

THE USE OF ORGANIC LIGANDS TO STUDY THE MOLECULAR
MECHANISMS OF ANGIOGENESIS AND IMMUNOREGULATION

by

Benjamin E. Turk

B.A., Chemistry and Biochemistry
Oberlin College, 1990

Submitted to the Department of
Chemistry in Partial Fulfillment of
the Requirements of the Degree of

Doctor of Philosophy
in Biological Chemistry

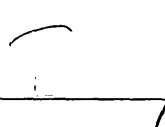
at the

Massachusetts Institute of Technology

February 1999

©1999 Massachusetts Institute of Technology
All rights reserved

Signature of Author

 _____

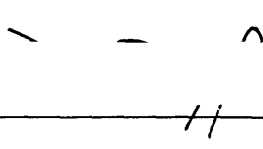
Department of Chemistry
January 14, 1999

Certified by

Jun Liu

Associate Professor of Chemistry and Biology
Thesis Supervisor

Accepted by

 _____

Dietmar Seyferth

~~Chairman, Departmental~~ Committee on Graduate Students

Science

This doctoral thesis has been examined by a Committee of the Department of Chemistry as follows:

Professor JoAnne Stubbe _____
Chairperson

Professor Jun O. Liu _____
Thesis Supervisor

Professor Stephen J. Lippard _____

THE USE OF ORGANIC LIGANDS TO STUDY THE MOLECULAR MECHANISMS OF ANGIOGENESIS AND IMMUNOREGULATION

by

Benjamin E. Turk

Submitted to the Department of Chemistry
on January 14, 1999 in Partial Fulfillment of the
Requirements for the Degree of Doctor of Philosophy

ABSTRACT

TNP-470, a synthetic derivative of the natural product fumagillin, and the synthetic teratogen thalidomide are both in clinical trials for cancer due to their ability to inhibit angiogenesis. The mechanism of action for either of these compounds, however, is not understood at the molecular level. TNP-470 and the related natural product ovalicin were found to covalently and specifically inhibit methionine aminopeptidase 2, and a significant correlation was found for a series of drug analogs for their ability to inhibit the enzyme and inhibit the growth of cultured endothelial cells. Endothelial cells treated with TNP-470 were found to be defective in their ability to remove the amino-terminal methionine residue from a subset of cellular proteins, providing a potential mechanism for the growth inhibitory activity of the drug. Ovalicin was initially discovered as an immunosuppressive agent, and it was found that TNP-470 also possesses immunosuppressive activity. A strong correlation was found between the ability of drug analogs to inhibit the proliferation of endothelial cells and lymphocytes, suggesting that the two activities share a common molecular basis. Studies on the effect of TNP-470 on the cell division cycle in endothelial cells revealed that the drugs inhibits the induction of cyclin E-dependent kinase activity, suggesting that the compounds inhibit growth during the mid- to late-G1 phase of the cell cycle.

Thalidomide has also been shown to possess anti-inflammatory properties, perhaps due to its ability to inhibit the production of TNF- α from activated monocytes. Thalidomide was found to bind to α_1 -acid glycoprotein, a serum protein which has been implicated in cytokine regulation. A series of tetrafluorophthalimide analogs of thalidomide were synthesized and shown to be highly potent inhibitors of TNF- α production. These novel compounds appear to act by a mechanism distinct from thalidomide. Two specific tetrafluorophthalimide binding proteins were identified: a novel homolog of the redox protein thioredoxin and a glutathione-dependent dehydroascorbate reductase homolog. These proteins may play a role in the oxidative regulation of signal transduction pathways leading to inflammatory cytokine induction.

Thesis Supervisor: Jun O. Liu

Title: Associate Professor of Chemistry and Biology

Acknowledgments

First and foremost, I need to thank Jun Liu, my advisor, who provided the impetus for all of the work described in this thesis. Jun has an irrepressible enthusiasm for science, and has always made himself available to discuss both the larger issues and finer details. I had the fortune of being present as he built from scratch what has emerged as an incredible and exciting interdisciplinary research program. The Liu lab is truly a place where the work you do is limited only by your interests.

Of course I am also deeply indebted to various members of the Liu lab with whom I have worked closely over the years. Eric Griffith has been my close collaborator on the TNP-470 work. From day one, it has been clear that Eric was scientifically years ahead of his contemporaries. I have benefited greatly from our countless discussions, whether they be about MetAP2, Gojira, or The King. Ed Licitra and I never shared a project, but I credit him for stimulating my interest in signal transduction and cell biology in general. I wish Ed the best of luck in whatever program he decides to enter following med school. Without the formidable synthetic chemistry skills of Zhuang Su, none of the TNP-470 work would have been possible. Zhuang's passion for chemistry and disaster films also contributed mightily to the energy level (and volume) of the lab. I would also like to recognize the contributions of Satomi Niwayama and Christine Loh, who worked on the tetrafluorophthalimide project, and with whom I had many stimulating discussions.

I would also like to thank the rest of the Liu group, past and present, for making the lab a terrific and friendly environment in which to work: Sara Verilli, Suming Kong, Fei Xiong, Rachel Brenner, Matt Bogyo, Luo Sun, Hongsi Jiang, Angelo Mondragon, Chris Armstrong, Hong-Duk Youn, Alex Akhiezer, Boris Dai, Yi Zhang, Ling-Hua Zhang, Hideaka Kakeya and Weifeng Liu. And I would be remiss without acknowledging the help of Jun's parade of assistants over the years, in particular Alicia Kikuchi, Mary Taddia, Maria Josefson, and especially Maureen Coleman.

I should also thank my neighbors on the first floor of the Center for Cancer Research, in particular Christy, Marianne, Tara, Bryan, Charles, and Ping, from whom I may have actually picked up some immunology. Oh yeah, and thanks for the pre-hybe, Jainzhu.

I thank those with whom I lunched on a daily basis: Bill Kobertz (destroy that photograph, if you please), Dave Wang (I thought you said they didn't put *any* air in), Linda Shimizu, Martha Rook (bourbon!), and Jeff Eckert (chaotic evil though he may be). We should also like to thank Matt Bogyo (f--king baby! Pretty sneaky, Sis). And let's not forget lunch bunch mark II: Peter, Bob and Eva. The constant factor being Evan Powers, of course, who has been my friend and sometime roommate since the beginning. Thanks, Evan, for accompanying me to smoky clubs and hosting PIGG in the early days, introducing me to some out-I-mean-like-*way*-out-as-in-snap-your-fingers-for-applause

jazz later on, for the gossip, for the bile-venting sessions, for never complaining about the mess, and for discussing some chemistry here and there.

I would like to recognize a couple of non-scientists (imagine!) for keeping me sane throughout these six plus years. I owe a lot to Steven Seidenberg for his friendship, his musicianship (?), and for thinking more deeply about evolution than any of the biologists I know. And my time in Boston would have been significantly less bearable without the companionship of Erica Rubin, who among other things taught me something (I think) about the mind, and who took me to Orgonon and Schoodic.

Finally I would like to thank Mom, Dad, and my brother Greg for a lifetime of love and support.

Rest in Peace: Kobo Abe, Linus Pauling, Carl Sagan, Alice Rugen, Derek Gross. You are missed.

Table of Contents

Abstract	3
Acknowledgments	4
Table of Contents	6
List of Abbreviations	8
List of Figures	9
List of Tables	12
Chapter 1. Angiogenesis and small molecule angiogenesis inhibitors	13
Angiogenesis	13
Tumor growth is angiogenesis-dependent	14
The angiogenic switch	15
Angiogenesis inhibitors as anticancer drugs	18
Fumagillin, TNP-470, and ovalicin	20
Thalidomide	24
References	27
Chapter 2. Identification of methionine aminopeptidase 2 as the common target for the angiogenesis inhibitors TNP-470 and ovalicin	32
Abstract	32
Introduction	32
Materials and Methods	33
Results	39
Discussion	50
References	58
Chapter 3. Inhibition of MetAP2 by TNP-470 and ovalicin in endothelial cells	61
Abstract	61
Introduction	61
Materials and Methods	70
Results	74
Discussion	94
References	99
Chapter 4. A common mode of action for the anti-angiogenic and immunosuppressive properties of TNP-470 and ovalicin	102
Abstract	102
Introduction	102

Materials and Methods	106
Results	111
Discussion	119
References	126
Chapter 5. Effects of TNP-470 on the cell division cycle	129
Abstract	129
Introduction	129
Materials and Methods	135
Results	136
Discussion	144
References	150
Chapter 6. Binding of thalidomide to α_1 -acid glycoprotein	153
Abstract	153
Introduction	153
Materials and Methods	155
Results	160
Discussion	167
References	169
Chapter 7. Studies on the mechanism of action of tetrafluorophthalimide inhibitors of cytokine induction in monocytes	172
Abstract	172
Introduction	172
Materials and Methods	176
Results	183
Discussion	198
References	205

List of Abbreviations

AGP	α_1 -acid glycoprotein
AIPPS	azidoiodophenylpropionyl succinimide
BAEC	bovine aortic endothelial cell
bFGF	basic fibroblast growth factor
Cdk	cyclin-dependent kinase
CKI	cyclin-dependent kinase inhibitor
Con A	concanavalin A
DMSO	dimethyl sulfoxide
ECM	extracellular matrix
eIF	eukaryotic initiation factor
ELISA	enzyme-linked immunosorbent assay
EMSA	electrophoretic mobility shift assay
eNOS	endothelial nitric oxide synthase
FBS	fetal bovine serum
GAPDH	glyceraldehyde-3-phosphate dehydrogenase
GST	glutathione S-transferase
HRI	heme regulated inhibitor kinase
HUVEC	human umbilical vein endothelial cell
IEF	isoelectric focusing
IL	interleukin
JNK	c-Jun N-terminal kinase
LPS	lipopolysaccharide
MALDI	matrix-assisted laser desorption/ionization
MetAP	methionine aminopeptidase
MHC	major histocompatibility complex
MMP	matrix metalloprotease
NEPHGE	non-equilibrium pH gradient electrophoresis
ORF	open reading frame
PAGE	polyacrylamide gel electrophoresis
PBMC	peripheral blood mononuclear cell
PDE	phosphodiesterase
PI	propidium iodide
PI3K	phosphoinositide 3'-kinase
PMA	phorbol myristate acetate
PMSF	phenylmethylsulfonyl fluoride
P/S	penicillin and streptomycin
SDS	sodium dodecyl sulfate
TNF- α	tumor necrosis factor- α
TOF	time of flight
uPA	urokinase plasminogen activator
VEGF	vascular endothelial growth factor

List of Figures

- Figure 1.1. Angiogenesis inhibitors related to fumagillin and thalidomide.
- Figure 2.1. The chemical structures of fumagillin, ovalicin, ovalicin photoaffinity label, biotin conjugates and synthetic analogs.
- Figure 2.2. Photoaffinity labeling of BAEC and mouse embryo extracts reveals a common binding protein for both TNP-470 and ovalicin.
- Figure 2.3. Isolation of p67 from mouse embryo extracts using biotin-fumagillin and biotin-ovalicin conjugates.
- Figure 2.4. MALDI-TOF mass spectrum of tryptic digest of p67.
- Figure 2.5. MetAP2 is highly conserved among eukaryotes.
- Figure 2.6. Western blot analysis confirms the identity of p67 as MetAP2.
- Figure 2.7. The biotin conjugates of fumagillin and ovalicin form stable adducts with MetAP2.
- Figure 2.8. Drug binding does not alter the protective effect of MetAP2 on eIF-2 α phosphorylation.
- Figure 2.9. TNP-470 and ovalicin specifically inhibit MetAP2 in vivo in yeast.
- Figure 2.10. Pharmacological correlation between inhibition of the methionine aminopeptidase activity of MetAP2 and inhibition of BAEC proliferation using fumagillin and ovalicin analogs.
- Figure 3.1. Two families of MetAP.
- Figure 3.2. Removal of the initiator methionine from proteins can potentially affect their activity in a number of ways.
- Figure 3.3. Sensitivity of various endothelial cell lines to TNP-470.
- Figure 3.4. Human endothelial cell lines express comparable levels of both MetAP1 and MetAP2 mRNA regardless of sensitivity to TNP-470.
- Figure 3.5. Analysis of protein myristoylation in BAECs in the presence and absence of TNP-470 by one dimensional SDS-PAGE.
- Figure 3.6. Analysis of protein myristoylation in BAECs in the presence and absence of TNP-470 by two dimensional gel electrophoresis.
- Figure 3.7. TNP-470 affects the migration of several protein spots by two dimensional electrophoresis.
- Figure 3.8. Two dimensional electrophoretic analysis followed by silver staining of protein extracts from cells treated with or without TNP-470.

Figure 3.9. Two dimensional electrophoretic analysis followed by silver staining of protein extracts from cells treated with or without TNP-470.

Figure 3.10. Purification of GAPDH from BAECs treated with or without TNP-470.

Figure 3.11. Two dimensional electrophoresis of GAPDH purified from TNP-470-treated and untreated BAECs.

Figure 3.12. Purification of GST- π from BAECs treated with or without TNP-470.

Figure 4.1. Structures of TNP-470, fumagillin, and ovalicin, illustrating the atom numbering system referred to in the text.

Figure 4.2. Correlation between inhibition of endothelial cell proliferation and the MLR for TNP-470, ovalicin, and derivatives.

Figure 4.3. Ovalicin and TNP-470 do not effect Con A-stimulated IL-2 production.

Figure 4.4. Ovalicin inhibits Con A-stimulated mouse lymphocyte proliferation.

Figure 4.5. TNP-470 inhibits the IL-2-dependent proliferation of T cell blasts.

Figure 4.6. Ovalicin and TNP-470 do not effect expression of CD25 (IL-2R α) in Con A stimulated mouse lymphocytes.

Figure 4.7. Inhibition of cell proliferation by immunosuppressive drugs.

Figure 5.1 The eukaryotic cell division cycle.

Figure 5.2. S49.1 cells have a prolonged G₁ phase when treated with TNP-470.

Figure 5.3. TNP-470 increases the G₂/M phase in BAECs.

Figure 5.4. TNP-470 does not prolong the passage of HUVECs through G₂ or M phase.

Figure 5.5. TNP-470 prevents entry of synchronized HUVECs into S phase.

Figure 5.6. TNP-470 inhibits activation of cyclin E-dependent kinase.

Figure 6.1A. Structure of thalidomide.

Figure 6.1B. Preparation of thalidomide photoaffinity labels AIPPOT and [¹²⁵I]AIPPOT.

Figure 6.2. Effect of thalidomide on the secretion of TNP- α by LPS-stimulated human peripheral blood monocytes.

Figure 6.3. Labeling of bovine thymus S100 fraction with [¹²⁵I]AIPPOT.

Figure 6.4. Two dimensional gel electrophoresis of [¹²⁵I]AIPPOT-labeled bovine thymus extract.

Figure 6.5. Purified thalidomide binding proteins.

Figure 6.6. Comparison of peptide sequences derived from the purified thalidomide binding protein and those of human AGP.

Figure 6.7. Labeling of human AGP with increasing concentrations of cold competitors.

Figure 7.1. Structures of thalidomide and analogs.

Figure 7.2. Inhibition of TNF- α production from LPS-stimulated THP-1 cells by thalidomide and analogs.

Figure 7.3. Synthesis of thalidomide analogs.

Figure 7.4. Inhibition of TNF- α production from LPS-stimulated THP-1 cells by compound **5** and its tetrafluorinated analog **7**.

Figure 7.5. Tetrafluorophthalimides affect TNF- α production at the transcriptional level.

Figure 7.6. Tetrafluorophthalimides do not bind to α_1 -AGP.

Figure 7.7. Detection of tetrafluorophthalimide binding proteins by photoaffinity labeling.

Figure 7.8. Affinity purification of p40.

Figure 7.9. Sequence of human tetrafluorophthalimide binding protein p40, aligned with the yeast 27.5 kD homolog and tobacco thioredoxin.

Figure 7.10. Effect of tetrafluorophthalimide **7** on NF- κ B activation.

Figure 7.11. Affinity purification of p30.

Figure 7.12. Purified p30.

Figure 7.13. Confirmation that p30 is identical to the recently cloned homolog of glutathione-dependent dehydroascorbate reductase.

Figure 7.14. Alignment of human p30 with a recently cloned glutathione-dependent dehydroascorbate reductase from rat.

List of Tables

Table 1.1. Angiogenesis inhibitors currently undergoing clinical trials for cancer.

Table 2.1. Potency of fumagillin and ovalicin analogs for inhibition of BAEC proliferation and MetAP2 enzymatic activity.

Table 3.1. Molecular weights of tryptic peptides from the 37 kD protein indicate that it is identical to GAPDH.

Table 3.2. Molecular weights of tryptic peptides from the 16 kD protein indicate it to be cyclophilin A.

Table 3.3. Amino terminal sequence analysis of GAPDH purified from TNP-470-treated and untreated BAECs.

Table 3.4. Amino terminal sequence of purified GST- π from cells grown to confluence in the presence or absence of TNP-470.

Table 4.1. IC₅₀ values for TNP-470 and ovalicin analogs in various assays.

Table 7.1. The MALDI-TOF mass spectrum of a tryptic digest of p30 suggests identity with a recently cloned glutathione-dependent dehydroascorbate reductase homolog.

Chapter 1

Angiogenesis and small molecule angiogenesis inhibitors

Angiogenesis

The formation of blood vessels during embryonic development in vertebrates occurs by two distinct mechanisms. The vascular framework is initially laid down by vasculogenesis, the de novo formation of blood vessels concomitant with the differentiation of angioblast precursors into endothelial cells, the cells which line all blood vessels (1,2). Subsequent blood vessel growth occurs by angiogenesis, whereby new vessels are formed by either splitting or sprouting from previously existing ones. Whereas splitting angiogenesis predominates in some embryonic tissues, such as the lung and heart, sprouting angiogenesis is responsible for vascularization of the developing brain and kidney, and is the only type known to occur in adults (2). Further vascular remodeling occurs after the onset of circulation, which involves both additional angiogenesis and regression of pre-existing vessels to produce the hierarchical system of veins, arteries, and capillaries characteristic of the adult circulatory system.

Sprouting angiogenesis is a complex process which involves the coordination of a series of component events (3,4). The vessel from which the new sprout arises must be rendered discontinuous by local breakdown of the basement membrane, the layer of extracellular matrix (ECM) which surrounds the endothelial cell tube. Vascular discontinuity is enhanced by endothelial cell retraction. Endothelial cells then change shape and invade the surrounding tissue, accompanied by mitogen-driven cell proliferation at the leading edge of the developing sprout. Cells more proximal to the original vessel cease proliferation and adhere tightly to each other, giving rise to the new capillary tube. Eventually, the sprouting endothelial cell tubes fuse into loops which support circulation.

Whereas extensive angiogenesis occurs in the developing embryo and during postnatal growth, angiogenesis in the adult is restricted to aspects of the reproductive cycle in females, such as follicle maturation during ovulation and the regrowth of the

endometrium following menstruation, to wound healing, and to pathological states such as cancer, retinal neovascularization, and arthritis (5,6). Accordingly, endothelial cells are among the most quiescent in the body, with an estimated 0.01% believed to be in the cell cycle at a given time, compared to 14% for gut epithelial cells (5). In response to the appropriate physiological or pathological signals, however, these cells rapidly switch to a highly proliferative state.

Tumor growth is angiogenesis-dependent

A variety of evidence supports the theory that the growth of solid tumors and metastases are dependent on angiogenesis (6,7,8,9). Vascularization promotes tumor progression both by providing a means for the exchange of nutrients, oxygen, and waste products and by releasing paracrine growth factors that act on the tumor cells. Thus without the induction of new blood vessels, a tumor will be restricted to a microscopic size. In some cases it has been documented that cells in such microscopic tumors in fact proliferate at the same rate as do cells in larger, vascularized solid tumors, but that cell numbers are kept in check by an increased rate of cell death due either to necrosis or apoptosis. Seminal experiments by Judah Folkman and co-workers in the early 1970s first illustrated the requirement for angiogenesis in tumor growth (10). Tumors were implanted into the iris of a rabbit, an avascular site. Initially, a tumor would grow slowly, but induced the outgrowth of vessels from the host, presumably due to the action of a secreted factor. In a matter of days, these vessels would reach the tumor implant. The tumor would then become vascularized and grow rapidly and exponentially. If the tumors were instead implanted in the anterior vitreous chamber such that blood vessels could not reach them, they failed to grow beyond a millimeter in diameter, though the cells would continue to proliferate. Such tumors could be left in the vitreous chamber for over a month and then retransplanted to the retina, which would result in vascularization and rapid growth.

In addition to primary tumors, the development of metastases also requires angiogenesis (7,9). Vascularization of the primary tumor promotes the shedding of tumor cells into the circulation, particularly because angiogenic vessels are leaky and thus permeable to cells. High hydrostatic pressure within the tumor mass arising from the leaky vasculature also promotes efflux of cells. In addition, matrix-degrading enzymes which are active during endothelial cell invasion can promote dissociation of cells from the tumor mass. Cells shed from angiogenic tumors are also likely to be angiogenic when they arrive at the site of metastasis. Like primary tumors, those which are not limited to a microscopic size until they also become angiogenic (11).

The angiogenic switch

Observations in experimental animals and in human patients support the idea that the switch from a non-angiogenic state to an angiogenic state, in which the developing tumor now induces blood vessel growth and invasion from the surrounding tissue, is a definable and requisite event in tumor progression (3). Tumor progression is generally regarded as proceeding through discrete morphologically distinct stages, which reflect the accumulation of genetic and epigenetic changes in the tumor cells. Such stages can be detected in certain transgenic mouse models for cancer. Expression of the SV40 T antigen under the insulin promoter in mice causes the development of pancreatic islet cell carcinomas. While all islets are initially normal, about half eventually become hyperplastic, in which proliferation increases but neovascularization has not occurred. Only 1-2% progress to solid tumors, which are highly vascularized. A discrete angiogenic stage occurs in about 10% of the islets as judged by the ability of explants to attract endothelial cells in vitro (12). These observations imply that the ability to recruit new blood vessels is necessary but not sufficient for the progression to full-blown solid tumors. Similarly, biopsies reveal that discrete stages are evident during the development of breast cancer in human patients, including carcinoma-in-situ, a more localized stage which precedes invasive carcinoma. Using endothelial cell markers as a measure for the

extent of vascularization in tumor biopsies it was shown that only a subset of carcinomas-in-situ were vascularized and therefore angiogenic (13,14). This observation places an angiogenic stage in between non-angiogenic carcinoma-in-situ and fully invasive carcinoma.

The angiogenic switch reflects a shift in the balance of endogenous activators and inhibitors of angiogenesis, which normally serve to keep the vasculature quiescent (3,6). A number of secreted proangiogenic factors have been identified which can promote angiogenesis in vitro and in vivo. In the context of tumor angiogenesis, these factors are generally believed to be produced by the tumor itself, though some angiogenesis inducers may be produced by hematopoietic cells (macrophages, lymphocytes, and mast cells) recruited to the tumor, and perhaps by the surrounding stroma as a consequence of induction by the tumor. Those which have been principally associated with tumor angiogenesis include vascular endothelial growth factor (VEGF, also known as vascular permeability factor, or VPF), and the acidic and basic fibroblast growth factors (aFGF and bFGF). Each of these factors is sufficient to induce blood vessel growth when implanted within an avascular site such as the rabbit cornea. These factors are able to trigger the entire angiogenic cascade by means of their pleiotropic effects on endothelial cells (7,15). VEGF increases vascular permeability, causing leakage of serum proteins into the extravascular space. Serum plasminogen is activated to plasmin at the endothelial cell surface as a consequence of VEGF-induced upregulation of urokinase plasminogen activator (uPA) and its receptor (uPAR) in endothelial cells. Plasmin can thereby locally catalyze the proteolytic activation of matrix metalloproteases (MMPs) necessary for breakdown of the basement membrane. Plasmin and MMPs are also important for penetration of the growing sprout through the fibrinous layer which forms as a consequence of vascular leakage (15,16). VEGF also upregulates integrin $\alpha_v\beta_3$, which is considered to be a marker for vessels undergoing active angiogenesis. Ligation of $\alpha_v\beta_3$ imparts a survival signal to dividing endothelial cells and is required to prevent their death by apoptosis (17). Integrin $\alpha_v\beta_3$ promotes the directed degradation of the extracellular

matrix by binding directly to MMP-2 (also called gelatinase A), thereby recruiting it to the endothelial cell surface (18). bFGF has been shown to induce the expression of proteases and $\alpha_v\beta_3$ as well, and also to downregulate other integrins, such as $\alpha_6\beta_4$, which allows loosening of endothelial cell-basement membrane adhesion and thus promotes vascular discontinuity and invasion (7,15). Both VEGF and bFGF are potent endothelial cell mitogens, and synergize with each other in this regard. Several lines of evidence have established roles for these factors in angiogenesis. Expression of VEGF correlates with the onset of angiogenesis in tumors, during the female reproductive cycle, and during embryogenesis, and its receptors (VEGF-R1 and VEGF-R2) are restricted in expression to endothelial cells. Mice lacking either VEGF receptor or having only one copy of the gene encoding VEGF die embryonically due to serious defects in vasculogenesis (19). Though expression of bFGF is widespread, the protein lacks a standard signal sequence and its release from cells does not appear to occur via the normal secretory pathway. Thus bFGF expression may not correlate with the presence of the active factor (3,7). In addition, secreted bFGF binds heparin and is likely to be sequestered in the extracellular matrix, where it may be released during breakdown as described above. Antibodies against either bFGF or VEGF will block or retard tumor growth in certain mouse models (4). Retroviral delivery of a dominant negative mutant of the type 2 VEGF receptor (VEGF-R2, also called Flk-1 in mice) to endothelial cells in a mouse brain tumor model also decreased tumor growth (20).

Upregulation of angiogenesis inducers during tumor progression occurs by several mechanisms. VEGF is activated in hypoxic cells (7). In several cases activation of oncogenes has been tied to upregulation of angiogenesis inducers (6). For example, activation of Ha-Ras and Src induce VEGF expression in some cell lines. Ras, Src, and Yes can also upregulate uPA in some cell types, which promotes basement membrane degradation as described above. The loss of the von Hippel Lindau tumor suppressor gene results in stabilization of the VEGF mRNA (2).

A variety of endogenous protein inhibitors of angiogenesis have also been identified and there is evidence that their downregulation must occur in order for blood vessels to grow (3,6). Among the first to be identified was thrombospondin, which is produced in high levels by untransformed cells and at low levels in tumor cell lines. Loss of wild type p53, a common event in tumor progression, results in downregulation of thrombospondin, and is likely to be a genetic component of the angiogenic switch in some cancers. More recently, several circulating antiangiogenic proteins have been identified in mouse models for cancer metastasis. These factors include angiostatin, an internal fragment of plasminogen, and endostatin, a carboxy terminal fragment of collagen type XVIII (21,22). Both are in fact produced by primary tumors and act to suppress the growth of metastases. Surgical removal of the primary tumor gives rise to rapid growth of metastases, a situation observed with some human cancers (9). Presumably the growth of the primary tumor is supported by high local concentrations of activators, as discussed above. How these various protein inhibitors suppress angiogenesis is not well understood. Angiostatin may work by inducing apoptosis of growing endothelial cells, whereas endostatin appears to compete with angiogenesis inducers for binding to heparin (23,24).

Angiogenesis inhibitors as anticancer drugs

The requirement of angiogenesis for tumor growth has led to the proposal that inhibition of angiogenesis should represent a novel form of anticancer therapy. Indeed, a number of antiangiogenesis drugs are currently in clinical trials for a variety of cancers (Table 1.1, 25). Such inhibitors may be directed against any of the various steps in the angiogenesis process, and may be either proteins or small molecules (4). MMP inhibitors, such as marimastat, prevent ECM breakdown, an early step in angiogenesis, and several are currently in phase III clinical trials for a variety of solid tumors. Their efficacy may also reflect their ability to directly inhibit tumor cell invasiveness. Interferon- α inhibits endothelial cell growth and migration and has proven effective in

Table 1.1. Angiogenesis inhibitors currently undergoing clinical trials for cancer (25).

Drug	Mechanism	Trial
Marimastat	MMP inhibitor	Phase III
Bay 12-9566	MMP inhibitor	Phase III
Ag3340	MMP inhibitor	Phase III
MMI270	MMP inhibitor	Phase I
COL-3	MMP inhibitor	Phase I
Platelet factor-4	Endothelial cell growth inhibitor	Phase II
Interleukin 12	Endothelial cell growth inhibitor	Phase I/II
Vitaxin	Antibody to $\alpha_v\beta_3$	Pre-phase II
RhuMad VEGF	Antibody to VEGF	Phase II
SU5416	Inhibitor of VEGF-R kinase	Phase II
Interferon- α	Endothelial cell growth inhibitor	Phase I/II
ZD0101	Targets inflammatory response to blood vessels	Phase II
TNP-470	Endothelial cell growth inhibitor	Phase II
Thalidomide	Mechanism unknown	Phase II
Carboxyamino-triazole	Endothelial cell growth and migration inhibitor	Phase I/II
Squalamine	Endothelial cell growth inhibitor	Phase II/II
IM862	Mechanism unknown	Phase II

managing life-threatening childhood hemangiomas (8). Carboxyamino-triazole and platelet factor-4 also inhibit the growth of endothelial cells and are in phase II trials for several solid tumors. Blocking antibodies against integrin $\alpha_v\beta_3$ and VEGF are also undergoing clinical trials for cancer. Highly anticipated due to striking results in animal models, human clinical trials of the anti-angiogenic polypeptides angiostatin and endostatin have not yet begun.

The advantages of antiangiogenesis therapy over conventional chemotherapy are theoretically numerous (8,9). Angiogenesis inhibitors should be less generally cytotoxic

than conventional drugs and therefore should not produce the severe side effects typically associated with chemotherapy such as nausea, hair loss, and bone marrow suppression. Since the endothelial cells targeted by anti-angiogenesis drugs are in direct contact with the bloodstream, drug delivery problems should not be as much of an issue. Importantly, drug resistance, which arises in 30% of patients undergoing chemotherapy, does not seem to arise with anti-angiogenic therapy (9,26). Tumor cells develop drug resistance due to their inherent genomic instability, which gives rise to selectable variants. Primary cells, such as endothelial cells, should not be subject to the same selection because genetic alterations occur much less frequently. This principle is evident in the clinic, where bone marrow suppression continues to occur throughout repeated cycles of chemotherapy, and where resistance to experimental antiangiogenic drugs has not been observed. In mouse tumor models, repeated cycles of endostatin treatment allows for successive rounds of tumor regression and regrowth without the development of resistance (27). Curiously, in each of several different models, tumors failed to regrow following cessation of endostatin treatment after a number of cycles, perhaps due to exhaustion of the proliferative potential of the tumor-associated endothelial cells. Such results have raised hopes that this next generation of anti-angiogenesis drugs may revolutionize the treatment of cancer.

Fumagillin, TNP-470, and ovalicin

Two classes of small molecule angiogenesis inhibitors to receive attention in recent years are those related to fumagillin and thalidomide (Figure 1.1). Prior to its rediscovery as an angiogenesis inhibitor, fumagillin had been known for over 40 years. In 1949, it was first identified as an active fraction from culture supernatants of the fungus *Aspergillus fumigatus* which could suppress replication of a *Staphylococcus* phage without affecting the growth of the bacteria itself (28). Soon thereafter the drug was found to have potent antiprotozoal activities, which prompted human clinical trials to test fumagillin as an anti-amoebic agent (29,30). Dose-limiting side effects, however, prevented its widespread clinical use. Interestingly, demonstration that the compound inhibited the growth of some

tumor cells in culture led to testing of fumagillin in mice as an anticancer drug (31). The increase in survival time and decrease in tumor growth observed in animals even prompted testing in a small group of human patients. No clinical efficacy was observed, perhaps due to the relatively low doses administered. Today fumagillin is sold principally for agricultural use as an anti-protozoal agent to treat nosema disease, a hive-decimating scourge of beekeepers.

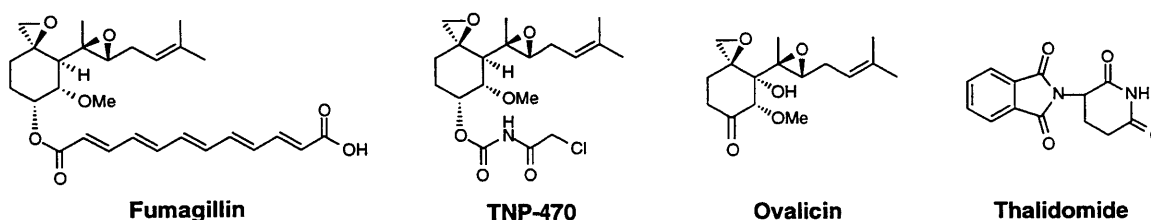


Figure 1.1. Angiogenesis inhibitors related to fumagillin and thalidomide.

The accidental fungal contamination of an endothelial cell culture led to the rediscovery of fumagillin as an angiogenesis inhibitor, in a manner which mirrored Fleming's discovery of penicillin (32). Ingber, while a postdoctoral fellow in Folkman's laboratory, noted that endothelial cells near the contaminant were rounded, suggesting that their ability to proliferate was impaired. Purification of the active principle from culture supernatants of the contaminating *Aspergillus* revealed it to be fumagillin. Subsequently, fumagillin was demonstrated to inhibit endothelial cell proliferation in vitro and to inhibit blood vessel growth in vivo. Due to the induction of severe weight loss in mice, the compound could not be used in models of tumor growth in vivo. Accordingly, a series of fumagillin analogs were prepared in an effort to find more potent angiogenesis inhibitors which might have fewer side effects. Among those synthesized, the most potent was the compound TNP-470 (originally named AGM-1470), in which the decatetraenoyl group of fumagillin was replaced with a chloroacetylcarbamoyl moiety (Figure 1.1). TNP-470 reversibly inhibits endothelial cell proliferation with an IC_{50} in the low picomolar range, while micromolar concentrations of the drug are cytotoxic (33). TNP-470 has been

shown to inhibit angiogenesis in a variety of contexts in vivo, including spontaneous vascularization of the chicken egg chorioallantoic membrane and bFGF-induced blood vessel growth in the rat cornea (32,33). Importantly, systemic administration of TNP-470 inhibits the growth of both blood vessels and solid tumors in mice.

Another structural analog of fumagillin, the natural product ovalicin, was also known for some time before it was found to be an angiogenesis inhibitor. Initially isolated in 1962 from culture supernatants of the fungus *Pseudeurotium ovalis*, the compound was shown to be potently immunosuppressive (34). In animals, the drug inhibits antibody production, reduces spleen weight in immunized animals, prolongs the survival of skin grafts, and reduces significantly the symptoms of experimental allergic encephalomyelitis (35,36). In vitro, the drug inhibits mitogen-induced lymphocyte proliferation, providing a potential explanation for its effects in animals (37). Human clinical trials, however, were halted when it was found that ovalicin caused a dramatic decrease in platelet count in some patients, ceasing further development of the drug (34). Around the same time, ovalicin was also isolated from a separate fungus in a screen for compounds that could stimulate lettuce seed germination in the dark (38). More recently, the structural similarity between fumagillin and ovalicin prompted the finding that ovalicin also inhibits angiogenesis, having a potency for the inhibition of endothelial cell growth rivaling that of TNP-470 (39). The relationship between these varied activities of ovalicin is unclear.

As the most active compound in its class, TNP-470 has been extensively studied in animals as an anticancer agent. Compared with its high potency as an inhibitor of endothelial cell growth, inhibition of tumor cell proliferation in vitro generally requires much higher concentrations of the drug (32). The efficacy displayed by TNP-470 in a variety of animal models for cancer has therefore been attributed to its effects on blood vessels and not to direct inhibition of tumor cell growth. Systemic administration of TNP-470 can inhibit the growth of a variety of solid tumors implanted subcutaneously in

mice, including Lewis lung carcinoma, B16 melanoma, M5076 reticulum cell sarcoma, and Walker 256 carcinoma (32,40). In some cases inhibition of tumor growth has been correlated with decreases in vascularization of the tumor. The drug also inhibits the growth of several human tumors implanted into nude mice (41,42). In each case, tumors grow more slowly as a consequence of drug treatment, but tumor regression does not occur. TNP-470 on its own can dramatically decrease the number of metastases in several rodent models, including tumors which spread to the lung, lymph nodes, and liver (40,43). These observations are significant in that they support the notion that metastases require the induction of blood vessels to grow to visible dimensions. In addition, these studies illustrate that anti-angiogenic drugs can work in animal models in which the progression of cancer parallels human cancer development more closely than when tumors are simply implanted subcutaneously. In this regard, it is also notable that combination therapy with TNP-470 and two other angiogenesis inhibitors, minocycline and interferon α/β , slows the growth of islet cell carcinoma in transgenic mice expressing the SV40 T antigen under control of the insulin promoter, in which tumors arise in the context of solid tissue (44). In addition, TNP-470 alone could prevent formation of primary liver tumors in carcinogen-treated rats (45). While these studies indicate that TNP-470 can prevent tumor formation and growth, the effects combination therapy with conventional cytotoxic drugs or radiation can be more than additive in mouse tumor models, leading in some cases to long term survival (46,47). Such successes in animal tests have led to human clinical trials with TNP-470 for several solid tumors, including Kaposi's sarcoma, prostate cancer, cervical carcinoma, glioblastoma, pancreatic cancer, and renal cancer (48). Preliminary results have not been conclusive with regard to efficacy, but as anticipated, side effects have generally been much less severe than with conventional chemotherapy .

Despite having progressed to human clinical trials, little is known regarding the molecular mechanism of action of the class of drugs comprising fumagillin, ovalicin, and TNP-470. The drugs appear to cause their target cells to arrest in the G₁ phase of the cell cycle, apparently subsequent to immediate early gene induction by mitogens (37,49,50,

51). How these compounds inhibit cell proliferation is not clear. Presumably cell cycle arrest occurs as a consequence of inhibiting some protein or proteins essential for cell cycle progression. Identification of such a protein would thus provide basic information regarding the mechanisms of cell growth, and would identify a potential target for the development of future angiogenesis inhibitors which could prove clinically important.

Thalidomide

Thalidomide, a synthetic derivative of glutamine, was first prepared in 1956 and found to have sedative-hypnotic properties (52). Widely used as a tranquilizer in Germany and other parts of Europe during the early 1960s, the drug was withdrawn from the market when it was determined to be the cause of an outbreak of serious birth defects in late 1961 (53,54). Nearly 10,000 children were born with thalidomide-induced malformations. The most common was severe phocomelia, or shortening of the limbs, though defects of the eyes, ears, respiratory system, and intestinal tract were also reported. Despite years of research, no clear cellular or molecular mechanism has emerged to explain the teratogenic effect of thalidomide. An intriguing observation, however, was recently made by D'Amato in Folkman's group (55). D'Amato reasoned that given the extensive angiogenesis which occurs during embryonic development, compounds which inhibit angiogenesis would be expected to be potent teratogens. Therefore a subset of known teratogenic compounds could in fact be angiogenesis inhibitors. Indeed, thalidomide turned out to prevent bFGF-induced neovascularization of the rabbit cornea when administered systemically, providing an attractive mechanism for its teratogenicity. The drug has been shown to inhibit VEGF-induced corneal angiogenesis as well (56). Interestingly, thalidomide did not inhibit endothelial cell growth in vitro, suggesting that the drug affects other steps in the angiogenic cascade, such as cell movement or invasion. Alternatively, thalidomide might require metabolic activation which can only occur in vivo. Oxidation of thalidomide to an arene oxide has previously been proposed to mediate the teratogenic action of thalidomide (57). The inhibition of endothelial cell

growth by thalidomide treated with liver microsomes was recently reported in support of this hypothesis (58). Microsomes from humans and rabbits, which are susceptible to thalidomide's teratogenicity could activate the drug, whereas microsomes from rodents, which are apparently insensitive to thalidomide, could not, supporting both the idea that metabolic activation was essential for thalidomide's angiogenesis inhibitory activity and that this activity underlies the teratogenic action of the drug. However, thalidomide has been shown inhibit angiogenesis in vivo in rodents, and while thalidomide does not induce the same types of malformations in mice and rats as it does in humans, a different spectrum of birth defects and embryotoxicity do occur in thalidomide-treated rodents (59,60,61). Thus a role for metabolic activation of thalidomide is still unclear, and further work will be needed to determine if the ability of the drug to inhibit angiogenesis indeed underlies its teratogenicity. The new findings, however, have prompted clinical trials for thalidomide for cancer and angiogenesis-dependent retinopathy.

Like ovalicin, knowledge an effect of thalidomide on the immune system predates its use as an angiogenesis inhibitor. In 1965 thalidomide was provided to soothe a leprosy patient undergoing erythema nodosum leprosum (ENL), the most severe inflammatory reaction associated with the disease (62). Surprisingly, the patient's symptoms cleared up rapidly, prompting a systematic trial of thalidomide to treat ENL. Thalidomide remains the drug of choice for this condition, and has proven to be effective in other inflammatory diseases of the skin (63). The anti-inflammatory activity of thalidomide has also led to its use against graft versus host disease following bone marrow transplantation and in treating oral and esophageal ulcers and wasting associated with HIV infection (64,65,66).

The anti-inflammatory activity of thalidomide has been attributed to its ability to inhibit the production of the inflammatory cytokine tumor necrosis factor- α (TNF- α) from lipopolysaccharide (LPS)-stimulated blood monocytes (67). Consistent with this observation, thalidomide lowers circulating TNF- α levels in ENL patients, and the drug can protect mice from lethal doses of LPS, a mouse model for septic shock (68,69). In

cultured cells, however, high concentrations of thalidomide unlikely to be achievable in vivo are required to inhibit production of the cytokine, indicating that either the drug's activity is potentiated by metabolic activation or that other mechanisms operate in vivo. In this regard thalidomide has been shown to lower levels of cell adhesion molecules expressed on both leukocytes and endothelial cells, which mediate inflammation by promoting extravasation of leukocytes from the bloodstream into surrounding tissues (70,71,72). It is possible that the in vivo efficacy of thalidomide reflects the synergistic effects of partial down-regulation of both inflammatory cytokines and adhesion molecules.

Despite increasing clinical use, the molecular basis for the varied activities of thalidomide is also not understood. The inhibition of TNF- α appears to be mediated by destabilization of its mRNA (73). Activation of the MAPK family protein kinases p38 and c-Jun N-terminal kinase (JNK) by LPS has been implicated in post-transcriptional regulation of TNF- α . A requirement for p38 for optimal TNF- α production has been suggested by the discovery of a class of pyridinylimidazole TNF- α production inhibitors which potently and specifically inhibit this kinase (74,75). Expression of a dominant negative allele of JNK in a mouse macrophage cell line inhibits expression from a TNF- α translational reporter construct but not a transcriptional reporter construct (76). Possible roles of the signaling pathways leading to p38 and JNK activation in thalidomide sensitivity have not been explored thus far. In addition, no protein target for thalidomide has been identified. Such studies have perhaps been hampered by the low potency of the drug; the IC₅₀ for TNF- α production is approximately 200 μ M, close to the solubility limit for the compound in water. The molecular target for thalidomide is likely to play a key role in the signaling cascade leading to cytokine induction in monocytes, and may provide a novel target for anti-inflammatory drug discovery. Such a protein may prove to play an important role in the regulation of angiogenesis as well.

References for Chapter One

1. Risau, W. (1995) Differentiation of endothelium. *FASEB J.* **9**, 926-933.
2. Risau, W. (1997) Mechanisms of angiogenesis. *Nature* **386**, 671-674.
3. Hanahan, D. and Folkman, J. (1996) Patterns and emerging mechanisms of the angiogenic switch during tumorigenesis. *Cell* **86**, 353-364.
4. Auerbach, W. and Auerbach, R. (1994) Angiogenesis inhibition: a review. *Pharmac. Ther.* **63**, 265-311.
5. D'Amore, P. A., and Thompson, R. W. (1987) Mechanisms of angiogenesis. *Ann. Rev. Physiol.* **49**, 453-464.
6. Bouck, N., Stellmach, V., and Hsu, S. C. (1996) How tumors become angiogenic. *Adv. Cancer Res.* **69**, 135-174.
7. Folkman, J. (1995) Tumor angiogenesis. In *The Molecular Basis of Cancer*, J. Mendelsohn, P. M. Howley, M. A. Israel, and L. A. Liotta, Eds. (W. B. Saunders, Philadelphia) 206-232.
8. Folkman, J. (1995) Clinical applications of research on angiogenesis. *New Engl. J. Med.* **333**, 1757-1763.
9. Folkman, J. (1995) Angiogenesis in cancer, vascular, rheumatoid, and other disease. *Nat. Med.* **1**, 27-31.
10. Gimbrone, M. A., Leapman, S. B., Cotran, R. S., and Folkman, J. (1972) Tumor dormancy in vivo by prevention of neovascularization. *J. Exp. Med.* **136**, 261-276.
11. Holmgren L., O'Reilly M. S., Folkman J. (1995) Dormancy of micrometastases: balanced proliferation and apoptosis in the presence of angiogenesis suppression. *Nat. Med.* **1**, 149-153.
12. Folkman J., Watson K., Ingber D., Hanahan D. (1989) Induction of angiogenesis during the transition from hyperplasia to neoplasia. *Nature* **339**, 58-61.
13. Weidner, N., Folkman, J., Pozza, F., Bevilacqua, P., Allred, E. N., Moore, D. H., Meli, S., and Gasparini, G. (1992) Tumor angiogenesis: a new significant and independent prognostic indicator in early-stage breast carcinoma. *J. Natl. Cancer Inst.* **84**, 1875-1887.
14. Guidi, A. J., Fischer, L., Harris, J. R., and Schnitt, S. J. (1994) Microvessel density and distribution in ductal carcinoma in situ of the breast. *J. Natl. Cancer Inst.* **86**, 614-619.
15. Senger, D. R. (1996) Molecular framework for angiogenesis: a complex web of interactions between extravasated plasma proteins and endothelial cell proteins induced by angiogenic cytokines. *Am. J. Pathol.* **149**, 1-7.
16. Hiraoka, N., Allen, E., Apel, I. J., Gyetko, M. R., and Weiss, S. J. (1998) Matrix metalloproteinases regulate neovascularization by acting as pericellular fibrinolysins. *Cell* **95**, 365-377.
17. Strömblad, S., and Cheresh, D. A. (1996) Integrins, angiogenesis, and vascular cell survival. *Chem Biol.* **3**, 881-885.
18. Brooks, P. C., Strömblad, S., Sanders, L. C., von Schalscha, T. L., Aimes, R. T., Stetler-Stevenson, W. G., Quigley, J. P., and Cheresh, D. A. (1996) Localization of

- matrix metalloproteinase MMP-2 to the surface of invasive cells by interaction with integrin $\alpha_v\beta_3$. *Cell* **85**, 683-693.
19. Hanahan, D. (1997) Signaling vascular morphogenesis and maintenance. *Science* **277**, 48-50.
 20. Millauer, B., Shawver, L. K., Plate, K. H., Risau, W., and Ullrich, A. (1994) Glioblastoma growth inhibited in vivo by a dominant-negative Flk-1 mutant. *Nature* **367**, 576-579.
 21. O'Reilly, M. S., Holmgren, L., Shing, Y., Chen, C., Rosenthal, R. A., Moses, M., Lane, W. S., Cao, Y., Sage, E. H., and Folkman, J. (1994) Angiostatin: a novel angiogenesis inhibitor that mediates the suppression of metastases by a Lewis lung carcinoma. *Cell* **79**, 315-328.
 22. O'Reilly, M. S., Boehm, T., Shing, Y., Fukai, N., Vasios, G., Lane, W. S., Flynn, E., Birkhead, J. R., Olsen, B. R., and Folkman, J. (1997) Endostatin: an endogenous inhibitor of angiogenesis and tumor growth. *Cell* **88**, 277-285.
 23. Claesson-Welsh, L., Welsh, M., Ito, N., Anand-Apte, B., Soker, S., Zetter, B., O'Reilly, M., and Folkman, J. (1998) Angiostatin induces endothelial cell apoptosis and activation of focal adhesion kinase independently of the integrin-binding motif RGD. *Proc. Natl. Acad. Sci. USA* **95**, 5579-5583.
 24. Hohenester, E., Sasaki, T., Olsen, B. R., and Timpl, R. (1998) Crystal structure of the angiogenesis inhibitor endostatin at 1.5 Å resolution. *EMBO J.* **17**, 1656-1664.
 25. Nelson, N. J. (1998) Inhibitors of angiogenesis enter phase III testing. *J. Natl. Cancer Inst.* **90**, 960-963.
 26. Kerbel, R. S. (1997) A cancer therapy resistant to resistance. *Nature* **390**, 335-336.
 27. Boehm, T., Folkman, J., Browder, T., and O'Reilly, M. S. (1997) Antiangiogenic therapy of experimental cancer does not induce acquired drug resistance. *Nature* **390**, 404-408.
 28. Hanson, F. R., and Elbe, E. (1949) An antiphage agent isolated from *Aspergillus* sp. *J. Bacteriol.* **58**, 527.
 29. McCowen, M. C., Callender, M. E., and Lawlis, J. F., Jr. (1951) Fumagillin (H-3), a new antibiotic with amebicidal properties. *Science* **113**, 202-203.
 30. Wilson, B. J. (1971) Miscellaneous *Aspergillus* toxins. In *Microbial Toxins*, Vol. 6. A. Ciegler, S. Kadis, and S. J. Ajl, Eds. (Academic Press, New York) 277-295.
 31. DiPaolo, J. A., Tarbell, D. S., Moore, G. E. (1959) Studies on the carcinolytic activity of fumagillin and some of its derivatives. *Antibiot. Ann.* **1958-1959**, 541-546.
 32. Ingber, D., Fujita, T., Kishimoto, S., Sudo, K., Kanamaru, T., Brem, H., and Folkman, J. (1990) Synthetic analogs of fumagillin that inhibit angiogenesis and suppress tumour growth. *Nature* **348**, 555-557.
 33. Kusaka, M., Sudo, K., Fujita, T., Marui, S., Itoh, F., Ingber, D., and Folkman, J. (1991) Potent anti-angiogenic action of AGM-1470: comparison to the fumagillin parent. *Biochem. Biophys. Res. Commun.* **174**, 1070-1076.
 34. Stähelin, H. F. (1996) The history of cyclosporin A (Sandimmune®) revisited: another point of view. *Experientia* **52**, 5-13.

35. Lazary, S., and Stähelin, H. (1969) Immunosuppressive effect of a new antibiotic: ovalicin. *Antibiot. Chemother.* **15**, 177-181.
36. Lazary, S., and Stähelin, H. (1968) Immunosuppressive and specific antimetabolic effects of ovalicin. *Experientia* **24**, 1171-1173.
37. Hartmann, G. R., Richter, H., Weiner, E. M., and Zimmermann, W. (1978) On the mechanism of action of the cytostatic drug anguidine and of the immunosuppressive agent ovalicin, two sesquiterpenes from fungi. *Planta Med.* **34**, 231-252.
38. Sassa, T., Kaise, H., Ogawa, Y., and Munakata, K. (1969) Isolation of a new lettuce seed germination stimulant. *Nature* **222**, 773-774.
39. Corey, E. J., Guzman-Perez, A., and Noe, M. C. (1994) Enantioselective synthesis of (-)-ovalicin, a potent inhibitor of angiogenesis, using substrate-enhanced asymmetric hydroxylation. *J. Am. Chem. Soc.* **116**, 12109-12110.
40. Yamaoka, M., Yamamoto, T., Masaki, T., Ikeyama, S., Sudo, K., and Fujita, T. (1993) Inhibition of tumor growth and metastasis of rodent tumors by the angiogenesis inhibitor *O*-(Chloroacetyl-carbamoyl)fumagillol (TNP-470; AGM-1470). *Cancer Res.* **53**, 4262-4267.
41. Yamaoka, M., Yamamoto, T., Ikeyama, S., Sudo, K., and Fujita, T. (1993) Angiogenesis inhibitor TNP-470 (AGM-1470) potently inhibits the tumor growth of hormone-independent human breast and prostate carcinoma cell lines. *Cancer Res.* **53**, 5233-5236.
42. Kanai, T., Konno, H., Tanaka, T., Matsumoto, K., Baba, M., Nakamura, S., and Baba, S. (1997) Effect of angiogenesis inhibitor TNP-470 on the progression of human gastric cancer xenotransplanted into nude mice. *Int. J. Cancer* **71**, 838-841.
43. Ohta, Y., Watanabe, Y., Tabata, T., Oda, M., Hayashi, Y., Endo, Y., Tanaka, M., and Sasaki, T. (1997) Inhibition of lymph node metastasis by an anti-angiogenic agent, TNP-470. *Br. J. Cancer* **75**, 512-515.
44. Parangi, S., O'Reilly, M., Christofori, G., Holmgren, L., Grosfeld, J., Folkman, J., and Hanahan, D. (1996) Antiangiogenic therapy of transgenic mice impairs *de novo* tumor growth. *Proc. Natl. Acad. Sci. USA* **93**, 2002-2007.
45. Ikebe, T., Yamamoto, T., Kubo, S., Hirohashi, K., Kinoshita, H., Kaneda, K., and Sakurai, M. (1998) Suppressive effect of the angiogenesis inhibitor TNP-470 on the development of carcinogen-induced hepatic nodules in rats. *Jpn. J. Cancer Res.* **89**, 143-149.
46. Kato, T., Sato, K., Kakinuma, H., and Matsuda, Y. (1994) Enhanced suppression of tumor growth by combination of angiogenesis inhibitor *O*-(Chloroacetyl-carbamoyl)fumagillol (TNP-470) and cytotoxic agents in mice. *Cancer Res.* **54**, 5143-5147.
47. Teicher, B. A., Holden, S. A., Ara, G., Alvarez Sotomayor, E., Huang, Z. D., Chen, Y.-N., and Brem, H. (1994) Potentiation of cytotoxic cancer therapies by TNP-470 alone and with other anti-angiogenic agents. *Int. J. Cancer* **57**, 920-925.
48. Castronovo, V., and Belotti, D. (1996) TNP-470 (AGM-1470): Mechanisms of action and early clinical development. *Eur. J. Cancer* **32A**, 2520-2527.

49. Kusaka, M., Sudo, K., Matsutani, E., Kozai, Y., Marui, S., Fujita, T., Ingber, D., and Folkman, J. (1994) Cytostatic inhibition of endothelial cell growth by the angiogenesis inhibitor TNP-470 (AGM-1470). *Br. J. Cancer* **69**, 212-216.
50. Abe, J., Zhou, W., Takua, N., Taguchi, J., Kurokawa, K., Kumada, M., and Takuwa, Y. (1994) A fumagillin derivative angiogenesis inhibitor, AGM-1470, inhibits activation of cyclin-dependent kinases and phosphorylation of retinoblastoma gene product but not protein tyrosyl phosphorylation or protooncogene expression in vascular endothelial cells. *Cancer Res.* **54**, 3407-3412.
51. Hori, A., Ikema, S., and Sudo, K. (1994) Suppression of cyclin D1 mRNA expression by the angiogenesis inhibitor TNP-470 (AGM-1470) in vascular endothelial cells. *Biochem. Biophys. Res. Commun.* **204**, 1067-1073.
52. Mellin, G. W., and Katzenstein, M. (1962) The saga of thalidomide: neuropathy to embryopathy, with case reports of congenital abnormalities. *New Engl. J. Med.* **267**, 1184-1193.
53. McBride, W. G. (1961) Thalidomide and congenital abnormalities. *Lancet* **ii**, 1358.
54. Lenz, W. (1962) Thalidomide and congenital abnormalities. *Lancet* **i**, 45.
55. D'Amato, R. J., Loughnan, M. S., Flynn, E., and Folkman, J. (1994) Thalidomide is an inhibitor of angiogenesis. *Proc. Natl. Acad. Sci. USA* **91**, 4082-4085.
56. Kruse, F. E., Joussen, A. M., Rohrschneider, K., Becker, M. D., and Volcker, H. E. (1998) Thalidomide inhibits corneal angiogenesis induced by vascular endothelial growth factor. *Graefes Arch. Clin. Exp. Ophthalmol.* **236**, 461-466.
57. Gordon, G. B., Spielberg, S. P., Blake, D. A., and Balasubramanian, V. (1981) Thalidomide teratogenesis: evidence for a toxic arene oxide metabolite. *Proc. Natl. Acad. Sci. USA* **78**, 2545-2548.
58. Bauer, K. S., Dixon, S. C., and Figg, W. D. (1998) Inhibition of angiogenesis by thalidomide requires metabolic activation, which is species-dependent. *Biochem. Pharmacol.* **55**, 1827-1834.
59. Kenyon, B. M., Browne, F., D'Amato R. J. (1997) Effects of thalidomide and related metabolites in a mouse corneal model of neovascularization. *Exp. Eye. Res.* **64**, 971-978.
60. Fickentscher, K., Kirfel, A., Will, G., and Köhler, F. (1977) Stereochemical properties and teratogenic activity of some tetrahydrophthalimides. *Mol. Pharmacol.* **13**, 133-141.
61. Parkhie, M., and Webb, M. (1983) Embryotoxicity and teratogenicity of thalidomide in rats. *Teratology* **27**, 327-332.
62. Sheskin, J. (1965) Thalidomide in the treatment of lepra reactions. *Clin. Pharmacol. Ther.* **6**, 303-306.
63. Koch, H. P. (1985) Thalidomide and congeners as anti-inflammatory agents. *Prog. Med. Chem.* **22**, 165-242.
64. Vogelsang, G. B., et al. (1992) Thalidomide for the treatment of chronic graft-versus-host disease. *N. Engl. J. Med.* **326**, 1055-1058.

65. Jacobson, J. M., et al. (1997) Thalidomide for the treatment of oral aphthous ulcers in patients with human immunodeficiency virus infection. *N. Engl. J. Med.* **336**, 1487-1493.
66. Reyes-Terán, G., Sierra-Madero, J. G., Martínez del Cerro, V., Arroyo-Figueroa, H., Pasquetti, A., Calva, J. J., and Ruiz-Palacios, G. M. (1996) Effects of thalidomide on HIV-associated wasting syndrome: a randomized, double-blind, placebo-controlled clinical trial. *AIDS* **10**, 1501-1507.
67. Sampaio, E. P., Sarno, E. N., Galilly, R., Cohn, Z. A., and Kaplan, G. (1991) Thalidomide selectively inhibits tumor necrosis factor α production by stimulated human monocytes. *J. Exp. Med.* **173**, 699-703.
68. Sarno, E. N., Grau, G. E., Vieira, L. M. M., and Nery, A. C. (1991) Serum levels of TNF- α and IL-1 β during leprosy reactional states. *Clin. Exp. Immunol.* **84**, 103-108.
69. Corral, L. G., Muller, G. W., Moreira, A. L., Chen, Y., Wu, M., Stirling, D., and Kaplan, G. (1996) Selection of novel analogs of thalidomide with enhanced tumor necrosis factor α inhibitory activity. *Mol. Med.* **2**, 506-515.
70. Neubert, R., Nogueira, A. C., and Neubert, D. (1993) Thalidomide derivatives and the immune system. 1. Changes in the pattern of integrin receptors and other surface markers on T lymphocyte subpopulations of marmoset blood. *Arch. Toxicol.* **67**, 1-17.
71. Nogueira, A. C., Neubert, R., Helge, H., and Neubert, D. (1994) Thalidomide and the immune system: 3. Simultaneous up- and down-regulation of different integrin receptors on human white blood cells. *Life Sci.* **55**, 77-92.
72. Nogueira, A. C., Gräfe, M., and Neubert, R. (1995) Effect of thalidomide and some derivatives on the adhesion of lymphocytes to endothelial cells. *Naunyn-Schmeideberg's Arch. Pharmacol.* **351S**, R130.
73. Moreira, A. L., Sampaio, E., Zmuidzinas, A., Frindt, P., Smith, K. A., and Kaplan, G. (1993) Thalidomide exerts its inhibitory action on tumor necrosis factor α by enhancing mRNA degradation. *J. Exp. Med.* **177**, 1675-1680.
74. Lee, J. C., et al. (1994) A protein kinase involved in the regulation of inflammatory cytokine biosynthesis. *Nature* **372**, 739-742.
75. Pritchett, W., Hand, A., Shields, J., and Dunnington, D. (1995) Mechanism of action of bicyclic imidazoles defines a translational regulatory pathway for tumor necrosis factor alpha. *J. Inflamm.* **45**, 97-105.
76. Swantek, J. L., Cobb, M. H., and Geppert, T. D. (1997) Jun N-terminal kinase/stress-activated protein kinase (JNK/SAPK) is required for lipopolysaccharide stimulation of tumor necrosis factor alpha (TNF- α) translation: glucocorticoids inhibit TNF- α by blocking JNK/SAPK. *Mol. Cell. Biol.* **17**, 6274-6282.

Chapter 2

Identification of methionine aminopeptidase 2 as the common target for the angiogenesis inhibitors TNP-470 and ovalicin

Abstract

Inhibition of angiogenesis is emerging as a novel form of cancer therapy with numerous advantages over conventional cytotoxic drugs. The synthetic compound TNP-470, a derivative of the natural product fumagillin, was among the first anti-angiogenesis drugs to enter clinical trials. A close structural homolog, the fungal metabolite ovalicin, was originally identified as an immunosuppressive drug but has also been shown to inhibit angiogenesis. The drugs act by inhibiting endothelial cell proliferation, but the molecular basis for this activity is not known. We find that the two drugs bind to a common protein, methionine aminopeptidase type 2 (MetAP2). The drugs covalently inactivate the aminopeptidase activity of this enzyme, but do not affect the ability of the protein to inhibit the phosphorylation of eukaryotic initiation factor-2 α (eIF-2 α) by inhibitory kinases. Yeast deficient in MetAP1 were unable to grow in the presence of either drug, whereas the growth yeast deficient in MetAP2 was unaffected by either TNP-470 or ovalicin, indicating that the compounds inhibit the type 2 enzyme specifically. A significant correlation was found for a series of drug analogs between their activity as inhibitors of MetAP2 aminopeptidase activity and their ability to inhibit endothelial cell growth, which suggests that inhibition of MetAP2 mediates the anti-angiogenic activity of these drugs.

Introduction

Angiogenesis, the formation of new blood vessels from pre-existing ones, occurs extensively during embryonic development and postnatal growth in mammals (1). In the adult, however, the process is normally restricted to a few physiological circumstances, such as wound healing, corpus luteum formation, and regrowth of the endometrium during

the menstrual cycle (2,3). A number of pathological states, however, including diabetic retinopathy and arthritis, are angiogenesis-dependent (4). In particular, the growth of solid tumors is severely restricted without the induction of new blood vessels to supply nutrients and oxygen (4,5,6). Compounds which inhibit angiogenesis are therefore currently being explored as novel therapies for cancer. Angiogenesis inhibitors appear to lack the side effects and problems with drug resistance associated with conventional cytotoxic chemotherapy (7).

TNP-470 (also known as AGM-1470, Figure 2.1), a synthetic analog of the natural product fumagillin, was among the first small molecule angiogenesis inhibitors to enter clinical trials (8,9). The closely related compound ovalicin, which was originally identified as an immunosuppressive drug, has also been shown to inhibit angiogenesis (10,11). Though they are potent inhibitors of endothelial cell proliferation in vitro and in vivo, little is known about their mechanism of action. TNP-470 appears to arrest cells in the G₁ phase of the cell cycle, but has no effect on early growth factor induced events, such as tyrosine phosphorylation and induction of immediate early genes such as c-Myc and c-Fos (12,13,14). The molecular basis for cell cycle arrest mediated by these drugs is unknown. In order to elucidate these mechanisms, we sought to identify cellular binding proteins for TNP-470 and ovalicin. We report the covalent binding of both drugs to a bifunctional protein, methionine aminopeptidase 2 (MetAP2)/p67 inhibitor of eIF-2 α phosphorylation. TNP-470 and ovalicin are found to irreversibly inhibit the aminopeptidase activity of the protein, and do not appear to affect the homologous MetAP1 enzyme. Using a series of drug analogs, we find a strong correlation between inhibition of endothelial cell proliferation and inhibition of MetAP2, suggesting that this enzyme mediates the anti-angiogenic activity of these compounds.

Materials and Methods

Synthesis of fumagillin and ovalicin analogs. All compounds used except the photoaffinity label were synthesized in the Liu group by Zhuang Su. All analogs of

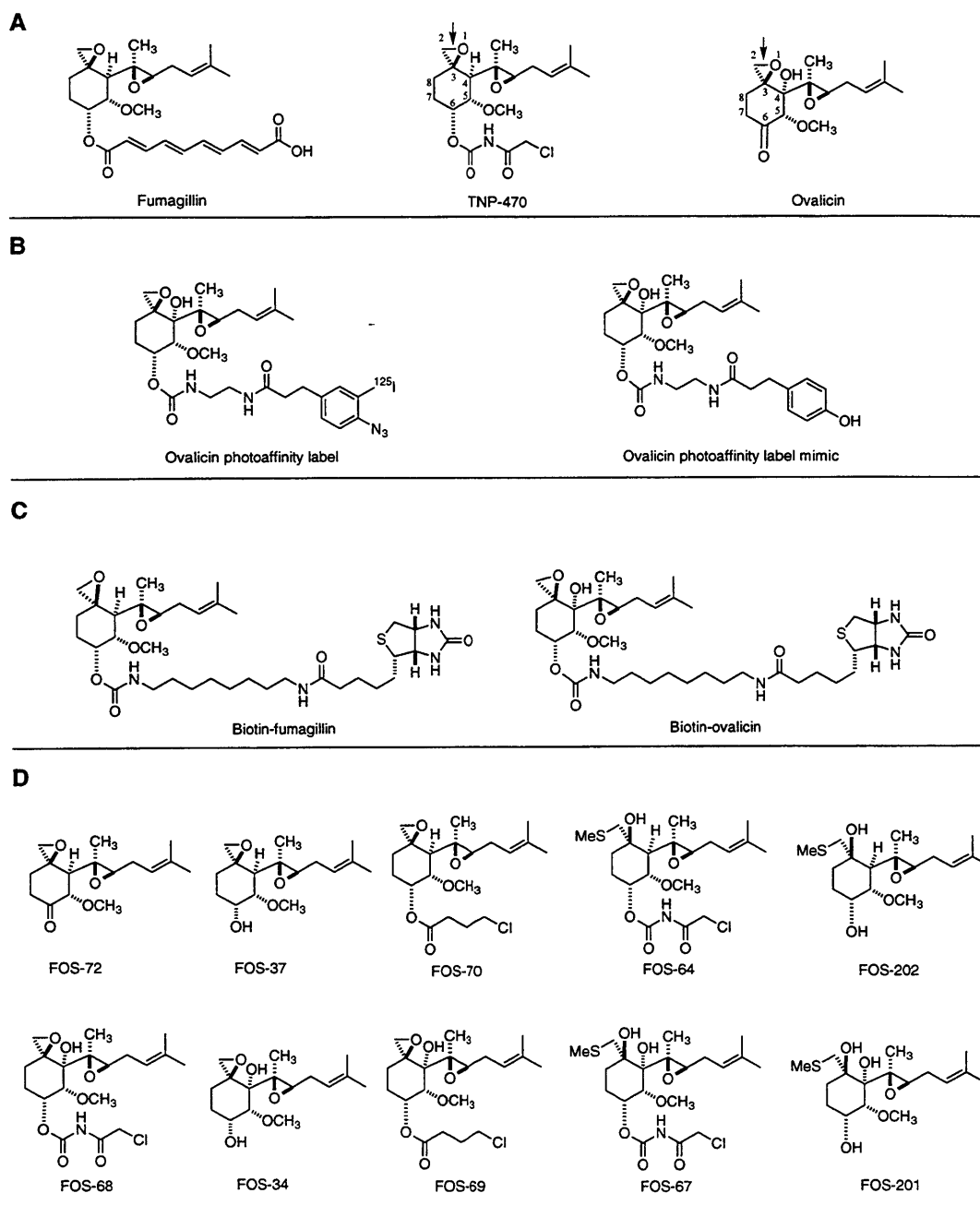


Figure 2.1. The chemical structures of fumagillin, ovalicin, ovalicin photoaffinity label, biotin conjugates and synthetic analogs. (A) Fumagillin, TNP-470, and ovalicin. The epoxides at C-2 and C-3 of TNP-470 and ovalicin are highlighted by arrows and numbering of the six-membered ring system is indicated. (B) Ovalicin photoaffinity label and its mimic. (C) Biotin-fumagillin and biotin-ovalicin conjugates. (D) Synthetic analogs of fumagillin and ovalicin.

fumagillin, including TNP-470, were synthesized according to literature procedures (15). All analogs of ovalicin and the biotin-fumagillin and biotin-ovalicin conjugates were synthesized using modified procedures. All compounds were characterized by ¹H NMR, IR and mass spectrometry.

Ovalicin photoaffinity label. Aminoethylcarbamoyldeoxyfumagillol (0.4 mg) was taken up in EtOH (50 μL) and mixed with [¹²⁵I] 3-(3-azido-4-iodophenyl)propionylsuccinimide (carrier-free, 25 μCi) in 5 μL EtOAc in a reaction vial (16). The vial was sealed and incubated in the dark for 1 hr. The reaction mixture was concentrated to dryness under a stream of Ar, suspended in neat EtOAc, and chromatographed on silica gel. The product eluted in 5% MeOH/EtOAc. Fractions containing product as judged by thin layer chromatography were pooled and the solvent removed under a stream of Ar. The product was suspended in neat MeOH and stored at -80°C in the dark.

Photoaffinity labeling. Labeling reactions (25 μl) included 4 mg/ml protein from cell or tissue extract, cold competitor drug or 0.2% EtOH carrier as indicated, and 40 μCi/ml ovalicin photolabel in labeling buffer (20 mM Tris•HCl, pH 7.5, 100 mM NaCl). Reaction mixtures were incubated on ice in the dark for 1 hr and then irradiated in a Stratalinker (Stratagene) at 254 nm (0.2 J/cm²) with samples 12 cm from the source lamps. Reactions were quenched by adding 1.5 μl β-mercaptoethanol (to 5% final concentration) followed by 7.5 μl 5 x SDS sample buffer (10% SDS, 0.5 M Tris•HCl, pH 6.8, 40% glycerol, 0.1 mg/ml bromophenol blue) and heated in a boiling water bath for 3 min. Samples were analyzed by 10% SDS/PAGE (see Chapter 3), followed by autoradiography.

BAEC (bovine aortic endothelial cell) proliferation assay. The assay was performed in the Liu lab by Eric Griffith. BAEC were trypsinized and plated into 96-well plates at a density of 2000 cells per well. After the cells adhered to the plate, compounds dissolved in ethanol (final concentration of 0.5%) were added to the cultures. Three days later, 25 μl of 2.5 mg/ml (3-[4,5-Dimethylthiazol-2-yl]-2,5-diphenyl tetrazolium bromide (MTT) solution was added to the cultures. After an additional 4 hr incubation, 100 μl of

10% SDS/0.01 N HCl solution was added to the culture. The absorbance at 600 nm was determined 12 hr later using a Titertek Multiscan Plus plate reader.

Affinity binding assay. Performed by Eric Griffith in the Liu lab. Mouse embryo extracts were prepared from 14.5 d.p.c. (days post conception) mouse embryos. Embryos were dissected and Dounce homogenized (30 strokes) in 4 ml/g lysis buffer (20 mM Tris•HCl, pH 7.1, 100 mM KCl, 0.2% Triton X-100, 2 µg/ml leupeptin, 2 µg/ml aprotinin, 2 µg/ml soybean trypsin inhibitor). Lysates were centrifuged at 10,000 x g for 20 min. The resulting supernatant was centrifuged at 50,000 x g for 30 min. The supernatant was either used immediately or frozen at -80 °C for storage. Extract (200 µl) was incubated for 30 min with 50 µM competitor or ethanol control at 4 °C. Following competition, the extract was incubated with the conjugate ligands (1 µM) for 1 hr at 4 °C. Immobilized streptavidin (40 µl of a 1:1 suspension in lysis buffer) was added and the mixture was incubated at 4°C for 1 hr. The beads were pelleted at 10,000 rpm in a microcentrifuge for 5 min and washed twice with 600 µl lysis buffer for 5 min. SDS sample buffer (40 µl) was added and the samples were boiled for 10 min. The mixture was loaded on a 12% SDS-PAGE gel and silver stained.

Identification of p67 by mass spectrometry. Purification of p67 and tryptic digestion was performed by Eric Griffith in the Liu lab as follows. The affinity binding experiment was scaled up by using 3 mL of mouse embryo extract (16 mg/mL) and increasing the amount of biotin-fumagillin, immobilized streptavidin and other reagents and solutions proportionally. The partially purified p67 was released from immobilized streptavidin by boiling in sample buffer for 10 min before loading onto a 10% SDS-polyacrylamide gel. After electrophoresis, the gel was silver stained to visualize p67. The 67-kD band was excised, reduced and alkylated with iodoacetamide, followed by digestion with trypsin and extraction as previously described (17).

Mass spectrometry was performed by Zuchun Wu in the laboratory of Klaus Biemann as follows. The extract of the tryptic peptide mixture was dried in a Speedvac and the residue was dissolved in 3.5 µl of 7% aqueous formic acid. About 0.5 µl of this

solution and 0.5 μ l of the standard (peptides corresponding to amino acids 4-10 and 18-39 of ACTH, 50-100 fmol each) were placed onto a thin film of α -cyano-4-hydroxycinnamic acid deposited on the sample plate of a PerSeptive Biosystems Voyager-Elite MALDI-TOF mass spectrometer and evaporated to dryness. Fig. 3B represents the spectrum obtained by summation of 256 N₂ laser pulses. The instrument was operated in the reflectron mode with delayed extraction (18) Under these conditions, the resolution is at least >4000, sufficient to resolve the isotopic multiplets with the mass accuracy being over 50 ppm.

The human MetAP2 sequence (Swiss-prot Accession No. P50579) was used to search the EST database. A total of 13 overlapping mouse clones were found (Accession numbers: AA175951, AA172540, AA023796, AA185067, AA175099, AA138570, L26708, AA204267, AA175131, AA212018, AA242695, AA408613 and D21545). They were assembled into single cDNA encoding the full length MetAP2.

Western blotting. Performed by Eric Griffith in the Liu laboratory. Recombinant human MetAP2 was expressed and purified as previously reported (19). Samples were transferred to nitrocellulose at 50V for 1 hr at 4°C. The nitrocellulose was treated overnight with blocking solution (5% BSA, 2% Nonfat milk, 0.02% NaN₃ in PBS). The membrane was incubated with rabbit anti-human MetAP2 polyclonal antibodies (1:500) for 1 hr at room temperature, followed by incubation with sheep anti-rabbit IgG-HRP. MetAP2 was visualized with the chemiluminescent ECL kit (Amersham) as per manufacturer's instructions.

Detection of biotin-fumagillin and biotin-ovalicin covalently associated with MetAP2. Performed by Eric Griffith in the Liu laboratory. Recombinant human MetAP2 (100 ng) was incubated in 40 μ l binding buffer (20 mM Tris•HCl, pH 7.1, 100 mM KCl, 0.2% Triton X-100) in the presence or absence of competitors for 1 hr followed by incubation with the biotin conjugates (1 μ M) at 4 °C for 2 hr. 40 μ l of 2 x SDS sample buffer was added, and the samples were boiled for 10 min. Following SDS-PAGE, the samples were transferred to nitrocellulose at 50V for 1 hr at 4 °C and blocked

overnight in blocking solution (5% BSA, 2% Nonfat milk, 0.02% NaN₃ in PBS). The membrane was incubated with rabbit anti-human MetAP2 antibodies (1:500) for 1 hr at room temperature, followed by incubation with sheep anti-rabbit IgG-HRP or incubated with streptavidin-HRP (1:1000) for 1 hr and visualized with the chemiluminescent ECL kit (Amersham), as per manufacturer's instructions.

MetAP enzymatic assay. Performed by Shaoping Chen in the laboratory of Yie-Hwa Chang at St. Louis University. Recombinant human MetAP2 was expressed and purified from insect cells as previously described (19). To determine the effect of ovalicin and TNP-470 as well as their derivatives on MetAP activity, various amounts of these inhibitors was added to buffer H (10 mM HEPES, pH 7.35, 100 mM KCl, 10% glycerol, and 0.1 M Co²⁺) containing 1 nM of purified human MetAP2, and incubated at 37 °C for 30 min. To start the enzymatic reaction, Met-Gly-Met-Met was added to a concentration of 1 mM to the reaction mixture. Released methionine was quantified at different time points (0, 2, 3 and 5 min) using the method of Zuo et al. (20).

Phosphorylation assay for eIF-2 α . Performed by Maryam Rolfie-Kolpin and Jane-Jane Chen of the MIT HST division and Eric Griffith in the Liu laboratory. Recombinant human MetAP2 was incubated with TNP-470 or ethanol carrier alone and dialyzed into 20 mM Tris•HCl, pH 7.8, 100 mM KCl. Modified or control MetAP2 (0.6 μ g) was incubated with purified eIF-2 (0.3 μ g) in 20 mM Tris•HCl, pH 7.8, 40 mM KCl, and 2 mM MgOAc₂ on ice for 1 hr, Recombinant HRI (0.25 ng) and [γ -³²P]ATP were then added to a final total volume of 20 μ l and the reaction mixture was further incubated at 37 °C for 10 min. The labeled eIF-2 α was analyzed by 10% SDS-PAGE followed by autoradiography. The phosphorylated bands were quantified by NIH Image 1.60 software.

Yeast growth assay. Performed by Shaoping Chen in the laboratory of Yie-Hwa Chang. Wild-type (YPH500 (MAT α ura3-52 lys2-801 ade2-101 trp1- Δ 63 his3- Δ 200), map1 null [XLP101 (map1::HIS3)], and map2 null [XLP201 (map2::URA3)] yeast cells were grown in YEPD at 30°C to an OD₆₀₀ of 1 and then plated out in parallel onto a YEPD plates

containing either no drug, 50 nM TNP-470, or 50 nM ovalicin. The plates were incubated at 30°C for four days.

Results

To identify proteins which bind to TNP-470 and ovalicin, we applied two approaches in parallel, photoaffinity labeling and affinity chromatography. Structure-activity data on fumagillin analogs indicated that modifications to the C-6 sidechain permitted retention of activity, while other modifications were not tolerated (15). Accordingly, probes were synthesized by affixing a radioactively tagged phenyl azide photocrosslinking moiety (16) to this site in ovalicin, or by tethering biotin to the corresponding site in either ovalicin or fumagillin (Figure 2.1). Each of the affinity probes retained significant, though reduced activity when assayed in a bovine aortic endothelial cell (BAEC) proliferation assay.

Incubation of BAEC extracts with the ovalicin photoaffinity label followed by irradiation resulted in the labeling of a series of proteins (Figure 2.2). Preincubation of the lysate with excess ovalicin prevented the labeling of a single protein band of approximately 67 kD, suggesting that this protein binds specifically to ovalicin, whereas the other labeled proteins interact non-specifically with the photoaffinity probe. Furthermore, labeling of the 67 kD protein could also be prevented by preincubation with TNP-470, indicating that the two drugs bind to a common protein.

To facilitate purification of the 67 kD protein, we required a more abundant source of protein than cultured cells. Given that extensive angiogenesis occurs in later developing embryos, we examined extracts of mouse embryos (14.5 days post conception) for the presence of the protein. Increased amounts of the protein could be detected by photoaffinity labeling in the mouse embryo extracts over BAEC extracts (Figure 2.2). Interestingly, treatment of mouse embryo extracts with the photoaffinity label without subsequent irradiation still resulted in efficient labeling of the 67 kD protein which could also be competed by ovalicin or TNP-470, indicating that the compounds are likely to bind to the protein covalently.

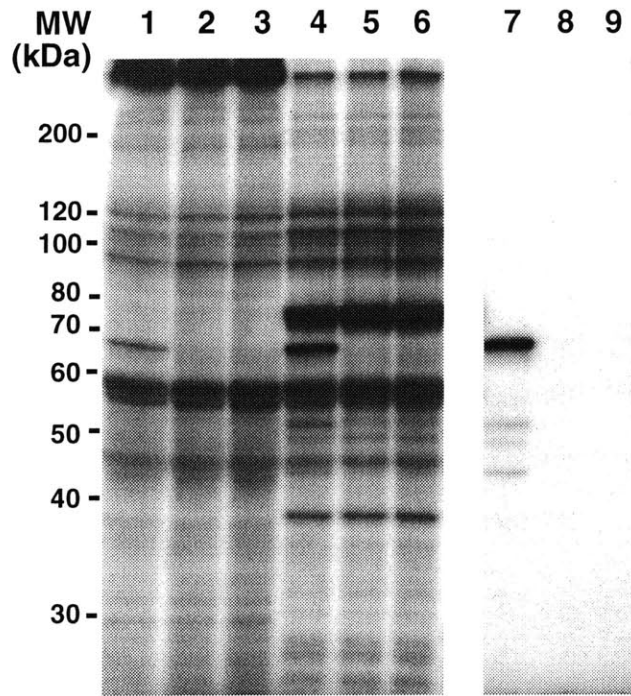


Figure 2.2. Photoaffinity labelling of BAEC and mouse embryo extracts reveals a common binding protein for both TNP-470 And ovalicin. Lanes 1-3, ovalicin photoaffinity labeling of BAEC extracts: 1, no competitor; 2, + 1 μM ovalicin; 3, + 1 μM TNP-470. Lanes 4-6, ovalicin photoaffinity labeling of mouse embryo extract: 4, no competitor; 5, + 1 μM ovalicin; 6, + 1 μM TNP-470. Lanes 7-9, mouse embryo extract incubated with ovalicin photoaffinity label without irradiation: 7, no competitor; 8, + 1 μM ovalicin; 9, + 1 μM TNP-470.

To purify the 67 kD protein, mouse embryo extracts were incubated with either the biotin-ovalicin or the biotin-fumagillin conjugate followed by isolation of the complexes on immobilized streptavidin. SDS-PAGE followed by silver staining of the isolated proteins revealed a bound 67 kD protein (Figure 2.3). Addition of excess ovalicin or TNP-470 with the biotin conjugates resulted in the disappearance of this band. To identify this protein, the affinity purification was performed on a larger scale and approximately 600 ng of the protein was isolated. The protein band was excised from the silver-stained gel and digested with trypsin. Tryptic peptides were extracted from the gel and subjected to matrix-assisted laser desorption/ionization-time of flight (MALDI-TOF) mass spectrometry. The resulting spectrum contained 17 tryptic peptide-derived peaks, which were used to search the EMBL protein database (Figure 2.4). 15 of the peaks corresponded to peptides predicted to be present in both rat and human MetAP2 (Figure 2.5). The peaks at m/z 2136.15 and 2122.11 are derived from the same peptide (residues 452-469) in which the carboxy-terminal cysteine residue (C468) has reacted partially with monomeric acrylamide. The sole peak that was unaccounted for, m/z 1228.68, may have resulted from an unidentified post-translational modification of MetAP2.

Rat MetAP2 has a calculated molecular mass of 53 kD, but has been shown to migrate at 67 kD on SDS-PAGE (21). Though no mouse homolog of MetAP2 has been cloned, a putative open reading frame (ORF) could be constructed from overlapping sequences in the expressed sequence tag (EST) database. The mouse ORF has 97% sequence identity at the amino acid level with rat MetAP2, which itself is 94% identical to the human protein (Figure 2.5). All 16 tryptic peptides identified by mass spectrometry matched the theoretical peptides from the mouse ORF. It is therefore likely that the isolated protein is the mouse homolog of MetAP2.

To confirm the identity of the isolated protein as MetAP2, we repeated the affinity purification using the biotin-drug conjugates and analyzed the proteins retained on immobilized streptavidin by Western blot using polyclonal antibodies against human MetAP2 (Figure 2.6). The bound proteins indeed reacted with the MetAP2 antibodies.

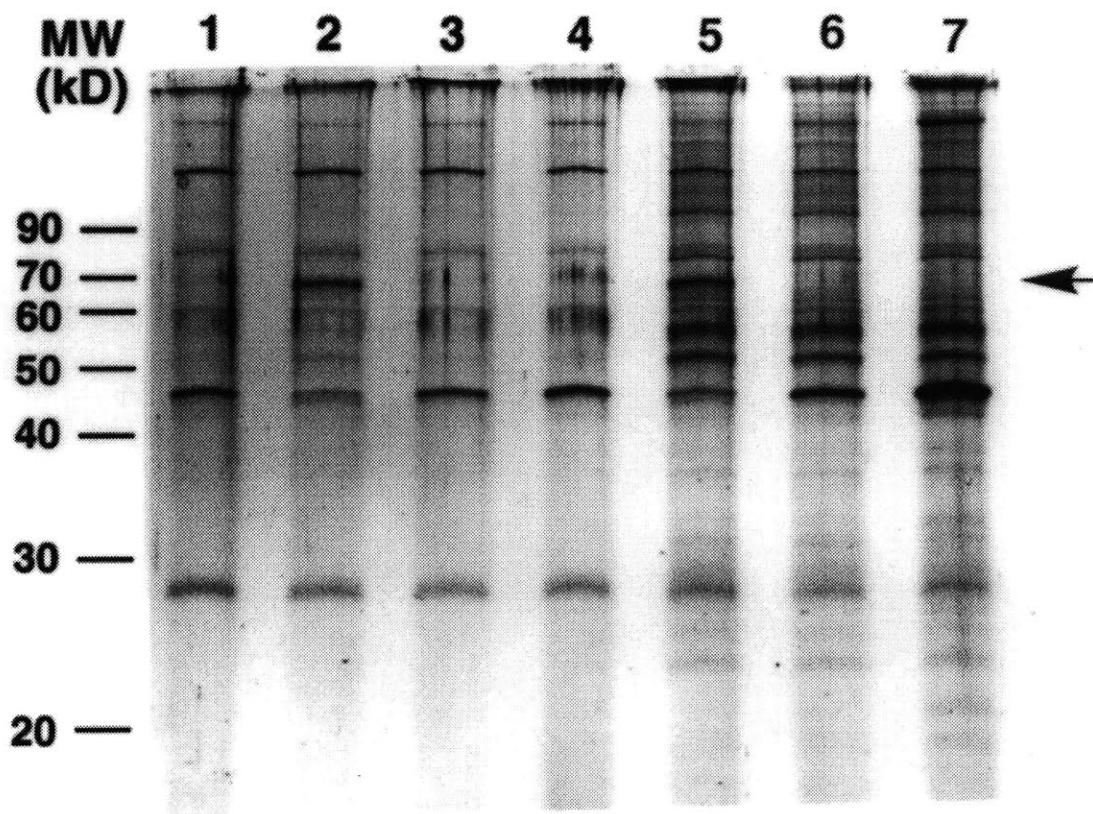


Figure 2.3. Isolation of p67 from mouse embryo extracts using biotin-fumagillin and biotin-ovalicin conjugates. Mouse embryo extracts were incubated with competing drugs for 30 min followed by incubation with biotin-fumagillin or biotin-ovalicin conjugate for 1 hr. Immobilized streptavidin was added for 1 hr. Samples were analyzed by SDS-PAGE followed by silver staining. Lane 1, immobilized streptavidin control; 2, biotin-fumagillin conjugate alone; 3, biotin-fumagillin conjugate with TNP-470 competition; 4, biotin-fumagillin conjugate with ovalicin competition; 5, biotin-ovalicin conjugate alone; 6, biotin-ovalicin conjugate with TNP-470 competition; 7, biotin-ovalicin conjugate with ovalicin competition.

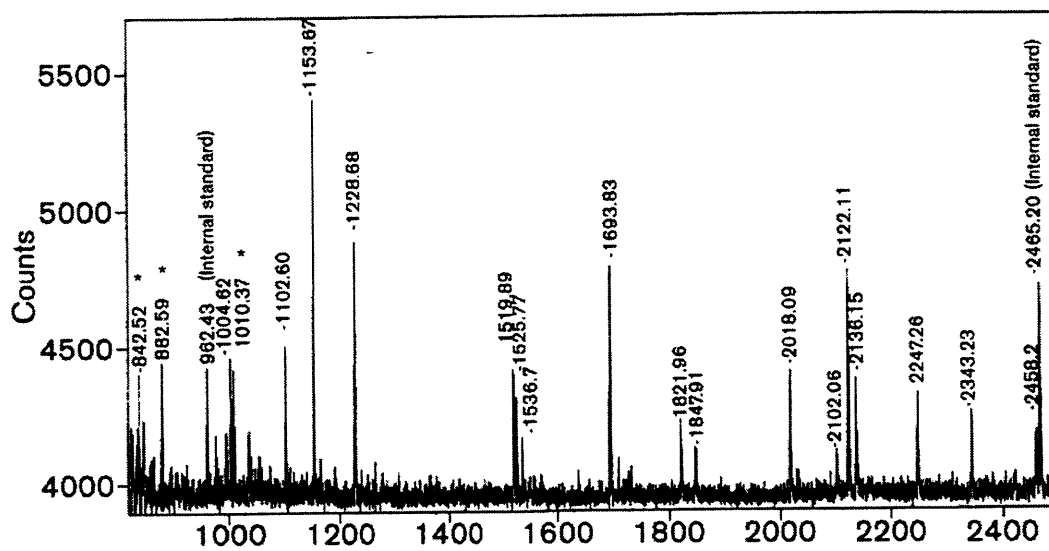


Figure 2.4. MALDI-TOF mass spectrum of tryptic digest of p67. The m/z values are monoisotopic. Peaks marked (*) are also present in the spectrum from a blank sample.

In addition, the isolated protein migrated at the same molecular weight on SDS-PAGE as did recombinant human MetAP2. These experiments establish the common 67 kD binding protein for TNP-470 and ovalicin to be MetAP2.

The initial photoaffinity labeling studies implicated the interaction between MetAP2 and ovalicin/TNP-470 to be covalent. This interaction is likely to be mediated by one or both of the epoxide groups common to the two drugs. To confirm the covalent nature of the complex, the biotin-fumagillin and biotin-ovalicin conjugates were incubated with recombinant human MetAP2 either alone or in the presence of excess competitor drug. The complexes were then boiled in SDS-containing buffer and subjected to SDS-PAGE followed by electrophoretic transfer to nitrocellulose membrane. Probing of the membrane with streptavidin conjugated to horseradish peroxidase allowed for covalent incorporation of biotin into proteins to be detected by enhanced chemiluminescence (Figure 2.7). SDS-stable incorporation of biotin could be detected only in MetAP2 incubated with biotin-fumagillin or biotin-ovalicin alone, and not with protein incubated with either free biotin or with the biotin-drug conjugates in the presence of either ovalicin or TNP-470. Maintenance of the drug-protein complexes under highly denaturing conditions as demonstrated with both the biotin-drug conjugates and photoaffinity label strongly suggests the interaction to be covalent.

MetAP2 is a bifunctional protein. It catalyzes the co-translational removal of N-terminal methionine residues from nascent proteins (22). The protein also inhibits the phosphorylation of eIF-2 α by inhibitory kinases, thus acting as a positive regulator of translation (21,23,24). To better understand how binding of TNP-470 and ovalicin to MetAP2 might lead to inhibition of cell growth, we examined the effect of the drugs on both activities in vitro. First, we tested whether the drugs could inhibit the aminopeptidase activity of MetAP2. Using a tetrapeptide substrate, we found that preincubation of purified recombinant human MetAP2 with either drug potently inhibited the aminopeptidase activity. The IC₅₀ values were estimated to be 1 nM for TNP-470 and 0.4 nM for ovalicin when tested against 1 nM MetAP2 (Table 2.1).

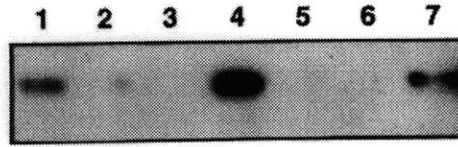


Figure 2.6. Western blot analysis confirms the identity of p67 as MetAP2. Samples were prepared as in Figure 2.3, transferred to nitrocellulose and incubated with rabbit anti-human MetAP2 polyclonal antibodies followed by incubation with anti-rabbit IgG-HRP. Lane 1, biotin-fumagillin conjugate alone; 2, biotin-fumagillin conjugate with TNP-470 competition; 3, biotin-fumagillin conjugate with ovalicin competition; 4, biotin-ovalicin conjugate alone; 5, biotin-ovalicin conjugate with TNP-470 competition; 6, biotin-ovalicin conjugate with ovalicin competition; 7, 10 μ g recombinant MetAP2.

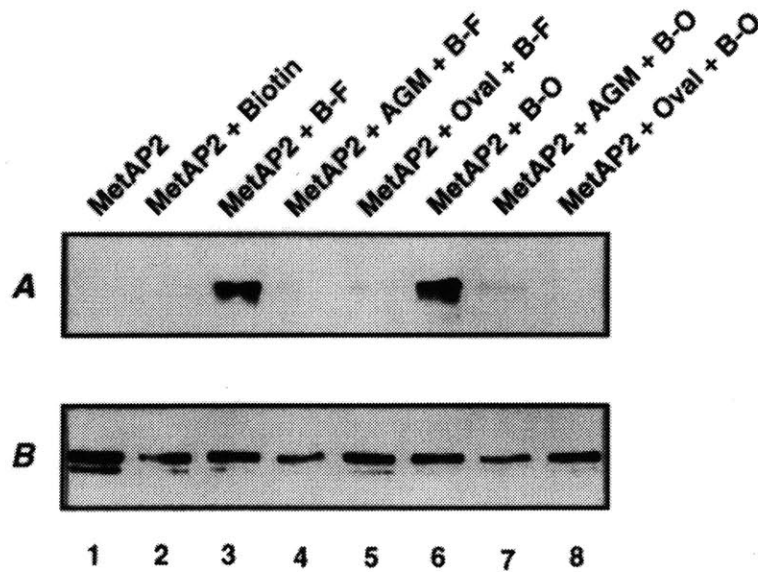


Figure 2.7. The biotin conjugates of fumagillin and ovalicin form stable adducts with MetAP2. Recombinant human MetAP2 was incubated with the biotin conjugates in the presence or absence of competitors. Samples were denatured, boiled in a SDS and β -mercaptoethanol-containing buffer, transferred to nitrocellulose. The biotin conjugates bound to the protein were detected using streptavidin-HRP (panel A), and MetAP2 was detected using anti-human MetAP2 followed by anti-rabbit IgG-HRP (panel B). Abbreviations: B-F, biotin-fumagillin; B-O, biotin-ovalicin; AGM, TNP-470; Oval, ovalicin.

To determine whether TNP-470 and ovalicin could potentially affect the ability of MetAP2 to regulate translation, we studied the effect of the drugs on the activity of MetAP2 towards inhibiting the phosphorylation of eIF-2 α by the heme-regulated inhibitor kinase (HRI). Our initial attempts to assess the effects of the drugs in this assay were complicated as the drugs appeared to stimulate both the autophosphorylation of HRI and its phosphorylation of eIF-2 α . We attribute this effect to non-specific modification of cysteine sidechains of HRI by the epoxide groups of both drugs, as a number of thiol-modifying reagents have been shown to stimulate HRI kinase activity (25). To circumvent this problem, we first incubated MetAP2 with TNP-470 and then subjected the drug-protein complexes to extensive dialysis to remove unreacted drug. When assayed for methionine aminopeptidase activity, this drug-protein complex was completely inactive, whereas a sample treated with carrier solvent alone and dialyzed in an identical manner retained full activity. The TNP-470-MetAP2 complex was then tested for its ability to inhibit eIF-2 α phosphorylation by HRI. We found that MetAP2 bound by TNP-470 is equally as effective as free MetAP2 at inhibiting the phosphorylation of eIF-2 α , while neither the free nor bound protein inhibited HRI autophosphorylation (Figure 2.8). This experiment appears to rule out the possibility that misregulation of translation underlies the inhibition of endothelial cell proliferation by TNP-470 and ovalicin.

Eukaryotes possess two homologous MetAPs, MetAP1 and MetAP2 (22,26). In the yeast *Saccharomyces cerevisiae*, deletion of the gene encoding either MetAP alone results in slow growth, while deletion of both MetAPs is lethal. Because we did not detect binding to MetAP1 by either photoaffinity labeling or by affinity chromatography, TNP-470 and ovalicin appear to specifically inhibit MetAP2. To further explore the specificity of the compounds for MetAP2 over MetAP1, we tested the compounds for their ability to inhibit the growth of various yeast strains. Both wild type yeast and yeast strains lacking either MetAP1 (*map1*) or MetAP2 (*map2*) were plated onto media containing either 50 nM TNP-470, 50 nM ovalicin, or no drug (Figure 2.9). Although

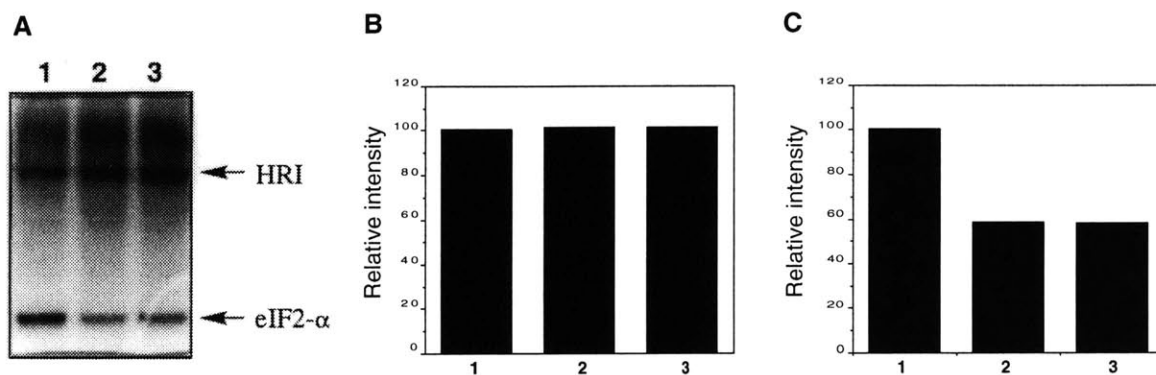


Figure 2.8. Drug binding does not alter the protective effect of MetAP2 on eIF-2 α phosphorylation. (A) Autoradiogram of eIF-2 α phosphorylation by HRI. Lane 1, eIF-2 α + HRI; 2, eIF-2 α + MetAP2 + HRI; 3, eIF-2 α + MetAP2-TNP-470 + HRI. (B) Quantitation of HRI autophosphorylation. (C) Quantitation of eIF-2 α phosphorylation.

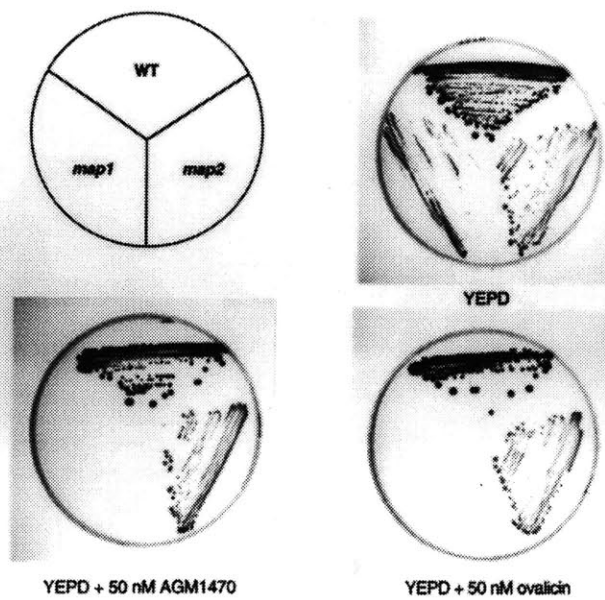


Figure 2.9. TNP-470 and ovalicin specifically inhibit MetAP2 in vivo in yeast. Wild type (WT), *map1*, and *map2* yeast strains were plated on the yeast growth medium YEPD, or YEPD containing either 50 nM TNP-470 or 50 nM ovalicin. The plates were incubated at 30°C for four days before being photographed.

wild type and *map2* mutant yeast were resistant to the drug, the growth of *map1* mutant yeast was completely inhibited under these conditions. These results indicate that MetAP2, but not MetAP1, is inhibited by the drugs in vivo.

As both TNP-470 and ovalicin inhibit the aminopeptidase activity of MetAP2 without affecting its ability to regulate translation, we suspected that inhibition of MetAP2 might mediate the effect of these drugs on cell proliferation. As an initial step towards testing this hypothesis, we examined the activity of a series of TNP-470 and ovalicin analogs for their abilities to inhibit MetAP2 aminopeptidase activity in vitro and to inhibit the growth of cultured BAECs (Table 2.1). A significant correlation ($P > 0.001$) was found between the potency of compounds in the inhibition of BAEC proliferation and the inhibition of MetAP2 activity (Figure 2.10). Importantly, no derivative was found which showed high potency in one assay but no activity in the other. This correlation provides support for the notion that inhibition of MetAP2 underlies the anti-angiogenic effects of TNP-470 and ovalicin.

Discussion

The covalent inactivation of MetAP2 by TNP-470 and ovalicin is the first demonstration of a cellular binding protein for this class of angiogenesis inhibitors. MetAP2 is a cobalt-dependent peptidase which catalyzes the co-translational removal of amino-terminal methionine residues from nascent polypeptides (22). All eukaryotes appear to possess two homologous methionine aminopeptidases, MetAP1 and MetAP2 (22,26). TNP-470 and ovalicin inhibit MetAP2 potently and specifically, as the growth of yeast possessing only MetAP1 is not inhibited by the drugs. Furthermore, the correlation among drug analogs between inhibition of MetAP2 in vitro and inhibition of cultured endothelial cell growth suggests that MetAP2 is the physiological target of these drugs.

MetAP2 is a bifunctional protein, which raises the question as to whether the growth inhibitory effects of TNP-470 and ovalicin are mediated by decreased protein synthesis, which would occur if the ability of the protein to prevent the phosphorylation

Table 2.1. Potency of Fumagillin and Ovalicin Analogs for Inhibition of BAEC Proliferation and MetAP2 Enzymatic Activity.

Compound	Proliferation IC ₅₀ (nM)	MetAP2 IC ₅₀ (nM)
TNP-470	0.037 ± 0.0024	1.0 ± 0.3
Ovalicin	0.018 ± 0.0059	0.4 ± 0.2
FOS-72	0.013 ± 0.0015	6 ± 2
FOS-68	0.46 ± 0.26	2.0 ± 0.8
FOS-69	0.31 ± 0.066	0.10 ± 0.03
FOS-70	0.12 ± 0.01	3.5 ± 1.8
FOS-37	9.5 ± 4.6	8 ± 2
FOS-34	2.2 ± 1.4	4 ± 1
FOS-64	110 ± 18	3,000 ± 1,000
FOS-67	40 ± 4	400 ± 200
FOS-201	56 ± 34	45 ± 12
FOS-202	2,800 ± 2,300	5,000 ± 2,000

IC₅₀s were calculated as the average of at least three experiments fit using Deltagraph Pro 3.5 software.

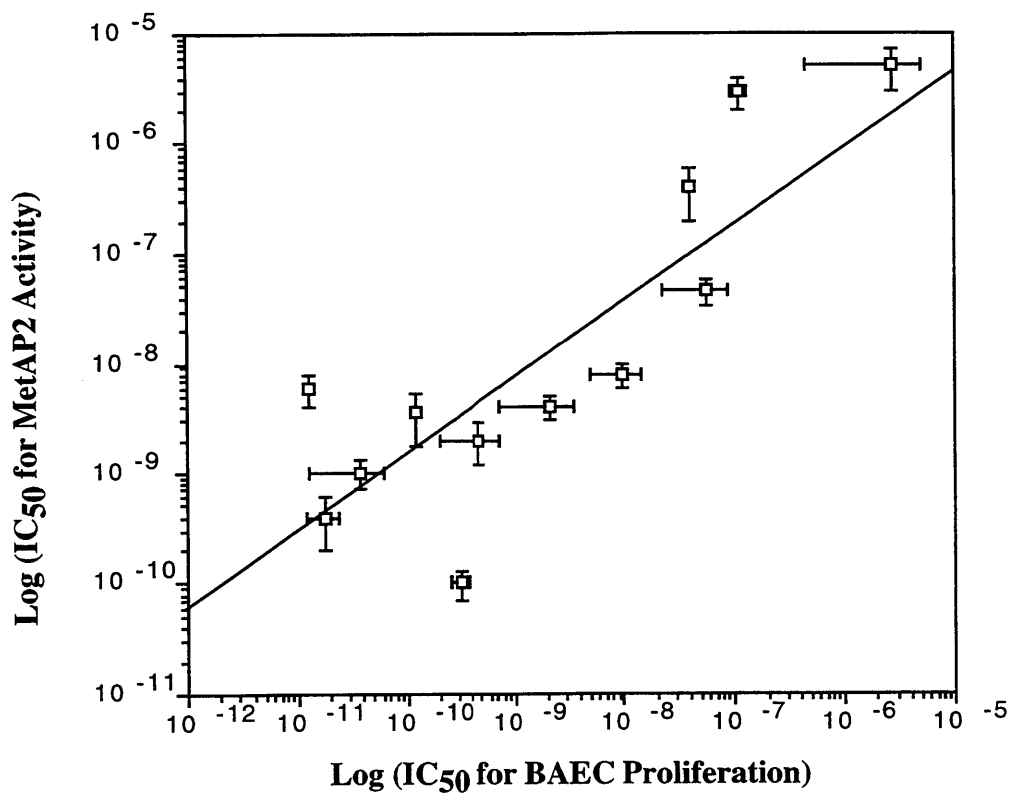


Figure 2.10. Pharmacological correlation between inhibition of the methionine aminopeptidase activity of MetAP2 and inhibition of BAEC proliferation using fumagillin and ovalicin analogs. Values were taken from Table 2.1.

of eIF-2 α were compromised by drug binding (23,24). Previous studies with ovalicin have indicated a decrease in protein synthesis in drug-treated cells, but that this decrease occurs subsequent to decreases in DNA synthesis, suggesting that it is a consequence and not a cause of decreased proliferation (27). In addition, TNP-470 was reported to have no overall effect on protein synthesis (12). These reports are consistent with our observation that the in vitro phosphorylation of eIF-2 α is not effected by the drugs.

TNP-470 possesses three potentially reactive groups, a chloroacetyl moiety and two epoxides, any of which might mediate the covalent interaction with MetAP2. Since the covalent interaction was shown using derivatives with either a biotin moiety or radioactive label at the C6 position, the chloroacetyl group appears to be dispensable for covalent binding. The fact that ovalicin and other compounds bearing a keto, hydroxyl, or chlorobutoyl group at the C6 position can be highly potent, as inhibitors of both MetAP2 and endothelial cell proliferation argues that the chloroacetyl group is dispensable for activity as well. In contrast, compounds in which the spiro epoxide group (indicated by an arrow in Figure 2.1A) has been opened with thiomethane are much less potent than their unmodified derivatives in both assays. This suggests that an intact spiro epoxide is required for high activity, perhaps because it mediates the covalent interaction between the drugs and MetAP2. Studies subsequent to the work described in this chapter have confirmed this prediction. The use of modified biotin-fumagillin conjugates in which the ring epoxide, the sidechain epoxide, or both were converted to alkenes were tested in the covalent drug binding assay depicted in Figure 2.7 (28). Only analogs with an intact spiro epoxide formed specific covalent adducts with MetAP2. In addition, the recently solved X-ray crystal structure of MetAP2 bound to fumagillin indicates that formation of the covalent adduct involves opening of the ring epoxide (29). The structure has also been solved with bound TNP-470, and in this case the protein also forms a covalent adduct via the ring epoxide, with the chloroacetyl group remaining unmodified (J. Clardy, personal communication). Together these results confirm the

importance of the ring epoxide for the potent and covalent inactivation of MetAP2 by TNP-470 and ovalicin.

The selectivity of this class of drugs for MetAP2 over MetAP1 is interesting given the structural similarity between the two classes of enzyme, particularly in the active site where drug binding occurs (29,30). Fumagillin in fact has been found to form an adduct with MetAP from *E. coli*, which is most closely related to the MetAP1 enzymes of eukaryotes, though comparatively high concentrations of drug and long incubation times are required (31). Characterization of this adduct revealed that fumagillin forms a covalent bond with H79 of *E. coli* MetAP, a residue which is conserved among both MetAP families. Indeed, a fluorescent fumagillin derivative was found to form a covalent adduct with the corresponding residue in human MetAP2, H231 (28). Furthermore, the crystal structure of the MetAP2-fumagillin adduct indicates that a covalent bond forms by the nucleophilic opening of the ring epoxide by H231 (29). Site-directed mutagenesis has confirmed that this residue is essential for both covalent drug binding and catalysis (28). The selectivity of the drugs for MetAP2 is therefore not due to the absence of a suitable reactive group in MetAP1. Modeling of the active site residues of MetAP2 bound to fumagillin superimposed with free *E. coli* MetAP (whose crystal structure has also been solved) provides an explanation for the observed specificity (29,30). Accommodation of fumagillin into the *E. coli* MetAP binding pocket results in a configuration in which His-79 (equivalent to human MetAP2 His-231) is too far away from the ring epoxide to allow covalent bond formation. Theoretical movement of fumagillin to enable covalent adduct formation results in steric clashes between functional groups of the drug and protein side chains, and also would break favorable interactions, such as the one between the ring-opened epoxide oxygen and one of the cobalt atoms. Covalent reaction of fumagillin, TNP-470, and ovalicin with the MetAP1-type enzymes would therefore be expected to occur much less efficiently than with MetAP2.

Methionine aminopeptidase activity appears to be essential for cell growth. Prokaryotes are inviable if their single MetAP is deleted (32). In yeast, deletion of the gene encoding either of the two MetAPs alone results in slow growth, whereas yeast lacking both genes are inviable (19). The majority of cytosolic proteins appear to undergo removal of their amino-terminal methionine, and such processing is essential for the activity of certain proteins. Amino-terminal protein myristoylation requires prior removal of the initiator methionine and is important for the function of proteins such as the Src-family tyrosine kinases, ADP ribosylation factor, and endothelial nitric oxide synthase (33,34). The amino-terminal residue of a protein can also dramatically effect its rate of degradation according to the N-end rule, so that loss of MetAP activity could lead to aberrant levels of certain proteins (35). Failure to undergo amino-terminal processing could also affect the ability of a protein to fold or function properly.

While possession of a single active MetAP is likely to be a general requirement for cell growth in humans, different cell types and cell lines exhibit varied sensitivity to TNP-470, suggesting differences in their degree of dependence specifically on MetAP2 (8). Primary endothelial cells cannot grow in low concentrations of TNP-470, for example, while transformed endothelial cell lines tend to be resistant to the drug (36). Similarly, mitogen-stimulated primary T cells are sensitive to ovalicin, whereas the transformed Jurkat human T cell line is resistant (27, B. E. Turk and J. O. Liu, unpublished observations). Drug resistance does not always accompany transformation, however, as a variety of transformed cells sensitive to TNP-470 have been described, including the mouse T cell lymphoma S49.1 (27). In at least one instance, a transformed cell line has been reported to be fumagillin-sensitive, while a non-transformed revertant cell line was resistant (37). In addition, some primary cell types, such as mouse embryonic fibroblasts, are not sensitive to TNP-470 (E. C. Griffith and J. O. Liu, unpublished observations).

Sensitivity to TNP-470 and ovalicin might occur by one of several mechanisms. As MetAP activity appears to be essential for cell growth, sensitive cell types may

exclusively express MetAP2. MetAP activity would thus be eliminated by drug treatment. In such cases the acquisition of resistance by transformation or otherwise would be associated with increased MetAP1 expression. Alternatively, MetAP1 and MetAP2 may process different substrates in cells. Initiator methionine processing appears to depend principally on the identity of the second translated residue, with efficient cleavage generally occurring when it is relatively small and uncharged, though exceptions to this rule have been found (38,39,40,41). The substrate specificities of yeast MetAP1 and MetAP2, porcine MetAP2, and human MetAP2 have been examined in vitro using peptide substrates, though a systematic comparison using identical substrates has not been performed (19,26,42,43). Each enzyme appears to have substrate specificity which parallels the general rules for methionine removal in cells, though the yeast MetAP1 cleaves peptides in which the second residue is valine or threonine somewhat less efficiently than those in which the second residue is glycine. How this in vitro behavior might correspond to in vivo specificity is not clear. The slow growth phenotype of yeast lacking MetAP1 indicates that these cells are compromised in their ability to process substrates essential for optimal growth. This could be due either to a decrease in overall nonspecific MetAP activity or due to a partial or complete defect in the ability to process MetAP1 specific substrates. Overexpression of MetAP2 reverses the growth defect in MetAP1 deficient cells, whereas low level expression of MetAP2 cannot, suggesting that while MetAP2 can process MetAP1 substrates important for optimal growth, it probably does so less efficiently than MetAP1 (19,44). These observations point to the existence of substrates at least partially specific to either MetAP whose processing is essential for optimal growth in yeast. Direct evidence for the existence of specific substrates, however, is lacking. The ability of yeast deficient in either MetAP1 or MetAP2 alone to process various substrate proteins, for example, has not been examined.

The existence of substrates efficiently processed only in the presence normal levels of MetAP2 activity in mammalian cells is therefore plausible. Under this

assumption, there are several ways in which a mammalian cell may be sensitive to TNP-470 and ovalicin. One way is for there to be a specific MetAP2 substrate essential for cell growth whose activity or stability is dependent on removal of its amino-terminal methionine. In this scenario, the acquisition of resistance to the drugs would reflect a loss in the requirement for this protein for cell growth. Loss of dependence on particular growth promoting pathways commonly occurs as a consequence of transformation, which might explain the association sometimes observed between transformation and drug resistance. Alternatively, an inhibitor of cell growth could be stabilized or activated by aberrant amino-terminal processing as a consequence of decreased MetAP2 activity. Loss of such an inhibitor could contribute to both transformation and drug resistance. The identification of such target substrates will further elucidate the mechanism of action of TNP-470 and ovalicin, and may reveal novel proteins involved in the regulation of cell growth.

References for Chapter 2

1. Risau, W. (1997) Mechanisms of angiogenesis. *Nature* **386**, 671-674.
2. D'Amore, P. A., and Thompson, R. W. (1987) Mechanisms of angiogenesis. *Ann. Rev. Physiol.* **49**, 453-464.
3. Bouck, N., Stellmach, V., and Hsu, S. C. (1996) How tumors become angiogenic. *Adv. Cancer Res.* **69**, 135-174.
4. Folkman, J. (1995) Angiogenesis in cancer, vascular, rheumatoid, and other disease. *Nat. Med.* **1**, 27-31.
5. Gimbrone, M. A., Leapman, S. B., Cotran, R. S., and Folkman, J. (1972) Tumor dormancy in vivo by prevention of neovascularization. *J. Exp. Med.* **136**, 261-276.
6. Hanahan, D. and Folkman, J. (1996) Patterns and emerging mechanisms of the angiogenic switch during tumorigenesis. *Cell* **86**, 353-364.
7. Folkman, J. (1995) Clinical applications of research on angiogenesis. *New Engl. J. Med.* **333**, 1757-1763.
8. Ingber, D., Fujita, T., Kishimoto, S., Sudo, K., Kanamaru, T., Brem, H., and Folkman, J. (1990) Synthetic analogs of fumagillin that inhibit angiogenesis and suppress tumour growth. *Nature* **348**, 555-557.
9. Castronovo, V., and Belotti, D. (1996) TNP-470 (AGM-1470): Mechanisms of action and early clinical development. *Eur. J. Cancer* **32A**, 2520-2527.
10. Lazary, S., and Stähelin, H. (1969) Immunosuppressive effect of a new antibiotic: ovalicin. *Antibiot. Chemother.* **15**, 177-181.
11. Corey, E. J., Guzman-Perez, A., and Noe, M. C. (1994) Enantioselective synthesis of (-)-ovalicin, a potent inhibitor of angiogenesis, using substrate-enhanced asymmetric hydroxylation. *J. Am. Chem. Soc.* **116**, 12109-12110.
12. Kusaka, M., Sudo, K., Matsutani, E., Kozai, Y., Marui, S., Fujita, T., Ingber, D., and Folkman, J. (1994) Cytostatic inhibition of endothelial cell growth by the angiogenesis inhibitor TNP-470 (AGM-1470). *Br. J. Cancer* **69**, 212-216.
13. Abe, J., Zhou, W., Takua, N., Taguchi, J., Kurokawa, K., Kumada, M., and Takuwa, Y. (1994) A fumagillin derivative angiogenesis inhibitor, AGM-1470, inhibits activation of cyclin-dependent kinases and phosphorylation of retinoblastoma gene product but not protein tyrosyl phosphorylation or protooncogene expression in vascular endothelial cells. *Cancer Res.* **54**, 3407-3412.
14. Hori, A., Ikema, S., and Sudo, K. (1994) Suppression of cyclin D1 mRNA expression by the angiogenesis inhibitor TNP-470 (AGM-1470) in vascular endothelial cells. *Biochem. Biophys. Res. Commun.* **204**, 1067-1073.
15. Marui, S., Itoh, F., Kozai, Y., Sudo, K., and Kishimoto, S. (1992) Chemical modification of fumagillin. I. 6-O-Acyl, 6-O-sulfonyl, 6-O-alkyl and 6-O-(N-substituted carbamoyl)fumagillols. *Chem. Pharm. Bull.* **40**, 96-101.
16. Lowndes, J. M., Hokin-Neaverson, M., and Ruoho, A. E. (1988) N-(3-(p-azido-m-[¹²⁵I]iodophenyl)propionyl)-succinimide— a heterobifunctional reagent for the synthesis of radioactive photoaffinity ligands: synthesis of a carrier-free ¹²⁵I-labeled cardiac glycoside photoaffinity label. *Anal. Biochem.* **168**, 39-47.

17. Shevchenko, A., Wilm, M., Vorm, O., and Mann, M. (1996) Mass spectrometric sequencing of proteins from silver-stained polyacrylamide. *Anal. Chem.* **68**, 850-858.
18. Vestal, M. L., Juhase, P., & Martin, S. A. (1995) Delayed extraction matrix-assisted laser desorption time-of-flight mass spectrometry. *Rapid Commun. Mass Spectrom.* **9**, 1044-1050.
19. Li, X. and Chang, Y.-H. (1996). Evidence that the human homologue of a rat initiation factor-2 associated protein (p67) is a methionine aminopeptidase. *Biochem. Biophys. Res. Commun.* **227**, 152-159.
20. Zuo, S., Guo, Q., Ling, C., and Chang, Y.-H. (1995). Evidence that two zinc fingers in the methionine aminopeptidase from *Saccharomyces cerevisiae* are important for normal growth. *Mol. Gen. Genetics* **246**, 247-253.
21. Wu, S., Gupta, S., Chatterjee, N., Hileman, R. E., Kinzy, T. G., Denslow, N. D., Merrick, W. C., Chakrabarti, D., Osterman, J. C., and Gupta, N. K. (1993). Cloning and characterization of complementary DNA encoding the eukaryotic initiation factor-2 associated 67-kDa protein (p67). *J. Biol. Chem.* **268**, 10796-10801.
22. Arfin, S. M., Kendall, R. L., Hall, L., Weaver, L. H., Stewart, A. E., Matthews, B. W., and Bradshaw, R. A. (1995). Eukaryotic methionyl aminopeptidases: two classes of cobalt-dependent enzymes. *Proc. Natl. Acad. Sci. USA* **92**, 7714-7718.
23. Datta, B., Chakrabarti, D., Roy, A. L., and Gupta, N. K. (1988). Roles of a 67-kDa polypeptide in reversal of protein synthesis inhibition in heme-deficient reticulocyte lysate. *Proc. Natl. Acad. Sci. USA* **85**, 3324-3328.
24. Ray, M. K., Datta, B., Chakraborty, A., Chattopadhyay, A., Meza-Keuthen, S., and Gupta, N. K. (1992). The eukaryotic initiation factor 2-associated 67-kDa polypeptide (p67) plays a critical role in regulation of protein synthesis initiation in animal cells. *Proc. Natl. Acad. Sci. USA* **89**, 539-543.
25. Gross, M. and Rabinovitz, M. (1972). Control of globin synthesis by hemin: factors influencing formation of an inhibitor of globin chain initiation in reticulocyte lysates. *Biochim. Biophys. Acta* **287**, 340-352.
26. Li, X. and Chang, Y.-H. (1995). Amino-terminal protein processing in *Saccharomyces cerevisiae* is an essential function that requires two distinct methionine aminopeptidases. *Proc. Natl. Acad. Sci. USA* **92**, 12357-12361.
27. Hartmann, G. R., Richter, H., Weiner, E. M., and Zimmermann, W. (1978) On the mechanism of action of the cytostatic drug anguidine and of the immunosuppressive agent ovalicin, two sesquiterpenes from fungi. *Planta Med.* **34**, 231-252.
28. Griffith, E. C., Su, Z., Niwayama, S., Ramsay, C. A., Chang, Y.-H., and Liu, J. O. (1998) Molecular recognition of angiogenesis inhibitors fumagillin and ovalicin by methionine aminopeptidase 2. *Proc. Natl. Acad. Sci. USA* **95**, 15183-15188.
29. Liu, S., Widom, J., Kemp, C. W., Crews, C. M., and Clardy, J. (1998) Structure of human methionine aminopeptidase-2 complexed with fumagillin. *Science* **282**, 1324-1327.

30. Roderick, S. L., and Matthews, B. W. (1993) Structure of the cobalt-dependent methionine aminopeptidase from *Escherichia coli*, a new type of proteolytic enzyme. *Biochemistry* **32**, 3907-3912.
31. Lowther, W. T., McMillen, D. A., Orville, A. M., and Matthews, B. W. (1998) The anti-angiogenic agent fumagillin covalently modifies a conserved active-site histidine in the *Escherichia coli* methionine aminopeptidase. *Proc. Natl. Acad. Sci. USA* **95**, 12153-12157.
32. Chang, S. Y., McGary, E. C., and Chang, S. (1989). Methionine aminopeptidase gene of *Escherichia coli* is essential for cell growth. *J. Bacteriol.* **171**, 4071-4072.
33. Gordon, J. I., Duronio, R. J., Rudnick, D. A., Adams, S. P., and Gokel, G. W. (1991) Protein N-myristoylation. *J. Biol. Chem.* **266**, 8647-8650.
34. Nathan, C. and Xie, Q. (1994) Nitric oxide synthases: roles, tolls, and controls. *Cell* **78**, 915-918.
35. Varshavsky, A. (1996) The N-end rule: functions, mysteries, uses. *Proc. Natl. Acad. Sci. USA* **93**, 12142-12149.
36. Antoine, N., Greimers, R., De Roanne, C., Kusaka, M., Heinen, E., Simar, L. J., & Castronovo, V. (1994) AGM-1470, a potent angiogenesis inhibitor, prevents the entry of normal but not transformed endothelial cells into the G₁ phase of the cell cycle. *Cancer Res.* **54**, 2073-2076.
37. Jenkins, D. C., Stables, J. N., Wilkinson, J., Topley, P., Holmes, L. S., Linstead, D. J., and Rapson, E. B. (1993) A novel cell-based assay for the evaluation of anti-*ras* compounds. *Br. J. Cancer* **68**, 856-861.
38. Huang, S., et al. (1987) Specificity of cotranslational amino-terminal processing of proteins in yeast. *Biochemistry* **26**, 8242-8246.
39. Moerschell, R. P., Hosokawa, Y., Tsunasawa, S., and Sherman, F. (1990) The specificities of yeast methionine aminopeptidase and acetylation of amino-terminal methionine in vivo. *J. Biol. Chem.* **265**, 19638-19643.
40. Flinta, C., Persson, B., Jörnvall, H., and von Heijne, G. (1986) Sequence determinants of cytosolic N-terminal protein processing. *Eur. J. Biochem.* **154**, 193-196.
41. Boissel, J.-P., Kasper, T. J., and Bunn, H. F. (1988) Cotranslational amino-terminal processing of cytosolic proteins: cell-free expression of site directed mutants of human hemoglobin. *J. Biol. Chem.* **263**, 8443-8449.
42. Chang, Y.-H., Teichert, U., and Smith, J. A. (1990) Purification and characterization of a methionine aminopeptidase from *Saccharomyces cerevisiae*. *J. Biol. Chem.* **265**, 19892-19897.
43. Kendall, R. L., and Bradshaw, R. A. (1992) Isolation and characterization of the methionine aminopeptidase from porcine liver responsible for the co-translational processing of proteins. *J. Biol. Chem.* **267**, 20667-20673.
44. Klinkenberg, M., Ling, C., and Chang, Y.-H. (1997) A dominant negative mutation in *Saccharomyces cerevisiae* methionine aminopeptidase-1 affects catalysis and interferes with the function of methionine aminopeptidase-2. *Arch. Biochem. Biophys.* **347**, 193-200.

Chapter 3

Inhibition of MetAP2 by TNP-470 and ovalicin in endothelial cells

Abstract

The angiogenesis inhibitors TNP-470 and ovalicin specifically inhibit methionine aminopeptidase 2 (MetAP2) in vitro. Inhibition of MetAP2 and changes in initiator methionine removal in drug-treated endothelial cells has not been demonstrated. Both drug-sensitive and insensitive endothelial cell lines express MetAP1 and MetAP2, indicating that drug sensitivity in mammalian cells is not simply due to the absence of compensating MetAP activity. With a single exception, detectable protein N-myristoylation is unaffected in sensitive endothelial cells treated with TNP-470, indicating that for proteins destined to be myristoylated, MetAP1 activity can generally compensate when MetAP2 is inactive. Analysis by two-dimensional gel electrophoresis of total protein extracts from cells pulse-labeled with [³⁵S]-methionine following TNP-470 treatment revealed changes in the migration of several newly synthesized proteins. Two of these proteins were identified by mass spectrometry to be glyceraldehyde-3-phosphate dehydrogenase (GAPDH) and cyclophilin A. Purification and amino-terminal sequencing of GAPDH from TNP-470-treated cells revealed partial retention of its initiator methionine compared to untreated cells. Amino-terminal processing of glutathione S-transferase- π (GST- π) was unaffected by TNP-470 treatment, indicating that methionine removal from some, but not all proteins is affected by inactivation of MetAP2. These studies indicate the possibility that amino-terminal processing defects of specific proteins resulting from TNP-470 treatment may result in decreased cell growth.

Introduction

The majority of proteins produced by both prokaryotes and eukaryotes bear modifications to their amino-termini (1,2). Among the most common of such

modifications for cytosolic proteins is removal of the initiator methionine residue. In prokaryotes, protein synthesis is initiated with N-formyl methionine (3). Removal of the formyl group occurs co-translationally on a subset of proteins and is a requirement for the subsequent co- or post-translational cleavage of the N-terminal methionine residue. Methionine removal is catalyzed by a single cobalt-dependent enzyme, methionine aminopeptidase (MetAP), which is essential for cell growth (4). In eukaryotes, where translation begins with free methionine, initiator methionine removal generally occurs co-translationally, when the nascent polypeptide chain is between 20 to 40 residues long (5). All eukaryotes appear to possess two MetAPs, a type 1 enzyme (MetAP1) and a type 2 enzyme (MetAP2) (6,7). Though conventionally regarded as cobalt-dependent, MetAP1 from yeast is in fact optimally activated by zinc under physiological glutathione concentrations, suggesting that MetAPs in general utilize zinc *in vivo* (8). Both enzymes bear a carboxy terminal catalytic domain homologous to prokaryotic MetAPs, including five absolutely conserved residues involved in metal coordination (Figure 3.1). MetAP1 and MetAP2 are distinguishable by having highest sequence homology to the corresponding prokaryotic MetAPs of eubacteria and archaeobacteria, respectively. In addition, the two enzymes possess unique N-terminal domains not present in their prokaryotic counterparts. In MetAP1, this domain contains two zinc finger motifs, while the amino-terminal domain in MetAP2 contains two polybasic stretches and one polyacidic stretch (6,7,9). The functions of these amino-terminal domains are not known, though they appear to be essential for proper activity as a yeast MetAP1 mutant lacking the amino-terminal zinc finger domains, while catalytically active *in vitro*, cannot function *in vivo* (10). These amino-terminal domains are thought to be involved in mediating protein-protein or protein-nucleic acid interactions which could target the MetAPs to their site of action on the ribosome.

Individual deletion of the gene encoding either MetAP in *S. cerevisiae* results in viable yeast with a slow growth phenotype, while yeast in which both genes have been removed are inviable, suggesting that methionine aminopeptidase activity is necessary for

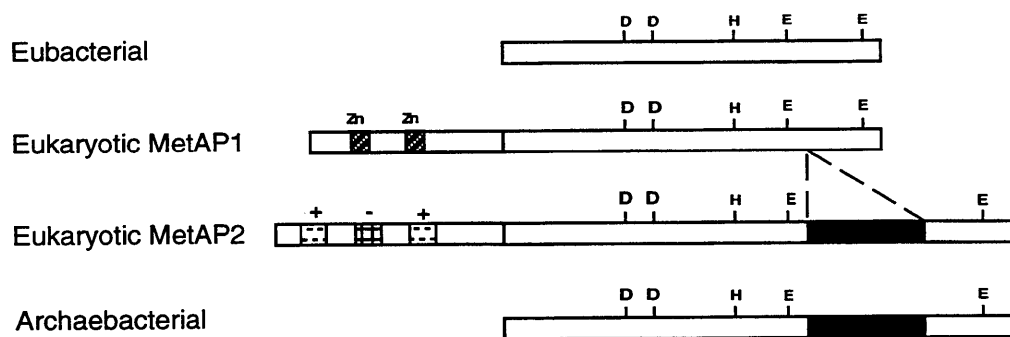


Figure 3.1. Two families of MetAP. The homologous catalytic domains are aligned with each other, with the residues involved in metal coordination shown. The two zinc finger motifs (Zn) of MetAP1 are indicated, as are the polybasic (+) and polyacidic (-) stretches of MetAP2.

survival in eukaryotes (7). MetAP2 was originally cloned in yeast as a high copy suppressor of the slow growth phenotype of MetAP1 mutants, though low levels of expression cannot complement the growth defect (7,11). These observations suggests that at wild type levels, MetAP1 and MetAP2 have different functions, perhaps in the processing of overlapping but distinct sets of protein substrates. Interestingly expression of a dominant negative MetAP1 mutant in yeast also interferes with the function of MetAP2, suggesting that the two enzymes might bind to a common set of regulatory proteins or compete for a common binding site on the ribosome (11).

Removal of the initiator methionine occurs for most but not all cytosolic proteins in eukaryotes. As indicated by studies of initiator methionine processing of amino-terminal hemoglobin mutants translated *in vitro* in a rabbit reticulocyte lysate system, cytochrome c and plant thaumatin mutants expressed in yeast, and surveys of proteins with known amino-terminal primary structure, the major determinant for methionine removal appears to be the identity of the second translated residue of a protein (12,13,14,15). Typically, the initiator methionine is removed only if the second residue is relatively small and uncharged, in particular if it is glycine, alanine, serine, threonine, valine, proline or cysteine. Exceptions to the rule exist, however, and indicate that in some cases further sequence context is likely to be important (14,16). Whether the two MetAP isoforms are responsible for cleaving different subsets of these substrates *in vivo* is not known. Studies on peptide substrates *in vitro* using purified protein indicate that yeast MetAP1 processes tripeptide substrates bearing valine or threonine in the penultimate position approximately 20-fold less efficiently than a tripeptide bearing alanine in the same position (17). Where tested, porcine, human, and yeast MetAP2 assayed against peptide substrates follow the expected trend with regards to the penultimate residue (7,18,19). While these studies suggest that some nascent protein substrates may be less efficiently processed by MetAP1 than by MetAP2 *in vivo*, it is not clear how these differences in activity *in vitro* might translate into differences in substrate specificities *in vivo*. For example, no studies have been done to examine the

substrate specificity for initiator methionine retention in the yeast mutants lacking one or the other MetAP.

There are several ways in which initiator methionine removal can affect the activity of cellular proteins (Figure 3.2). It is required, for example, for subsequent amino-terminal protein modifications, such as acetylation and myristoylation (1,2). N-terminal myristoylation, which is specific to eukaryotes, occurs co-translationally, is generally irreversible, and requires prior removal of the initiator methionine to produce a substrate bearing an amino-terminal glycine residue (20). Other sequence determinants, such as the presence of serine in position 5 and basic amino acid residues at positions 7 and 8, are not individually crucial but increase the tendency for myristoylation to occur. Myristoylation affects the function of different proteins in different ways. For some proteins myristoylation confers either constitutive or regulated membrane localization, which can be essential for proper function. Mutants of the protein kinase encoded by the *v-src* oncogene which cannot be myristoylated retain their kinase activity, but fail to become membrane-associated and lose the ability to transform cells (21). In some cases myristoylation does not direct proteins to the membrane but is crucial for protein-protein interactions, as in the case of many viral coat proteins, where myristoylation is required for assembly of infectious viral particles (22). For other proteins, such as the regulatory B subunit of the protein phosphatase calcineurin and the catalytic subunit of protein kinase A, myristoylation does not appear to be essential for function and its role is not clear. Yeast in which the gene encoding N-myristoyl transferase have been deleted are not viable due to the presence of proteins essential for growth which require myristoylation to function properly (23). It is thus conceivable that the lack of viability observed in MetAP1/MetAP2 double knockout yeast is entirely due to the requirement of methionine removal for subsequent myristoylation.

The majority of mature cytosolic proteins in eukaryotes, perhaps as many as 80%, are N-terminally acetylated (24). Acetylation also occurs co-translationally, either subsequently or alternatively to methionine removal, depending on the substrate (2,25).

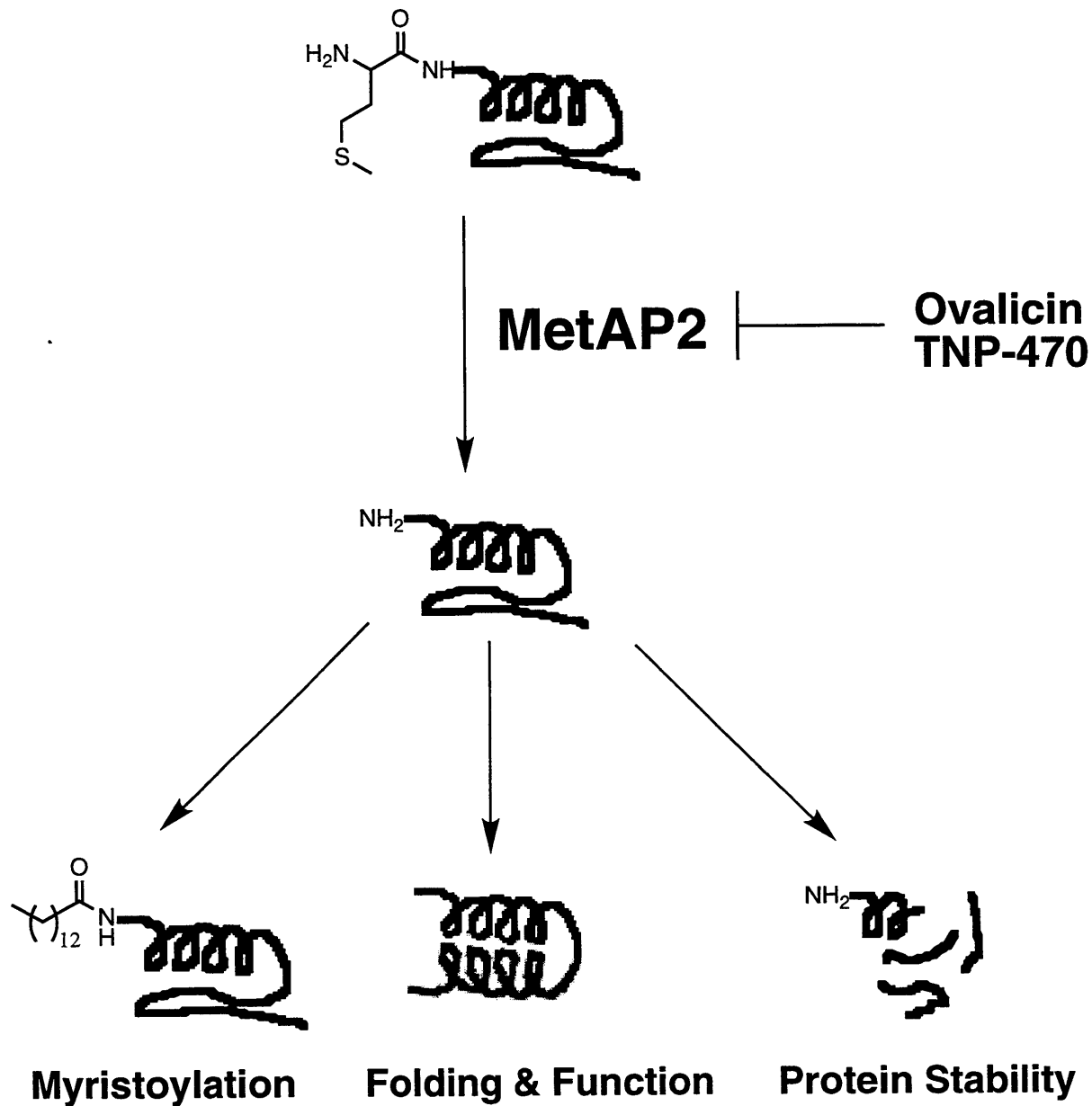


Figure 3.2. Removal of the initiator methionine from proteins can potentially affect their activity in a number of ways.

Acetylation substrates tend to either have small, uncharged residues (glycine, alanine, serine or threonine) at their amino-termini, or bear methionine at the amino-terminus and have glutamate, aspartate, or asparagine in the penultimate position (12-16). Analysis of model substrates in yeast and a survey of eukaryotic proteins with known N-terminal structure indicate that these rules do not hold as rigidly as the trends discussed above for methionine removal, indicating that residues in positions other than the first two are likely to dictate specificity of acetylation. While the significance of amino-terminal acetylation is not well understood, it is generally believed to be related to protein stability and turnover (1). Thus acetylation of the amino-terminus may protect a protein from degradation by exopeptidases and prolong its half-life, though there is no indication that acetylated proteins are generally turned over more slowly than non-acetylated ones. The notion that acetylation can affect protein turnover is supported by the observation that a hypoxanthine phosphoribosyltransferase variant which bears an amino-terminal proline residue turns over more rapidly than a variant bearing an acetylated alanine residue in the same position, though this difference cannot be unambiguously tied to acetylation (26). It is feasible, however, that inappropriate retention of a protein's amino-terminal methionine could prevent it from being acetylated, thereby reducing its half-life, which could result in lower levels of the affected protein.

The residue present at the amino-terminus of a protein can dramatically affect the rate of protein turnover in several ways that appear unrelated to acetylation. Studies by Varshavsky and co-workers in yeast have elucidated a pathway for protein degradation by what is termed the N-end rule (27). Expression of protein constructs bearing the protein ubiquitin fused to the amino-terminus in yeast leads to rapid proteolytic removal of the ubiquitin moiety at the site of fusion. This method allows for the production of proteins with any desired amino-terminal residue. Studies with this system indicate that the half life of a protein so produced depends entirely on the identity of the unmasked N-terminal residue. Generally, small amino-terminal residues (glycine, alanine, serine, threonine, valine and methionine) are stabilizing, producing proteins with half-lives on the

order of days, while larger residues are destabilizing, resulting in the rapid ubiquitin-dependent degradation of the protein within minutes. The observed trend appears to be thereby complementary to the trend for methionine removal, which indicates that the majority of cytosolic proteins are unlikely to be targets for this degradation pathway. However, the existence of MetAP substrates which are exceptions to the general rules for methionine removal raises the possibility that N-end rule substrates may exist which are produced by the standard protein maturation pathways employed in cells.

Residues at or near the amino-terminus of a protein may be important in determining protein half-life by mechanisms distinct from the N-end rule. Levels of the protein kinase encoded by the *c-mos* proto-oncogene (Mos) are controlled in part by changes in its rate of turnover, and the wild type protein (which bears an amino-terminal proline residue) is degraded rapidly when produced in *Xenopus* oocytes by microinjection of its mRNA (28). Using the microinjection assay to produce a series of mutants in the second codon, Sagata and co-workers showed that the turnover rate of the protein produced was dictated by the nature of the second translated residue in a manner unrelated to the predicted pattern for an N-end rule substrate. These mutations were found to affect the phosphorylation of a serine residue near the N-terminus which seems to be important for regulating the stability of Mos. Though not explicitly shown, it seems possible that retention of the amino-terminal methionine residue could also lead to differential phosphorylation and turnover, illustrating a mode of regulation of protein stability which could be employed for other proteins as well. The levels of several proteins involved in carbohydrate metabolism are rapidly degraded in yeast following shift from growth on a non-fermentable to a fermentable carbon source in a process called catabolite inactivation. Interestingly, mutation of the amino-terminal proline residue to serine or tryptophan eliminated catabolite inactivation of the enzyme fructose-1,6-bisphosphatase (29). The presence of proline at the amino-terminus of several other enzymes degraded during catabolite inactivation suggests that involvement of the amino-terminus may be a general feature of this process.

Processing of the amino-terminal methionine residue may be crucial for a protein to function properly. The refolding yield and solubility of wild type hen egg-white lysozyme produced in bacteria under conditions where the amino-terminal methionine is retained is poor compared to the native enzyme, which does not have methionine at its amino-terminus (30). This observation raises the possibility that some proteins may be unable to fold properly without correct removal of their initiator methionine. Human α - and β -globin chains normally undergo removal of their amino-terminal methionine residues to yield valine at their amino-termini. Hemoglobin prepared from a bacterial source which fails to undergo processing retains the ability to bind oxygen cooperatively, but binding is less sensitive to pH or the presence of organic phosphates (31). The N-terminal DNA binding domain of the transcription factor MEF2C displays increased binding specificity and bends DNA more sharply when a short extension (gly-gly-met) is appended to the amino-terminal glycine residue (32). These studies indicate that minor modifications to the amino-terminus of a protein can alter its biochemical behavior in potentially significant ways.

For a variety of reasons therefore the nature of the amino-terminus of a protein can be essential for its function, indicating that failure to cleave the initiator methionine of certain proteins will result in loss of function. The absolute requirement for MetAP activity for viability of both yeast and prokaryotes provides evidence that substrates essential for cell growth exist which do not function properly without proper amino-terminal processing. We and others have found that TNP-470, ovalicin, and fumagillin all covalently and specifically inactivate MetAP2 (Chapter 2, 33,34). As the growth of most mammalian cells and cell lines is not inhibited by these drugs, it would appear that unlike yeast, most mammalian cells do not require MetAP2 for optimal growth. Why the growth of endothelial cells and T lymphocytes is inhibited by TNP-470 and ovalicin is not clear. The simplest possible explanation is that these cell types do not express MetAP1, and thus inactivation of MetAP2 results in complete loss of MetAP activity necessary for cell growth. Alternatively, there may exist proteins essential for the growth

of drug sensitive cells which can be processed solely by MetAP2 and not by MetAP1, and whose activity or stability, for any of the reasons outlined above, requires removal of its initiator methionine. Alternatively, a protein which inhibits the growth of these cells may be stabilized by retention of its initiator methionine leading to its accumulation and cell cycle arrest. Herein we show that MetAP2 activity is inhibited in intact cells. Furthermore such inhibition is shown to result in altered amino-terminal processing of a subset of cellular proteins. These observations confirm the existence of specific MetAP2 substrates in vivo which cannot be processed in the absence of the enzyme, which suggests that that inhibition of MetAP2 by TNP-470 and ovalicin is a plausible mechanism leading to cell cycle arrest.

Materials and Methods

[Methyl-³H] Thymidine, EXPRESS [³⁵S] methionine/cysteine mixture, [γ -³²P] ATP, and ENHANCE fluorographic enhancer were purchased from DuPont/NEN Life Science.

[9,10(n)-³H] myristic acid was obtained as an ethanolic solution from Amersham and was concentrated to dryness and resuspended to 10 mCi/mL in EtOH prior to use.

Antibodies to GAPDH were obtained from Biodesign International. Antibodies to GST- π were from Medical and Biological Laboratories (Nagoya). BioMax and XOMat AR5 film for autoradiography were from Kodak. 1X SSC solution is 15 mM sodium citrate with 150 mM NaCl, pH 7.0. 1X Denhart's reagent is 0.02% Ficoll type 400, 0.02% polyvinylpyrrolidone, and 0.02% BSA.

Cell Culture. Unless otherwise indicated, cells were grown in a humidified incubator at 37°C in an atmosphere of 5% CO₂. Bovine aortic endothelial cells (BAECs) were cultured in DME (low glucose) containing 10% fetal bovine serum (FBS) and 50 units/mL penicillin plus 50 μ g/mL streptomycin (P/S). Human umbilical vein endothelial cells (HUVECs) were obtained from Clonetics and cultured in EGM-2 (Clonetics). HUV-EC-C cells were obtained from the American Type Culture Collection (ATCC) and cultured in Kaign's modification of Ham's F12 media containing 10% FBS, 100 μ g/mL heparin,

and 30 µg/mL endothelial cell growth supplement (Sigma or Clonetics), and P/S. Flasks and plates were pretreated with endothelial cell attachment factor (Sigma). ECV-304 cells (ATCC) were maintained in M199 with 10% FBS and P/S. EA.hy926 cells, a generous gift of Dr. Cora-Jean Edgell (University of North Carolina, Chapel Hill), were grown in DME containing HAT and 10% FBS.

Cell proliferation assay (MTT). HUV-EC-C cells (5000 per well), BAECs, or EA.hy926 cells (2000 per well) were seeded into 96-well plates and grown for 96 h in the presence of varying concentrations of drugs or carrier alone (0.5% ethanol). 3-(4,5-Dimethylthiazol-2-yl)-2,5-diphenyltetrazolium bromide (MTT, 25 µL, 10 mg/mL in PBS) was added during the final 4 h after which cells were extracted with 100 µL of 10% SDS with 0.1 M HCl per well for 16 hr at 37°C. Plates were read at 600 nm.

Cell proliferation assay (³H thymidine incorporation). Cells prepared as described above were seeded into 96-well plates and grown in the presence of drug or carrier alone (0.5% EtOH) for 72 hr. Cells were pulsed with [³H] thymidine (6.7 Ci/mmol, 1 µCi per well) for the final 6 to 18 hr of culture and harvested with a semiautomated cell harvester onto glass fiber papers for scintillation counting.

Labeling of probe for Northern blot analysis. Purified restriction digested probe (50 ng) was labeled using High Prime DNA labeling mix (containing Klenow enzyme, Boehringer Mannheim) with 50 µCi [³²P]-dCTP in a volume of 20 µL for 10 min at 37°C. Probes were purified using NucTrap size exclusion columns (Stratagene) and incorporated radioactivity determined by scintillation counting.

Northern blot analysis. Total RNA was prepared from a single confluent flask of HUV-EC-C, ECV304, or EA.hy926 cells by direct lysis in 10 mL Tri Reagent (Molecular Research Center, Inc.). After incubating at room temperature 5 min, the extract was washed with 0.2 volumes of CHCl₃, allowed to separate 5 min and then centrifuged at 12,000 x g for 15 min at 4°C. RNA was precipitated from the aqueous layer by adding 0.5 volumes isopropanol, mixing, incubating at room temperature 5 min and centrifuging at 12,000 x g for 8 min at 4°C. The pellet was washed with 75% EtOH, air-dried, and

suspended in 50 μ L diethyl pyrocarbonate treated water. A total of 8.4 μ g RNA from each sample was electrophoresed in a 1% agarose gel run in 20 mM MOPS, pH 7.0, 8 mM NaCl, 1 mM EDTA with 16.2% formalin. RNA was transferred to nitrocellulose overnight by capillary action. The membrane was heated at 80°C for 2 hr in vacuo. To probe for RNA expression, the membrane was treated with prehybridization fluid (50% formamide, 5X SSC, 5X Denhart's reagent, 500 μ g/mL salmon sperm DNA, and 2% SDS) for 2 hr at 42°C and then treated with 32 P-labeled specific DNA probe (5×10^6 cpm) in hybridization fluid (50% formamide, 5X SSC, 1X Denhart's reagent, 100 μ g/mL salmon sperm DNA, 2% SDS, and 10% dextran sulfate) overnight at 42°C. The membrane was then washed twice with 2X SSC plus 0.1% SDS, once with 0.2X SSC plus 0.1% SDS, and once with 0.1X SSC plus 0.1% SDS prior to exposure to X-ray film. Prior to re-probing for a different message, the membrane was first boiled in 1% SDS, 10 mM Tris HCl, pH 7.4, 1 mM EDTA for 10 min and rinsed with 4X SSC.

Electrophoresis. SDS-PAGE was performed as described by Laemmli (35), using 2% SDS, 50 mM Tris HCl, pH 6.8, 5% β -mercaptoethanol, with 0.1% bromophenol blue as loading buffer. Isoelectric focusing (IEF) and non-equilibrium pH gradient electrophoresis (NEPHGE) were performed as described (36,37) except that ampholytes used were purchased from Bio-Rad Laboratories. For IEF, samples were made up to 1% SDS with 20 mM DTT, heated in a boiling water bath for 3 min, and cooled to ambient temperature after which 1/10th volume of 2D gel loading buffer (9M urea, 4% CHAPS, 1% DTT, 2% ampholytes, pH 3-10) was added.

Analysis of protein myristoylation. BAECs were trypsinized from confluent plates, seeded into plates (10^5 cells/cm²) and allowed to recover 4 hr at 37°C. After drug or EtOH carrier treatment for the indicated time, the media was removed and replaced with labeling media (DME with low glucose, 5% dialyzed FBS, and 5 mM sodium pyruvate) containing drug or carrier. [3 H] myristic acid (54 Ci/mmol, 10 mCi/mL in EtOH) was added to a final concentration of 50 μ Ci/mL and cells were incubated for the indicated times. After washing once with PBS, cells were harvested by direct lysis into either SDS-

PAGE loading buffer or 2D gel loading buffer. Extracts were incubated at room temperature for 2 hr, frozen on dry ice/EtOH and stored at -20°C until analysis by either one- or two-dimensional gel electrophoresis as described above. Gels were stained with Coomassie blue, impregnated with an autoradiography enhancer (NEN Enhance), dried, and exposed to X-ray film to visualize spots.

Analysis of total protein synthesis and turnover. BAECs were plated into 6-well dishes and grown to 50% confluence. Cells were treated for 4 hr with TNP-470 (50 nM) or EtOH carrier alone (0.5 %), at which time the media was removed and replaced with labeling media (methionine-free DME containing 5% dialyzed FBS, 1mL). After incubating 10 min at 37°C, media was replaced with fresh labeling media (0.5 mL) containing 0.5 mCi/mL [³⁵S] methionine (NEN EXPRESS label, >1000 Ci/mmol) including TNP-470 or carrier. Cells were incubated 30 min at 37°C, washed once with complete media, and then cultured in fresh complete media for various times. Cells were washed with PBS and harvested directly into 150 µL 2D gel loading buffer either immediately or at 1 hr, 4 hr, or 16 hr following the pulse. Extracts were kept at room temperature 1 hr, frozen on dry ice EtOH, and stored at -20°C until analysis by two dimensional gel electrophoresis (NEPHGE/SDS-PAGE). Gels were silver stained, dried, and exposed to BioMax film.

Mass spectrometry. Samples were prepared from silver-stained polyacrylamide gels and analyzed by MALDI-TOF mass spectrometry as described in Chapter 2 by Susan Wolf in the laboratory of Klaus Biemann.

Purification of GAPDH for amino-terminal sequence analysis. BAECs were plated at 1/3 confluence and treated with either 50 nM TNP-470 or 0.1% EtOH carrier alone in 15 cm plates (six of each type) for 72 hr. Cells were detached by treating with 1 mM EDTA in PBS, pelleted, washed once with PBS and lysed by homogenization in hypotonic buffer as described in Chapter 7. Lysates were centrifuged at 16,000 x g for 10 min at 4°C. Supernatants were dialyzed for 18 hr with one change into dialysis buffer (30 mM sodium phosphate, pH 6.0, 1 mM DTT, and 1 mM EDTA). Samples were assayed

for protein by Bradford assay (Bio Rad), and 1 mg of protein was brought to a volume of 2 mL with dialysis buffer and added to 0.35 mL of AMP-agarose beads. Samples were incubated at 4°C for 20 hr with rotating. The bead suspensions were transferred to columns, drained, washed with 5 column volumes of dialysis buffer, and then eluted with four 350 μ L portions of elution buffer (30 mM sodium phosphate, pH 7.5, 1 mM DTT, 1 mM EDTA, and 1 mM NAD⁺). Eluates were concentrated to 125 μ L under reduced pressure, and then subjected to SDS-PAGE. Samples were transferred to PVDF membrane in 10 mM CAPS, pH 11, 10% MeOH at 20 V for 2 hr at 4°C. The membrane was stained with Ponceau S (0.2% in 1% HOAc), destained with ddH₂O. Bands were excised and submitted to the MIT Biopolymers laboratory for sequence analysis.

Purification of GST- π for amino-terminal sequence analysis. BAECs were plated at low density (20% confluence) and allowed to grow to confluence in the presence or absence of 50 nM TNP-470. Cells treated with TNP-470 were exchanged into fresh media containing drug after 3 days. Cells were washed once with cold PBS and then extracted into lysis buffer (0.5% triton X100, 50 mM HEPES, pH 7.3, 250 mM NaCl, 1 mM DTT, 1 mM EDTA, 1 μ g/mL aprotinin, 25 μ M leupeptin, 1 mM PMSF, 1 mL per 15 cm plate) by scraping into a microcentrifuge tube and incubating at 4°C for 30 min with rotating. Extracts were centrifuged 10 min at 16,000 x g at 4°C to remove debris, frozen on dry ice/EtOH, and stored at -80°C until use. To purify GST, 1.2 mL of each lysate was incubated with 100 μ L glutathione sepharose 4B (Pharmacia) for 2 hr at 4°C with rotating. Beads were pelleted and washed 3 times for 5 min at 4°C with lysis buffer, suspended in SDS-PAGE loading buffer, and heated in a boiling water bath for 10 min. Samples were prepared for N-terminal analysis as described above for GAPDH, except that blots were stained with Coomassie Brilliant Blue (0.1% in 1% HOAc, 40% MeOH) to visualize protein bands.

Results

Primary endothelial cells and T lymphocytes are sensitive to TNP-470 and ovalicin, but most other cell types, including many transformed cells, are not. A possible explanation for this observation would be that endothelial cells lack MetAP1, which would mean that treatment with TNP-470 or ovalicin would result in complete loss of MetAP activity in these cells. Cells would be thereby unable to proliferate, by analogy with *map1* mutant yeast. To address this possibility, we examined expression levels of both MetAP1 and MetAP2 mRNA in a series of endothelial cell lines, each derived from human umbilical vein endothelial cells (HUVECs). While proliferation of the cell line HUV-EC-C is inhibited by TNP-470, growth of ECV304 cells is largely unaffected, and EA.hy926 cells are only partially sensitive to the drug (Figure 3.3). All three cell lines, however, express MetAP1 and MetAP2 mRNA at comparable levels by Northern blot analysis (Figure 3.4). It is therefore unlikely that TNP-470 treatment completely inhibits MetAP activity in sensitive cells or that resistance is conferred by high levels of expression of either protein.

If inhibition of MetAP2 peptidase activity underlies cell cycle arrest induced by TNP-470 and ovalicin, then protein substrates must exist which cannot be efficiently processed by MetAP1. Several approaches were therefore taken to determine if cells treated with the drugs have specific defects in methionine processing. First, protein myristoylation was examined. Bovine aortic endothelial cells (BAECs) were pretreated with TNP-470 and then labeled with [³H] myristic acid, which is metabolically converted to myristoyl CoA and incorporated into proteins as N-myristoyl groups (38). Labeled cell extracts were subjected to SDS-PAGE followed by fluorography. Samples were run in duplicate and one set of lanes each was treated with either Tris buffer or 1M hydroxylamine, which cleaves thioester bonds, to ensure that the incorporated radioactivity was due to myristoylation and not due to S-palmitoylation as a consequence of metabolic conversion of the labeled myristate to palmitate. A series of myristoylated protein bands could be detected by this procedure (Figure 3.5). For most of the detected proteins, no differences in the intensity of labeling were observed between untreated cells

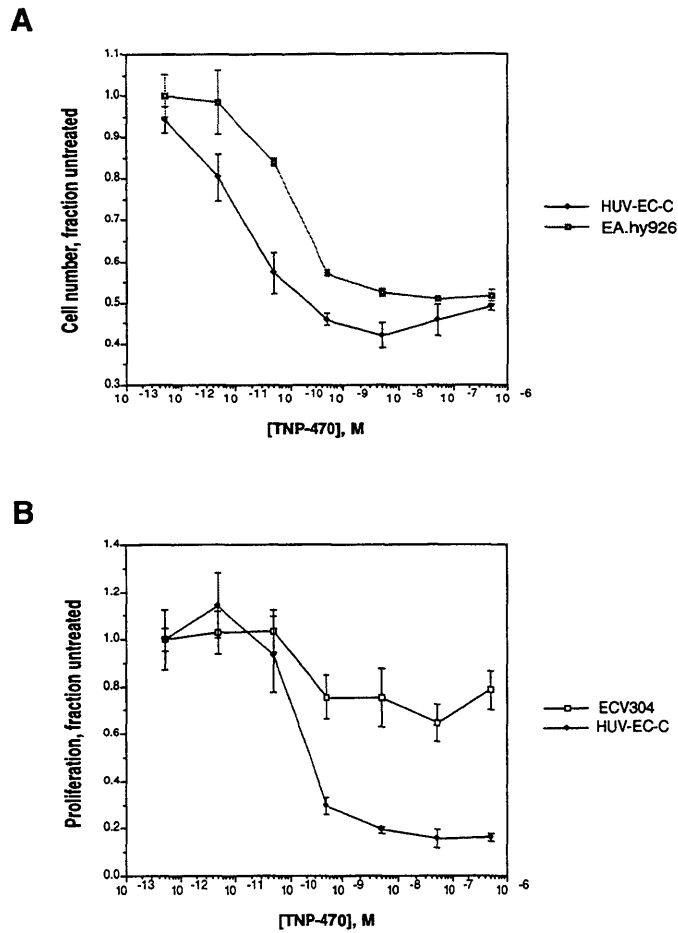


Figure 3.3. Sensitivity of various endothelial cell lines to TNP-470. Cells were grown in 96-well plates in the presence of varying concentrations of TNP-470 for 3 days and then proliferation was analyzed by either [³H] thymidine incorporation (A, HUV-EC-C and ECV-304) or MTT assay (B, HUV-EC-C and EA.hy926).

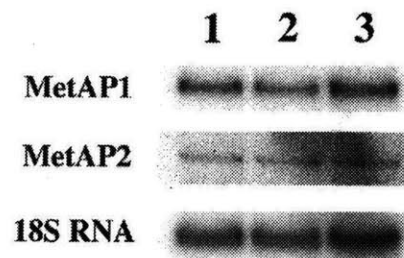


Figure 3.4. Human endothelial cell lines express comparable levels of both MetAP1 and MetAP2 mRNA regardless of sensitivity to TNP-470. Levels of MetAP1 mRNA, MetAP2 mRNA, and control 18S rRNA expression in HUV-EC-C (lane 1), EA.hy926 (lane 2), and ECV-304 (lane 3) cells were determined by Northern blot analysis.

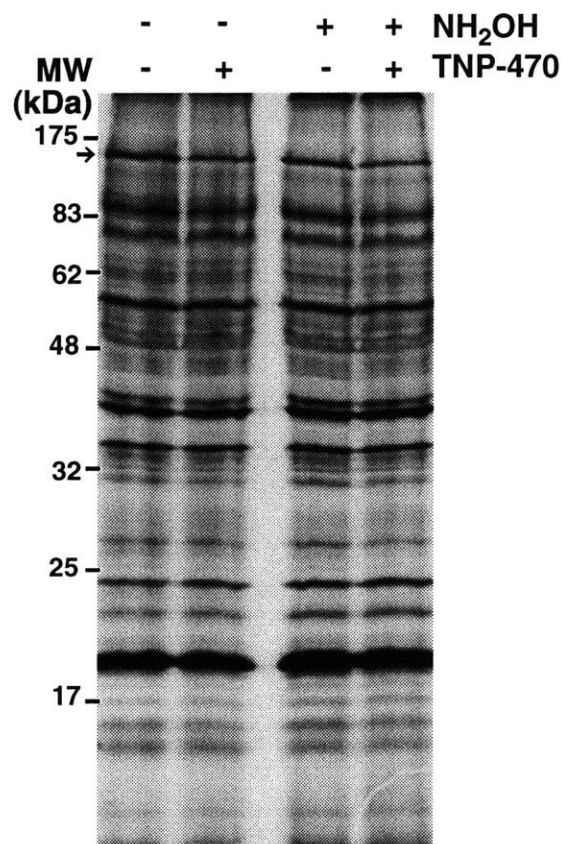


Figure 3.5. Analysis of protein myristoylation in BAECs in the presence or absence of TNP-470 by one dimensional SDS-PAGE. Cells were pretreated with 50 nM TNP-470 or carrier solvent alone as indicated for 48 hr prior to labeling for 4 hr with [³H] myristic acid. Extracts were run on SDS-PAGE (10%), and lanes were treated either with 1M Tris HCl, pH 7.0 or 1M hydroxylamine, pH 7.0 as indicated prior to fluorography. The band of roughly 150 kD molecular weight which decreases with TNP-470 treatment is indicated with an arrow.

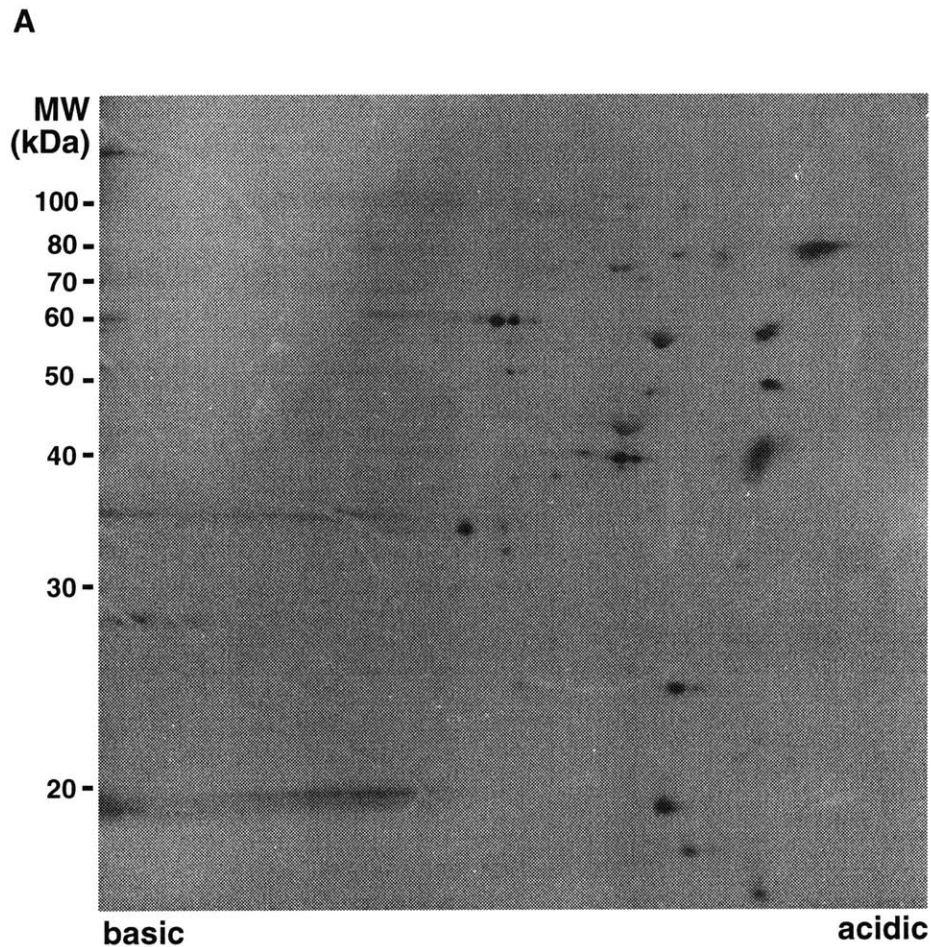
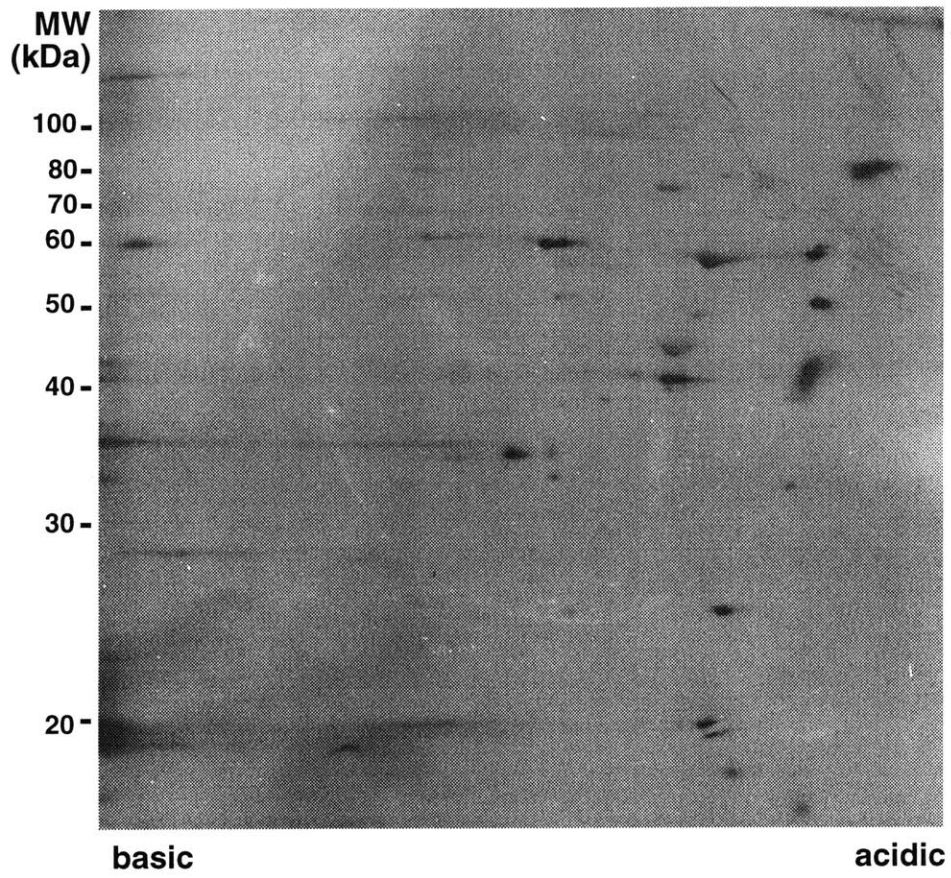


Figure 3.6. Analysis of protein myristoylation in BAECs in the presence or absence of TNP-470 by two dimensional gel electrophoresis. Cells were pre-treated with 50 nM TNP-470 or carrier solvent alone (0.1% EtOH) for 4 hr followed by [³H] myristic acid labeling for 16 hr. Extracts were analyzed by two dimensional electrophoresis, using isoelectric focusing for the first dimension and SDS-PAGE (12%) for the second dimension. This page: A. Extracts from cells treated with carrier solvent alone. Following page: B. Extracts from TNP-470 treated cells.

B



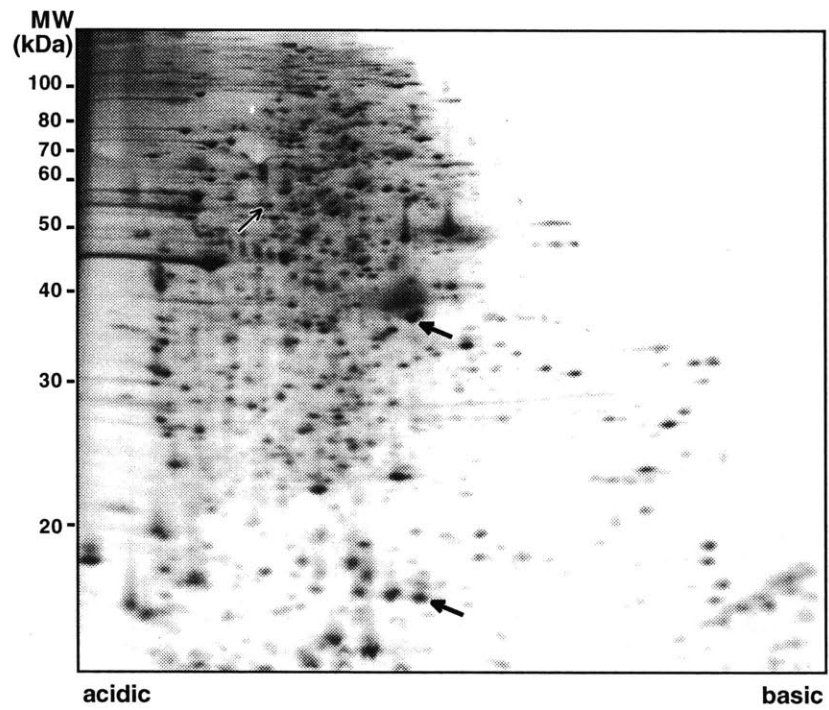
and cells treated with TNP-470. The only exception is a single protein band of approximately 150 kD molecular weight, which is decreased approximately two-fold in intensity from cells treated with TNP-470. To determine whether the myristoylation of a subset of proteins which could not be visualized by one-dimensional electrophoresis was affected by TNP-470 treatment, extracts were analyzed by two-dimensional electrophoresis as well (Figure 3.6). No proteins could be detected which appeared to be differentially myristoylated in TNP-470-treated cells. Though it is possible that there are scarce myristoylated proteins which could not be detected by this method, it would appear that for the great majority of proteins destined for myristoylation, MetAP1 can compensate in the absence of MetAP2 activity.

Given the precedent for effects on turnover rate consequent to changes the amino-terminus of a protein, we examined whether TNP-470 treatment affected the half-life of any cellular proteins. To do this, cells were pre-treated with TNP-470 or carrier solvent alone and then pulse labeled with [³⁵S] methionine. Following the pulse, cells were exchanged into fresh media containing excess cold methionine and extracts prepared at various times thereafter. To allow observation of as many proteins as possible, extracts were analyzed by two dimensional electrophoresis followed by autoradiography. Autoradiograms for samples collected immediately following the pulse and 16 hr later are shown in Figure 3.7. Despite detection of several rapidly degraded proteins (with half-lives less than 16 hr), clear differences in the turnover rate of any protein due to TNP-470 treatment were not observed. However, several protein spots, which migrated at roughly 16 kD, 37 kD, and 56 kD molecular weight, displayed altered mobility when visualized by autoradiography from cells treated with TNP-470 (Figure 3.7). Interestingly, these changes in mobility were not evident when proteins from extracts prepared immediately following the pulse were visualized by silver stain, but the mobility of the 37 kD and the 56 kD protein began to change at later time points (20 hr following initiation of drug treatment) (Figures 3.8 and 3.9). This observation suggests that the altered mobilities observed are due to modifications which occur to proteins synthesized only subsequently

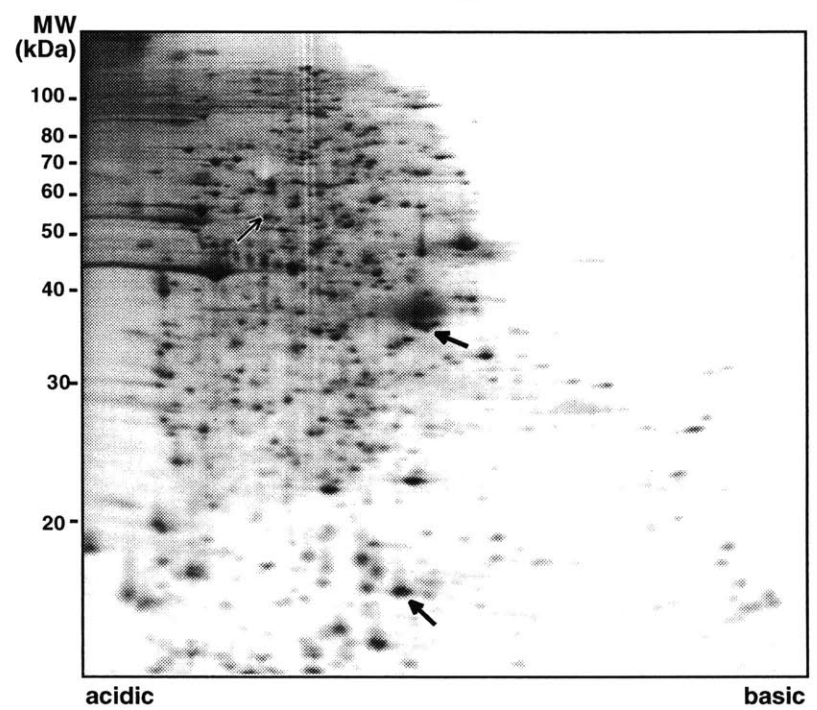
Figure 3.7. TNP-470 affects the migration of several protein spots by two dimensional electrophoresis. Cells were pretreated with 50 nM TNP-470 for 4 hr prior to pulse labeling with [³⁵S] methionine. Extracts were prepared either immediately following the pulse (A) or after a 16 hr chase with excess cold methionine (B). Proteins with altered migration are indicated with arrows in panel A.

A

-TNP-470, 0 hr

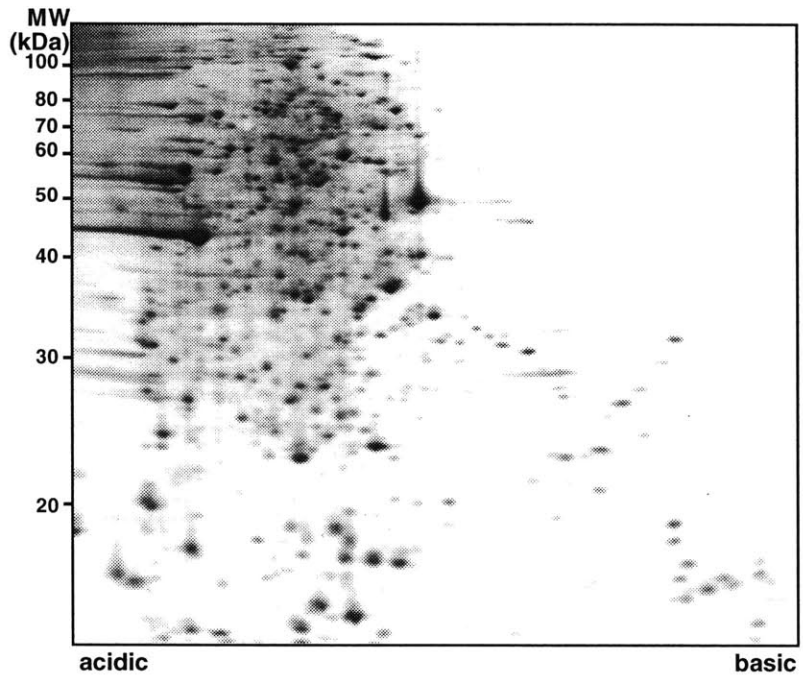


+TNP-470, 0 hr



B

-TNP-470, 16 hr



+TNP-470, 16 hr

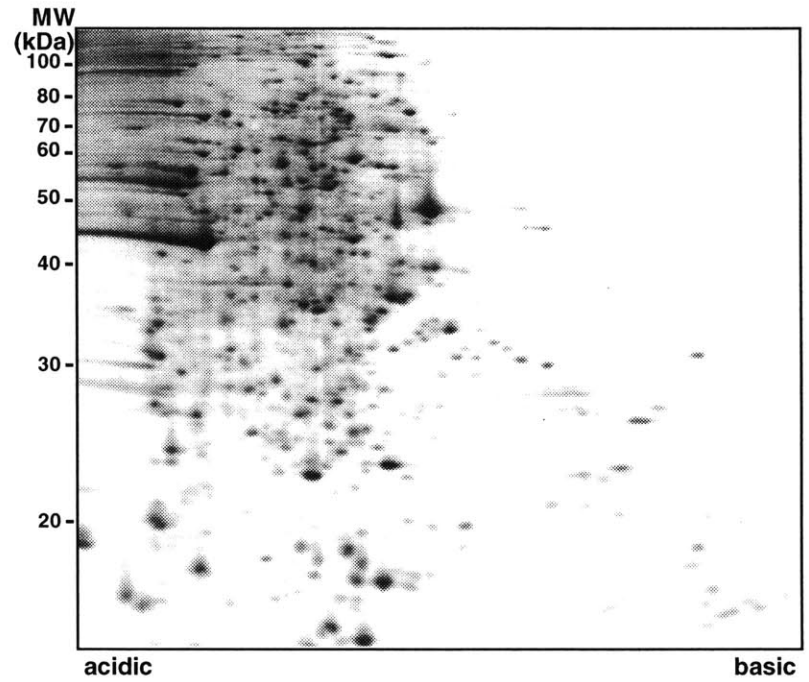
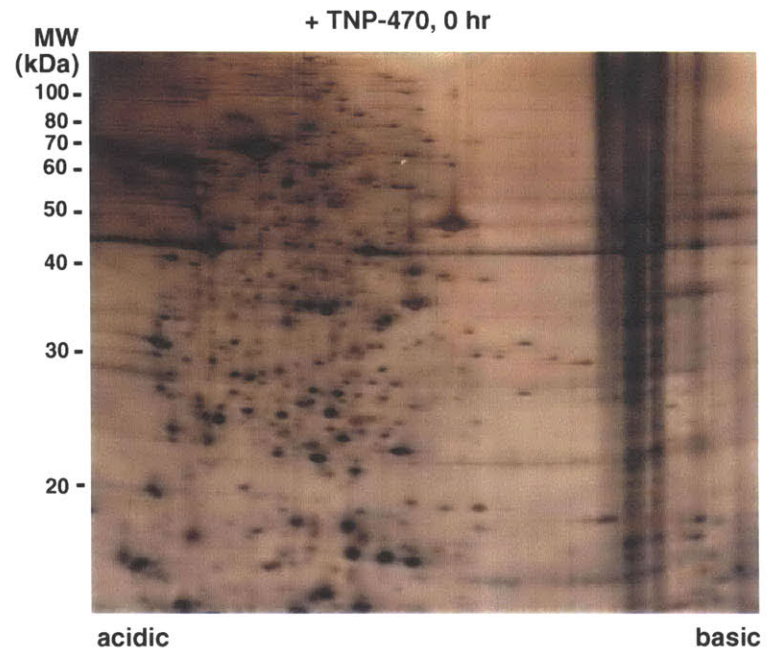
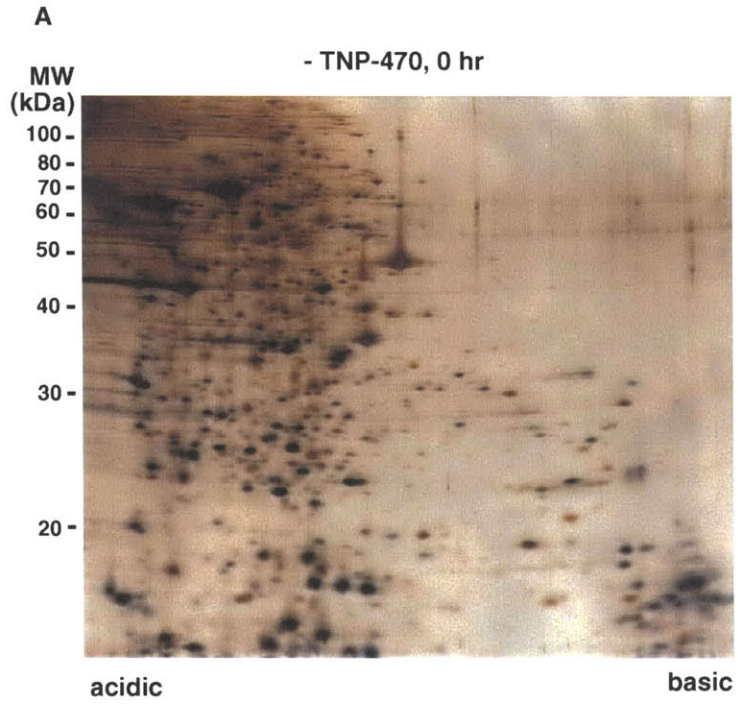


Figure 3.8. Two dimensional electrophoretic analysis followed by silver staining of protein extracts from cells treated with or without TNP-470. The same gels shown in Figure 3.6 were silver stained prior to drying and autoradiography.



B

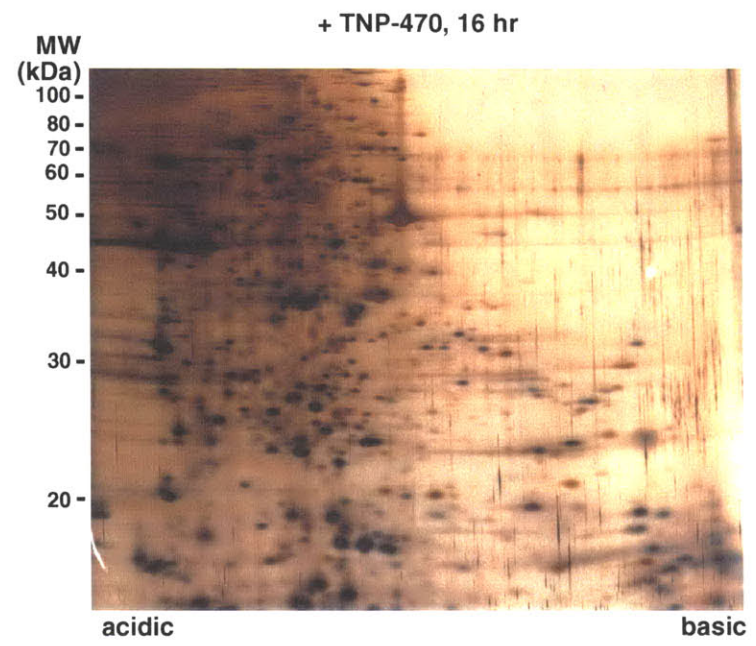
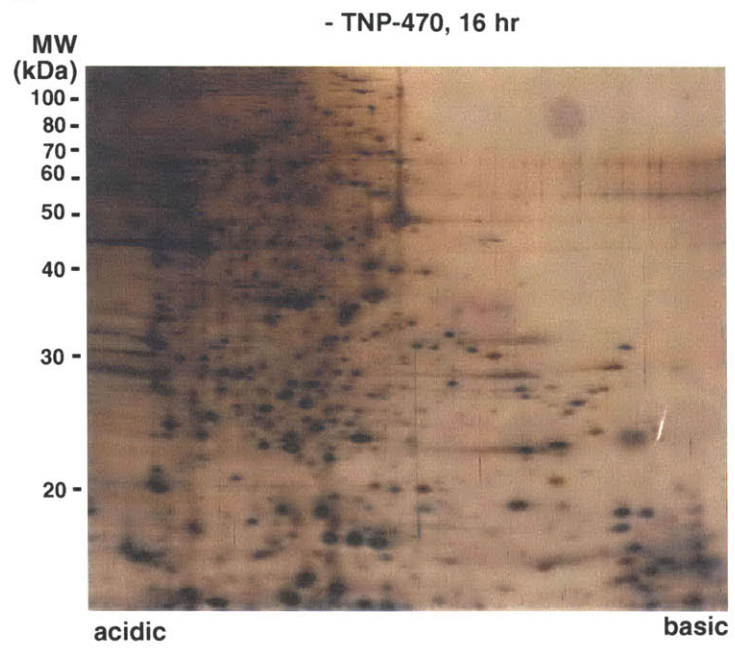


Figure 3.9. Two dimensional electrophoretic analysis followed by silver staining of protein extracts from cells treated with or without TNP-470. Enlarged view of the gels shown in Figure 3.8 reveals altered migration of the 38 kD protein at the later time point.

- TNP-470

+ TNP-470

0 hr



16 hr



to drug treatment. The ability to detect a partial change in mobility of the 37 kD and 56 kD proteins by silver stain at later times probably indicates that turnover of a detectable fraction of the protein has occurred by that time.

To study this modification further, the 37 kD and 16 kD proteins, which were relatively abundant as judged from intensity of silver staining, were identified by MALDI-TOF mass spectrometry analysis of in-gel tryptic digests (39). Mass spectra of tryptic peptides from the 37 kD protein revealed 16 peptides, which were used to search the protein databank. Of the 16 masses, nine matched predicted peptides from the enzyme glyceraldehyde-3-phosphate dehydrogenase (GAPDH) with high accuracy (Table 3.1). Two additional peptides appear to result from modification of cysteine residues of GAPDH with monomeric acrylamide. The nature of the remaining five peptides is not known, but may reflect allelic differences between the isolated protein and the sequence in the protein databank, or possibly unknown post-translational modifications to GAPDH. The assignment of this protein as GAPDH is also consistent with its observed molecular weight of 37 kD. The mass spectrum from the tryptic digest of the 16 kD protein contained 12 peaks distinct from background. Of these, 11 matched peptides derived from the peptidyl prolyl cis-trans isomerase cyclophilin A, including three which were modified by acrylamide as above (Table 3.2).

Interestingly, both GAPDH and cyclophilin A from bovine sources have their initiator methionine residues removed co-translationally to yield mature proteins with unmodified valine residues at their amino-termini, raising the possibility that their shifts in mobility following drug treatment are due to retention of the initiator methionine. To investigate this possibility we chose to purify and determine the amino-terminal sequence of GAPDH from cells treated with TNP-470. GAPDH was chosen over cyclophilin A as its rate of turnover appeared to be more rapid (Figure 3.9). BAECs were treated for 72 hr with either 50 nM TNP-470 or carrier solvent alone and extracts prepared by hypotonic lysis. GAPDH was purified by affinity chromatography on AMP-agarose (40). As judged by immunoblotting, TNP-470 treatment had little effect on levels of the enzyme,

Table 3.1. Molecular weights of tryptic peptides from the 37 kD protein indicate that it is identical to GAPDH. Peptides predicted to be modified on cysteine residues by monomeric acrylamide are indicated with an asterisk (*).

Measured mass (Da)	Calculated mass (Da)	GAPDH peptide	Location in sequence
783.344	-	-	-
795.426	795.425	LTGMAFR	225-231
806.397	-	-	-
977.55	977.542	KAITIFQER	70-77
1033.61	-	-	-
1213.58	-	-	-
1358.71	1358.681	VVDLMVHMASKE	321-332
1369.78	1369.744	GAAQNIPASTGAAK	198-212
1461.87	1461.832	LEKPAKYDEIKK	246-257
1556.83	1556.811	VPTPNVSVVDLTCR	232-245
1570.88	1570.826	VPTPNVSVVDLTCR	232-245*
1615.93	1615.881	AITIFQERDPANIK	70-83
1763.83	-	-	-
1795.83	-	-	-
1848.01	1848.936	IVSNASCTTNCLAPLAK	143-159*
2213.08	2213.11	VIISAPSADAPMFVMGVNHEK	116-136

Table 3.2. Molecular weights of tryptic peptides from the 16 kD protein indicate it to be cyclophilin A. Peptides predicted to be modified on cysteine residues by monomeric acrylamide are indicated with an asterisk (*).

Measured mass (Da)	Calculated mass (Da)	Cyclophilin A peptide	Location in sequence
686.371	686.399	HVVFGK	125-130
737.349	737.358	TAENFR	31-36
777.341	777.347	GSCFHR	49-54*
1055.53	1055.541	VSFELFADK	19-27
1132.61	1132.604	KITIADCGQI	154-163*
1140.57	1140.558	FDDENFILKH	82-90
1379.79	1379.758	VSFELFADKVPK	19-30
1505.78	1505.746	VKEGMNIVEAMER	131-143
1564.76	-	-	-
1612.76	1612.761	IIPGFMCQGGDFTR	55-68*
1817.95	1817.896	SIYGEKFDENFILK	76-90
1946.01	1946.002	VNPTVFFDIAVDGEPLGR	1-18

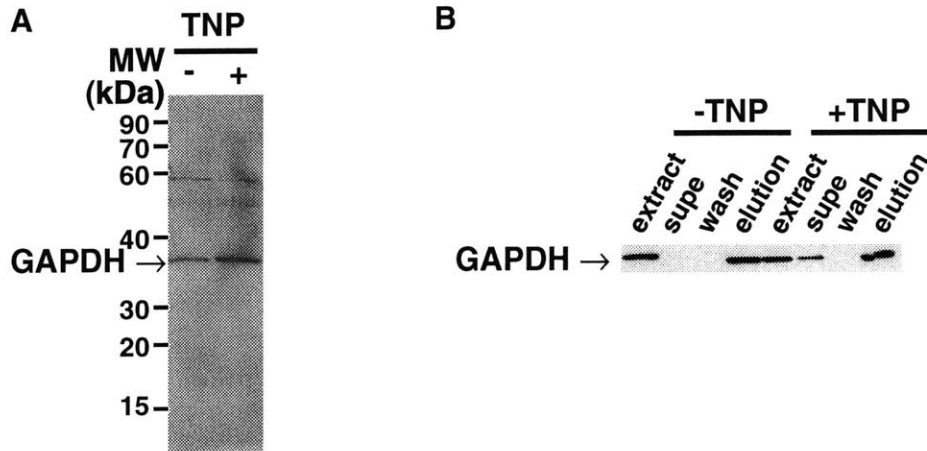


Figure 3.10. Purification of GAPDH from BAECs treated with or without TNP-470. Cells were treated for 72 hr with 50 nM TNP-470 or carrier solvent alone. GAPDH was isolated from extracts by AMP-agarose affinity chromatography. A, Silver stain of purified material. B, Western blotting with GAPDH antibodies. Equal proportions of the extracts, AMP-agarose bead supernatants, column wash, and 1 mM NAD elution fractions were loaded in each lane.

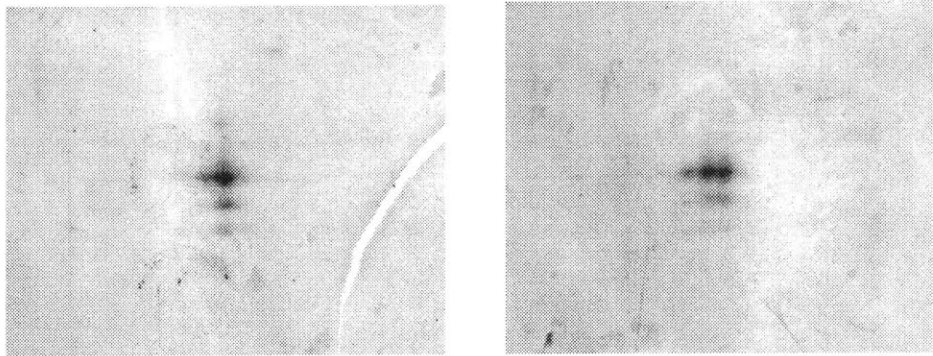


Figure 3.11. Two dimensional electrophoresis of GAPDH purified from TNP-470-treated and untreated BAECs. Purified material identical to that shown in figure 3.9A was subjected to two dimensional electrophoresis (NEPGE/SDS-PAGE). Gels were silver stained to visualize protein. Left panel, GAPDH isolated from control cells. Right panel, GAPDH isolated from TNP-470 treated cells.

Table 3.3. Amino terminal sequence analysis of GAPDH purified from TNP-470-treated and untreated BAECs. The remainder of protein samples shown in figure 3.11 was run on SDS-PAGE, blotted to PVDF membrane, and sequenced by Edman degradation. The picomolar amount of each amino acid is given for each cycle.

Cycle	Literature sequence	Control cells	TNP-470-treated cells
1	V	V (44.1), M (0)	V (13.6), M (17.0)
2	K	K (47.7), V (0)	K (19.1), V (10.6)
3	V	V (42.2), K (3.0)	V (15.7), K (17.0)
4	G	G (34.3), V (2.0)	G (17.2), V (12.2)
5	V	V (36.7), G (2.4)	V (16.4), G (14.8)
6	N	N (23.1), V (4.8)	N (9.9), V (13.5)

and recovery from both drug-treated and untreated cells was nearly quantitative (Figure 3.10). Two dimensional gel analysis of the purified protein from TNP-470-treated cells revealed an approximately one to one mixture of the two closely migrating forms, while the material from untreated cells was almost exclusively a single species (Figure 3.11).

Purified material from both preparations was separated by SDS-PAGE, electrophoretically transferred to PVDF membrane, and their amino-terminal sequences were determined by Edman degradation. While the N-terminal sequence of the protein purified from untreated cells was identical to the predicted sequence for bovine GAPDH with complete removal of the initiator methionine (41), the protein from TNP-470-treated cells appeared to be a mixture of GAPDH with the methionine retained and with the methionine removed in roughly equal amounts (Table 3.1). This establishes that complete processing of the N-terminal methionine from GAPDH requires MetAP2 activity, and that this activity is inhibited in intact cells by TNP-470. Taken together with the observation that protein myristoylation is not generally effected by the drug, this result indicates that the amino-terminal processing of some, but not all, proteins is diminished in TNP-470 treated cells. It is formally possible, however, that the defect in GAPDH processing was simply due to an overall decrease in MetAP activity in cells, which may

have led to subtle decreases in myristoylation which could not be detected in our experiments.

In order to observe directly whether MetAP2 was required for complete amino-terminal methionine removal from all proteins, we chose to examine the amino-terminus of other cytosolic proteins. Bovine glutathione S-transferase- π (GST- π) is normally processed by removal of its initiator methionine to produce the mature protein with an unblocked amino-terminal proline residue (42). We isolated GST- π from cells treated with or without 50 nM TNP-470 by affinity chromatography on glutathione sepharose (Figure 3.12). In order to ensure that the protein analyzed was synthesized subsequent to drug treatment, cells were plated at low density and allowed to grow to confluence under both conditions. As TNP-470 decreases the growth rate of BAECs dramatically, drug treated cells did not reach confluence until 7 days following replating, while carrier treated cells reached confluence after only 2 days. Western blotting confirmed that approximately 75% of the protein present in extracts was synthesized during the last 6 days of drug treatment, as there was four-fold more GST- π present in equal proportions of extracts prepared 7 days after initiating drug treatment compared with extract from an identical plate made one day following drug treatment (Figure 3.12). Amino-terminal sequencing of the purified protein revealed that approximately 80% of the protein had its initiator methionine removed, while roughly 20% retained the methionine, regardless of whether it was from drug treated or untreated cells (Table 3.2). This indicates that in contrast with GAPDH, MetAP2 activity is dispensable for normal processing of GST- π , illustrating that specific MetAP2 substrates do exist within cells.

Discussion

All endothelial cell lines tested, regardless of their degree of sensitivity to TNP-470, were shown to express the genes encoding both MetAP1 and MetAP2 at comparable levels. This result indicates that the situation in mammalian cells is likely to be more complex than in *map1* mutant yeast, where inhibition of MetAP2 by drug cannot be compensated

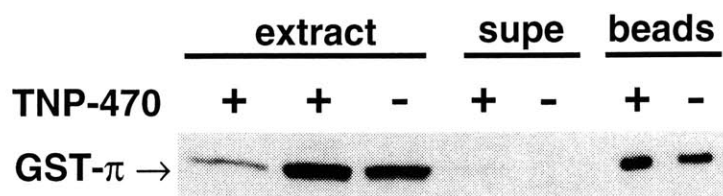


Figure 3.12. Purification of GST- π from BAECs treated with or without TNP-470. BAECs plated at equal densities were grown to confluence in the presence or absence of TNP-470 or harvested after 24 hr TNP-470 treatment. GST- π was isolated from extracts with glutathione-agarose beads. As indicated, equal proportions of crude protein extracts, glutathione-agarose bead supernatants, or material retained on glutathione-agarose beads was separated by SDS-PAGE and analyzed by Western blot with anti-GST- π antibodies. Lane 1, plate harvested after 24 hr TNP-470 treatment. Lanes 2-7, plates treated as indicated and harvested at confluence.

Table 3.4. Amino terminal sequence of purified GST- π from cells grown to confluence in the presence or absence of TNP-470. The remainder of the samples shown in figure 3.12 was electrophoresed, blotted onto PVDF membrane, and sequenced by Edman degradation. The molar amount of each amino acid present in each cycle is indicated.

Cycle	Literature sequence	Control cells	TNP-470-treated cells
1	P	P (11.7), M (1.6)	P (19.2), M (2.8)
2	P	P (12.7)	P (19.5)
3	Y	Y (13.4), P (2.1)	Y (20.5), P (3.8)
4	T	T (9.7), Y (3.3)	T (14.1), Y (5.5)
5	I	I (13.6), T (1.9)	I (22.8), T (3.3)
6	V	V (10.8), I (2.8)	V (17.6), I (5.9)

for by other MetAP activity. An attractive possibility is that specific proteins exist which can only be efficiently processed by MetAP2. Analysis of GAPDH isolated from TNP-470-treated cells indicates this to be the case. Though only half of the GAPDH isolated from drug-treated cells had failed to undergo amino-terminal processing, the fraction of the enzyme with altered mobility by two dimensional electrophoresis appears closer to 70% when examined by autoradiography, a ratio which reflects the constitution of protein synthesized only during the pulse period in the absence of MetAP2 activity and not pre-existing protein (see Figure 3.7). Thus a portion of the protein isolated was likely to be present prior to drug treatment, indicating that an even smaller fraction the protein (perhaps 30%) synthesized in the absence of MetAP2 activity undergoes methionine removal.

The fact that GAPDH has a valine residue in its second translated position may indicate that nascent proteins with penultimate valine residues are generally poor substrates for MetAP1. In this regard it is interesting that the other protein identified whose mobility is altered on two dimensional gels by drug treatment, cyclophilin A, also bears a valine residue in the same position, though it is not known whether this aberrant migration also results from failure to remove the initiator methionine. These observations

concur with studies on the substrate specificity of yeast MetAP1 on tripeptide substrates in vitro (17). In the same study, it was found that tripeptides containing serine or threonine residues in the second position are cleaved with similarly poor efficiency (roughly twenty fold lower than an optimal tripeptide with an alanine residue in position two). Whether initiator methionine retention of proteins with serine or threonine in the second translated position will turn out to be compromised in cells treated with TNP-470 remains to be seen. Such a possibility is particularly intriguing given the tendency for proteins with amino-terminal serine or threonine residues to be acetylated (12-16). Failure to remove the initiator methionine in this situation would result in the presence of an abnormal positively charged group at the amino-terminus, which may contribute to changes in activity.

We observed a decrease in incorporation of labeled myristate for only a single detectable protein upon with TNP-470 treatment. While this is likely to reflect decreased myristoylation of this unknown protein, it may also reflect the presence of lower levels of the protein in TNP-470-treated cells. In either case, our observations indicate that at least for most proteins destined to be myristoylated, MetAP1 can compensate in the absence of MetAP2 activity. This may be due to the fact that all myristoylated proteins bear glycine residues at their amino-termini and thus the nascent proteins are processed equally well by either MetAP, as suggested by in vitro studies with peptide substrates (7,17-19). Given that it appears in some cases that sequence context beyond the second translated residue is important for determining the fate of the initiator methionine, it is possible that the substrate specificities of MetAP1 and MetAP2 also bear subtle differences from one another which are dictated by other residues as well, which may account for the single myristoylated protein of 150 kD whose labeling is decreased by drug treatment, and may mean that there are other such proteins outside of our limits of detection which fail to be myristoylated in the presence of TNP-470. It was recently reported that myristoylation of endothelial nitric oxide synthase (eNOS) is decreased by 50% in BAECs treated with TNP-470 (43). However, high concentrations (5 μ M),

which correlated with cytotoxicity rather than growth arrest, were used in this study, indicating that inhibition of eNOS myristoylation (and cell death) may have resulted from non-specific effects such as inhibition of MetAP1 as well as MetAP2. The molecular weight of eNOS is consistent with it being identical to the protein observed in our experiments, indicating the possibility that eNOS myristoylation is hampered by specific inhibition of MetAP2. Experiments to examine this possibility are currently underway.

A crucial component to understanding the mechanism of action of TNP-470 and ovalicin lies in the identity of these specific MetAP2 substrates whose activity is affected by differential methionine removal. At this time it is not known what fraction of cellular proteins are specifically processed by MetAP2. A number of proteins involved in cell cycle regulation, such as cyclin E, pRb, and Cdk4, are predicted to have their initiator methionine residues removed as judged by the identity of their second translated residues (44), though it is not known if maintenance of the amino-terminal methionine on any of these proteins would affect their activity. The Src family protein tyrosine kinases, which are myristoylated, play an essential role in cell cycle progression, and are likely to be inactive in this regard without proper localization (21,45). Such kinases may be expressed at low levels and were thus below the limit of detection in our endothelial cell protein myristoylation assay. The possibility that the myristoylation of various Src family kinases is diminished by TNP-470 treatment is the subject of current investigation.

References for Chapter 3

1. Kendall, R. L., Yamada, R., and Bradshaw, R. A. (1990) Cotranslational amino-terminal processing. *Meth. Enzymol.* **185**, 398-407.
2. Bradshaw, R. A., Brickey, W. W., and Walker, K. W. (1998) N-Terminal processing: the methionine aminopeptidase and N^α-acetyl transferase families. *Trends. Biochem. Sci.* **23**, 263-267.
3. Meinnel, T., Mechulam, Y., and Blanquet, S. (1993) Methionine as translation start signal: a review of the enzymes of the pathway in *Escherichia coli*. *Biochimie* **75**, 1061-1075.
4. Chang, S.-Y., McGary, E. C., and Chang, S. (1989) Methionine aminopeptidase gene of *Escherichia coli* is essential for cell growth. *J. Bacteriol.* **171**, 4071-4072.
5. Jackson, R., and Hunter, T. (1970) Role of methionine in the initiation of haemoglobin synthesis. *Nature* **227**, 672-676.
6. Arfin, S. M., Kendall, R. L., Hall, L., Weaver, L. H., Stewart, A. E., Matthews, B. W., and Bradshaw, R. A. (1995). Eukaryotic methionyl aminopeptidases: two classes of cobalt-dependent enzymes. *Proc. Natl. Acad. Sci. USA* **92**, 7714-7718.
7. Li, X. and Chang, Y.-H. (1995). Amino-terminal protein processing in *Saccharomyces cerevisiae* is an essential function that requires two distinct methionine aminopeptidases. *Proc. Natl. Acad. Sci. USA* **92**, 12357-12361.
8. Walker, K. W., and Bradshaw, R. A. (1998) Yeast methionine aminopeptidase I can utilize either Zn²⁺ or Co²⁺ as a cofactor: a case of mistaken identity? *Protein Sci.* **7**, 2684-2687.
9. Chang, Y.-H., Teichert, U., and Smith, J. A. (1992) Molecular cloning, sequencing, deletion, and overexpression of a methionine aminopeptidase gene from *Saccharomyces cerevisiae*. *J. Biol. Chem.* **267**, 8007-8011.
10. Zuo, S., Guo, Q., Ling, C., and Chang, Y.-H. (1995) Evidence that two zinc fingers in the methionine aminopeptidase from *Saccharomyces cerevisiae* are important for normal growth. *Mol. Gen. Genetics* **246**, 247-253.
11. Klinkenberg, M., Ling, C., and Chang, Y.-H. (1997) A dominant negative mutation in *Saccharomyces cerevisiae* methionine aminopeptidase-1 affects catalysis and interferes with the function of methionine aminopeptidase-2. *Arch. Biochem. Biophys.* **347**, 193-200.
12. Huang, S., et al. (1987) Specificity of cotranslational amino-terminal processing of proteins in yeast. *Biochemistry* **26**, 8242-8246.
13. Moerschell, R. P., Hosokawa, Y., Tsunasawa, S., and Sherman, F. (1990) The specificities of yeast methionine aminopeptidase and acetylation of amino-terminal methionine in vivo. *J. Biol. Chem.* **265**, 19638-19643.
14. Flinta, C., Persson, B., Jörnvall, H., and von Heijne, G. (1986) Sequence determinants of cytosolic N-terminal protein processing. *Eur. J. Biochem.* **154**, 193-196.
15. Boissel, J.-P., Kasper, T. J., and Bunn, H. F. (1988) Cotranslational amino-terminal processing of cytosolic proteins: cell-free expression of site directed mutants of human hemoglobin. *J. Biol. Chem.* **263**, 8443-8449.

16. Tsunasawa, S., Stewart, J. W., and Sherman, F. (1985) Amino-terminal processing of mutant forms of yeast iso-1-cytochrome *c*. *J. Biol. Chem.* **260**, 5382-5392.
17. Chang, Y.-H., Teichert, U., and Smith, J. A. (1990) Purification and characterization of a methionine aminopeptidase from *Saccharomyces cerevisiae*. *J. Biol. Chem.* **265**, 19892-19897.
18. Kendall, R. L., and Bradshaw, R. A. (1992) Isolation and characterization of the methionine aminopeptidase from porcine liver responsible for the co-translational processing of proteins. *J. Biol. Chem.* **267**, 20667-20673.
19. Li, X. and Chang, Y.-H. (1996). Evidence that the human homologue of a rat initiation factor-2 associated protein (p67) is a methionine aminopeptidase. *Biochem. Biophys. Res. Commun.* **227**, 152-159.
20. Towler, D. A., Gordon, J. I., Adams, S. P., and Glaser, L. (1988) The biology and enzymology of eukaryotic protein acylation. *Ann. Rev. Biochem.* **57**, 69-99.
21. Kamps, M. P., Buss, J. E., and Sefton, B. M. (1985) Mutation of NH₂-terminal glycine of p60^{src} prevents both myristoylation and morphological transformation. *Proc. Natl. Acad. Sci. USA* **82**, 4625-4628.
22. Gordon, J. I., Duronio, R. J., Rudnick, D. A., Adams, S. P., and Gokel, G. W. (1991) Protein N-myristoylation. *J. Biol. Chem.* **266**, 8647-8650.
23. Johnson, D. R., Bhatnagar, R. S., Knoll, L. J., and Gordon, J. I. (1994) Genetic and biochemical studies of protein myristoylation. *Ann. Rev. Biochem.* **63**, 869-914.
24. Brown, J. L. and Roberts, W. K. (1976) Evidence that approximately eighty per cent of the soluble proteins from Ehrlich ascites cells are N^α-acetylated. *J. Biol. Chem.* **251**, 1009-1014.
25. Pestana, A. and Pitot, H. C. (1975) Acetylation of nascent polypeptide chains on rat liver polyribosomes in vivo and in vitro. *Biochemistry* **14**, 1404-1412.
26. Johnson, G. G. and Chapman, V. M. (1987) Altered turnover of hypoxanthine phosphoribosyltransferase in erythroid cells of mice expressing *Hprt a* and *Hprt b* alleles. *Genetics* **116**, 313-320.
27. Varshavsky, A. (1996) The N-end rule: functions, mysteries, uses. *Proc. Natl. Acad. Sci. USA* **93**, 12142-12149.
28. Nishizawa, M., Okazaki, K., Furuno, N., Watanabe, N., and Sagata, N. (1992) The 'second-codon' rule and autophosphorylation govern the stability and activity of Mos during the meiotic cell cycle in *Xenopus* oocytes. *EMBO J.* **11**, 2433-2446.
29. Hämmerle, M., Bauer, J., Rose, M., Szallies, A., Thumm, M., Düsterhus, S., Mecke, D., Entian, K.-D., and Wolf, D. H. (1998) Proteins of newly isolated mutants and the amino-terminal proline are essential for ubiquitin-proteasome-catalyzed catabolite degradation of fructose-1,6-bisphosphatase of *Saccharomyces cerevisiae*. *J. Biol. Chem.* **273**, 25000-25005.
30. Mine, S., Ueda, T., Hashimoto, Y., and Imoto, T. (1997) Improvement of the refolding yield and solubility of hen egg-white lysozyme by altering the Met residue attached to its N-terminus to Ser. *Protein Eng.* **10**, 1333-1338.

31. Hoffman, S. J., Looker, D. L., Roehrich, J. M., Cozart, P. E., Durfee, S. L., Tedesco, J. L., and Stetler, G. L. (1990) Expression of fully functional tetrameric human hemoglobin in *Escherichia coli*. *Proc. Natl. Acad. Sci. USA* **87**, 8521-8525.
32. Meierhans, D. and Alleman, R. K. (1998) The N-terminal methionine is a major determinant of the DNA binding specificity of MEF-2C. *J. Biol. Chem.* **273**, 26052-26060.
33. Griffith, E. C., Su, Z., Turk, B. E., Chen, S., Chang, Y.-W., Wu, Z., Biemann, K., Liu, J. O. (1997) Methionine aminopeptidase (type 2) is the common target for angiogenesis inhibitors TNP-470 and ovalicin. *Chem. Biol.* **4**, 461-471.
34. Sin, N., Meng, L., Wang, M. Q. W., Wen, J., Bornmann, W. G., and Crews, C. M. (1997) The anti-angiogenic agent fumagillin covalently binds and inhibits the methionine aminopeptidase, MetAP2. *Proc. Natl. Acad. Sci. USA* **94**, 6099-6103.
35. Laemmli, U. K. (1970) Cleavage of structural proteins during the assembly of the head of bacteriophage T4. *Nature* **227**, 680-685.
36. O'Farrell, P. Z., and Goodman, H. M. (1976) Resolution of simian virus 40 proteins in whole cell extracts by two-dimensional electrophoresis: heterogeneity of the major capsid protein. *Cell* **9**, 289-298.
37. O'Farrell, P. Z., Goodman, H. M., and O'Farrell, P. H. (1977) High resolution two-dimensional electrophoresis of basic as well as acidic proteins. *Cell* **12**, 1133-1142.
38. Magee, A. I., Wootton, J., and de Bony, J. (1995) Detecting radiolabeled lipid-modified proteins in polyacrylamide gels. *Meth. Enzymol.* **250**, 330-337.
39. Shevchenko, A., Wilm, M., Vorm, O., and Mann, M. (1996) Mass spectrometric sequencing of proteins from silver-stained polyacrylamide. *Anal. Chem.* **68**, 850-858.
40. Alexander, M., Curtis, G., Avruch, J., and Goodman, H. M. (1985) Insulin regulation of protein biosynthesis in differentiated 3T3 adipocytes: regulation of glyceraldehyde-3-phosphate dehydrogenase. *J. Biol. Chem.* **260**, 11978-11985.
41. Kulbe, K. D., Jackson, K. W., and Tang, J. (1975) Evidence for a liver-specific glyceraldehyde-3-phosphate dehydrogenase. *Biochem. Biophys. Res. Commun.* **67**, 35-42.
42. Ahmad, H., Sing, S. V., Medh, R. D., Ansari, G. A. S., Kurosky, A., and Awasthi, Y. C. (1988) Differential expression of α , μ , and π classes of isozymes of glutathione S-transferase in bovine lens, cornea, and retina. *Arch. Biochem. Biophys.* **256**, 416-426.
43. Yoshida, T., Kaneko, Y., Tsukamoto, A., Han, K., Ichinose, M., and Kimura, S. (1998) Suppression of hepatoma growth and angiogenesis by a fumagillin derivative TNP470: Possible involvement of nitric oxide synthase. *Cancer Res.* **58**, 3751-3756.
44. NCBI Entrez protein database. Accession numbers: 3041657 (cyclin E), 793995 (pRb), and 1168867 (cdk4).
45. Roche, S., Koegl, M., Barone, M. V., Roussel, M. F., and Courtneidge, S. A. (1995) DNA synthesis induced by some but not all growth factors requires Src family protein tyrosine kinases. *Mol. Cell. Biol.* **15**, 1102-1109.

Chapter 4

A common mode of action for the anti-angiogenic and immunosuppressive properties of TNP-470 and ovalicin

Abstract

TNP-470 (1), a synthetic derivative of the natural product fumagillin (2), potently inhibits angiogenesis in vivo and the growth of endothelial cell cultures in vitro. The structurally related natural product ovalicin (3) also inhibits angiogenesis but possesses potent immunosuppressive activity. The recent finding that all three drugs bind and inhibit the same target, methionine aminopeptidase 2 (MetAP2), raised the question of whether TNP-470 is also immunosuppressive and whether inhibition of MetAP2 underlies both activities of ovalicin. To address these questions, we synthesized a series of analogs of TNP-470 and ovalicin and tested them for their abilities to inhibit the proliferation of either endothelial cell or mixed lymphocyte cultures. TNP-470 and its analogs were found to possess both immunosuppressive and anti-angiogenic activities. A strong correlation was observed between the ability of compounds to inhibit bovine and human endothelial cell growth and their ability to inhibit the mouse mixed lymphocyte reaction (MLR), implying that the two activities share a common molecular basis, i.e., inhibition of MetAP2. Interestingly, ovalicin and several other compounds behaved differently in the human MLR than in either the mouse MLR or human endothelial cell proliferation assays, pointing to possible species-specific and cell type-specific differences in the metabolism or uptake of these compounds. Ovalicin and TNP-470 were not found to inhibit IL-2 production or upregulation of CD25, but rather to inhibit IL-2-dependent T cell proliferation.

Introduction

The success of organ transplantation is generally limited by rejection of the graft by the host immune system (1). Whereas only a small fraction of naive T lymphocytes carried

by the host organism are specific to a typical infectious agent, a relatively large proportion will be reactive against a graft from a genetically distinct individual, largely due to the presence of foreign major histocompatibility complex (MHC) molecules (2). This incompatibility gives rise to a rapid and strong immune response. For this reason, successful organ transplantation requires the use of immunosuppressive drugs, which inhibit the expansion of T cells reactive against the donor graft (3,4). Early immunosuppressive therapy employed combinations of cytotoxic compounds, which are selectively toxic to rapidly dividing cells, and corticosteroids, which are both cytotoxic and modulate cytokine production by lymphoid cells (3,4). As immunosuppressive therapy must be maintained indefinitely for most organs, serious side effects associated with these drugs prevented their widespread use.

The development of cyclosporin A in the early 1970s revolutionized the practice of transplant medicine and allowed both the number of transplants performed and the number of organ types suitable for transplantation to increase dramatically (4,5). While unequaled in its selectivity for the immune system, cyclosporin A is also restricted by side effects such as nephrotoxicity, which has stimulated the search for a next generation of less toxic immunosuppressive drugs which may be applicable to a wider range of disorders, such as autoimmune diseases.

T cell activation, the primary event in a graft rejection response, can be regarded as a stepwise process (6). Engagement of the T cell receptor by its cognate ligand, the MHC-peptide complex, triggers a signal transduction cascade culminating in the activation of genes required to drive cell proliferation. A crucial part of this response is the production of the autocrine growth factor interleukin-2 (IL-2) (6,7). The effects of cyclosporin A are largely attributed to its ability to inhibit IL-2 production by activated T lymphocytes; addition of excess IL-2 can reverse the effects of the drug on T cell proliferation in vitro (8). The molecular basis for inhibition of IL-2 by cyclosporin A has been elucidated in recent years (9). The drug binds to a protein called cyclophilin, which possesses peptidyl-prolyl cis-trans isomerase activity. Interestingly, the more recently

discovered drug FK506, which also inhibits IL-2 production though it bears no structural similarity to cyclosporin A, binds to a distinct protein (FKBP) which has the same enzymatic activity. Suppression of IL-2 production, however, does not occur by inhibiting the rotamase activity of these enzymes. Both the cyclosporin A-cyclophilin and FK506-FKBP complexes bind to and inhibit the protein phosphatase calcineurin. Calcineurin plays a key role in relaying signals from the T cell receptor to the nucleus during T cell activation. T cell receptor engagement results in an influx of calcium ions to the cell cytosol, and calcineurin is thereby activated by binding to the calcium sensing protein calmodulin. An important substrate for calcineurin is the transcription factor NF-AT (nuclear factor of activated T cells) which translocates to the nucleus following dephosphorylation by calcineurin where it participates directly in the induction of the IL-2 gene (10).

Other immunosuppressive compounds appear to act at distinct steps in the T cell activation cascade. The marine natural product discodermolide has been shown to downregulate the IL-2 receptor by an unknown mechanism, thereby preventing cells from responding to IL-2 (11). Rapamycin, which bears structural similarity to FK506, blocks IL-2-dependent T cell proliferation (12). Like FK506, rapamycin binds to FKBP, but the complex does not inhibit calcineurin. Rather, the rapamycin-FKBP complex binds to and inhibits a protein kinase called FRAP (also known as RAFT) (13). FRAP acts as an intermediary in the growth factor-mediated regulation of the translation of specific proteins which presumably play a role in promoting cell cycle progression through the G₁ phase.

The fungal metabolite ovalicin (3) was discovered in the 1960s and showed promise as a potent immunosuppressive drug prior to the development of cyclosporin A (14). It has been shown to inhibit antibody responses, reduce spleen weight, and prolong skin graft survival in mice, and to inhibit the development of experimental allergic encephalomyelitis in rats (15,16). In addition, ovalicin was shown to inhibit the proliferation of mouse and human mixed lymphocyte cultures, a cellular assay measuring

alloantigen-stimulated T cell proliferation (17,18). Ovalicin went as far as to be tested in human clinical trials but was discontinued due to serious side effects (14). The mechanism of action of the drug has never been determined. The emergence of the structurally similar compounds TNP-470 (1) and fumagillin (2) as angiogenesis inhibitors led to the observation that ovalicin inhibits the growth of endothelial cells as well (19,20). This structural similarity begs the speculation that TNP-470 may also possess immunosuppressive activity, which could have implications for its use in the clinic. Paradoxically, TNP-470 has been shown to enhance, rather than inhibit, T-cell dependent B lymphocyte proliferation in vitro and in mice (21,22).

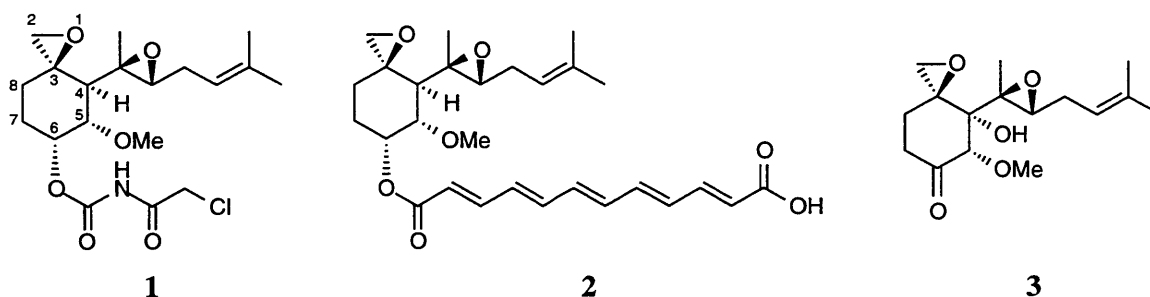


Figure 4.1. Structures of TNP-470 (1), fumagillin (2), and ovalicin (3), illustrating the atom numbering system referred to in the text.

Recently, we and others showed that TNP-470, fumagillin, and ovalicin all covalently bind and inactivate a common target, MetAP2 (23,24, see Chapter 2). Using a series of drug analogs, we found a strong correlation between the ability of compounds to inhibit the growth of cultured endothelial cells and to inhibit MetAP2 activity. However, it remains unknown whether MetAP2 inhibition also mediates the immunosuppressive activity of ovalicin. As both TNP-470 and ovalicin appear to share the same molecular target, it is even more puzzling that the aforementioned difference exists between the apparent immunostimulatory activity of TNP-470 and the immunosuppressive activity of ovalicin. To explore the relationship between the anti-angiogenic and immunosuppressive properties of these compounds, we tested a variety of TNP-470 and ovalicin derivatives for their effects on mouse and human mixed lymphocyte cultures. We

report that TNP-470 possesses potent antiproliferative activity against both mouse and human mixed lymphocyte cultures. We found a strong correlation between the activities of all analogs tested in the endothelial cell proliferation assay and the MLR, implying that there is a common molecular basis for the anti-angiogenic and immunosuppressive activities of this class of drugs. Surprisingly, we also found that the activity of several compounds diverged greatly between the mouse and human MLR. Inhibition of human endothelial cell growth correlated better with inhibition of the mouse MLR than the human MLR, indicating that there may be cell-type specific differences in availability and metabolism of TNP-470, ovalicin and their analogs that vary between species. Additionally, we investigated the site in the T cell activation pathway which is inhibited by ovalicin and TNP-470. While IL-2 production is unaffected by drug treatment, IL-2-induced cell proliferation is inhibited by TNP-470, indicating a mode of action similar to rapamycin.

Materials and Methods

All compounds used were synthesized by Zhuang Su in the Liu laboratory. Solvents were reagent grade and dried prior to use in most cases. Moisture-sensitive reactions were carried out in a flame-dried apparatus under a N₂ atmosphere. Column chromatographic separations were performed with TSI Chemical silica gel 60 (230-400 mesh). The products were dried under high vacuum over night or over P₂O₅ at ambient temperature. TLC was performed with Merck silica gel 60 *F*₂₅₄ precoated plates and products were detected with UV light, I₂, 10% H₂SO₄ in MeOH, KMnO₄ solution (2.0 g KMnO₄, 4.0 g Na₂CO₃, 100 mL H₂O) or *p*-anisaldehyde solution (3.7 mL *p*-anisaldehyde, 1.5 mL AcOH, 5 mL H₂SO₄, 135 mL EtOH). IR spectroscopy was performed with a Perkin-Elmer FT IR spectrometer. NMR spectra were acquired using a Varian VXR-500 spectrometer (¹H, 500 MHz), in CDCl₃; Chemical shifts are reported as ppm downfield from TMS internal standard. MS was performed with Finnegan MATT-8200 spectrometer. Compounds **1**, **5**, **8**, **12**, and **14** were prepared as described (25-27).

(3S,4R,5R,6R)-4-[(1'S,2'S)-1',2'-Epoxy-1',5'-dimethyl-4'-hexenyl]-5-methoxy-6-O-(N-chloroacetyl)carbamoyl-1-oxaspiro[2.5]octane-4,6-diol (6). To a stirred solution of **9** (35 mg, 0.12 mmol) in 3 mL of CH₂Cl₂ was added chloroacetyl isocyanate (56 mg, 40 mL, 0.47 mmol) at 0 °C. The reaction mixture was stirred for 1.5 h at room temperature, then diluted with ethyl acetate and washed with saturated aqueous NaHCO₃ and brine. The organic phase was dried over anhydrous MgSO₄ and concentrated in vacuo. The residue was chromatographed on silica gel (ether/hexane, 1:2 used as the eluent) to give 39 mg (77.7%) of the product as colorless oil. IR (neat) cm⁻¹: 3466, 3282, 2964, 2935, 1753, 1719, 1497, 1221, 1197, 1101, 1076; ¹H NMR (500 MHz, CDCl₃): 8.16 (1H, S), 5.57 (1H, q, *J* = 3.4 Hz), 5.16 (1H, t, *J* = 7.3 Hz), 4.48 (2H, s), 3.65 (1H, d, *J* = 3.9 Hz), 3.48 (3H, s), 3.09 (1H, s), 2.99 (1H, t, *J* = 6.8 Hz), 2.97 (1H, d, *J* = 4.4 Hz), 2.54 (1H, d, *J* = 4.4 Hz), 2.50-2.36 (2H, m), 2.18-2.10 (1H, m), 2.06-1.90 (2H, series of m), 1.73 (3H, s), 1.65 (3H, s), 1.33 (3H, s), 1.08 (1H, m); MS (FAB) *m/z*: 440.2 (M+Na⁺, 100).

(3S,4R,5R,6R)-4-[(1'S,2'S)-1',2'-Epoxy-1',5'-dimethyl-4'-hexenyl]-5-methoxy-6-O-(4''-chlorobutyryl)-1-oxaspiro[2.5]octane-4,6-diol (7). 4-Chlorobutyryl chloride (18 mg, 14 mL, 0.13 mmol) was added to a magnetically stirred solution of **9** (25 mg, 0.084 mmol) and dimethylaminopyridine (DMAP, 15 mg) in CH₂Cl₂ (4 mL) at 0 °C. After stirring for overnight, the reaction was diluted with CHCl₃ and which was washed with saturated aqueous NH₄Cl solution. The organic phase was dried, filtered, and evaporated. Chromatography of the residue on silica gel (eluted with 25% ethyl acetate in hexanes) resulted in 31 mg (91.5%) of the product as a colorless oil. IR (neat) cm⁻¹: 3514, 2935, 1728, 1443, 1376, 1245, 1202, 1173, 1144, 1101, 1004, 956, 927; ¹H NMR (500 MHz, CDCl₃): 5.60 (1H, dd, *J* = 3.4 and 7.8 Hz), 5.18 (1H, t, *J* = 7.5 Hz), 3.63 (1H, d, *J* = 3.9 Hz), 3.61 (2H, t, *J* = 6.5 Hz), 3.46 (3H, s), 3.02 (1H, t, *J* = 6.5 Hz), 2.96 (1H, d, *J* = 4.4 Hz), 2.87 (1H, s), 2.55 (1H, d, *J* = 6.8 Hz), 2.53 (1H, d, *J* = 7.3 Hz), 2.51 (1H, d, *J* = 4.4 Hz), 2.43-2.33 (2H, series of m), 2.18-2.07 (3H, series of m), 1.80-1.84 (2H, series of m),

1.74 (3H, s), 1.65 (3H, s), 1.34 (3H, s), 1.14 (1H, dt, $J = 4.4, 13.7$ Hz); MS(FAB) m/z : 425.1 (M+Na⁺, 100).

(3S,4R,5R,6R)-4-[(1'S,2'S)-1',2'-Epoxy-1',5'-dimethyl-4'-hexenyl]-5-methoxy-1-oxaspiro[2.5]octane-4,6-diol (9). To a stirred solution of ovalicin (**3**, 100 mg, 0.34 mmol) in 5 mL of 1,4-dioxane was added sodium borohydride (25.5 mg, 0.67 mmol) at 0 °C. The reaction mixture was stirred for 30 min at room temperature, after which the reaction was quenched by adding saturated aqueous NH₄Cl and extracted with CHCl₃. The combined organic extracts were dried, filtered, and evaporated, and the residue was chromatographed on silica gel (elution with 50% ether in hexane). There was 95 mg (93.7%) of the desired product as a colorless oil. IR (neat) cm⁻¹: 3442, 2925, 1439, 1415, 1381, 1201, 1137, 1108, 1030, 981, 923, 801; ¹H NMR (500 MHz, CDCl₃): 5.16 (1H, t, $J = 7.5$ Hz), 4.45-4.38 (1H, m), 4.02 (1H, d, $J = 9.3$ Hz), 3.57 (1H, s), 3.50 (1H, t, $J = 3.4$ Hz), 3.50 (3H, s), 2.95 (1H, d, $J = 4.4$ Hz), 2.87 (1H, t, $J = 6.35$ Hz), 2.52-2.50 (1H, m), 2.54 (1H, d, $J = 4.4$ Hz), 2.44-2.35 (1H, m), 2.18-2.10 (1H, m), 2.07-2.00 (1H, 2m), 1.84-1.75 (1H, m), 1.73 (3H, s), 1.65 (3H, s), 1.33 (3H, s), 1.01-0.94 (1H, 2m); MS(FAB) m/z : 321.4 (M+Na⁺, 100).

(1R,2S,3R,4R)-1-Methylthiomethylene-2-[(1'S,2'S)-1',2'-epoxy-1',5'-dimethyl-4'-hexenyl]-3-methoxycyclohexane-1,2,4-triol (11). To a stirred solution of **9** (26 mg, 0.087 mmol) in 2 mL of DMF was added CH₃SH (18 mg, 0.26 mmol) at room temperature. The reaction mixture was stirred for 1.5 h, then diluted with ethyl acetate and washed with saturated aqueous NaHCO₃ and brine. The organic phase was dried over anhydrous MgSO₄ and concentrated in vacuo, and the residue was chromatographed on silica gel (ethyl acetate/hexane, 1:2 used as the eluent) to give 21 mg (70.0%) of the product as colorless oil. IR (neat) cm⁻¹: 3430, 2924, 1441, 1382, 1324, 1154, 1100, 1057, 1037, 833; ¹H NMR (500 MHz, CDCl₃): 5.19 (1H, t, $J = 7.3$ Hz), 4.33-4.29 (1H, m), 3.70 (1H, br., s), 3.49 (3H, s), 2.97 (1H, t, $J = 6.5$ Hz), 2.90 (1H, d, $J = 13.2$ Hz), 2.76 (1H, d, $J = 13.2$ Hz), 2.60-2.40 (2H, m), 2.25-2.17 (1H, m), 2.14 (3H, s), 1.97-1.81 (3H,

m), 1.73 (3H, s), 1.66 (3H, s), 1.62-1.54 (1H, m), 1.49 (3H, s); MS(FAB) *m/z*: 469.5 (M+Na⁺, 100).

(1R,2S,3R,4R)-1-Methylthiomethylene-2-[(1'S,2'S)-1',2'-epoxy-1',5'-dimethyl-4'-hexenyl]-3-methoxy-4-O-(N-chloroacetyl)carbamoyl-cyclohexane-1,2,4-triol (13).

To a stirred solution of **11** (30 mg, 0.087 mmol) in 2.5 mL of CH₂Cl₂ was added chloroacetyl isocyanate (11 mg, 8 mL, 0.094 mmol) at 0 °C. The reaction mixture was stirred for 1.5 h at room temperature, then diluted with ethyl acetate and washed with saturated aqueous NaHCO₃ and brine. The organic phase was dried over anhydrous MgSO₄ and concentrated in vacuo. The residue was chromatographed on silica gel (ether/hexane, 1:2 used as the eluent) to give 35 mg (86.3%) of the product as colorless oil. IR (neat) cm⁻¹: 3485, 3263, 2964, 2925, 1753, 1719, 1501, 1376, 1202, 1158, 1105, 1072, 1028; ¹H NMR (500 MHz, CDCl₃): 8.26 (1H, br., s), 5.51 (1H, d, *J* = 2.9 Hz), 5.18 (1H, t, *J* = 7.3 Hz), 4.42 (2H, s), 3.81 (1H, br., s), 3.43 (3H, s), 3.05 (1H, t, *J* = 6.6 Hz), 2.95 (1H, d, *J* = 13.7 Hz), 2.84 (1H, m), 2.48-2.40 (1H, m), 2.23-2.16 (1H, m), 2.14 (3H, s), 2.04-1.97 (1H, dm), 1.95-1.80 (2H, series of m), 1.78-1.50 (3H, series of m), 1.72 (3H, s), 1.66 (3H, s), 1.47 (3H, s); MS(FAB) *m/z*: 488.1 (M+Na⁺, 100).

Cell Culture. To isolate splenocytes, mice were sacrificed by asphyxiation, and their spleens were removed and pulverized between ground glass slides. Cells were filtered through nylon mesh and erythrocytes lysed in 17 mM TrisHCl/140 mM NaCl for 5 min at 37 °C. Intact cells were washed several times in 4% fetal bovine serum (FBS) in PBS and resuspended in culture medium (RPMI with 10% FBS, 50 μM β-mercaptoethanol, 50 units/mL penicillin and 50 μg/mL streptomycin). Human PBMCs were isolated by step gradient centrifugation on Ficoll-Paque Plus (Pharmacia) and cultured in RPMI containing 10% human type AB serum, 50 μM β-mercaptoethanol, 50 units/mL penicillin and 50 μg/mL streptomycin. HUV-EC-C cells were obtained from the American Type Culture Collection and cultured in Kaign's modification of Ham's F12 media containing 10% FBS, 100 μg/mL heparin, and 30 μg/mL endothelial cell growth supplement (Sigma), 50

units/mL penicillin and 50 µg/mL streptomycin. Flasks and plates were pretreated with endothelial cell attachment factor (Sigma).

Mixed Lymphocyte Reaction. For the mixed lymphocyte reaction, splenocytes from responder (Balb/c) and stimulator (C57/Black 6) mice (5×10^5 of each per well) or human PBMCs from two donors (1×10^5 of each per well) were cultured in a volume of 200 µL in U-bottom 96-well plates in the presence of varying concentrations of drugs or carrier alone (0.5% ethanol) for either 96 h (mouse) or 154 h (human). Cells were treated with 1 µCi [methyl- ^3H] thymidine (6.7 Ci/mmol) per well for the last 8 h of culture and then harvested onto glass fiber paper for scintillation counting.

Preparation of T cell blasts. Mouse splenocytes or lymph node cells were plated into 24-well plates at a density of 2×10^6 /mL and stimulated with 5 µg/mL concanavalin A (Con A) for 48 hr. Cultures were expanded into media containing 100 U/mL IL-2 (Pharmacia). To measure IL-2 dependent proliferation, confluent T cell blasts were diluted tenfold into 96-well plates in either media alone or media containing IL-2 plus varying concentrations of drug or carrier alone (0.5% EtOH). Plates were incubated for 48 hr and labeled with [^3H] thymidine, harvested and counted as described above.

Concanavalin A (Con A)-dependent proliferation. Mouse splenocytes or lymph node cells were plated into 96-well plates at 10^6 /mL (200 µL per well). Drugs and Con A were added to the indicated concentration and plates were incubated 48 hr, labeled and harvested as described above.

Analysis of IL-2 production and IL-2 receptor expression by murine splenocytes. Single cell suspensions of splenocytes from a C57/Black 6 mouse were prepared as described above. Cells were aliquotted into 96-well plates at 10^6 cells/mL (200 µL per well) and treated with drug at the indicated concentration or carrier solvent alone (0.5% EtOH) followed by Con A to a final concentration of 1 µg/mL. After 22 hr at 37 °C in a humidified incubator, cells were harvested by centrifugation. Supernatants were analyzed for IL-2 by enzyme-linked immunosorbent assay (ELISA). Cells pooled from two identically treated wells were suspended in 47 µL 4% FBS in PBS. F_cBlock (1 µL, 0.5

mg/mL) was added, and cells were incubated 5 min on ice prior to the addition of FITC conjugated anti-CD25 (1 μ L, 0.5 mg/mL, Pharmingen) and PE conjugated anti-Thy 1.2 (1 μ L, 0.2 mg/mL, Pharmingen). Cells were incubated on ice in the dark for 20 min. Cells were washed by adding 3 mL 4% FBS/PBS, pelleted, and resuspended in 0.5 mL 4% FBS/PBS containing 1 μ g/mL PI, and analyzed by flow cytometry.

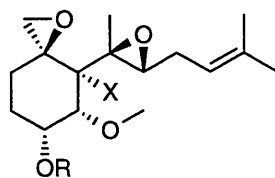
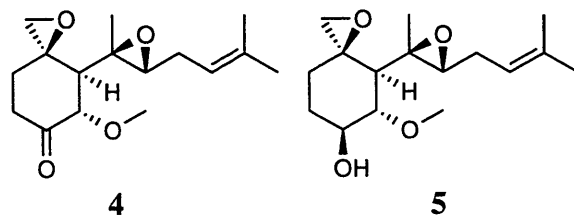
Endothelial Cell Proliferation Assay. HUV-EC-C cells (5000 per well) or BAECs (2000 per well) were seeded into 96-well plates and grown for either 96 h (HUV-EC-C) or 72 hr (BAECs) in the presence of varying concentrations of drugs or carrier alone (0.5% ethanol). 3-(4,5-Dimethylthiazol-2-yl)-2,5-diphenyltetrazolium bromide (MTT, 25 μ L, 10 mg/mL in PBS) was added during the final 4 h after which cells were extracted with 100 μ L of 10% SDS/0.1 M HCl per well for 16 h at 37 °C. Plates were read at 600 nm.

Results

To explore the relationship between inhibition of MetAP2, and the anti-angiogenic and immunosuppressive properties of TNP-470 and ovalicin, we synthesized a series of analogs with a wide spectrum of potencies for determining the degree of correlation between those activities. In addition, as TNP-470 (1), fumagillin (2), and ovalicin (3) have all been shown to covalently inactivate MetAP2, we were interested in evaluating the relative contributions of the electrophilic chloroacetyl and epoxide groups of TNP-470 (1) to the activity. Thus, compounds bearing a variety of substituents at the C-6 position of the cyclohexyl ring were prepared with either a hydrogen (fumagillin series) or an hydroxyl group (ovalicin series) at the C-4 position of the ring (Scheme 4.1). In addition, several analogs were synthesized in which the spiro (C-3) epoxide was opened with thiomethane (Scheme 4.2). Compounds in the fumagillin series were prepared according to published procedures (25-27); those in the ovalicin series were prepared analogously as described in the Materials and Methods section.

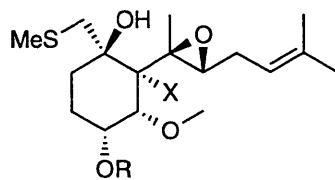
We have shown previously that these compounds are active to varying degrees in inhibition of both MetAP2 enzymatic activity in vitro and endothelial cell proliferation in

Scheme 4.1



	X	R
6	OH	CONHCOCH ₂ Cl
7	OH	CO(CH ₂) ₃ Cl
8	H	CO(CH ₂) ₃ Cl
9	OH	H
10	H	H

Scheme 4.2



	X	R
11	OH	H
12	H	H
13	OH	CONHCOCH ₂ Cl
14	H	CONHCOCH ₂ Cl

cell culture (Chapter 2). In this study, we measured the activity of compounds **1-14** in the mouse MLR (Table 4.1). TNP-470 and fumagillin were found to be potent inhibitors of mouse MLR, indicating that they possess intrinsic immunosuppressive activity. Interestingly, the fumagillin analog (**4**) in which the sidechain at C-6 was removed and replaced with a keto group as in ovalicin is the most potent analog, rivaling ovalicin for inhibition of mouse MLR. A similar trend was observed previously for endothelial cell inhibition, suggesting that the chloroacetyl group of TNP-470 is dispensable for its biological activity. Overall, there is a strong correlation between compounds that are active in the mouse MLR and compounds that are active at inhibiting bovine aortic endothelial cell (BAEC) proliferation (Figure 4.2), though compounds are in general approximately one order of magnitude less potent in the MLR. In both assays, compounds within either the ovalicin or the fumagillin series follow a predictable trend in activity depending on the substituent at the C-6 position, with hydroxyl, chlorobutoyl, chloroacetylcarbonyl, and carbonyl being the order of ascending activity. In contrast, all compounds in which the C-3 epoxide had been opened were much less active than their corresponding analogs with intact epoxides. An intact spiro epoxide moiety also appears essential for strong inhibition of MetAP2 by these compounds, which suggests that the epoxide rather than the chloroacetyl group mediates covalent inactivation of the enzyme (Table 4.1). These results imply that the inhibition of endothelial cell growth and the inhibition of lymphocyte proliferation by these compounds shares a common molecular basis, which is likely to be the inhibition of MetAP2.

As ovalicin has undergone and TNP-470 is currently undergoing human clinical trials, a subset of their synthetic analogs were also examined in the MLR performed with primary human peripheral blood mononuclear cells (PBMC, Table 1). Surprisingly, a number of compounds differed significantly in potency from the analogous mouse MLR and human endothelial cell proliferation assays. Most striking was the immunosuppressive parent drug ovalicin, which was over 1000-fold less active at inhibiting the proliferation of human cells compared to mouse cells. In contrast, ovalicin

Table 4.1. IC₅₀ values for TNP-470 and ovalicin analogs in various assays.^a

Compound	mouse MLR (nM)	human MLR (nM)	HUV-EC-C (nM)	BAEC (nM) ^b	MetAP2 (nM) ^b
1	1.63 ± 0.56	1.42 ± 0.40	0.0084 ± 0.0010	0.037 ± 0.0024	1.0 ± 0.3
2	2.32 ± 0.79	0.22 ± 0.07	0.0616 ± 0.0088	ND	ND
3	0.219 ± 0.011	601 ± 91	0.00253 ± 0.00051	0.018 ± 0.0059	0.4 ± 0.2
4	0.128 ± 0.033	0.29 ± 0.05	0.00202 ± 0.00045	0.013 ± 0.0015	6 ± 2
5	9.69 ± 0.54	0.41 ± 0.38	ND	ND	ND
6	7.23 ± 0.46	5.25 ± 5.78	0.0296 ± 0.0231	0.46 ± 0.26	2.0 ± 0.8
7	21.1 ± 9.2	ND	ND	0.31 ± 0.066	0.1 ± 0.03
8	43.8 ± 12.4	ND	ND	0.12 ± 0.01	3.5 ± 1.8
9	59.9 ± 15.1	89.8 ± 22.9	0.187 ± 0.111	2.2 ± 1.4	4 ± 1
10	199 ± 75	88.6 ± 26.3	1.07 ± 0.33	9.5 ± 4.6	8 ± 2
11	108 ± 20	> 10000	23.7 ± 5.0	65 ± 34	400 ± 200
12	> 5000	> 100000	ND	2800 ± 2300	5000 ± 2000
13	810 ± 230	ND	ND	40 ± 4	400 ± 200
14	877 ± 158	ND	ND	110 ± 18	3000 ± 1000

^aValues represent the mean ± SD for representative experiments performed in triplicate.

^bFor details see Chapter 2. MetAP2 assays were done using recombinant human protein.

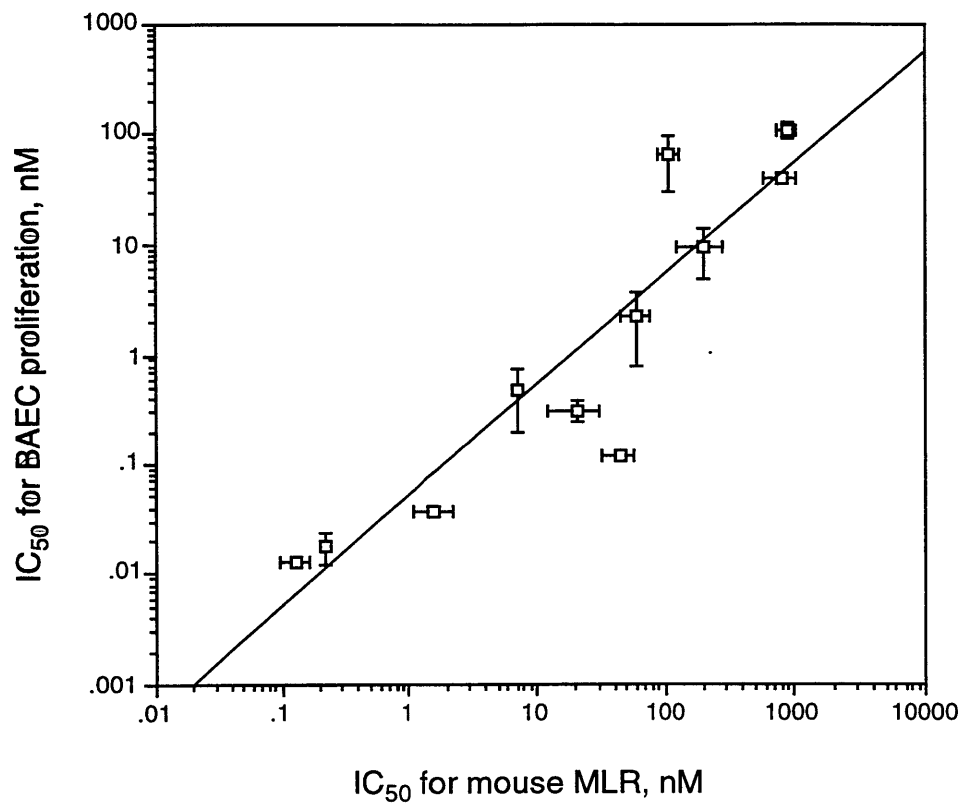


Figure 4.2. Correlation between inhibition of endothelial cell proliferation and the MLR for TNP-470, ovalicin and derivatives.

exhibited little toxicity in rodents but was found to be severely neurotoxic in higher animals. The opposing trends of the immunosuppressive activity and neurotoxicity may account for the failure of ovalicin to have become a useful immunosuppressive drug. Epimerization of the C-6 hydroxyl group of **10** generates **5**, which was not only more active against the MLR for both species but over 20-fold more potent in the human than in the mouse MLR. The potency of **5** in the mouse MLR is similar to that ($IC_{50} = 34$ nM) of a known immunosuppressive natural product, FR65814, which is structurally identical to **5** except the 5-methoxy substituent is replaced by a hydroxyl group (28). Despite these exceptions, there still appears to be a correlation between modifications that enhance or diminish activity in the mouse MLR and those that do in the human MLR. The C-3 epoxide group, for example, appears to be essential for activity in the human MLR as well.

In order to determine whether the differences observed between mouse and human lymphocyte proliferation were due entirely to species differences, we tested the same subset of compounds for their ability to inhibit the growth of HUV-EC-C cells, a human umbilical vein endothelial cell-derived line which is sensitive to TNP-470 (Table 1). We found a stronger correlation between the activity of compounds in this assay and the BAEC inhibition assay or the mouse MLR than the human MLR. Ovalicin (**3**), for example, is among the most potent inhibitors of HUV-EC-C cell growth. These results suggest that there is something unique about human lymphocytes that makes them respond differently to a subgroup of ovalicin and fumagillin analogs.

To further explore the mechanism of immunosuppression by this class of drugs, we chose to determine the step of the T cell activation pathway blocked by ovalicin and TNP-470. We first examined IL-2 production from Con A-stimulated splenocytes (Figure 4.3). Splenocytes were treated with Con A in the presence of either ovalicin or TNP-470 and IL-2 levels in the supernatants were determined by ELISA. Neither drug had any significant effect on Con A-induced IL-2 production at concentrations which caused potent inhibition of Con A-induced proliferation (Figure 4.4). Under these

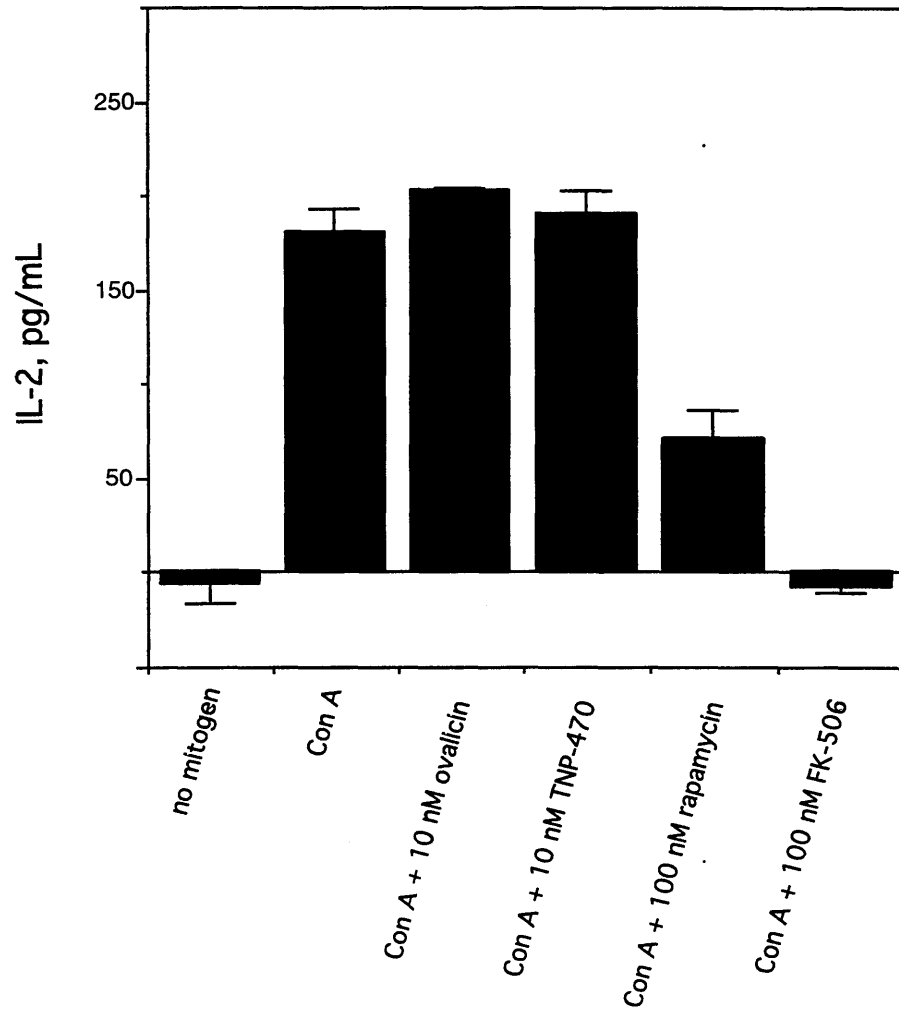


Figure 4.3. Ovalicin and TNP-470 do not effect Con A-stimulated IL-2 production. Splenocytes were stimulated with Con A and culture supernatants were analyzed for IL-2 by ELISA 22 hr later.

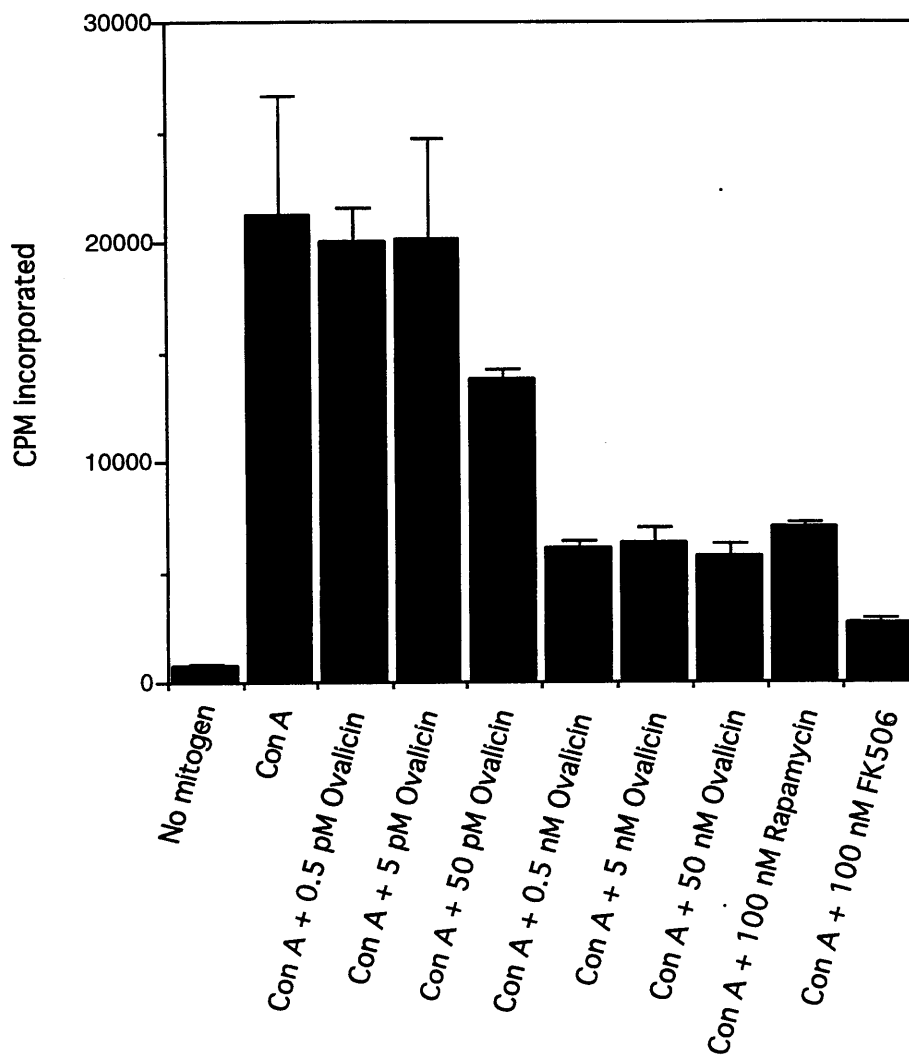


Figure 4.4. Ovalicin inhibits Con A-stimulated mouse lymphocyte proliferation. Splenocytes were incubated with 1 $\mu\text{g}/\text{mL}$ Con A in the presence of indicated drug for 48 hr and proliferation was assayed by [^3H] thymidine incorporation.

conditions, rapamycin caused partial inhibition of IL-2 production, while FK506 completely abrogated IL-2 production.

To determine whether the drugs affected the IL-2 signaling pathway in a manner similar to rapamycin, we examined the sensitivity of T cell blast proliferation to TNP-470. Splenocytes treated with Con A proliferate vigorously for several days and then rapidly stop due to consumption of endogenously generated growth factors. However, cells can be maintained as blasts by the addition of exogenous IL-2. TNP-470 potently inhibited the proliferation of T lymphocyte blasts, which was entirely dependent on added IL-2 (Figure 4.5). During T cell activation, the p70 α chain of the IL-2 receptor, CD25, is upregulated to allow assembly of the high affinity trimeric IL-2 receptor complex (29). Failure to upregulate CD25 could theoretically prevent responsiveness to IL-2 and IL-2 dependent proliferation. To test this possibility, we examined expression of CD25 following Con A stimulation of splenocytes in the presence of TNP-470 and ovalicin (Figure 4.6). Neither drug had any effect on the upregulation of CD25 in T cells at concentrations sufficient to greatly inhibit proliferation. As anticipated, rapamycin also had no effect, whereas FK506 caused a partial decrease in receptor expression. These results indicate that TNP-470 and ovalicin, like the immunosuppressant rapamycin, block the IL-2 dependent signaling pathway.

Discussion

The striking structural similarity between TNP-470 and ovalicin and the recent finding that both bind to the common molecular target MetAP2 appears to contradict reports that TNP-470 has immunostimulatory activity while ovalicin is immunosuppressive. In this study, we measured the effect of both TNP-470 and ovalicin in the MLR and found that TNP-470 does possess potent immunosuppressive activity. Though previous reports have indicated that lymphocyte proliferation is in fact potentiated by TNP-470, those experimental conditions differed from ours in several respects (21,22). Most notably, PHA was used as a mitogen, whereas our experiments used allogenic stimulation.

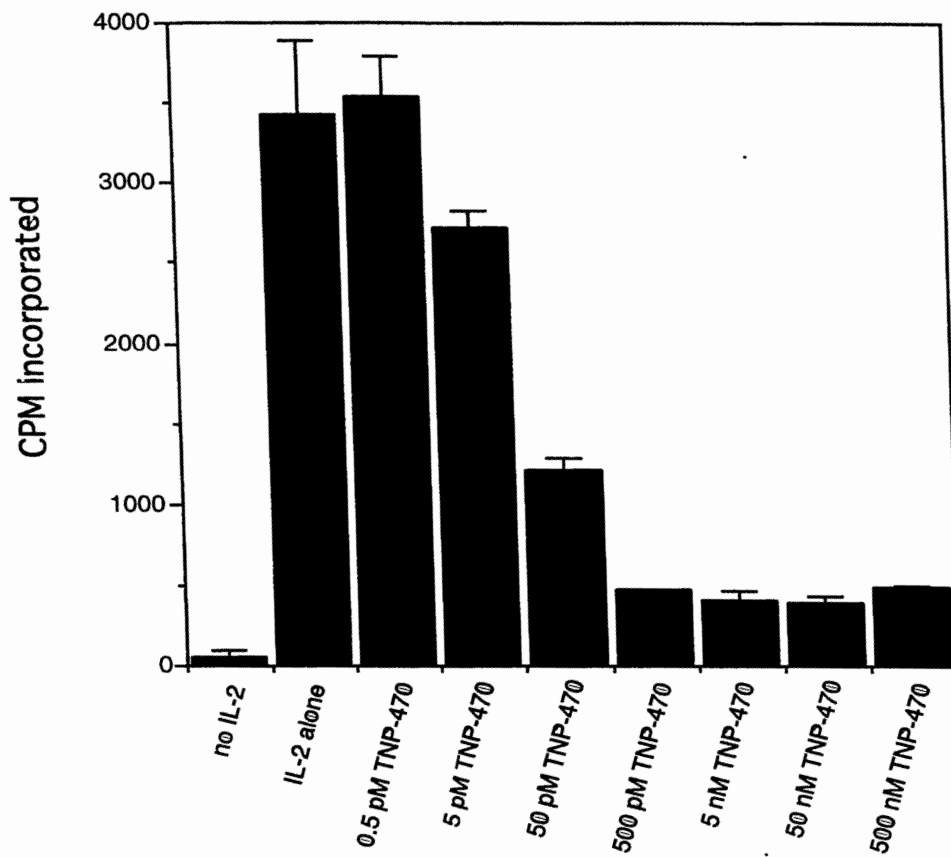


Figure 4.5. TNP-470 inhibits the IL-2 dependent proliferation of T cell blasts.

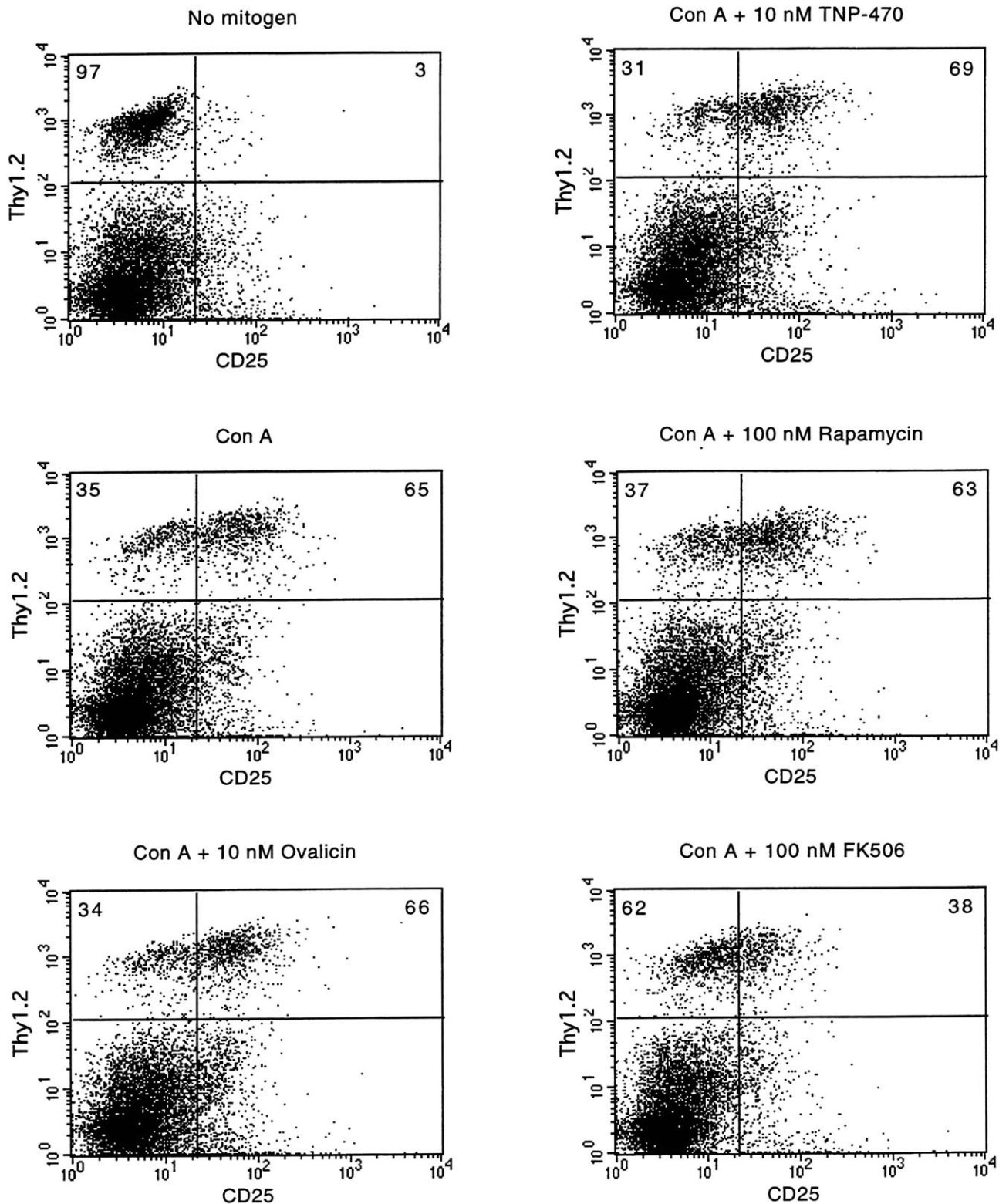


Figure 4.6. Ovalicin and TNP-470 do not effect expression of CD25 (IL-2R α) in Con A-stimulated mouse lymphocytes. Cells were isolated and stimulated as described in Materials and Methods in the presence of the indicated drug, stained with FITC-labeled α -Thy1.2 and PE-labeled α -CD25, and analyzed by flow cytometry. Numbers within the upper quadrants indicate the percentage of the Thy1.2 positive cells (T lymphocytes) which have CD25 levels above or below the indicated threshold.

Using PHA as a mitogen, we have also observed modest increases in human PBMC proliferation caused by ovalicin (B. T. and J. L., unpublished data). Mitogenic stimulus-dependent differences in the effect of TNP-470 on lymphocyte proliferation have been observed by others as well (30). As PHA-induced mitogenesis is not mediated by a single receptor but by nonspecific crosslinking of many cell-surface molecules, it is possible that PHA treatment may trigger pathways that are not sensitive to inhibition by TNP-470 or its analogs. Those pathways may not be activated during T cell receptor-mediated signaling such as that provided by allogenic stimulus in the MLR.

Among the analogs we synthesized from fumagillin and ovalicin, compound **4** in which the sidechain containing chloroacetyl group at C-6 of TNP-470 was replaced with a carbonyl group is the most potent inhibitor of angiogenesis and the MLR. The chloroacetyl group in TNP-470 is therefore not essential for either the anti-angiogenic or the immunosuppressive activity of TNP-470. In contrast, opening of the spiro epoxide group led to a dramatic decrease in the activity of TNP-470, suggesting a key role of the epoxide group in the binding of these drugs to MetAP2.

The activities of TNP-470 and ovalicin analogs in the mouse MLR correlates well ($r^2 = 0.83$) with their activities for the inhibition of BAEC proliferation, though approximately ten-fold higher concentrations of drugs were required to elicit the same degree of inhibition in the MLR compared with the BAEC assay. The reason for this discrepancy is unknown, but the high degree of correlation argues for a common underlying molecular mechanism for both processes. This contention is consistent with previous observations that inhibition of lymphocyte proliferation by ovalicin and inhibition of endothelial cell proliferation by TNP-470 both result from cytostatic growth arrest in the G₁ phase of the cell cycle (17,18,31-33). Structural features important for high potency in both cellular assays are also key to the inhibition of MetAP2 (see Table 1), suggesting that inhibition of this enzyme mediates both the anti-angiogenic and immunosuppressive activities of the drugs. Our observation that IL-2 dependent proliferation is inhibited by the drugs, whereas upregulation of IL-2 and CD25 are not,

also bears similarity to the situation with endothelial cells, where proliferation induced by growth factors (bFGF and VEGF) is blocked by the drugs (19). Interestingly, growth of the IL-2-dependent transformed cell line CTLL-2 was not affected by ovalicin, which parallels the tendency for transformed endothelial cell lines to lose sensitivity to TNP-470. Blockade of IL-2-dependent proliferation suggests the mode of action of ovalicin and TNP-470 to be similar to rapamycin (Figure 4.7), which also inhibits endothelial cell growth (34). Whether the drugs effect the same translational regulatory pathway targeted by rapamycin remains to be determined, though it seems unlikely given that ovalicin and TNP-470 do not appear to directly affect growth-factor induced increases in overall translation (17,31), while rapamycin does. TNP-470 does appear to arrest endothelial cells at a similar point in the cell cycle as rapamycin (see Chapter 5), though it may do so by interfering with a distinct pathway.

Interestingly, we also observed significant differences in the activity of several compounds between the human and mouse MLR. The most striking decrease in activity toward human cells was seen for ovalicin (3), even though this compound went as far as human clinical trials, a fate undoubtedly based at least to some degree on the initial demonstration of its potent immunosuppressive activity in rodents. Though such observations might indicate species-specific differences in a drug's molecular target which confer differential binding specificities for analogous drugs, this does not appear to be so in the case of TNP-470 or ovalicin, as inhibition of human endothelial cell proliferation correlates better with inhibition of the mouse MLR than with inhibition of the human MLR (see Table 1). In contrast to ovalicin, compound 5 with an inverted stereochemistry at C-6, inhibits human MLR more potently than the mouse MLR. It is possible that there are cell type-specific differences in either the uptake, compartmentalization or metabolism of these drugs that are particular to humans.

The activity of TNP-470 in the MLR warrants reconsideration of its possible immunosuppressive properties in vivo. Immunosuppressive side effects, however, have not been reported for TNP-470 in either animal models or human clinical trials (35). The

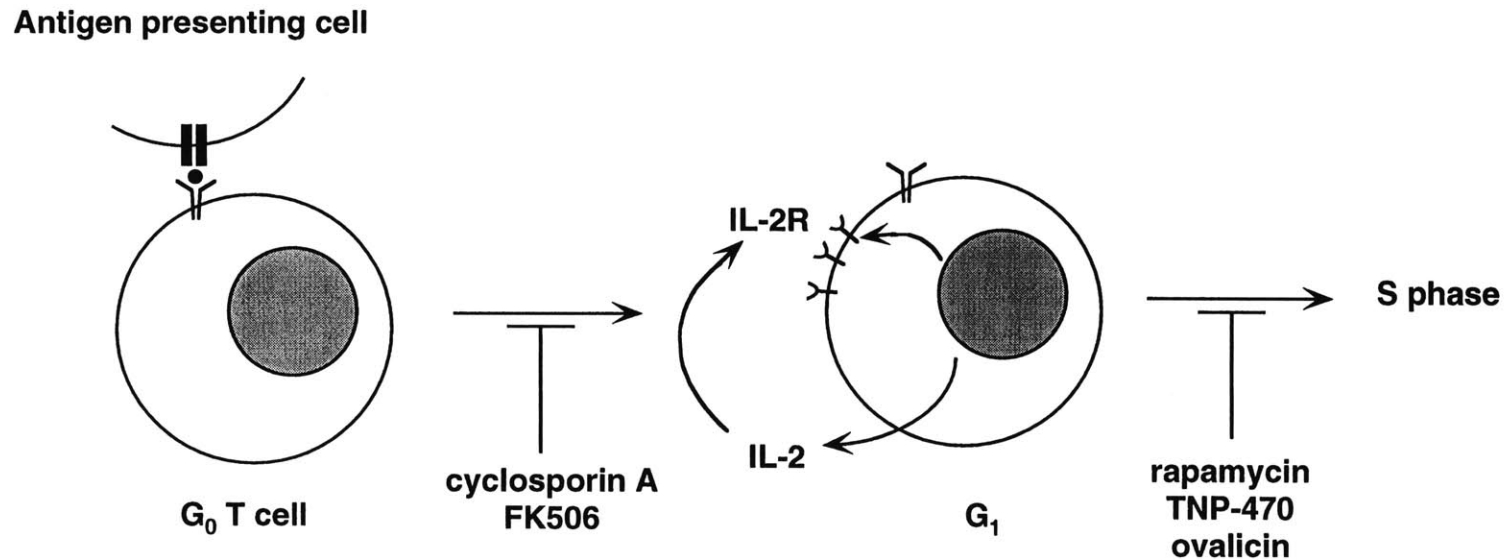


Figure 4.7. Inhibition of cell proliferation by immunosuppressive drugs. Cyclosporin A and FK506 prevent progression from G₀ to G₁ by blocking the production of the autocrine growth factor IL-2. TNP-470 and ovalicin inhibit IL-2 dependent progression through G₁ in a manner similar to rapamycin.

apparent lack of immunosuppressive activity of TNP-470 in vivo may be attributed to a combination of a lower sensitivity of lymphocytes to the drug and rapid clearance of TNP-470 from the serum (36). We have shown that human lymphocytes are over 100-fold less sensitive to TNP-470 than human endothelial cells (Table 1). In addition, it has been demonstrated that TNP-470 has a short serum half life of less than one hour (36). The lack of continuous exposure to TNP-470 may be sufficient to block endothelial cell proliferation without significantly affecting lymphocytes, offering an effective therapeutic window in which beneficial anti-tumor activity can be observed clinically without undesirable immunosuppressive side effects. These observations also demonstrate that despite an apparently common mode of action, it may be possible to find clinically useful angiogenesis-inhibitory compounds which possess little immunomodulatory activity.

References for Chapter 4

1. Roser, B. J. (1984) Mechanisms of graft rejection. In *Transplantation Immunology: Clinical and Experimental*. R. Y. Calne, Ed. (Oxford University Press, Oxford) 186-194.
2. Wood, K. J. (1992) Tolerance to alloantigens. In *Transplantation Immunology: Clinical and Experimental*. R. Y. Calne, Ed. (Oxford University Press, Oxford) 81-103.
3. White, D. J. G., and Calne, R. Y. (1984) Chemical immunosuppression. In *Transplantation Immunology: Clinical and Experimental*. R. Y. Calne, Ed. (Oxford University Press, Oxford) 254-277.
4. Thomson, A. W., Woo, J., and Cooper, M. (1992) Mode of action of immunosuppressive drugs with particular reference to the molecular basis of macrolide induced immunosuppression. In *The Molecular Biology of Immunosuppression*. A. W. Thomson, Ed. (John Wiley & Sons, Chichester) 153-180.
5. Lindholm, A. and Kahan, B. D. (1993) The use of cyclosporin in organ transplantation. In *T-Cell-Directed Immunointervention*. J.-F. Bach, Ed. (Blackwell, Oxford) 77-100.
6. Crabtree, G. R. (1989) Contingent genetic regulatory events in T lymphocyte activation. *Science* **243**, 355-361.
7. Smith, K. A. (1987) Interleukin 2. *Ann. Rev. Immunol.* **2**, 319-333.
8. Granelli-Piperno, A. (1993) Cellular mode of action of cyclosporin A. In *T-Cell-Directed Immunointervention*. J.-F. Bach, Ed. (Blackwell, Oxford) 3-25.
9. Schreiber, S. L., and Crabtree, G. R. (1992) The mechanism of action of cyclosporin and FK506. *Immunol. Today* **13**, 136.
10. Jain, J., McCaffrey, P. G., Miner, Z., Kerppola, T. K., Lambert, J. N., Verdine, G. L., Curran, T., and Rao, A. (1993) The T-cell transcription factor NFATp is a substrate for calcineurin and interacts with Fos and Jun. *Nature* **365**, 352-355.
11. Longley, R. E., Caddigan, D., Harmody, D., Gunasekera, M., and Gunasekera, S. P. (1991) Discodermolide— a new, marine-derived immunosuppressive compound. I. In vitro studies. *Transplantation* **52**, 650-656.
12. Bierer, B. E., Mattila, P. S., Standaert, R. F., Herzenberg, L. A., Burakoff, S. J., Crabtree, G., and Schreiber, S. L. (1990) Two distinct signal transmission pathways in T lymphocytes are inhibited by complexes formed between an immunophilin and either FK506 or rapamycin. *Proc. Natl. Acad. Sci. USA* **87**, 9231-9235.
13. Brown, E. J., and Schreiber, S. L. (1996) A signaling pathway to translational control. *Cell* **86**, 517-520.
14. Stähelin, H. F. (1996) The history of cyclosporin A (Sandimmune®) revisited: another point of view. *Experientia* **52**, 5-13.
15. Lazary, S., and Stähelin, H. (1968) Immunosuppressive and specific antimitotic effects of ovalicin. *Experientia* **24**, 1171-1173.

16. Lazary, S., and Stähelin, H. (1969) Immunosuppressive effect of a new antibiotic: ovalicin. *Antibiot. Chemother.* **15**, 177-181.
17. Hartmann, G. R., Richter, H., Weiner, E. M., and Zimmermann, W. (1978) On the mechanism of action of the cytostatic drug anguidine and of the immunosuppressive agent ovalicin, two sesquiterpenes from fungi. *Planta Med.* **34**, 231-252.
18. Zimmermann, W. A. and Hartmann, G. R. (1981) On the mode of action of the immunosuppressive sesquiterpene ovalicin. *Eur. J. Biochem.* **118**, 143-150.
19. Ingber, D., Fujita, T., Kishimoto, S., Sudo, K., Kanamaru, T., Brem, H., and Folkman, J. (1990) Synthetic analogs of fumagillin that inhibit angiogenesis and suppress tumour growth. *Nature* **348**, 555-557.
20. Corey, E. J., Guzman-Perez, A., and Noe, M. C. (1994) Enantioselective synthesis of (-)-ovalicin, a potent inhibitor of angiogenesis, using substrate-enhanced asymmetric hydroxylation. *J. Am. Chem. Soc.* **116**, 12109-12110.
21. Antoine, N., Bours, V., Heinen, E., Simar, L. J., and Castronovo, V. (1995) Stimulation of human B-lymphocyte proliferation by AGM-1470, a potent inhibitor of angiogenesis. *J. Natl. Cancer Inst.* **87**, 136-139.
22. Antoine, N., Daukandt, M., Heinen, E., Simar, L. J., and Castronovo, V. (1996) In vitro and in vivo stimulation of the murine immune system by AGM-1470, a potent angiogenesis inhibitor. *Am. J. Pathol.* **148**, 393-398.
23. Griffith, E. C., Su, Z., Turk, B. E., Chen, S., Chang, Y.-W., Wu, Z., Biemann, K., Liu, J. O. (1997) Methionine aminopeptidase (type 2) is the common target for angiogenesis inhibitors TNP-470 and ovalicin. *Chem. Biol.* **4**, 461-471.
24. Sin, N., Meng, L., Wang, M. Q. W., Wen, J., Bornmann, W. G., and Crews, C. M. (1997) The anti-angiogenic agent fumagillin covalently binds and inhibits the methionine aminopeptidase, MetAP2. *Proc. Natl. Acad. Sci. USA* **94**, 6099-6103.
25. Marui, S., Itoh, F., Kozai, Y., Sudo, K., and Kishimoto, S. (1992) Chemical modification of fumagillin. I. 6-O-Acyl, 6-O-sulfonyl, 6-O-alkyl and 6-O-(N-substituted carbamoyl)fumagillols. *Chem. Pharm. Bull.* **40**, 96-101.
26. Marui, S., Yamamoto, T., Sudo, K., Akimoto, H., and Kishimoto, S. (1995) Chemical modification of fumagillin. III. Modification of the spiro-epoxide. *Chem. Pharm. Bull.* **43**, 588-593.
27. Kishimoto, S.; Fujita, T. U.S. Patent 5 204 345, 1993.
28. Hatanaka, H.; Kino, T.; Hashimoto, M.; Tsurui, Y.; Kuroda, A.; Tanaka, H.; Goto, T.; Okuhara, M. *J. Antibiotics* **1988**, 8, 999.
29. Minami, Y., Kono, T., Miyazaki, T., and Taniguchi, T. (1993) The IL-2 receptor complex: its structure, function, and target genes. *Ann. Rev. Immunol.* **11**, 245-267.
30. Berger, A. E., Dortch, K. A., Staite, N. D., Mitchell, M. A., Evans, B. R., Holm, M. S. (1993) Modulation of T lymphocyte function by the angiogenesis inhibitor AGM-1470. *Agents Actions* **39**, C86-C88.
31. Kusaka, M., Sudo, K., Matsutani, E., Kozai, Y., Marui, S., Fujita, T., Ingber, D., and Folkman, J. (1994) Cytostatic inhibition of endothelial cell growth by the angiogenesis inhibitor TNP-470 (AGM-1470). *Br. J. Cancer* **69**, 212-216.

32. Abe, J., Zhou, W., Takua, N., Taguchi, J., Kurokawa, K., Kumada, M., and Takuwa, Y. (1994) A fumagillin derivative angiogenesis inhibitor, AGM-1470, inhibits activation of cyclin-dependent kinases and phosphorylation of retinoblastoma gene product but not protein tyrosyl phosphorylation or protooncogene expression in vascular endothelial cells. *Cancer Res.* **54**, 3407-3412.
33. Hori, A., Ikema, S., and Sudo, K. (1994) Suppression of cyclin D1 mRNA expression by the angiogenesis inhibitor TNP-470 (AGM-1470) in vascular endothelial cells. *Biochem. Biophys. Res. Commun.* **204**, 1067-1073.
34. Kanda, S., Hodgkin, M. N., Woodfield, R. J., Wakelam, M. J., Thomas, G., and Claesson-Welsh, L. (1997) Phosphatidylinositol 3'-kinase-independent p70 S6 kinase activation by fibroblast growth factor receptor-1 is important for proliferation but not differentiation of endothelial cells. *J. Biol. Chem.* **272**, 23347-23353.
35. Castronovo, V., and Belotti, D. (1996) TNP-470 (AGM-1470): Mechanisms of action and early clinical development. *Eur. J. Cancer* **32A**, 2520-2527.
36. Figg, W. D., Pluda, J. M., Lush, R. M., Saville, M. W., Wyvill, K., Reed, E., and Yarchoan, R. (1997) The pharmacokinetics of TNP-470, a new angiogenesis inhibitor. *Pharmacotherapy* **17**, 91-97.

Chapter 5

Effects of TNP-470 on the cell division cycle

Abstract

The angiogenesis inhibitor TNP-470 and the immunosuppressive drug ovalicin have been shown to inhibit progression through the G_1 phase of the cell cycle in human endothelial cells and T lymphocytes, respectively, though the molecular details of this blockade are unclear. Using the S49.1 T lymphoma cell line, we show that the drugs cause prolongation of G_1 phase but not a G_1 arrest. While progression through G_1 is effected specifically in human umbilical vein endothelial cells (HUVECs), bovine aortic endothelial cells (BAECs) appear to be delayed in both the G_1 and G_2/M phases when treated with TNP-470, suggesting that the drug affects cell cycle progression varies among species. In HUVECs, the G_1 delay is associated with inhibition of cyclin E-dependent kinase activity, suggesting that the TNP-470 effect occurs during mid to late G_1 , and providing a possible molecular explanation for inhibition of cell cycle progression by the drug.

Introduction

Under appropriate conditions, growth factor stimulation of quiescent cells triggers them to enter the cell division cycle (1). The cell cycle is divided into distinct phases: the S phase, in which DNA synthesis occurs, the M phase, mitosis, and two intervening gap phases, G_1 and G_2 (Figure 5.1). Growth factor withdrawal, terminal differentiation, and loss of cell adhesion can cause normal cells to exit the cell cycle following mitosis and enter a distinct quiescent state, G_0 . Growth factors are needed for cells to remain in the cell cycle only during a portion of the G_1 phase up to a point termed the restriction point, after which cells will continue through the S, G_2 and M phases even if growth factors are withdrawn (2). Cell cycle entry and progression are controlled by the activity of a family of protein serine-threonine kinases, the cyclin-dependent kinases (Cdks) (1,2). Distinct Cdk family members are important for progression at different points in the cell cycle.

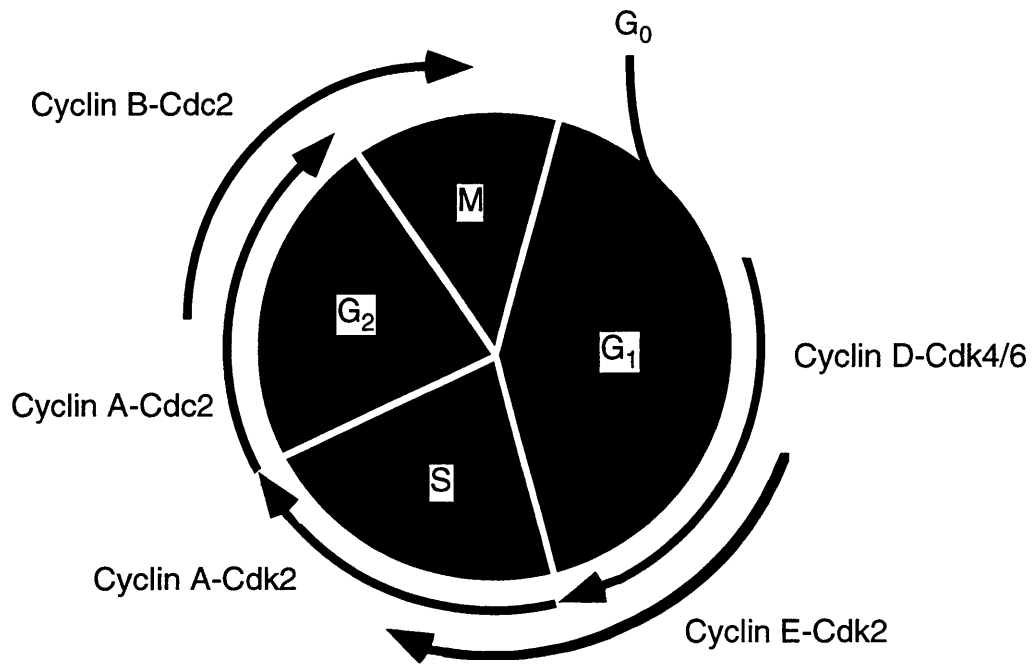


Figure 5.1. The eukaryotic cell division cycle.

Though Cdk protein levels are generally low in quiescent cells and rise during entry into the cell cycle, they remain constant in cycling cells. Cdk activity, however, is periodic, and is controlled by several factors. Association of the Cdk with a member of the cyclin family of regulatory proteins, whose levels vary with position in the cell cycle, is required for kinase activity and influences substrate specificity. The cyclin-Cdk complexes most important for progression through G_1 and into S phase are complexes composed of cyclin D bound to either Cdk4 or Cdk6, whose activities are the first to appear following growth factor stimulation, and the cyclin E-Cdk2 complex, which is active later in G_1 and early in S phase (Figure 5.1).

Cdk activity is inhibited by binding of a member of one of two families of inhibitory proteins, termed CKIs, to the cyclin-Cdk complex (2,3). The INK4 family, composed of p16^{INK4a}, p15^{INK4b}, p18^{INK4c}, and p19^{INK4d}, specifically inhibit the cyclin D-Cdk4 and cyclin D-Cdk6 complexes. The other family, which includes p21^{WAF1}, p27^{Kip1} and p57^{Kip2}, inhibit both the cyclin D and cyclin E containing Cdk complexes. In addition, Cdks are subject to positive and negative regulatory phosphorylation at distinct sites (4).

Phosphorylation of specific substrate proteins by Cdks drives cell cycle progression. A key target for Cdks during progression through G_1 is the protein product of the retinoblastoma susceptibility gene (pRb) (2,5). During early G_1 , pRb is hypophosphorylated and considered to be in the active state. Active pRb forms a complex with E2F family transcription factors, rendering them unable to activate transcription. As G_1 progresses, pRb is phosphorylated, first by cyclin D-dependent kinases and then by cyclin E-Cdk2, on distinct sites. The resulting inactive hyperphosphorylated protein dissociates from E2F, allowing transcription of E2F target genes. These genes encode proteins important for cell cycle progression and DNA replication, such as dihydrofolate reductase, cyclin E, and E2F itself. Phosphorylation of pRb by cyclin D dependent kinases is critical to pRb inactivation. Cells lacking the Rb gene can still progress to S phase in the absence of cyclin D dependent kinase activity,

implying that pRb is the only substrate of these kinases important for cell cycle progression (6,7). Prior phosphorylation of pRb by cyclin D dependent kinases appears to be required for subsequent phosphorylation by cyclin E-Cdk2, and it is likely that phosphorylation by both kinases is necessary for inactivation of pRb (8,9).

Phosphorylation of pRb by cyclin E-dependent kinase may inactivate the protein towards as yet unidentified binding partners other than the E2F proteins (5). It is likely that there are cyclin E-Cdk2 substrates other than pRb important for cell cycle progression, including perhaps proteins at origins of replication which might directly regulate initiation of DNA synthesis (2).

Signaling from growth factor receptors results in the activation of multiple pathways which are important for the sequential activation of Cdks. Growth factor receptors generally possess either intrinsic (as in the FGF and VEGF receptors) or associated (as in the T cell receptor) tyrosine kinase activity in their cytoplasmic domains (10). Receptor autophosphorylation triggers association of signaling molecules via modular domains which recognize phosphotyrosine in the context of specific surrounding sequence motifs. Binding of the adaptor molecule Grb2 via its SH2 domain to activated receptor tyrosine kinases results in the recruitment of the associated Sos protein to the plasma membrane, where it can act to catalyze guanine nucleotide exchange in the small GTPase molecule Ras. Ras plays a crucially important role in progression through G₁ (11,12). Ras activates the MAP kinase cascade, which results in the expression of the immediate early genes c-Jun and c-Fos. The AP-1 transcription factor, which is comprised of the Jun/Fos heterodimer, is involved in induction of the cyclin D1 gene (13). Increasing cyclin D1 levels is therefore an important function of Ras during early G₁; a requirement for Ras later in G₁ has also been inferred from microinjection experiments though the target genes are not known (12).

Ras activation alone, however, is insufficient for entry into S phase, indicating the need for other growth-promoting pathways. The immediate early gene c-Myc has been shown to cooperate with Ras in the activation of cyclin E-dependent kinase activity and S

phase entry (14,15). Activation of the c-Myc gene occurs independently of Ras and appears to depend on the growth factor-induced activation of Src family tyrosine kinases by an unknown mechanism (16). c-Myc is a transcription factor whose target genes include those encoding ornithine decarboxylase and dihydroorotase, biosynthetic enzymes important for S phase (14). In addition, c-Myc may directly affect the cell cycle machinery via induction of cyclin E and the Cdc25a gene, which encodes the Cdk2-activating phosphatase. c-Myc also cooperates with Ras to decrease levels of the p27^{Kip1} CKI by an unknown mechanism.

Other growth promoting pathways feed into the Cdk machinery. Activation of phosphoinositide 3'-kinase (PI3K) by Ras gives rise to phospholipid products which activate several downstream targets, including the rapamycin-sensitive protein kinase FRAP, which defines a translational control pathway (17). Though the FRAP-sensitive mRNAs involved in promoting cell growth have not been established, it appears as if downregulation of p27^{Kip1} is an important downstream event (18). Growth factor-induced activation of Rho, a small GTPase in the Ras superfamily, also appears to be required for Ras-induced cell proliferation, perhaps due to its ability to decrease the level of the CKI p21^{WAF1} (19).

Small molecules which inhibit cell cycle progression can do so by any of a variety of mechanisms. Some compounds act as direct inhibitors of the growth-regulating signal transduction pathways. Examples include rapamycin, described above, wortmannin, which inhibits PI3K, and Src family kinase inhibitors, such as herbimycin A (20,21). Other compounds activate cellular checkpoint control pathways which exist to ensure that cell cycle progression occurs in an orderly manner. DNA damaging agents arrest cells in either G₁ or G₂ by activating distinct checkpoint pathways (4). One such pathway involves activation of the tumor suppressor p53, which stimulates transcription of target genes such as p21^{WAF1} important for mediating cell cycle arrest. Compounds which deplete deoxyribonucleotide triphosphate pools needed for DNA synthesis also activate a p53-dependent checkpoint pathway which occurs during S phase. General inhibitors of

protein or RNA synthesis and inhibitors of protein degradation typically cause cells to arrest in more than one phase of the cell cycle, presumably due to either the disappearance of rapidly turned over proteins which positively regulate growth or the stabilization of negative regulators (22).

Another set of compounds acts indirectly by inhibiting biosynthetic pathways necessary for the activity of growth-promoting molecules (22). Lovastatin, an HMG-CoA reductase inhibitor, arrests cells in G_1 by, among other things, cutting off the supply of farnesyl pyrophosphate, thereby preventing farnesylation of Ras which is required for its activity. TNP-470 and ovalicin, by virtue of their inhibition of MetAP2, can be regarded as members of this class of compounds. Whereas MetAP2 is not likely to be involved directly in a signaling cascade which promotes cell growth, its action may be required to maintain a growth regulatory protein in an active state. The identities of such target molecules remain unknown. The way in which TNP-470 and ovalicin affect cell cycle progression, including their effects on the cell cycle machinery, is an important aspect of their mechanism of action. Such information would reveal the point in the cell cycle where the downstream targets of MetAP2 play a crucial role, either by virtue of direct involvement in signal transduction or in the activation of known checkpoint pathways. For example, upregulation of p21^{WAF1} might point to activation of a p53-dependent checkpoint pathway, whereas a failure to downregulate p27^{Kip1} in response to growth factors may indicate an effect on a signaling pathway similar to rapamycin.

Previous work on TNP-470 indicates that it cytostatically and reversibly arrests endothelial cells in the G_1 phase of the cell cycle in human endothelial cells (23). Similarly, ovalicin prevents the initial onset of DNA synthesis in mitogen-stimulated lymphocytes, consistent with a similar mechanism of growth inhibition by the two drugs (24). Attempts to investigate effects of TNP-470 on the cell cycle machinery has met with conflicting results. One study reported a failure to induce cyclin D1 in human endothelial cells treated with TNP-470, though concentrations of drug much higher than necessary to inhibit cell growth were needed (25). In another report, more moderate

concentrations of TNP-470 caused a failure to induce the cyclin A gene, consistent with a G₁ arrest (26). A slight decrease in cyclin E mRNA was observed, along with a slight decrease in Cdk2 activity. No effect on cyclin D1 mRNA induction was observed, nor were effects on c-Fos or c-Myc induction. However, levels of cyclin E protein were not investigated, and Cdk2 activity was only observed at a single time point following growth factor stimulation. The regulation of Cdk2 by both cyclin E and cyclin A at different points in the cell cycle also complicates the interpretation. Yet another report, which studied the effects of TNP-470 on vascular smooth muscle cells, demonstrated an effect on Cdk2 activity which was not apparent upon initial induction the kinase but occurred at later time points following growth factor treatment (27). Cyclin D1 induction was unaffected, but Cdk2 induction was impaired, though at a time when kinase activity was unaffected. Levels of Cdk2 protein were not investigated, nor were cyclin E or cyclin A levels. Sorting out the effects of TNP-470 on these various molecules involved in cell cycle progression will be imperative in elucidating the mechanism of action of the drug. Decreases in the activity of certain proteins may point to the identification of crucial MetAP2 substrates in drug-sensitive cells, for example.

Materials and Methods

Cell Culture. BAECs and HUVECs were cultured as described in Chapters 2 and 3 respectively. S49.1 cells were grown in DME with 10% FBS and P/S. Cell proliferation was measured by tritiated thymidine incorporation as described in chapter 4.

Cell cycle analysis. Adherent cells were harvested by trypsinization. Cells were pelleted and resuspended to 2×10^6 /mL in propidium iodide (PI) stain solution (3% PEG 8000, 50 μ g/mL PI, 0.1% triton X100, 0.5 mg/mL RNase A, and 4 mM sodium citrate, pH 7.2) and incubated 20 min at 37°C in the dark. An equal volume of PI salt solution (3% PEG 8000, 50 μ g/mL PI, 0.1% triton X100, and 0.4 M NaCl) was added and the suspension kept at 4°C in the dark for a period of 1 to 16 hr prior to analysis by flow cytometry. Cell cycle data was fit using ModFit software.

Cell synchronization. HUVECs were plated at 3000 cells per cm² in complete medium and allowed to recover for 30 hr. Cells were washed once with PBS, incubated in 0.25% FBS in EBM-2 for 34 hr, and then restimulated with complete media (EGM-2). To synchronize at the G₁/S boundary, hydroxyurea was added to 1 mM at 12 hr post-restimulation and cells incubated for a further 18 hr.

Immunoprecipitation and kinase assays. Modified from Ezhevsky, *et al.* (8). Cyclin E antibodies (clone HE111) and control mouse IgG were purchased from Santa Cruz Biotechnology. Cells were washed once with cold PBS and extracted with lysis buffer (0.1% NP-40, 50 mM HEPES, pH 7.3, 250 mM NaCl, 2 mM EDTA, 1 mM DTT, 1 µg/mL aprotinin, 1 µg/mL leupeptin, 1 mM PMSF, 0.5 mM sodium pyrophosphate, 0.1 mM Na₃VO₄, 5 mM NaF, 0.5 mL per 75 cm²) by scraping into microcentrifuge tubes and incubating at 4°C for 30 min with rotating. Debris were removed by centrifugation at 16,000 x g for 10 min at 4°C and supernatants were frozen on dry ice/EtOH and stored at -80 °C until use. Protein concentration was determined by Bradford assay and equal amounts of protein were used for analysis. Antibodies were added (2 µg per sample) and incubated on ice for 2 to 4 hr prior to the addition of 20 µL of protein A/G agarose (for mouse antibodies). After 1 hr at 4°C with rotating, the beads were pelleted by centrifugation, washed three times for 5 min with 0.75 mL lysis buffer and then once with kinase buffer (50 mM HEPES, pH 7.3, 10 mM MgCl₂, 1 mM DTT, 10 µM cold ATP) and resuspended in 25 µL kinase buffer containing γ-[³²P]ATP (10 µCi, 3000 Ci/mmol) and 2 µg of Histone H1 substrate. Mixtures were incubated at 30°C for 30 min and then quenched by adding 15 µL of 4X SDS-PAGE loading buffer and heating in a boiling water bath for 10 min. Samples were subjected to SDS-PAGE (12% acrylamide) as described in Chapter 3, dried and analyzed by autoradiography.

Results

Sensitive cell types treated with TNP-470 have reduced yet detectable levels of DNA synthesis (23). Consistent with this observation, we have observed that bovine aortic

endothelial cells (BAECs) treated with TNP-470 remain capable of growing to confluence, albeit at a much slower rate (see Chapter 3). Such observations are consistent with several possibilities. One possibility is that a population of cells contains subpopulations of drug sensitive cells, which undergo cell cycle arrest, and drug resistant cells whose proliferation is unaffected by the drug. Drug resistance in this scenario could either be a stable characteristic endowed by genetic variation or more transient in nature. Alternatively, progression through the cell cycle could be slowed down but not arrested in all cells within the population. Treatment of human endothelial cells with TNP-470 has been reported to result in accumulation in the G_1 phase of the cell cycle, though detectable numbers of cells remain in S phase and G_2/M phase (23). To distinguish between these possibilities, we chose to treat sensitive cells with TNP-470 followed by treatment with the drug nocodazole, which causes a solid cell cycle block during M phase (28). As cells in M phase have a two-fold greater DNA content than cells in G_1 , the phases can be distinguished by flow cytometry following staining with the fluorescent DNA intercalator propidium iodide. As BAECs are primary cells and divide relatively slowly in culture, treatment with nocodazole for a time sufficient to synchronize the population in M phase was not possible due to cytotoxicity induced by prolonged drug treatment. We therefore required a sensitive cell type with a shorter cell cycle. The S49.1 mouse T lymphoma has been reported to be sensitive to low concentrations of ovalicin and divides approximately twice a day during exponential growth (24). As expected, S49.1 cells are also sensitive to TNP-470, and treatment with the drug caused accumulation of cells in G_1 (Figure 5.2). A short treatment with nocodazole was sufficient to completely synchronize cells in M phase, as judged by DNA content. If cells are treated with TNP-470 for 24 hr and then nocodazole is added to the culture for an additional 36 hr, virtually the entire population accumulates in M phase. It therefore appears as if TNP-470 does not cause S49.1 cells to arrest, but merely delays their progression through G_1 .

Treatment of subconfluent HUVECs results in an increase in the proportion of cells in G_1 with a decrease in the proportion of cells in both S and G_2/M , consistent with

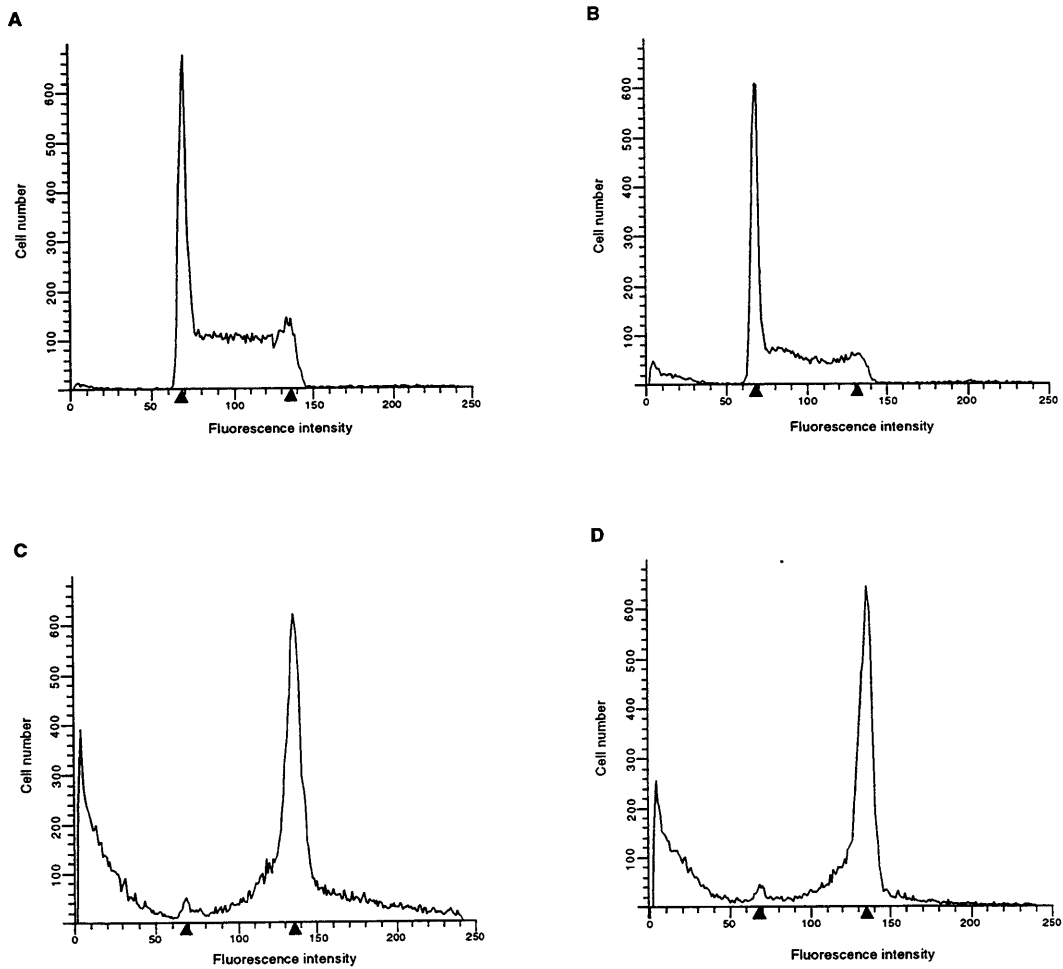


Figure 5.2. S49.1 cells have a prolonged G1 phase when treated with TNP-470. S49.1 cells were analyzed for cell cycle distribution by propidium iodide fluorescence flow cytometry following various drug treatments. The two arrowheads indicate the positions of the G1 and G2/M phases. A, No drug. B, 10 nM TNP-470, 24 hr. C, 100 nM Nocodazole, 12 hr. D, 10 nM TNP-470, 24 hr, followed by 100 nM nocodazole, 16 hr.

previous reports (data not shown, 23). TNP-470 treatment of BAECs, however, while decreasing the S phase population, appears to cause both the G₁ and G₂/M populations to increase (Figure 5.3A). While this result suggests that progression through both G₁ and G₂ or M is prolonged by TNP-470 in BAECs, the effect on G₂/M is subtle compared to the effect on G₁. In order to establish whether the drug causes prolonged G₂/M in BAECs, we examined the behavior of synchronized cells as they pass through G₂ and M in the presence and absence of TNP-470. Treatment with hydroxyurea causes cells to arrest at the G₁/S boundary due to depletion of deoxyribonucleotide pools; drug washout allows rapid and complete reversal of the block (29). BAECs were treated for 24 hr with 1 mM hydroxyurea, after which point drug was removed by washing the cells and replacing the culture media. At this point, either TNP-470 or carrier solvent alone was added to the cells. Cell cycle progression was analyzed over time by flow cytometry (Figure 5.3B). Following washout a population of cells remained in G₁ due to either incomplete synchronization or contact inhibition of cell growth. TNP-470 had no effect on S phase entry of the synchronized population. Whereas the G₂/M phase population was maximal in cells without TNP-470 8 hr following release from the hydroxyurea block, G₂/M remained highly populated up to 34 hr following release into TNP-470, indicating that passage through G₂ and/or M phase is prolonged by drug treatment. In contrast, transit through G₂/M by human umbilical vein endothelial cells (HUVECs) synchronized with hydroxyurea is unaffected by TNP-470 treatment, confirming that the drug specifically effects the G₁ phase in these cells (Figure 5.4).

To clarify the molecular mechanisms of growth inhibition by TNP-470, we chose to examine the effect of the drug on Cdk activities important for progression through G₁ in HUVECs (Figure 5.1). Growth factor starvation for 36 hr renders HUVECs quiescent as judged by a greatly reduced proportion of cells in S and G₂/M compared with cells maintained in complete media. Consistent with previous observations, growth factor restimulation of quiescent HUVECs was found to result in asynchronous entry into S phase as judged by either [³H] thymidine incorporation or by flow cytometry (29, data

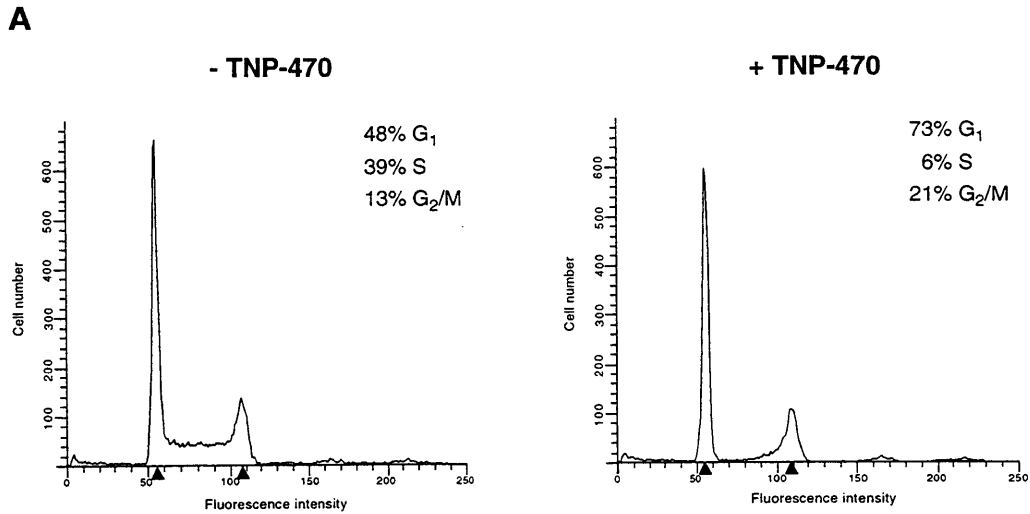
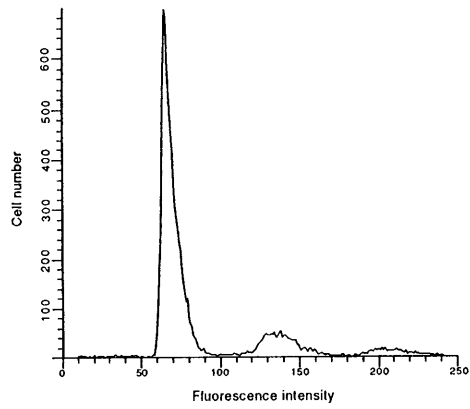


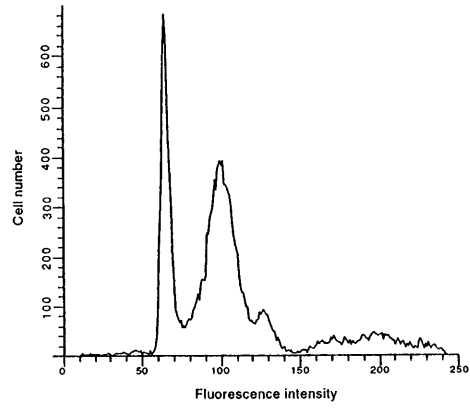
Figure 5.3. TNP-470 increases the G₂/M phase in BAECs. BAECs were analyzed for DNA content by propidium iodide fluorescence flow cytometry following various drug treatments. This page: A, Cells were analyzed following 24 hr treatments with either carrier solvent alone (left panel) or 10 nM TNP-470 (right panel). Cell cycle distribution is indicated in the inset. Following two pages: B, BAECs were synchronized by treating with hydroxyurea. Cells were harvested and analyzed at the times indicated following release from the block into media containing either carrier solvent alone (top panels) or 10 nM TNP-470 (bottom panels).

B

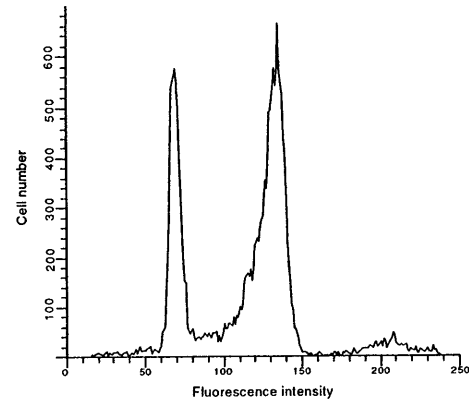
0 hr



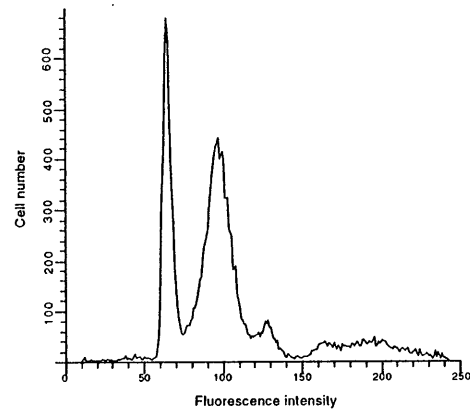
4 hr



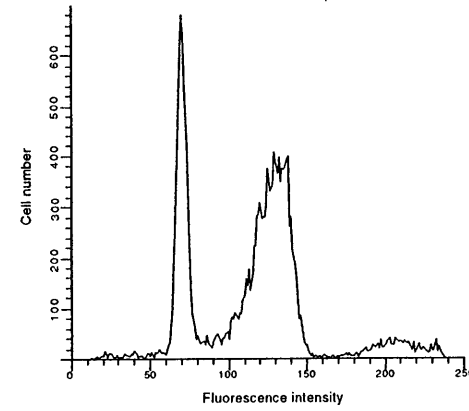
8 hr



- TNP-470



+ TNP-470

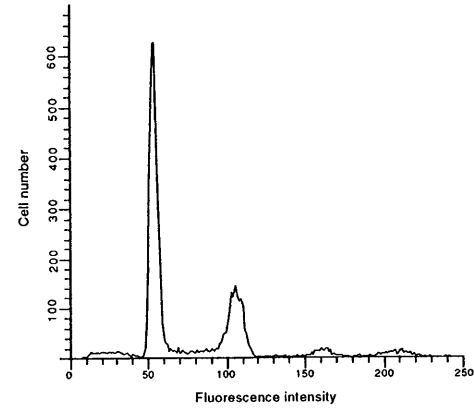
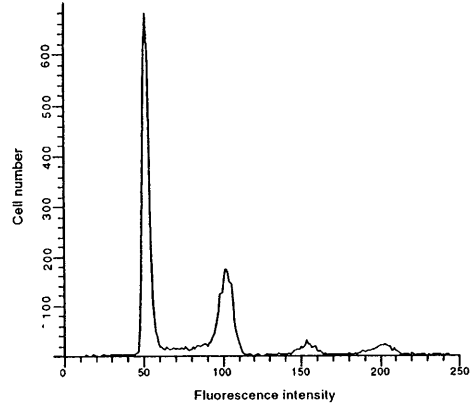
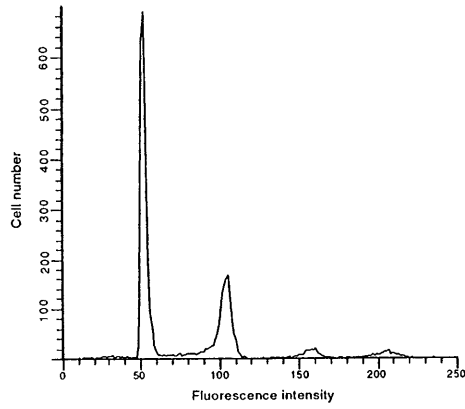


B, contd.

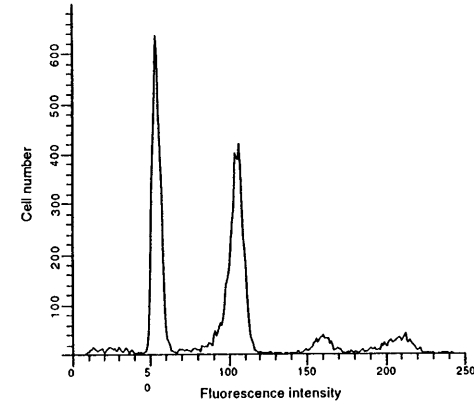
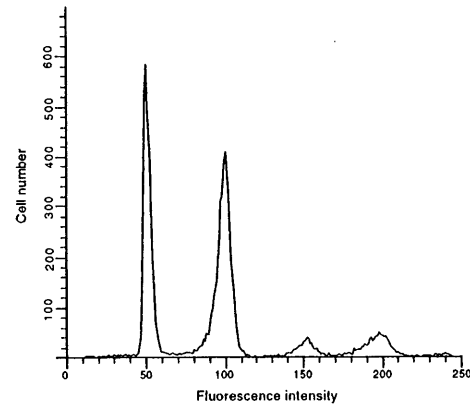
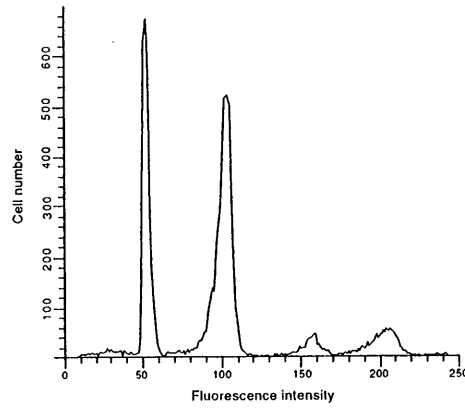
15 hr

24 hr

34 hr



- TNP-470



+ TNP-470

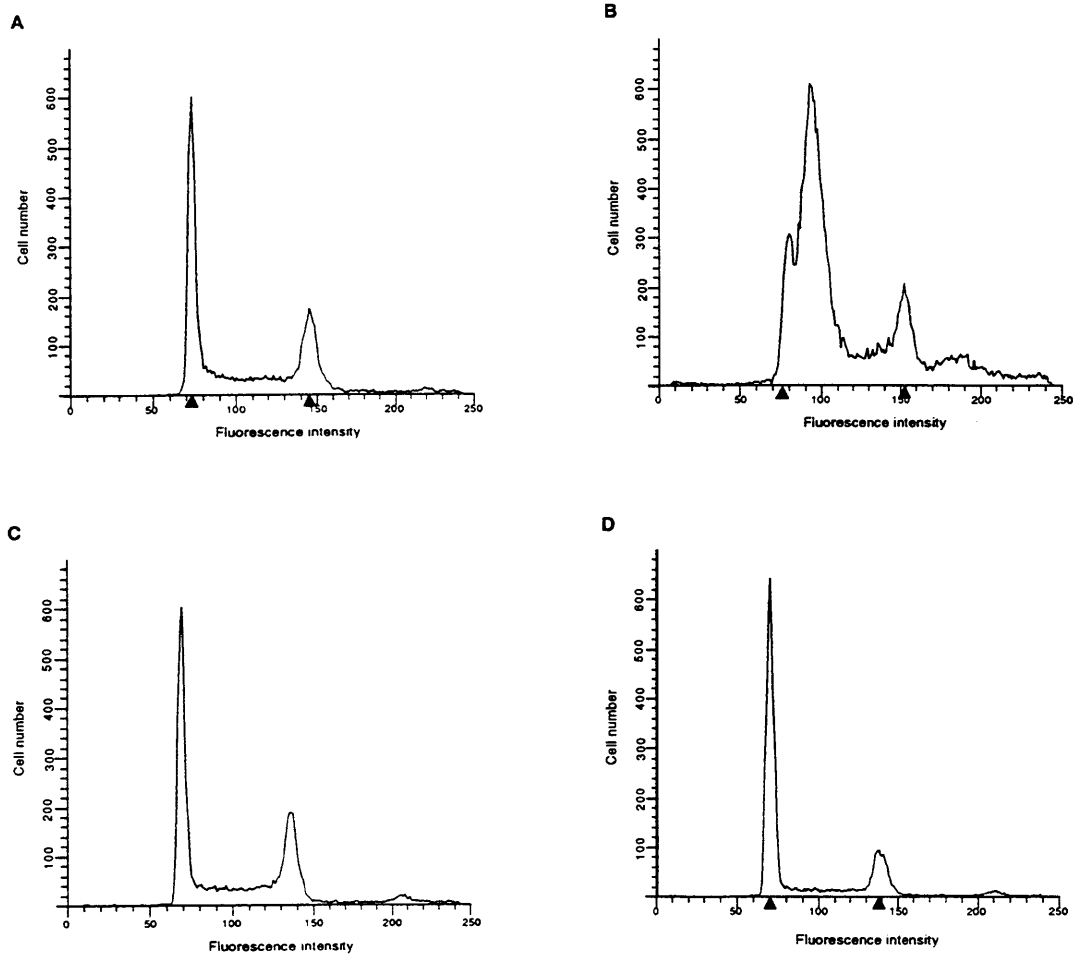


Figure 5.4. TNP-470 does not prolong the passage of HUVECs through G2 or M phase. HUVECs were either left untreated (A), or synchronized by treatment with 1 mM hydroxyurea for 24 hr (B through D). Cells were harvested and analyzed by PI fluorescence flow cytometry either immediately following hydroxyurea treatment (B), or 24 hr following washout of the hydroxyurea into media containing either no drug (C) or 10 nM TNP-470 (D).

not shown). To observe cyclin E dependent kinase activity, cells were treated with hydroxyurea starting 12 hr following restimulation and harvested 16 hr later. Such treatment results in a population of cells with about two thirds at the G₁/S boundary (29), a time when cyclin E dependent kinase activity is high (Figures 5.5 and 5.6). Addition of 10 nM TNP-470 during restimulation results in a significant decrease in S phase entry (Figure 5.5). The same concentration of drug causes inhibition of cyclin E dependent kinase activity (Figure 5.6). Taken together with previous observations that TNP-470 does not affect immediate early gene induction (25,26), this result indicates that TNP-470 causes a delay in cell cycle progression at a point in mid to late G₁, prior to maximal activation of cyclin E dependent kinases.

Discussion

The ability to trap TNP-470-sensitive cells in M phase by applying nocodazole subsequent to TNP-470 indicates that all cells within the drug-treated population escape G₁ phase. These observations are consistent with prior work which indicated that a detectable though reduced proportion of endothelial cells are in S phase following drug treatment. The appearance of resistance to TNP-470, which would be expected if a subpopulation of cells within a culture were stably drug resistant, has not been observed previously, even with prolonged drug treatment in endothelial cells (23). These results indicate instead that TNP-470 prolongs the G₁ phase of sensitive cells but does not cause G₁ arrest.

Cell cycle prolongation as opposed to arrest may occur if the molecular target of the drug contributes to but is not essential for cell cycle progression. Rapamycin treatment for example also delays entry into S phase but does not result in G₁ arrest (30). This may indicate the presence of homologous proteins which can compensate for loss of FRAP function, the existence of parallel pathways which regulate translational control that are only partially redundant with the FRAP pathway, or that activated translation is not an absolute requirement for S phase entry. A similar situation may apply to specific

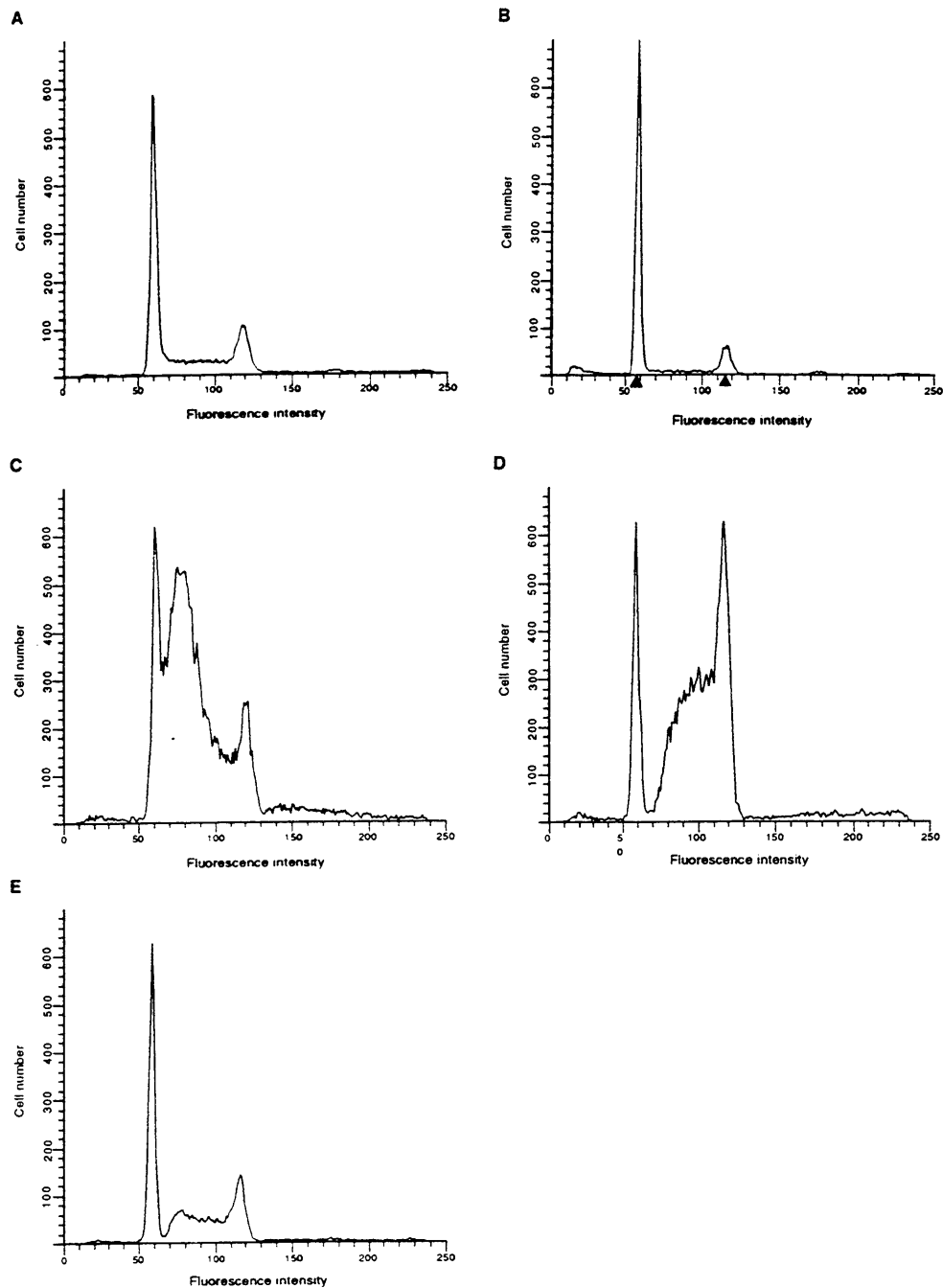


Figure 5.5. TNP-470 prevents entry of synchronized HUVECs into S phase. HUVECs were rendered quiescent by growth factor starvation and then restimulated with complete growth media containing 10 nM TNP-470 or carrier solvent alone. Hydroxyurea was added from 12 to 28 hr post-restimulation as described in Materials and Methods. Cells were harvested either immediately or 2 hr after exchange into fresh media without hydroxyurea. Cells were analyzed by PI fluorescence flow cytometry. A, Untreated asynchronous cells. B, Quiescent cells harvested prior to restimulation. C, Cells treated with hydroxyurea alone and harvested prior to washout. D, Cells treated with hydroxyurea alone and harvested 2 hr after washout. E, Cells treated with hydroxyurea with TNP-470 and harvested 2 hr following washout.

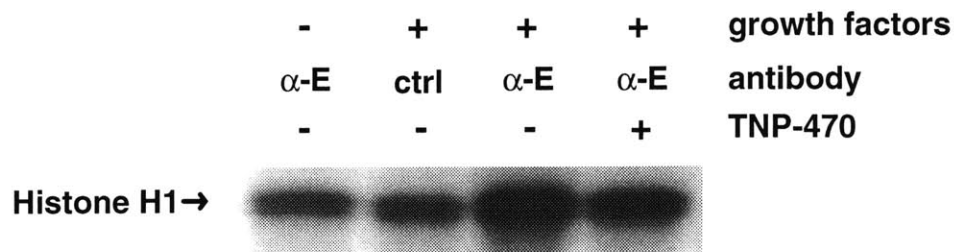


Figure 5.6. TNP-470 inhibits activation of cyclin E-dependent kinase. Cells were synchronized by growth factor starvation and restimulated with growth factors in the presence or absence of 10 nM TNP-470 or harvested prior to restimulation as indicated. Hydroxyurea was added to growth factor-stimulated cells after 12 hr, and cells were harvested 16 hr later. Lysates were analyzed by immunocomplex kinase assay using either control mouse IgG (ctrl) or anti-cyclin E (α -E) antibodies as indicated.

MetAP2 targets that regulate cell growth which are inactivated or activated by TNP-470 treatment. Because TNP-470 acts indirectly via inhibition of MetAP2, however, other scenarios are also possible. For example, a MetAP substrate crucial for cell growth may be partially processed by MetAP1 in the absence of MetAP2 activity, as in the case of glyceraldehyde-3-phosphate dehydrogenase (see Chapter 3). The amount of active protein would thus be decreased but not eliminated, which could prolong G₁ if the target protein were rate limiting for G₁ progression. Alternatively, inhibition of methionine processing may result in a protein which retains some but not all of its activity. In a situation where methionine retention leads to increased stability and thus higher levels of a CKI, for example, levels may not be high enough to completely inhibit its target Cdk(s).

The observation that TNP-470 causes slower progression through G₂/M as well as G₁ in BAECs is surprising given that it appears to exclusively arrest in G₁ in all other sensitive cell types that have been tested. This observation suggests that BAECs exclusively require for MetAP2 activity for timely passage through either G₂, M, or both. This requirement may reflect either multiple specific MetAP2 substrates which are important in different phases of the cell cycle, or a single target (or set of targets) which is important for progression through more than one phase. The protein kinase Src, for example, is required for progression through both G₁ and G₂ and does not function properly without amino-terminal methionine removal (31,32).

The differences between human and bovine endothelial cells could indicate that MetAP1 from the two species has different substrate specificities, which would result in differences in the particular protein which are not processed in the absence of MetAP2. Alternatively, the amino-terminal sequences of the key substrate(s) important for G₂/M progression may differ between species, such that the human protein is efficiently processed by MetAP1, whereas the bovine isoform is not. A further possibility is that bovine and human endothelial cells differ in their requirements for a particular MetAP2 substrate in G₂/M, or that endothelial cells from different tissues differ in such requirements.

We observed that TNP-470 causes a partial decrease in cyclin E-dependent kinase activity. Previous reports indicate that early growth factor-mediated events, such as immediate early gene induction, are not effected by TNP-470 (26). Taken together, these results suggest that TNP-470 affects cell cycle progression in mid to late G₁, prior to the onset of full cyclin E-Cdk2 activity. Further experiments will be needed to determine whether decreased cyclin E-dependent kinase activity reflects a cause or consequence of growth inhibition. A survey of the molecules known to be involved in activating cyclin E-Cdk2 should be particularly illuminating. For example, a failure to activate the kinase could be a result of failure to induce the genes encoding either cyclin E or Cdk2 in a timely manner, which would suggest that the TNP-470-mediated decrease in cyclin E-Cdk2 activity is secondary to failure to progress through G₁. Inhibition of cyclin E-Cdk2 by association of a CKI would also be informative. For example, the presence of p21^{WAF1} would suggest the activation of a checkpoint pathway and would implicate inhibition of the kinase as a causative factor in delayed progression through G₁. Inhibition of cell cycle progression by rapamycin, which also occurs during mid to late G₁, is associated with a failure to downregulate p27^{Kip1}, resulting in decreased cyclin E-dependent kinase activity (18). The observation that cells from mice lacking the Kip1 gene are still sensitive to rapamycin raises questions as to the importance of the CKI in mediating growth inhibition by the drug (33). It is possible, however, that the absence of p27 is compensated for by other family members such as p57^{Kip2}. Possible roles for these CKIs in TNP-470-mediated growth inhibition will be investigated in future studies.

Other possibilities include an effect on the phosphorylation state of Cdk2, which may itself be associated with decreased levels of either the Cdc25 phosphatase or a Cdk activating kinase. If an effect is observed on the level of a particular protein, it will be interesting to see whether this effect is mediated at the transcriptional or post-transcriptional level. In the context of MetAP2 inhibition, it is tempting to speculate that the effect of TNP-470 is mediated through an effect on the level of a cell cycle regulatory protein which is either stabilized or destabilized by failure to undergo proper amino-

terminal processing. Identification of such specific MetAP2 substrates is a crucial direction for future work in the field.

References for Chapter 5

1. Murray, A. M., and Hunt, T. (1993) *The Cell Cycle* (Oxford University Press, Oxford).
2. Sherr, C. J. (1995) Cancer cell cycles. *Science* **274**, 1672-1677.
3. Hunter, T. and Pines, J. (1994) Cyclins and cancer II: cyclin D and CDK inhibitors come of age. *Cell* **79**, 573-582.
4. Elledge, S. J. (1995) Cell cycle checkpoints: preventing an identity crisis. *Science* **274**, 1664-1672.
5. Mitnacht, S. (1998) Control of pRB phosphorylation. *Curr. Opin. Genet. Dev.* **8**, 21-27.
6. Lukas, J., Bartkova, J., Rohde, M., Strauss, M., and Bartek, J. (1995) Cyclin D1 is dispensable for G1 control in retinoblastoma gene-deficient cells independently of cdk4 activity. *Mol. Cell. Biol.* **15**, 2600-2611.
7. Lukas, J., Parry, D., Aagaard, L., Mann, D. J., Bartkova, J., Strauss, M., Peters, G., and Bartek, J. (1995) Retinoblastoma-protein-dependent cell-cycle inhibition by the tumour suppressor p16. *Nature* **375**, 503-506.
8. Ezhevsky, S. A., Nagahara, H., Vocero-Akbani, A. M., Gius, D. R., Wei, M. C., and Dowdy, S. F. (1997) Hypo-phosphorylation of the retinoblastoma protein (pRb) by cyclin D:Cdk4/6 complexes results in active pRb. *Proc. Natl. Acad. Sci. USA* **94**, 10699-10704.
9. Lundberg, A. S., and Weinberg, R. A. (1998) Functional inactivation of the retinoblastoma protein requires sequential modification by at least two distinct cyclin-cdk complexes. *Mol. Cell. Biol.* **18**, 753-761.
10. Ullrich A. and Schlessinger, J. (1990) Signal transduction by receptors with tyrosine kinase activity. *Cell* **61**, 203-12.
11. Roussel, M. F. (1998) Key effectors of signal transduction and G1 progression. *Adv. Cancer Res.* **74**, 1-24.
12. Dobrowolski, S., Harter, M., and Stacey, D. W. (1994) Cellular ras activity is required for passage through multiple points of the G₀/G₁ phase in BALB/c 3T3 cells. *Mol. Cell. Biol.* **14**, 5441-5449.
13. Brown, J. R., Nigh, E., Lee, R. J., Ye, H., Thompson, M. A., Saudou, F., Pestell, R. G., and Greenberg, M. E. (1998) Fos family members induce cell cycle entry by activating cyclin D1. *Mol. Cell. Biol.* **18**, 5609-5619.
14. Facchini, L. M., and Penn, L. Z. (1998) The molecular role of Myc in growth and transformation: recent discoveries lead to new insights. *FASEB J.* **12**, 633-651.
15. Leone, G., DeGregori, J., Sears, R., Jakoi, L., and Nevins, J. R. (1997) Myc and Ras collaborate in inducing accumulation of active cyclin E/Cdk2 and E2F. *Nature* **387**, 422-426.
16. Barone, M. V., and Courtneidge, S. A. (1995) Myc but not Fos rescue of PDGF signalling block caused by kinase-inactive Src. *Nature* **378**, 509-512.
17. Brown, E. J., and Schreiber, S. L. (1996) A signaling pathway to translational control. *Cell* **86**, 517-520.

18. Nourse, J., Firpo, E., Flanagan, W. M., Coats, S., Polyak, K., Lee, M.-H., Massague, J., Crabtree, G. R., and Roberts, J. M. (1994) Interleukin-2-mediated elimination of the p27^{Kip1} cyclin-dependent kinase inhibitor prevented by rapamycin. *Nature* **372**, 570-573.
19. Olson, M. F., Paterson, H. F., and Marshall, C. J. (1998) Signals from Ras and Rho GTPases interact to regulate expression of p21^{Waf1/Cip1}. *Nature* **394**, 295-298.
20. Chung, J., Grammer, T. C., Lemon, K. P., Kazlauskas, A., and Blenis, J. PDGF- and insulin-dependent pp70^{S6k} activation mediated by phosphatidylinositol-3-OH kinase. *Nature* **370**, 71-75.
21. Uehara, Y., Murakami, Y., Sugimoto, Y., and Mizuno, S. (1989) Mechanism of reversion of Rous sarcoma virus transformation by herbimycin A: reduction of total phosphotyrosine levels due to reduced kinase activity and increased turnover of p60^{v-src1}. *Cancer Res.* **49**, 780-785.
22. Hung, D. T., Jamison, T. J., and Schreiber, S. L. (1996) Understanding and controlling the cell cycle with natural products. *Chem. Biol.* **3**, 623-639.
23. Kusaka, M., Sudo, K., Matsutani, E., Kozai, Y., Marui, S., Fujita, T., Ingber, D., and Folkman, J. (1994) Cytostatic inhibition of endothelial cell growth by the angiogenesis inhibitor TNP-470 (AGM-1470). *Br. J. Cancer* **69**, 212-216.
24. Hartmann, G. R., Richter, H., Weiner, E. M., and Zimmermann, W. (1978) On the mechanism of action of the cytostatic drug anguidine and of the immunosuppressive agent ovalicin, two sesquiterpenes from fungi. *Planta Med.* **34**, 231-252.
25. Hori, A., Ikema, S., and Sudo, K. (1994) Suppression of cyclin D1 mRNA expression by the angiogenesis inhibitor TNP-470 (AGM-1470) in vascular endothelial cells. *Biochem. Biophys. Res. Commun.* **204**, 1067-1073.
26. Abe, J., Zhou, W., Takua, N., Taguchi, J., Kurokawa, K., Kumada, M., and Takuwa, Y. (1994) A fumagillin derivative angiogenesis inhibitor, AGM-1470, inhibits activation of cyclin-dependent kinases and phosphorylation of retinoblastoma gene product but not protein tyrosyl phosphorylation or protooncogene expression in vascular endothelial cells. *Cancer Res.* **54**, 3407-3412.
27. Koyama, H., Nishizawa, Y., Hosoi, M., Fukumoto, S., Kogawa, K., Shioi, A., and Morii, H. (1996) The fumagillin analogue TNP-470 inhibits DNA synthesis of vascular smooth muscle cells stimulated by platelet-derived growth factor and insulin-like growth factor-I: possible involvement of cyclin-dependent kinase 2. *Circ. Res.* **79**, 757-764.
28. Lanni, J. S. and Jacks, T. (1998) Characterization of the p53-dependent postmitotic checkpoint following spindle disruption. *Mol. Cell. Biol.* **18**, 1055-1064.
29. DiCaprio, J. A., Ludlow, J. W., Lynch, D., Furukawa, Y., Griffin, J., Piwnicka-Worms, H., Huang, C. M., and Livingston, D. M. (1989) The product of the retinoblastoma susceptibility gene has properties of a cell cycle regulatory element. *Cell* **58**, 1193-1198.
30. Chung, J., Kuo, C. J., Crabtree, G. R., and Blenis, J. (1992) Rapamycin-FKBP specifically blocks growth-dependent activation of and signaling by the 70 kd S6 protein kinases. *Cell* **69**, 1227-1236.

31. Roche, S., Koegl, M., Barone, M. V., Roussel, M. F., and Courtneidge, S. A. (1995) DNA synthesis induced by some but not all growth factors requires Src family protein tyrosine kinases. *Mol. Cell. Biol.* **15**, 1102-1109.
32. Roche, S., Fumagalli, S., and Courtneidge, S. A. (1995) Requirement for src family protein kinases in G₂ for fibroblast cell division. *Science* **269**, 1567-1569.
33. Nakayama, K., Ishida, N., Shirane, M., Inomata, A., Inoue, T., Shishido, N., Horii, I., Loh, D. Y., and Nakayama, K.-I. (1996) Mice lacking p27^{Kip1} display increased body size, multiple organ hyperplasia, retinal dysplasia, and pituitary tumors. *Cell* **85**, 707-720.

Chapter 6

Binding of thalidomide to α_1 -acid glycoprotein

Abstract

In addition to its well known sedative and teratogenic effects, thalidomide also possesses potent immunomodulatory and anti-inflammatory activities, being most effective against leprosy and chronic graft-versus-host disease. The immunomodulatory activity of thalidomide has been ascribed to the selective inhibition of tumor necrosis factor- α from monocytes. The molecular mechanism for the immunomodulatory effect of thalidomide remains unknown. To elucidate this mechanism, we synthesized an active photoaffinity label of thalidomide as a probe to identify the molecular target of the drug. Using the probe, we specifically labeled a pair of proteins of 43-45 kD with high acidity from bovine thymus extract. Purification of these proteins and partial peptide sequence determination revealed them to be α_1 -acid glycoprotein (AGP). We show that the binding of thalidomide photoaffinity label to authentic human AGP is competed with both thalidomide and the non-radioactive photoaffinity label at concentrations comparable to those required for inhibition of production of tumor necrosis factor- α from human monocytes, suggesting that AGP may be involved in the immunomodulatory activity of thalidomide.

Introduction

Thalidomide has a relatively simple chemical architecture (Figure 6.1), but exhibits a multitude of physiological activities on mammals. In addition to its sedative and teratogenic effects (1,2), thalidomide possesses significant and unique immunomodulatory and anti-inflammatory activities. It has been found to be effective against several immune disorders including chronic graft-versus-host disease (3), oral and oropharyngeal ulcers associated with HIV infection (4), erythema nodosum leprosum in leprosy (5) and several other inflammatory skin diseases (6). Most recently, thalidomide was found to have anti-angiogenic activity (7), raising the possibility that it may be used to treat certain types of angiogenesis-dependent diseases such as diabetic retinopathy and cancer.

The immunomodulatory effect and the related anti-inflammatory effect of thalidomide have attracted much attention in recent years. In searching for the cellular targets of thalidomide,

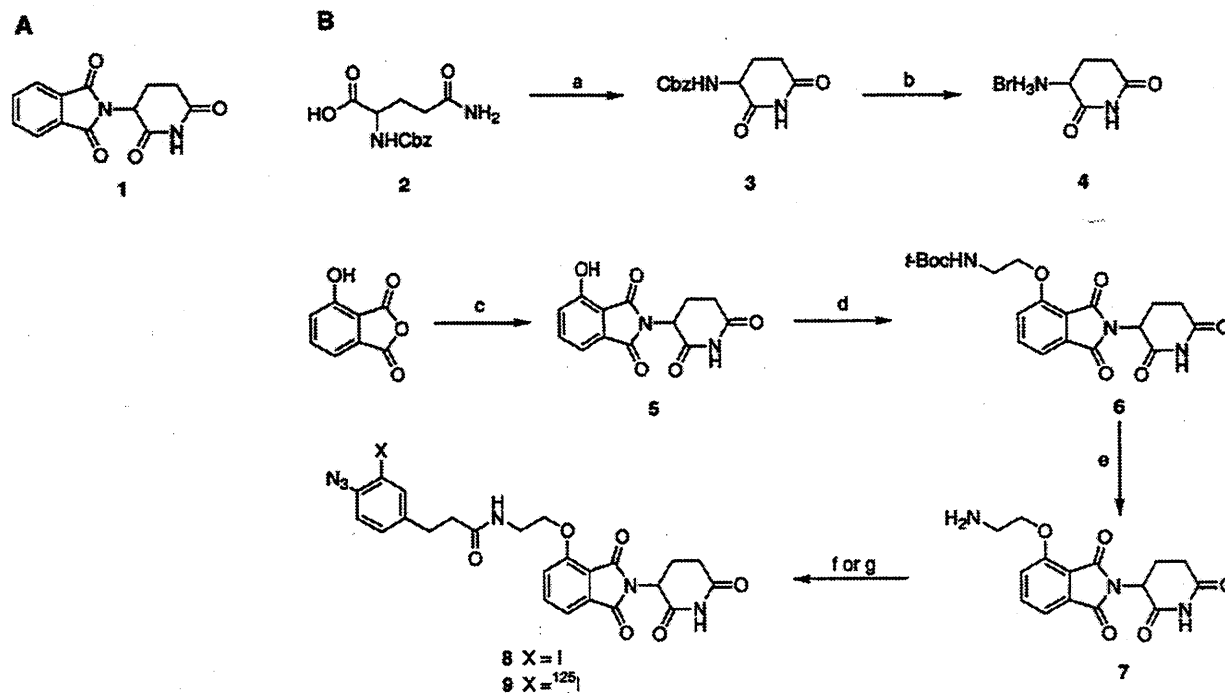


Figure 6.1. A. Structure of thalidomide (1). B. Preparation of thalidomide photoaffinity labels AIPPOT (8) and [^{125}I]AIPPOT (9). Reaction conditions: (a) SOCl_2 , 1 equivalent in dimethylformamide, 2 hr, -5°C . (b) 30% HBr/HOAc , 80 min., RT. (c) Compound 4, 1 equivalent, and triethylamine, 1 equivalent, in dimethylformamide, 24 hr at 60°C , 1 equivalent dicyclohexylcarbodiimide and catalytic dimethylaminopyridine added, continued at 60°C for 72 hr. (d) *N*-(*t*-Butoxycarbonyl)-aminoethyl bromide, 5 equivalents, and tetraethylammonium fluoride, 1 equivalent, 72 hr, RT. (e) 25% trifluoroacetic acid/ CH_2Cl_2 , 30 min., RT. (f) Azidoiodophenylpropionic acid succinimidyl ester, 1 equivalent, triethylamine, 2 equivalents in EtOAc, 40 hr, RT. (g) [^{125}I]Azidoiodophenylpropionic acid succinimidyl ester (carrier free) 100 μCi and 1 mg amine 7 in 0.5% $\text{Et}_3\text{N}/\text{EtOAc}$, 16 hr, RT.

several models of immune regulation have been examined. It was reported that the calcium-dependent lymphocyte proliferation in response to mitogen and alloantigens is inhibited by thalidomide (8). Neubert and coworkers uncovered several cell surface molecules whose expression is either enhanced or inhibited by the drug *in vivo* (9). Kaplan and colleagues found that thalidomide selectively inhibits the production of tumor necrosis factor- α (TNF- α) from stimulated human monocytes both *in vitro* and *in vivo* (10,11), providing a possible mechanism for both the immunomodulatory and the anti-inflammatory activities of the drug. This TNF- α inhibitory effect has been ascribed to enhanced mRNA degradation by the drug (12). Blockade of TNF- α production seems to underlie the inhibition of replication of the type 1 HIV in human monocytes by thalidomide (13). Further delineation of the inhibitory mechanism has been hampered, in large part, by the relatively low potency of the drug with an IC_{50} between 10 to 100 μ M for TNF- α inhibition (12,13).

In an effort to elucidate the molecular mechanism of immunomodulation by thalidomide in general and the molecular target responsible for its inhibition of TNF- α in particular, we have synthesized an active photoaffinity label derived from the drug. Using this photoaffinity label, we detected a pair of proteins that specifically bind to thalidomide. These thalidomide binding proteins have been identified as isoforms of α_1 -acid glycoprotein (AGP), indicating a potential role for AGP as a mediator of the drug's immunomodulatory effect.

Materials and Methods

Fresh calf thymus were obtained from Research 87, Medford, MA. Human AGP and *C. perfringens* Neuraminidase were from Sigma. Mouse anti-human TNF- α monoclonal antibodies used for ELISA were from Pharmingen. Carboxymethyl sepharose was from Pharmacia. Cbz-glutamine was purchased from Bachem Bioscience Inc. 125 I-labeled and unlabeled azidoiodophenylpropionic acid succinimidyl ester (14) were purchased from Dr. A. Ruoho, University of Wisconsin School of Medicine. NMR solvents were from Cambridge Isotope Laboratories. Propranolol and alprenolol were from Research Biochemicals International. All other chemicals were purchased from Aldrich Chemical Co.

General Synthetic Chemistry. Unless otherwise indicated, reagents were purchased from Aldrich and solvents from Aldrich or Mallinckrodt and were reagent grade or better. NMR

solvents were from Cambridge Isotope Laboratories. Dichloromethane was distilled under nitrogen from calcium hydride. Flash column chromatography was performed using Merck silica gel, 230-400 mesh. All compounds were analyzed by ^1H NMR using a Varian XL 300 Mhz spectrometer and by low resolution mass spectrometry. Where indicated, high resolution mass spectra were taken on a Finnegan MATT 8200 spectrometer.

Thalidomide. *N*-Phthaloylglutaric anhydride (4.96 g, 19.1 mmol) and urea (0.62 g, 10.3 mmol) were co-melted under an Ar atmosphere with stirring at 200 °C (15). After 20 min the reaction mixture was cooled to room temperature, and the resulting yellow solid was recrystallized from 2-ethoxyethanol (65 mL). Crystals were collected by suction filtration, washed three times with Et_2O , air dried, and then further dried in vacuo to afford 2.281 g thalidomide (46% yield). ^1H NMR ($\text{DMSO}-d_6$) δ 11.14 (s, 1H), 7.92 (m, 4H), 5.16 (dd, 1H), 2.89 (m, 1H), 2.52 (m, 2H), 2.07 (m, 1H).

***N*-Carbobenzoxy-2-aminoglutarimide.** Cbz-glutamine (0.5 g, 1.8 mmol) was dissolved in dimethylformamide under an atmosphere of Ar. The solution was cooled in an EtOH/dry ice bath and thionyl chloride (160 μL , 2.2 mmol) was added dropwise by syringe with stirring. The reaction vessel was transferred to an ice water bath and stirred for an additional 2 hr, after which time the solution was added to 190 mL 10% KOAc (aq) and the resulting mixture extracted twice with 200 mL Et_2O . The organic layers were dried over MgSO_4 , filtered, and the solvent removed under reduced pressure. The residue was chromatographed on silica gel in 1:1 $\text{CHCl}_3/\text{EtOAc}$. Removal of solvent under reduced pressure provided the product as an oily reddish solid (214 mg, 46% yield). ^1H NMR (CDCl_3) δ 8.24 (s, 1H), 7.34 (m, 5H), 5.63 (d, 1H), 5.12 (s, 2H), 4.35 (m, 1H), 2.48-2.84 (m, 3H), 1.88 (ddd, 1H).

2-Aminoglutarimide hydrobromide. HBr (30% solution in HOAc, 6mL) was added via syringe to a reaction vessel containing *N*-carbobenzoxy-2-aminoglutarimide (980 mg, 3.74 mmol) in a nitrogen atmosphere. The mixture was stirred 1 hr 10 min, at which point diethyl ether (15 mL) was added. The solid was collected by suction filtration, washed twice with diethyl ether, dried in air and in vacuo to provide 716 mg 2-aminoglutarimide hydrobromide as a pale green powder (92% yield). ^1H NMR ($\text{DMSO}-d_6$) δ 11.27 (s, 1H), 8.43 (s, 3H), 4.23 (d, 1H), 2.04-2.78 (m, 2H), 2.15 (m, 1H), 2.01 (m, 1H).

3-Hydroxythalidomide. 2-Aminoglutarimide hydrobromide (200 mg, 0.96 mmol) and 3-hydroxyphthalic anhydride (157 mg, 0.96 mmol) were dissolved in DMF under a nitrogen

atmosphere. Triethylamine (133 μ L, 0.96 mmol) was added via syringe and the solution heated to 60 °C in an oil bath for 4 hr. The mixture was then cooled to room temperature to add hydroxybenzotriazole (71 mg, 0.5 mmol) and dicyclohexylcarbodiimide (200 mg, 0.96 mmol), and then returned to the oil bath for an additional 24 hr. After cooling to room temperature, the reaction mixture was filtered and poured into brine, which was extracted twice with 3:5 CHCl₃/EtOAc. The organic fractions were dried with Na₂SO₄, filtered, and concentrated to an oil under reduced pressure. The residue was chromatographed twice on silica gel by loading in CHCl₃/EtOAc and eluting with neat EtOAc. Removal of the solvent under reduced pressure and in vacuo provided 109 mg of 3-hydroxythalidomide as a green-yellow solid (42% yield). ¹H NMR (DMSO-*d*₆) δ 11.17 (br s, 1H), 11.09 (s, 1H), 7.64 (m, 1H), 7.27 (m, 2H), 5.06 (dd, 1H), 2.87 (m, 1H), 2.48-2.61 (m, 2H), 2.02 (m, 1H).

***t*-Butoxycarbonylaminoethyl bromide.** Prepared by the reaction of di-*t*-butyl pyrocarbonate with aminoethyl bromide as previously reported (16) (49% yield). ¹H NMR (CDCl₃) δ 4.92 (br s, 1H), 3.50 (t, 2H), 3.43 (t, 2H), 1.42 (s, 9H).

3-(*t*-Butoxycarbonylaminoethoxy)thalidomide. 3-Hydroxythalidomide (12 mg, 0.044 mmol) was added to a mixture of DMF (0.8 mL), tetraethylammonium fluoride dihydrate (8 mg, 0.044 mmol), and molecular sieves (3 Å) with stirring, followed by the addition of *t*-butoxycarbonylaminoethyl bromide (30 mg, 0.132 mmol). The mixture was stirred under nitrogen for 72 hr, diluted with EtOAc (12 mL) and filtered. This solution was washed once with water and once with saturated aqueous NaHCO₃, dried with MgSO₄ and filtered. After removal of the solvent under reduced pressure, the residue was chromatographed on silica gel in 3:2 EtOAc/hexanes. Removal of the solvent produced 7 mg of the desired product as an oily solid (38% yield). ¹H NMR (CDCl₃) δ 8.069 (s, 1H), 7.67 (m, 1H), 7.47 (d, 1H), 7.22 (d, 1H), 5.23 (br s, 1H), 4.94 (dd, 1H), 4.21 (t, 2H), 3.59 (d, 2H), 2.71-2.92 (m, 3H), 2.13 (m, 1H), 1.42 (s, 9H).

3-(2-(3-Azido-2-iodophenyl)propionamido)ethoxythalidomide. *t*-Boc-aminoethoxythalidomide (4 mg) was dissolved in methylene chloride (1 mL) and an equal volume of 50% trifluoroacetic acid in methylene chloride added. The reaction was stirred for 30 min at room temperature. After the addition of 2 mL toluene, the solvent was removed under reduced pressure and the resulting oil was triturated twice with diethyl ether and dried in vacuo. The resulting white solid was dissolved in 2 mL EtOAc, and triethylamine (2 μ L) and 3-azido-2-

iodophenylpropionyl succinimide were added in the absence of direct light. The reaction was stirred in the dark for 40 hr and the product purified by chromatography on silica gel, eluting in 2% MeOH/EtOAc. Removal of the solvent under reduced pressure provided the product (4.0 mg) in 79% yield.

Thalidomide photoaffinity label, [¹²⁵I]3-(2-(3-Azido-4-iodophenylpropionamido)-ethoxy)thalidomide ([¹²⁵I]AIPPOT) (9). All procedures were performed in the absence of direct light. [¹²⁵I]Azidoiodophenylpropionic acid succinimidyl ester (120 mCi in 120 ml ethyl acetate) was concentrated under a stream of nitrogen to a volume of less than 5 ml. A suspension of 1 mg 3-(aminoethoxy)thalidomide in 100 µl ethyl acetate/0.5% triethylamine was added. The reaction mixture was left overnight at room temperature in a closed container. The product was purified by silica gel chromatography. Fractions were concentrated under a stream of nitrogen to <5 ml and then the product was resuspended in 100 ml methanol and stored at -80°C.

Monocyte Isolation and TNF- α Secretion Assay. Peripheral blood mononuclear cells were isolated from heparinized blood by centrifugation on Ficoll-Paque Plus (Pharmacia) step gradients. Cells were washed three times in cell culture medium (RPMI 1640). A monocyte-enriched fraction was isolated by suspending the cells to 2.5×10^6 /ml in complete medium (RPMI 1640 plus HEPES with 5% human AB serum, 50 units/ml penicillin, 50 µg/ml streptomycin and 2.5 mM L-glutamine) and allowing cells to adhere to plastic tissue culture plates in a humidified atmosphere of 5% CO₂ at 37 °C for three hours. Non-adherent cells were removed by washing with serum-free medium, and adherent cells were detached by scraping and washed twice with serum free medium. To assay for TNF- α production, cells were resuspended in complete medium to 10^6 cells/0.9 ml and plated at 0.45 ml per well in 24-well plates. Cells were allowed to adhere for two hours at 37 °C before drugs or analogs dissolved in dimethyl sulfoxide (DMSO) were added with a final concentration of 0.2% DMSO. This was followed by addition of lipopolysaccharide (LPS) (in 50 ml complete medium) to a final concentration of 1 µg/ml. Plates were incubated for 16 hours in a humidified incubator (37 °C/5% CO₂). Drug treatment did not significantly affect cell viability compared to DMSO controls, as judged by trypan blue exclusion. Culture supernatants were collected by centrifugation at 1300 x g for 6 minutes at 4 °C. TNF- α was assayed by ELISA using mouse anti-human TNF- α monoclonal antibodies from Pharmingen according to the supplier's instructions. The levels of TNF- α are derived from a second order polynomial standard curve ($r^2 > 0.995$ for each determination).

Preparation of Tissue Extracts. Freshly prepared bovine thymus tissue was shipped on ice and used the same day. Connective tissue was removed from organs and they were cut into small pieces and frozen in liquid nitrogen. Frozen chunks were weighed, powdered and then suspended in cytosol buffer (20 mM TrisHCl, pH 6.9, 100 mM NaCl, 2 mM β -mercaptoethanol, 0.02% NaN_3 , 5% glycerol, 1 mM phenylmethylsulfonyl fluoride), 1 ml/g of tissue, in a blender. Suspensions were dounce homogenized with ten up-and-down strokes and centrifuged at 9000 x g to remove most of the debris. The supernatant was centrifuged at 100,000 x g and the S100 fraction stored in aliquots at -80°C until needed.

Photoaffinity Labeling. Crude or partially purified tissue extract containing 5-20 μg of total protein or 0.1 μg of purified human AGP (Sigma) was diluted in labeling buffer (20 mM TrisHCl, pH 7.0, 50 mM NaCl, 1 mM MgCl_2 , 1 mM CaCl_2 , 0.5 mM EDTA) to a final volume of 45 μl . Drug or DMSO (0.5% volume) was added followed by incubation at 37°C for 30 min. Photoaffinity label ($\sim 1\mu\text{Ci}/\mu\text{l}$) was diluted five fold in labeling buffer in bulk immediately before use and 5 ml was added to each labeling tube in the absence of direct light. Samples were mixed and incubated at 37°C for 30 minutes in the dark, and then irradiated in a Stratalinker (Stratagene) at 254 nm with a total energy output of $3.3\text{ J}/\text{m}^2$. For one-dimensional SDS-PAGE, reactions were quenched by adding 3.5 μl β -mercaptoethanol followed by 18 μl 4x SDS-PAGE sample buffer (250 mM TrisHCl, pH 6.8, 40% glycerol, 5% SDS, 0.1 mg/ml bromophenol blue). Samples were heated in a boiling water bath for 3 minutes before they were subjected to SDS-PAGE. For two-dimensional electrophoresis, reactions were quenched by adding 5 μl 10% SDS/150 mM dithiothreitol. Samples were heated as above, cooled and 5 μl urea solution (65 mM dithiothreitol/4% CHAPS/9 M urea/5% Bio-Rad Bio-Lyte 3-10 ampholyte) was added. Samples were loaded onto IEF gels (4.5% acrylamide/0.4% bis-acrylamide/9.2 M urea/1% Bio-Lyte 5-7 ampholyte/4% Biolyte 3-10 ampholyte/1.5% CHAPS/0.5% NP-40, 14 cm x 2.5 mm) and run for 12 hr at 400 V followed by 2 hr at 1000 V in a Bio-Rad Protean II apparatus with 6 mM phosphoric acid in the lower chamber and 20 mM sodium hydroxide in the upper chamber. The SDS-PAGE dimension was 12% acrylamide/0.32% bis-acrylamide. Gels were stained with Coomassie Blue, dried onto blotting paper and exposed to X-ray film (Kodak XAR 5) or to phosphorimager cassettes (Molecular Dynamics). Labeling was quantified using ImageQuant software.

Protein Purification. All procedures were carried out at 4°C. To 20 ml of bovine thymus S100 fraction (9.2 mg/ml protein) was added 7.36 g (61%) ammonium sulfate with mixing. The mixture was incubated on a rotator for 16 hr followed by centrifugation at 12,000 x g for 15 minutes. To the supernatant was added 4.20 g (92%) ammonium sulfate and rotated for 8 hours. The mixture was centrifuged as before. The pellet was resuspended in 2 ml buffer containing 20 mM TrisHCl (pH 6.8) and 100 mM NaCl, and dialyzed into 20 mM sodium acetate, pH 4.1/20 mM NaCl overnight. The resulting suspension was centrifuged at 16,000 x g for 10 minutes to remove the precipitate and the supernatant was applied to a carboxymethyl sepharose column. The column was washed with the dialysis buffer. The flow-through fractions were pooled and dialyzed into 50 mM ammonium carbonate for 24 hours with one change of buffer. The sample was lyophilized overnight and resuspended in 20 µl H₂O.

Neuraminidase Digestion and Protein Sequencing. The purified thalidomide binding proteins (10 µl), 17 µl 0.1 M sodium acetate (pH 5.5) and 3 µl *C. perfringens* neuraminidase (Sigma Type V, 1 mU/µl) were mixed and incubated at 37°C for 5 hr. To the mixture were added 2.5 µl β-mercaptoethanol and 10 µl 4 x SDS sample buffer. The sample was heated in a boiling water bath for 3 minutes and subjected to SDS-PAGE as above. The proteins were then blotted onto PVDF membrane. The blot was stained with Ponceau S and destained briefly in doubly distilled water before the band corresponding to the thalidomide binding protein was sliced out. The membrane was submitted for proteolytic digestion with either Lys-C or chymotrypsin. Peptide fragments were separated by high performance liquid chromatography and sequenced by Edman degradation at the Harvard Microchemistry Facility and the MIT Biopolymers Lab.

Results

The relatively low potency of thalidomide as an inhibitor of TNF-α production suggests that thalidomide may have a low affinity for its target, making it difficult to employ conventional affinity chromatography to identify and purify the potential target proteins. We therefore resorted to the more sensitive method of photoaffinity labeling to identify thalidomide binding proteins. To make an active thalidomide photoaffinity label, we needed to define a position in thalidomide to which a radioactive photocrosslinking moiety may be attached without significantly abrogating its activity. A survey of the literature indicated that C-3 of the phthalimide group may be such a position as it has been shown that 3-hydroxythalidomide is

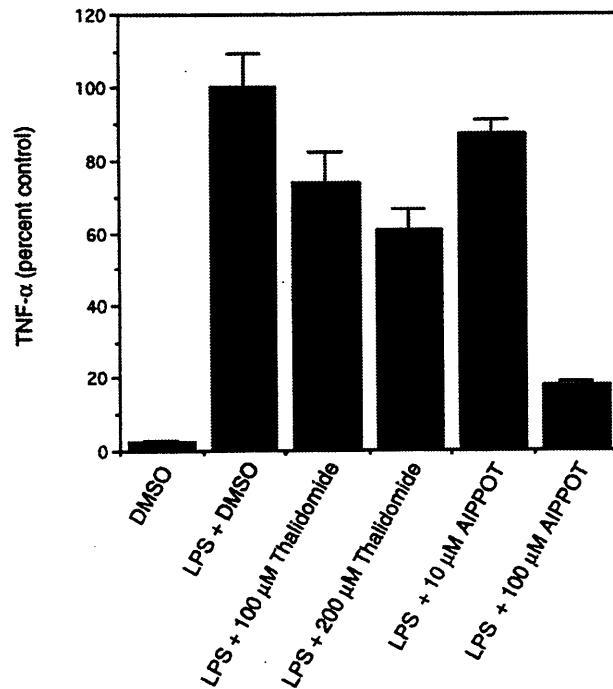


Figure 6.2. Effect of thalidomide and AIPPOT on the secretion of TNF- α by LPS-stimulated human peripheral blood monocytes. Monocytes were treated with 1 μ g/ml LPS for 16 hours in the presence of varying concentrations of drug or carrier alone (0.2% DMSO). The amount of TNF- α was determined in culture supernatants by ELISA. Results are expressed as the percentage of TNF- α produced compared to DMSO control and are the average of two experiments with separate donors each performed in triplicate. Error bars refer to SD.

active in animal models for both graft-versus-host disease (17) and embryopathy (18). We synthesized a non-radioactive photoaffinity label derived from thalidomide, 3-(2-(azido-iodophenylpropionamido)ethoxy)thalidomide (AIPPOT), by attaching a 4-azido-3-iodophenylpropionyl group onto 3-hydroxythalidomide via an ethanolamine linker (Figure 6.1). When the activity of the non-radioactive photoaffinity label was determined, it was found to be more active than thalidomide itself (Figure 6.2). While thalidomide inhibits TNF- α production with an IC₅₀ of over 200 μ M, its solubility limit in aqueous medium, the attachment of the side chain onto the 3-hydroxy group in the photoaffinity label resulted in an increase in its potency, with an IC₅₀ of less than 100 μ M.

We subsequently synthesized the radioactive photoaffinity label containing ¹²⁵I (Figure 6.1) and used it to identify potential thalidomide binding proteins in membrane and soluble extracts prepared from fresh bovine thymus, an abundant source of proteins from lymphoid cells. Although no specific proteins were detected in the membrane fraction (data not shown), treatment of the soluble extract with [¹²⁵I]AIPPOT followed by irradiation at 254 nm resulted in specific labeling of two proteins with apparent molecular mass of ca. 45 and 43 kD (Figure 6.3). This labeling can be competed with unmodified thalidomide at concentrations comparable to those required for TNF- α inhibition in the cellular assay (Figures 6.2 and 6.3).

To find an optimal procedure for isolating the putative thalidomide binding proteins, we determined, among other physical properties, their isoelectric points. Two-dimensional gel electrophoresis of labeled thymus extract revealed the putative thalidomide binding proteins to be extremely acidic with isoelectric points of ca. 3.5 (Figure 6.4). Moreover, the two labeled protein bands on one-dimensional SDS-PAGE were resolved into a series of spots in the IEF dimension. The unusually high acidity of the putative thalidomide binding proteins led us to search in the literature for proteins with similar isoelectric points. Indeed, we found that AGP, also called orosomuroid, was strikingly similar to the putative thalidomide binding proteins on a two-dimensional gel electrophoresis map with few other proteins in its neighborhood (19). This finding helped to simplify the isolation and identification of the thalidomide binding proteins.

Using the established purification procedures for AGP as a guide and the thalidomide photoaffinity labeling as an assay, we purified the thalidomide binding proteins to near homogeneity in two steps. Starting with crude bovine thymus extract, the thalidomide binding activity was concentrated in 61-92% ammonium sulfate precipitate (20). After dialysis into

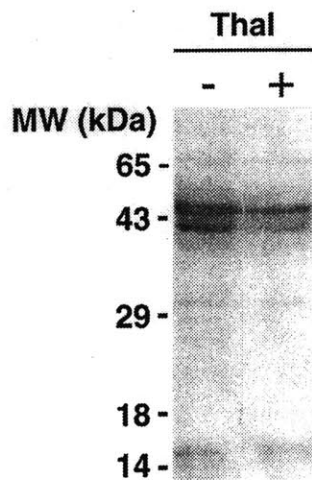


Figure 6.3. Labeling of bovine thymus S100 fraction with $[^{125}\text{I}]\text{AIPPOT}$. Soluble bovine thymus extracts were preincubated with 200 μM cold competitor thalidomide (+) or DMSO (-) carrier (0.5%) for 30 minutes before the addition of 1 μCi $[^{125}\text{I}]\text{AIPPOT}$ in the absence of direct light. After 30 minutes samples were irradiated, quenched with β -mercaptoethanol, and subjected to SDS-PAGE.

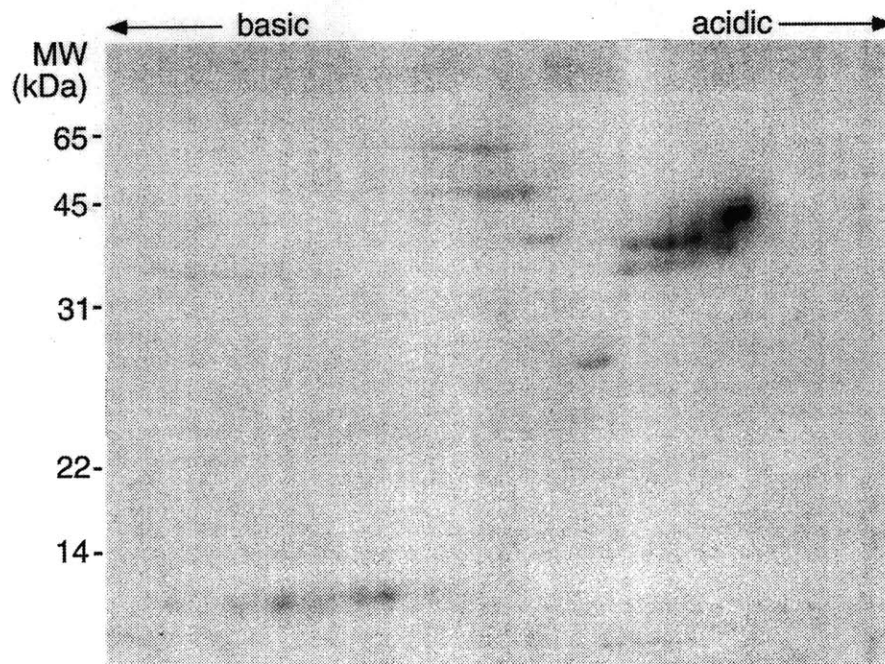


Figure 6.4. Two dimensional gel electrophoresis of $[^{125}\text{I}]\text{AIPPOT}$ -labeled bovine thymus extract.

acidic sodium acetate buffer, the thalidomide binding protein-containing fraction was subjected to weak cation exchange carboxymethyl sepharose chromatography (21). The thalidomide binding proteins were present in the flow-through fraction at pH 4.1, virtually free of other proteins (Figure 6.5, Lane 1). The N-termini of the proteins thus purified were blocked, in agreement with the known N-terminal pyroglutamate moiety of AGP (22). Since AGP is also known to have a high sialic acid content, we treated the purified thalidomide binding proteins with neuraminidase. Upon neuraminidase treatment, the two thalidomide binding protein bands were converted into a single protein band, suggesting that the two bands originated from the same protein with differential sialylation (Figure 6.5). Removal of the sialic acids also allowed for the subsequent proteolysis of the proteins and sequencing of the proteolytic fragments. The sequences of four proteolytic fragments were determined. All show high homology with human AGP (Figure 6.6). Although the bovine AGP has not been cloned, the four peptides sequences are 75% identical and 93% similar to human AGP (23). By comparison, rabbit AGP only bears 59% identity and 74% similarity to human AGP in the same regions, suggesting that the thalidomide binding proteins in bovine thymus extract are isoforms of the bovine AGP.

To confirm that AGP binds to thalidomide, we labeled commercially available AGP from several species. The labeling of human AGP with thalidomide photoaffinity label is shown in Figure 6.7. Indeed, [¹²⁵I]AIPPOT labels human AGP and this labeling is competed by both thalidomide and the non-radioactive AIPPOT, with the latter being more potent. The potencies of thalidomide and AIPPOT are in general agreement with the relative potency of these two compounds in the TNF- α secretion assay (Figure 6.2).

AGP in the plasma is known to bind to a large number of basic and occasionally neutral drugs and exert important effect on their pharmacokinetics (24). We compared the drug binding site for thalidomide and several other drugs using a competition assay in which the labeling of AGP by the thalidomide photoaffinity label was carried out in the presence of two known AGP-binding drugs, propranolol and alprenolol. As shown in Figure 6.7B, both propranolol and alprenolol compete effectively against the thalidomide photoaffinity label for AGP, with alprenolol being more potent than propranolol. It is likely that thalidomide binds to AGP at the same or an overlapping site as propranolol and alprenolol.

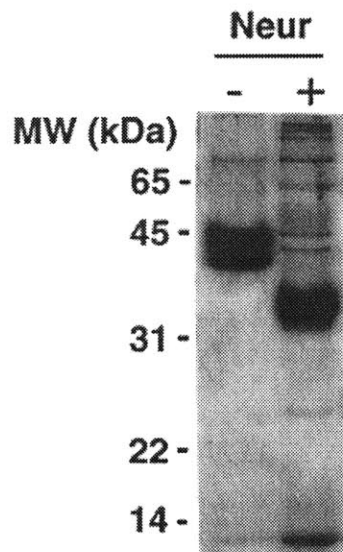


Figure 6.5. Purified thalidomide binding proteins. Proteins were purified as described in the Results section and aliquots incubated in 30 μ l digestion buffer in the presence or absence of 3 mU *C. perfringens* neuraminidase for 5 hr at 37 $^{\circ}$ C. Portions of the samples were subjected to SDS-PAGE followed by silver staining.

Bovine Peptide-1	FYIGSAF
	•••••
Human α_1 -AGP	FYIASAF
Bovine Peptide-2	AIQAAF
	•••••
Human α_1 -AGP	EIQAAF
Bovine Peptide-3	MLAASW
	•••••
Human α_1 -AGP	MLA-SY
Bovine Peptide-4	KXVGVXFYADK
	•••••
Human α_1 -AGP	KQYGLSFYADK

Figure 6.6. Comparison of peptide sequences derived from the purified thalidomide binding protein and those of human AGP. "X" in Bovine peptide-4 denotes unidentified residues.

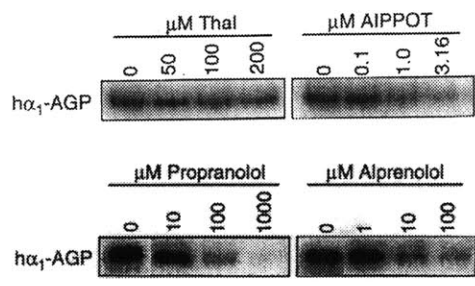


Figure 6.7. Labeling of human AGP with increasing concentrations of cold competitors. A sample of 0.1 μg human AGP per tube was preincubated with varying concentrations of competitor or with DMSO carrier alone (0.5%). $[^{125}\text{I}]\text{AIPPOT}$ (1 μCi per tube) was added, tubes were incubated 30 min, irradiated, quenched with β -mercaptoethanol and subjected to SDS-PAGE followed by autoradiography. A. Competition of labeling with thalidomide and AIPPOT. B. Competition with the β -blockers propranolol and alprenolol.

Discussion

Thalidomide is known to possess immunomodulatory and anti-inflammatory effects. However, the cellular and molecular mechanisms of these activities are not understood. Among the various cellular effects of thalidomide, the inhibition of TNF- α seems to offer a plausible mechanism for several known immunomodulatory activities of the drug. Using LPS-induced TNF- α secretion in human monocytes as an assay and an active thalidomide photoaffinity label as a probe, we isolated and identified two thalidomide binding proteins as isoforms of AGP.

AGP belongs to the class of acute phase proteins that are known to be induced in the liver in response to a wide variety of physiological stresses including inflammation, infection, pregnancy and malignancy (25,26). It is distinct from other serum proteins by its high carbohydrate content (over 40% by weight) and high acidity. Although it has been known for more than a century (27), the precise biological function of AGP still remains unknown. Nevertheless, a number of studies have pointed to potential roles of AGP in the regulation of the immune system and in inflammation. AGP was shown to have immunosuppressive activity in the mixed lymphocyte reaction (28) and an AGP-like immunosuppressive acidic protein was found from ascites fluids of cancer patients (29). The potential role of AGP in inflammation has been somewhat controversial. On the one hand, AGP was shown to exert a protective effect against TNF- α and LPS-induced lethality when it is administered intraperitoneally in mice (30). It has also been shown to inhibit platelet aggregation (31) and thus may be capable of preventing secretion of other pro-inflammatory factors. On the other hand, AGP was shown to potentiate LPS-induced secretion of such inflammatory cytokines as TNF- α and IL-1 in human monocytes *in vitro* (32). Since thalidomide inhibits LPS-induced TNF- α secretion, it will be interesting to see whether thalidomide acts by inhibiting AGP's potentiating activity for LPS. It also remains to be determined whether thalidomide has any effect on other immunomodulatory activities of AGP.

As an abundant plasma protein, AGP binds to many drugs and can modulate their metabolism (24). Those drugs include known β -blockers such as propranolol and alprenolol. Competition experiments indicate that thalidomide binds to the same site in AGP as propranolol and alprenolol. None of the drugs, however, possess the same unique immunomodulatory and anti-inflammatory activities of thalidomide. Whether binding of thalidomide to AGP confers a

unique conformational change to the protein leading to a gain of function remains to be investigated.

The primary source of AGP is known to be hepatocytes (33). However, it has been shown that lymphocytes, granulocytes and monocytes also express a membrane-associated form of AGP (34). It has also been reported that monocytes can serve as a source of soluble AGP (35). In fact, we have found that upon LPS stimulation, the promonocytic cell line THP-1 differentiated by treatment with $1\alpha, 25$ -dihydroxy vitamin D₃ produces large amount of AGP along with TNF- α (B.T. & J.L., unpublished results). These observations are consistent with the aforementioned immunomodulatory activities of AGP and suggest that AGP may play an important role in immunoregulation. The fact that thalidomide binds to AGP with high specificity implies that AGP may mediate the immunomodulatory effect of the drug.

References for Chapter 6

1. McBride, W. G. (1961) Thalidomide and congenital abnormalities. *Lancet* **ii**, 1358.
2. Lenz, W. (1962) Thalidomide and congenital abnormalities. *Lancet* **i**, 45.
3. Vogelsang, G. B., Taylor, S., Gordon, G., and Hess, A. D. (1986) Thalidomide, a potent agent for the treatment of graft-versus-host disease. *Transplant. Proc.* **18**, 904-906.
4. Jacobson, J. M., et al. (1997) Thalidomide for the treatment of oral aphthous ulcers in patients with human immunodeficiency virus infection. *N. Engl. J. Med.* **336**, 1487-1493.
5. Sheskin, J. (1965) Thalidomide in the treatment of lepra reactions. *Clin. Pharmacol. Ther.* **6**, 303-306.
6. Koch, H. P. (1985) Thalidomide and congeners as anti-inflammatory agents. In *Progress in Medicinal Chemistry* eds. Ellis, G. P. & West, G. B. (Elsevier Science Publishers, Amsterdam) pp. 166-242.
7. D'Amato, R. J., Loughnan, M. S., Flynn, E., and Folkman, J. (1994) Thalidomide is an inhibitor of angiogenesis. *Proc. Natl. Acad. Sci. USA* **91**, 4082-4085.
8. Keenan, R. J., Eiras, G., Bruckart, G. J., Stuart, R. S., Hardesty, R. L., Vogelsang, G., Griffith, B. P., and Zeevi, A. (1991) Immunosuppressive properties of thalidomide. *Transplant.* **52**, 908-910.
9. Nogueira, A. C., Neubert, R., Helge, H., and Neubert, D. (1994) Thalidomide and the immune system: 3. Simultaneous up- and down-regulation of different integrin receptors on human white blood cells. *Life Sci.* **55**, 77-92.
10. Sampaio, E. P., Sarno, E. N., Galilly, R., Cohn, Z. A., and Kaplan, G. (1991) Thalidomide selectively inhibits tumor necrosis factor α production by stimulated human monocytes. *J. Exp. Med.* **173**, 699-703.
11. Sampaio, E. P., Kaplan, G., Miranda, A., Nery, J. A. C., Miguel, C. P., Viana, S. M., and Sarno, E. N. (1993) The influence of thalidomide on the clinical and immunologic manifestation of erythema nodosum leprosum. *J. Inf. Dis.* **168**, 408-414.
12. Moreira, A. L., Sampaio, E. P., Zmuidzinas, A., Frindt, P., Smith, K. A., and Kaplan, G. (1993) Thalidomide exerts its inhibitory action on tumor necrosis factor α by enhancing mRNA degradation. *J. Exp. Med.* **177**, 1675-1680.
13. Makonkawkeyoon, S., Limson-Pobre, R. N. R., Moreira, A. L., Schauf, V., and Kaplan, G. (1993) Thalidomide inhibits the replication of human immunodeficiency virus type 1. *Proc. Natl. Acad. Sci. USA* **90**, 5974-5978.
14. Lowndes, J. M., Hokin-Neaverson, M., and Ruoho, A. E. (1988) N-(3-(p-azido-m-[¹²⁵I]iodophenyl)propionyl)-succinimide— a heterobifunctional reagent for the synthesis of radioactive photoaffinity ligands: synthesis of a carrier-free ¹²⁵I-labeled cardiac glycoside photoaffinity label. *Anal. Biochem.* **168**, 39-47.
15. Beckmann, V. R. (1962) Über das Verhalten von Thalidomid im Organismus. *Arzneim. Forsch.* **12**, 1095.
16. Ehrenstorfer-Schäfers, E.-M., Steiner, N., Altman, J., and Beck, W. (1990) Metal complexes of biologically important ligands, LV [1] Binding of steroidal hormones through α -amino acid ligands to platinum(II) and palladium(II). *Z. Naturforsch.* **45b**, 817-827.
17. Vogelsang, G. B., Hess, A. D., Gordon, G., Brundrette, R., and Santos, G. W. (1987) Thalidomide induction of bone marrow transplantation tolerance. *Transplant. Proc.* **19**, 2658-2661.

18. Boylen, J. B., Horne, H. H., and Johnson, W. J. (1964) Teratogenic effects of thalidomide and its metabolites on the developing chick embryo. *Can. J. Biochem.* **42** 35-42.
19. Golaz, O., Hughes, G. J., Frutiger, S., Paquet, N., Bairoch, A., Pasquali, C., Sanchez, J.-C., Tissot, J.-D., Appel, R. D., Walzer, C., Balant, L., and Hochstrasser, D. F. (1993) Plasma and red blood cell protein maps: update 1993. *Electrophoresis* **14**, 1223-1231.
20. Weimer, H. E., Mehl, J. W., and Winzler, R. J. (1950) Studies on the mucoproteins of human plasma. V. Isolation and characterization of a homogeneous mucoprotein. *J. Biol. Chem.* **185**, 561-568.
21. Bezkorovainy, A. (1965) Comparative study of the acid glycoproteins isolated from bovine serum, colostrum, and milk whey. *Arch. Biochem. Biophys.* **110**, 558-567.
22. Ikenaka, T., Bammerlin, H., Kaufmann, H., and Schmid, K. (1966) The amino-terminal peptide of alpha-1-acid glycoprotein. *J. Biol. Chem.* **241**, 5560.
23. Schmid, K., Kaufmann, H., Isemura, S., Bauer, F., Emura, J., Motoyama, T., Ishiguro, M., and Nanno, S. (1973) Structure of α_1 -acid glycoprotein. The complete amino acid sequence, multiple amino acid substitutions, and homology with the immunoglobulins. *Biochemistry* **12**, 2711-2724.
24. Kremer, J. M. H., Wilting, J., and Janssen, L. H. M. (1988) Drug binding to human α_1 -acid glycoprotein in health and disease. *Pharmacol. Rev.* **40**, 1-47.
25. Schmid, K. (1975) α_1 -Acid glycoprotein. In *The Plasma Proteins: Structure, Function and Genetic Control*, Ed. Putnam, F. W. (Academic Press, New York) pp. 184-228.
26. Arnaud, P., Miribel, L., and Roux, A. F. (1988) α_1 -Acid glycoprotein. *Meth. Enzymol.* **163**, 418-430.
27. Landwehr, H. A. (1882) Untersuchungen ueber das Mucin von Helix pomatia und ein neues Kohlenhydrat (Achrooglycogen) in der Weinbergschnecke. *Zeitschr. Physiol. Chem.* **6**, 74-77.
28. Bennett, M., and Schmid, K. (1980) Immunosuppression by human plasma α_1 -acid glycoprotein: Importance of the carbohydrate moiety. *Proc. Natl. Acad. Sci. U S A.* **77**, 6109-6113.
29. Tamura, K., Shebata, Y., Matsuda, Y., and Ishida, N. (1981) Isolation and characterization of an immunosuppressive acidic protein from ascitic fluids of cancer patients. *Cancer Res.* **41**, 3244-3252.
30. Libert, C., Brouckaert, P., and Fiers, W. (1994) Protection by α_1 -acid glycoprotein against tumor necrosis factor-induced lethality. *J. Exp. Med.* **180**, 1571-1575.
31. Costello, M., Fiedel, B. A., and Gweurz, H. (1979) Inhibition of platelet aggregation by native and desialised α_1 -acid glycoprotein. *Nature* **281**, 677-678.
32. Boutten, A., Dehoux, M., Deschenes, M., Rouzeau, J.-D., Bories, P. N., & Durand, G. (1992) α_1 -Acid glycoprotein potentiates lipopolysaccharide-induced secretion of interleukin-1 β , interleukin-6 and tumor necrosis factor- α in human monocytes and alveolar and peritoneal macrophages. *Eur. J. Immunol.* **22**, 2687-2695.
33. Jamieson, J. C., and Ashton, F. E. (1973) Studies on acute phase proteins of rat serum. 3. Site of synthesis of albumin and α_1 -acid glycoprotein and the contents of these proteins in liver microsome fractions from rats suffering from induced inflammation. *Can. J. Biochem.* **51**, 1034-1045.
34. Gahmberg, C. G., and Andersson, L. C. (1978) Leukocyte surface origin of human α_1 -acid glycoprotein (orosomuroid). *J. Exp. Med.* **148**, 507-521.

35. Nakamura, T., Board, P. G., Matsushita, K., Tanaka, H., Matsuyama, T. and Matsuda, T. (1993) α_1 -Acid glycoprotein expression in human leukocytes: Possible correlation between α_1 -acid glycoprotein and inflammatory cytokines in rheumatoid arthritis. *Inflammation* **17**, 33-45.

Chapter 7

Studies on the mechanism of action of tetrafluorophthalimide inhibitors of cytokine induction in monocytes

Abstract

Analogs of thalidomide in which the four hydrogen atoms of the phthalimide ring were replaced with fluorine were prepared in an effort to create more potent inhibitors of TNF- α production. Fluorination of thalidomide led to an increase in potency of over 500 fold, whereas the corresponding chlorinated and brominated compounds were much less active. Unlike thalidomide, these compounds inhibit the production of both IL-1 and IL-6 from stimulated monocytic cells in addition to TNF- α , and appear to work at the transcriptional level. As tetrafluorothalidomide does not bind to α_1 -acid glycoprotein, a known thalidomide binding protein, the existence of other possible target proteins was investigated. Photoaffinity labeling revealed that the tetrafluorophthalimides bind specifically to a 30 kD and a 40 kD protein. The 40 kD protein was affinity purified, sequenced, and identified as a novel homolog of thioredoxin. The 30 kD protein was purified and a tryptic digest subjected to mass spectrometry, which revealed it to be a recently identified protein with homology to a rat glutathione-dependent dehydroascorbate reductase. Binding of tetrafluorophthalimides to these proteins suggests a possible effect on redox-sensitive signaling pathways leading to cytokine induction in monocytes. The drugs had only a partial effect on activation of NF- κ B, a redox sensitive transcription factor known to be essential for TNF- α induction, pointing to the possibility that the activity of other transcription factors involved in cytokine induction are affected by the cellular redox environment.

Introduction

Interest in the teratogenic drug thalidomide (**1**) has increased in recent years due to its anti-inflammatory properties (*1*). Thalidomide is currently used in the clinic to treat

erythema nodosum leprosum (ENL) in leprosy patients, graft-versus-host disease, and HIV-associated wasting and ulcers (2-5). Its activity as an anti-inflammatory agent has been attributed to its ability to specifically inhibit the production of tumor necrosis factor- α (TNF- α) from monocytic cells (6). Inhibition of TNF- α production appears to be mediated by destabilization of the TNF- α mRNA (7).

Use of thalidomide is limited by side effects. In addition to being an extremely potent teratogen, it is also a sedative and causes peripheral neuropathy in some patients, which can become permanent if drug treatment is not immediately ceased (8-10). Recently, effort has been directed towards the development of thalidomide analogs which are more potent as TNF- α production inhibitors and might allow for therapeutic use in inflammatory diseases without undesirable side effects. One such strategy has involved consideration of the compound's chirality. Thalidomide has a single chiral center, at its α -carbon (Figure 1). It has been reported that the S(-)-isomer exclusively mediates the teratogenic effects of thalidomide in rabbits, whereas the R(+)-isomer is not teratogenic (11,12). However, oral administration of either isomer causes birth defects, perhaps due to acid-catalyzed epimerization of the drug in the stomach (13). In addition, a fast rate of epimerization has been observed in neutral aqueous solutions, indicating that even intravenous administration of the 'safe' isomer may cause birth defects in humans (14). To circumvent this problem, several groups have prepared thalidomide analogs that cannot readily epimerize. Replacement of the labile α -proton with a methyl group produces an analog which maintains its activity as a TNF- α production inhibitor (14). Studies with this compound indicate that the S(-)-isomer is a much more potent TNF- α production inhibitor than the other epimer, suggesting that it would be impossible to separate the anti-inflammatory and teratogenic activities of the drug on the basis of stereochemistry alone.

A group at Celgene Corporation has applied a more standard medicinal chemical approach to the discovery of more potent thalidomide analogs. Finding that an intact phthaloyl ring was essential for activity, the group prepared a series of analogs by

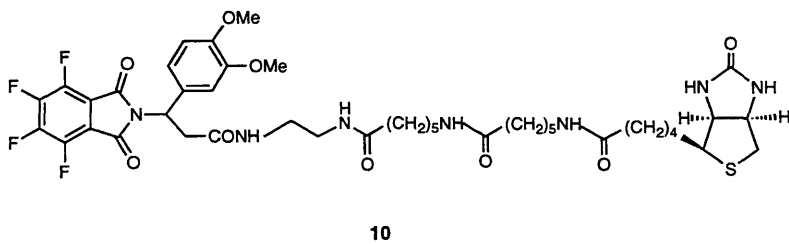
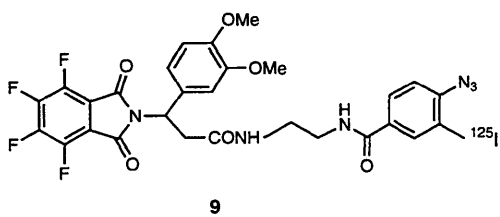
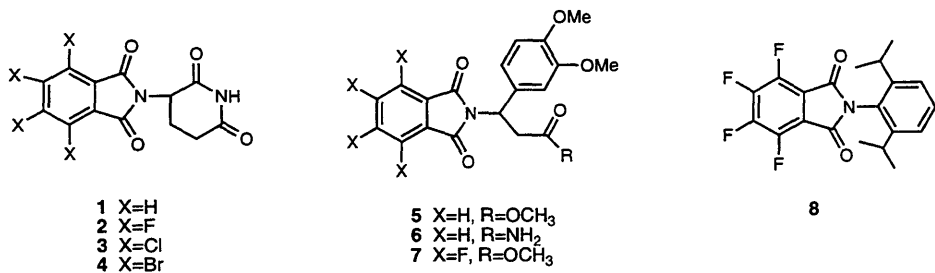


Figure 7.1. Structures of thalidomide and analogs.

modifying the glutarimide moiety (15). Accordingly, a series of phthalimidocinnamic acid derivatives was produced and tested for their ability to inhibit lipopolysaccharide (LPS)-stimulated TNF- α production from monocytes. Among the most potent compounds in this series was CC-1104 (5), which inhibits TNF- α production with an IC₅₀ of 6 μ M, approximately 30-fold more potently than thalidomide. A similar compound, CC-1069 (6), was found to be much more potent than thalidomide at protecting mice from lethal doses of LPS (16). Further increases were noted by amino substitution at either position on the phthalimide ring (15).

Hashimoto and co-workers have found that when the myelomonocytic cell line HL-60 is treated with PMA, thalidomide actually potentiates rather than inhibits TNF- α production (17). A series of phthalimides prepared in their laboratory, including analogs in which the glutarimide moiety was replaced with *o,o*-dialkylphenyl groups, was subsequently tested in this assay and found to have modestly increased activity compared with thalidomide (18). Intriguingly, tetrafluorophthaloyldiisopropylaniline (8), an analog in which each phthalimido proton was replaced with fluorine, was a highly potent potentiator of TNF- α production, with nanomolar concentrations of the compound inducing a five-fold increase in secreted TNF- α levels. This observation raises the question of whether 8 and other tetrafluorophthalimides, such as tetrafluorothalidomide (2), might act as potent inhibitors of TNF- α production from LPS-stimulated monocytic cells. Herein we find that tetrafluorothalidomide (2) is indeed a potent inhibitor of TNF- α production, with an IC₅₀ approximately 500-fold lower than the parent compound. Substitution with other halogens did not result in compounds with comparable activity. Compound 7, the tetrafluorinated analog of CC-1104 (5), was even more potent than tetrafluorothalidomide. The tetrafluorophthalimides appear to differ in their mechanism of action from thalidomide, however, as 2 and 7 also inhibit the production of IL-1 β and IL-6 from stimulated monocytic cells. In addition, unlike thalidomide, inhibition of TNF- α production appears to be mediated at the transcriptional level. To understand the mechanism of action of this new class of TNF- α production

inhibitors, two specific tetrafluorophthalimide binding proteins were purified and identified as novel homologs of thioredoxin and glutathione-dependent dehydroascorbate reductase, suggesting the possible regulation of redox-sensitive signaling pathways by these compounds.

Materials and Methods

Unless otherwise indicated, reagents were purchased from Aldrich and solvents from either Aldrich or Mallinckrodt and were reagent grade or better. NMR solvents were from Cambridge Isotope Laboratories. Flash column chromatography was performed using Merck silica gel, 230-400 mesh. All compounds were analyzed by ¹H NMR using a Varian XL 300 MHz spectrometer and by low resolution mass spectrometry. Where indicated, high resolution mass spectra were taken on a Finnegan MATT 8200 spectrometer. Antibodies to p30 were obtained from Dr. Michael Story at the MD Anderson Cancer Center at the University of Texas, Houston.

Tetrafluorothalidomide (2). Tetrafluorophthalic anhydride (43 mg, 0.2 mmol) and 2-aminoglutarimide hydrobromide (41 mg, 0.2 mmol, preparation described in Chapter 6) were dissolved in DMF in an Ar atmosphere. Triethylamine (27 μ L, 0.2 mmol) was added, and the solution stirred at 60°C for 16 hr. The solution was cooled in a dry ice/EtOH bath and thionyl chloride (32 μ L, 0.42 mmol) was added by syringe with stirring. The reaction vessel was transferred to an ice water bath and stirred for an additional 4 hr. The solution was poured into 10% aqueous KOAc (85 mL) and extracted three times with diethyl ether and then twice with EtOAc. The organic layers were dried with MgSO₄, filtered, concentrated under reduced pressure, combined, and chromatographed on silica gel in 3:2 hexanes/EtOAc. Removal of the solvent under reduced pressure afforded 15 mg tetrafluorophthalimide (22% yield). ¹H NMR (acetone-*d*₆) δ 10.00 (br s, 1H), 5.18 (dd, 1H), 2.91-3.02 (m, 1H), 2.67-2.80 (m, 2H), 2.20-2.27 (m, 1H).

Tetrachlorothalidomide (3). Prepared by Satomi Niwayama in the Liu laboratory analogously to tetrafluorothalidomide (2).

Tetrabromothalidomide (4). Prepared by Satomi Niwayama in the Liu laboratory analogously to tetrafluorothalidomide (2).

β -Amino-3,4-dimethoxydihydrocinnamic acid (12). Procedure is carried out as described (19) except that 3,4-dimethoxycinnamic acid is substituted for cinnamic acid, and the procedure is carried out on a smaller scale (2 g acid). 21% yield: $^1\text{H NMR}$ (D_2O) δ 2.86 (m, 2H), 3.89 (s, 3H), 3.90 (s, 3H), 4.64 (t, 1H), 7.10 (m, 3H).

Methyl β -amino-3,4-dimethoxydihydrocinnamate hydrochloride (13). Thionyl chloride (90 μL , 1.23 mmol) is added via syringe to 0.75 mL anhydrous methanol under Ar in an ice/water bath. β -Amino-3,4-dimethoxydihydrocinnamic acid (150 mg, 0.666 mmol) is added in portions with thorough mixing. The suspension is stirred at 0°C until the material dissolves (15 min) and then overnight at RT. The solvent is removed under reduced pressure and the product is suspended in ethyl ether, suction filtered, and washed with several volumes of ethyl ether. The resultant white powder is collected and dried in vacuo to yield 219.7 mg of the product (89% yield). $^1\text{H NMR}$ ($\text{DMSO}-d_6$) δ 3.05 (m, 2H), 3.56 (s, 3H), 3.74 (s, 3H), 3.76 (s, 3H), 4.52 (br m, 1H), 6.93-7.01 (m, 2H), 7.23 (s, 1H), 8.56 (br s, 3H).

CC-1104 (Methyl 3-phthalimido-3-(3,4-dimethoxyphenyl)propionate) (5). This procedure was adapted from a previously described method (20). Methyl β -amino-3,4-dimethoxydihydrocinnamate hydrochloride (45 mg, 0.16 mmol), carboethoxyphthalimide (36 mg, 0.16 mmol), and sodium carbonate (22 mg, 0.16 mmol) were taken up in 1:1 acetonitrile/water (2 mL) and stirred at room temperature for 1 hr. The acetonitrile was removed under reduced pressure. The resulting mixture is diluted with 20 mL water and extracted twice with 20 mL ethyl ether. The combined organic layers are dried with MgSO_4 , filtered and the solvent removed under reduced pressure. The resultant clear oil was chromatographed on silica gel in 1:1 hexanes/ethyl acetate to give 32 mg of an oily white solid (53% yield). $^1\text{H NMR}$ ($\text{DMSO } d_6$) δ 3.23 (dd, 1H), 3.61 (s, 3H), 3.75 (dd,

1H), 3.82 (s, 3H), 3.86 (s, 3H), 5.75 (dd, 1H), 6.79 (d, 1H), 7.09-7.11 (m, 2H), 7.55-7.80 (m, 4H). HR-MS 369.1211 (Calc. 369.1212).

Methyl β -tetrafluorophthaloyl-3,4-dimethoxydihydrocinnamate (7). Methyl β -amino-3,4-dimethoxydihydrocinnamate hydrochloride (48 mg, 0.17 mmol) and tetrafluorophthalic anhydride (38 mg, 0.17 mmol) were taken up in 5 mL glacial acetic acid. The mixture was refluxed under an argon atmosphere overnight. After removal of the solvent under reduced pressure, the residue is chromatographed on silica gel in 1:1 hexanes/ethyl ether to afford 43 mg of the product as a pale yellow powder (56%). ^1H NMR (CDCl_3) δ 7.04 (m, 2H), 6.79 (d, 1H), 5.67 (dd, 1H), 3.86 (s, 3H), 3.82 (s, 3H), 3.78 (m, 2H), 3.63 (s, 3H), 3.12 (dd, 1H). HR-MS 441.0835 (Calc. 441.0836).

***t*-Boc-Aminoethyl β -tetrafluorophthaloyl-3,4-dimethoxydihydrocinnamamide.** β -Tetrafluorophthaloyl-3,4-dimethoxydihydrocinnamate (13 mg, 0.03 mmol), DCC (7.5 mg, 0.037 mmol), and DMAP (1 mg) were dissolved in 2 mL CH_2Cl_2 under an Ar atmosphere. *t*-Boc-aminoethylamine (5.9 mg, 0.037 mmol) was added, and the mixture was stirred at room temperature for 16 hr. The reaction mixture was concentrated in vacuo and chromatographed on silica gel in 1:1 hexanes/ethyl acetate. Removal of the solvent under reduced pressure provided 5 mg of the product (30%). ^1H NMR (CDCl_3) δ 7.06 (m, 2H), 6.79 (d, 1H), 6.38 (br s, 1H), 5.72 (dd, 1H), 5.84 (br, 1H), 3.86 (s, 3H), 3.82 (s, 3H), 3.65 (dd, 1H), 3.10-3.38 (m, 4H), 2.92 (dd, 1H), 1.42 (s, 9H). HR-MS 569.17876 (Calc. 569.17851).

Cold tetrafluorophthalimide photoaffinity label. Synthesized by Satomi Niwayama in the Liu laboratory. *t*-Boc-Aminoethyl β -tetrafluorophthaloyl-3,4-dimethoxydihydrocinnamamide (6 mg, 0.01 mmol) was deprotected in 1 mL 25% trifluoroacetic acid in CH_2Cl_2 under an Ar atmosphere for 1.5 hr at RT. Toluene (1 mL) was added and the solvent removed under reduced pressure. The free amine was crystallized by the addition of ethyl ether and then reacted with an equimolar amount of AIPPS in 1 mL EtOAc using triethylamine (1 equivalent) as the base. After 16 hr the solvent was removed under reduced pressure and the product isolated by silica gel

chromatography in 30% hexanes in EtOAc. Removal of the solvent provided 4 mg of the product (40% yield). ¹H NMR (CDCl₃) δ 7.61 (s, 1H), 7.22 (m, 2H), 7.03 (m, 2H), 6.79 (d, 1H), 6.20 (br s, 1H), 5.92 (br s, 1H), 5.66 (dd, 1H), 3.86 (s, 3H), 3.82 (s, 3H), 3.62 (dd, 2H), 3.27 (m, 4H), 2.86 (m, 4H), 2.40 (t, 2H). HR-MS 768.08151 (Calc. 768.08147).

TNF- α production assay. Compounds were assayed by Satomi Niwayama in the Liu laboratory as follows. THP-1 cells were cultured in RPMI containing 25 mM HEPES (pH 7.3), 10 % FBS, penicillin and streptomycin, and were rendered LPS-responsive by culturing for 72 hr in the presence of 100 nM 1,25-dihydroxy vitamin D₃. Cells were plated at 10⁶ cells per well in 24-well tissue culture dishes. Drugs dissolved in DMSO (1 μ L) were added to a final concentration of 0.2% DMSO, followed by the addition of LPS in 50 μ L culture medium to a final concentration of 1 μ g/mL in 0.5 mL per well. Plates were incubated for 16 hr in a humidified incubator (37°C, 5% CO₂). Drug treatment did not significantly affect cell viability as judged by trypan blue exclusion. Culture supernatants were analyzed by ELISA using mouse anti-human TNF- α antibodies from PharMingen according to the supplier's instructions.

Northern blot analysis. Analysis was performed by Christine Loh in the Liu laboratory. Cells were treated as described and then total RNA was prepared using a Qiagen RNA preparation kit. RNA was electrophoresed, blotted to nitrocellulose and probed as in Chapter 3.

Preparation of cell lysates. HL-60 cells were pelleted and washed twice with PBS and once with hypotonic buffer (10 mM Tris HCl, pH 7.9, 1.5 mM MgCl₂, 10 mM KCl, 1 mM PMSF, 1 mM DTT, 200 μ g/mL aprotinin, 25 μ M leupeptin, and 10 μ g/mL pepstatin A). Cells were resuspended in three packed cell volumes of hypotonic buffer, incubated on ice for 10 min, and then lysed in a Dounce homogenizer with thirty up and down strokes. Debris and unlysed cells were pelleted by centrifugation for 10 min at 16,000 X g. Supernatants were collected and 1/11th volume of 10X cytosol buffer (100 mM Tris HCl, pH 7.9, 0.9 M NaCl, 2 mM EDTA, 50% glycerol) was added. Extracts were centrifuged at 100,000 X g for 1 hr. Protein concentration in supernatants was

determined by Bradford assay (Bio Rad). Extracts were frozen on dry ice/EtOH and stored at -80°C until use.

Photoaffinity labeling. Preparation and use of the thalidomide photoaffinity label was done as described in Chapter 6. Photoaffinity label **9** was prepared from *t*-Boc-aminoethyl β -tetrafluorophthaloyl-3,4-dimethoxydihydrocinnamamide by deprotection with trifluoroacetic acid and coupling with [¹²⁵I]AIPPS in an analogous manner.

Photoaffinity labeling was performed as described in Chapters 2 and 6.

Detection of tetrafluorophthalimide binding proteins by affinity chromatography.

HL-60 hypotonic extract (5 mg/mL protein) was precleared with streptavidin-agarose beads (Sigma) for 30 min at 4°C and then centrifuged to remove the beads. Precleared supernatant (300 μ L) was incubated with 3 μ M biotin conjugate **10** (synthesized by Satomi Niwayama in the Liu laboratory) in the presence of either 150 μ M **7** or carrier solvent alone (1% DMSO) for 2 hr on ice. Streptavidin-agarose beads were added (30 μ L in a volume of 75 μ L 20 mM Tris HCl, pH 7.4, 100 mM NaCl), and incubated for 1 hr with rotating at 4°C. Beads were pelleted and washed three times with wash buffer (0.6 mL 20 mM Tris HCl, pH 7.4, 100 mM NaCl, 5 min per wash). For detection of p40, beads were resuspended in SDS-PAGE loading buffer (60 μ L), heated in a boiling water bath for 10 min, and samples were subjected to SDS-PAGE (10% acrylamide) followed by silver staining. For detection of p30, protein was eluted from beads with five 100 μ L washes with SDS elution buffer (0.1% SDS, 10 mM Tris HCl, pH 7.5, and 1 mM DTT). Elutions were dried in vacuo, resuspended in 50 μ L water plus 2.5 μ L β -mercaptoethanol, heated in a boiling water bath for 10 min, and then subjected to two dimensional gel electrophoresis (IEF/SDS-PAGE) and silver staining as described in Chapter 6. For immunoblotting, beads were suspended in SDS-PAGE loading buffer, heated in a boiling water bath for 10 min. Following SDS-PAGE (12% acrylamide), samples were blotted to nitrocellulose and probed with p30 antiserum analogously to the procedure described in Chapter 2.

Purification of tetrafluorophthalimide binding proteins. HL-60 cells were grown in suspension in RPMI with 10% FBS, penicillin and streptomycin. The culture used as a source for p30 was grown by the Cell Culture Center (Minneapolis), and supplied as a frozen cell pellet.

For purification of p40, hypotonic extract from 4.5×10^8 HL-60 cells (3 mL) was precleared with immobilized streptavidin (Boehringer Mannheim) and then incubated with 3 μ M biotin conjugate **10** 2 hr on ice. Complexes were collected on immobilized streptavidin (500 μ L) by rotating 1.5 hr at 4°C. Beads were washed four times with hypotonic buffer, suspended in 400 μ L 2X SDS-PAGE loading buffer, and heated 10 min in a boiling water bath. The bead suspension was subjected to SDS-PAGE (10% acrylamide). The gel was stained with Coomassie Blue for 2 hr, destained with 10% HOAc, 10% MeOH for 16 hr, and then 30 min in 10% HOAc, 50% MeOH. After washing in ddH₂O for 30 min, p40 bands were excised. In gel digestion with Lys-C, HPLC separation and Edman sequencing of the resulting peptides was performed by the MIT Biopolymers laboratory.

For purification of p30, hypotonic extract from 4×10^9 HL-60 cells (8 mL) was precleared with glutathione Sepharose 4B (800 μ L) 45 min at 4°C with rotating. The suspension was centrifuged at 2000 X g for 2 min, and the supernatant was applied to a DEAE Sepharose column equilibrated to wash buffer (20 mM Tris HCl, pH 7.5, 100 mM NaCl, 1 mM DTT, and 25 μ M leupeptin). Flowthrough fractions were adjusted to 1 mM EDTA, 200 μ g/mL aprotinin, and 10 μ g/mL pepstatin A. Protein-containing fractions were pooled and concentrated to 2 mL by centrifugal filtration using Centriprep concentrators (Amicon). The concentrated sample was cleared with 225 μ L immobilized streptavidin for 1 hr at 4°C and centrifuged to remove beads. The supernatant was incubated with 3 μ M biotin conjugate **10** for 2 hr at 4°C, and then 90 μ L immobilized streptavidin beads were added followed by rotating for 1 hr at 4°C. The beads were washed four times with 1.2 mL wash buffer containing aprotinin, EDTA, and pepstatin A. Bound proteins were eluted by four 180 μ L washes with buffer containing 0.1% SDS,

12.5 mM Tris HCl, pH 6.8, 0.5% glycerol, and 1 mM DTT. Eluates were pooled and concentrated to 70 μ L in a speedvac, 3 μ L β -mercaptoethanol added, and the sample heated in a boiling water bath for 5 min. The sample was subjected to SDS-PAGE (12% acrylamide). The gel was silver stained as described (21) and the 30 kD band excised, digested with trypsin, and peptides extracted and subjected to MALDI-TOF mass spectrometry as described in Chapter 2. Methylation of the carboxylic acid groups was performed by suspending the peptide mixture in 10 μ L of 1% SOCl₂ in MeOH and heating to 50°C for 20 min, after which the sample was dried in vacuo (22).

Electrophoretic mobility shift assay (EMSA). Consensus NF- κ B binding site oligonucleotide (50 ng, Santa Cruz Biotechnology) was end labeled using T4 polynucleotide kinase (New England Biolabs) with 50 μ Ci [γ -³²P] ATP (3000 Ci/mmol) in 70 mM Tris HCl, pH 7.6, 10 mM MgCl₂, 5 mM DTT, and 0.1 mM EDTA (30 μ L) for 1 hr at 37°C. Labeled oligonucleotide was purified by electrophoresis in a 12% polyacrylamide native TBE gel. Incorporation of radioactivity was determined by scintillation counting.

THP-1 cells were treated with 1,25-dihydroxy vitamin D₃ as described above and suspended in fresh media to 10⁶ cells per mL (10 mL per sample). Cells were pretreated for 1 hr at 37°C with drug (1 μ M) or DMSO carrier control (0.1%) and then stimulated with 1 μ g/mL LPS for 30 min. Cells were harvested by scraping, pelleted at 4°C, and washed once with ice cold PBS. Nuclei were prepared by suspending cells in 900 μ L RSB (10 mM Tris HCl, pH 7.4, 10 mM NaCl, 3 mM MgCl₂, 0.5 mM DTT, 25 μ M leupeptin, 1 μ g/mL aprotinin, 1 mM PMSF, 0.1 mM EGTA) and then lysing by adding 5% NP40 (100 μ L), mixing and leaving on ice for 5 min. Nuclei were pelleted at 1800 X g for 5 min, washed with RSB, and repelleted at 4000 x g for 5 min. Nuclear extracts were prepared by resuspending nuclei in 30 μ L buffer C (23) (20 mM HEPES, pH 7.4, 420 mM NaCl, 1.5 mM MgCl₂, 0.2 mM EDTA, 25% glycerol, 0.01% NaN₃, 0.5 mM DTT, 1 mM PMSF, 25 μ M leupeptin, 1 μ g/mL aprotinin) and mixing for 30 min at 4°C. Extract was centrifuged for 10 min at 16,000 X g and an equal volume of buffer D (20 mM

HEPES, pH 7.4, 50 mM KCl, 0.2 mM EDTA, 0.01% NaN₃, 0.5 mM DTT, 1 mM PMSF, 25 μM leupeptin, 1 μg/mL aprotinin) was added to the supernatant.

EMSA was performed by incubating nuclear extract containing 8 μg total protein with 20,000 cpm oligonucleotide probe and 2 μg poly dIdC in a volume of 15 μL for 20 min at room temperature. Complexes were electrophoresed on 4.5% polyacrylamide/0.25X TBE native gels. Gels were dried immediately following electrophoresis and analyzed by autoradiography.

Reporter gene assays. The TNF reporter construct contains nucleotides -614 to +20 of the human TNF-α promoter upstream of the luciferase gene in the plasmid pGL2, and was obtained from Dr. S. McKnight, Tularik, Inc. The NF-κB reporter construct contains three copies of the NF-κB binding site from the mouse κ light chain enhancer upstream of the luciferase gene and was obtained from the laboratory of Dr. M. Karin, University of California, San Diego School of Medicine. THP-1 cells were transfected by the DEAE-dextran method with NF-κB-luciferase and TNF-luciferase reporter plasmids prepared using Qiagen EndoFree kits, 10 μg/10⁷ cells. 24 hr post-transfection, cells were pelleted and resuspended to 10⁶ cells per mL in fresh media and plated into 12-well plates (1 mL per well). Cells were preincubated for 1 hr with drug (1 μM) or DMSO carrier alone (0.2%) and then stimulated with 1 μg/mL LPS for 6 hr. Cells were harvested by scraping, lysed and analyzed for luciferase activity by luminometry using a luciferase assay kit (Promega).

Results

Tetrafluorothalidomide (**2**) was synthesized by coupling tetrafluorophthalic anhydride with 2-aminoglutarimide (Figure 7.1). The compound was tested for its ability to inhibit TNF-α production from the promonocytic cell line THP-1. Tetrafluorothalidomide potently inhibits TNF-α production with an IC₅₀ of ~500 nM in this assay (Figure 7.2). Compared with thalidomide (**1**), which has an IC₅₀ of over 200 μM, this represents a 500-fold increase in activity. To assess whether other halogen atoms have the same effect as

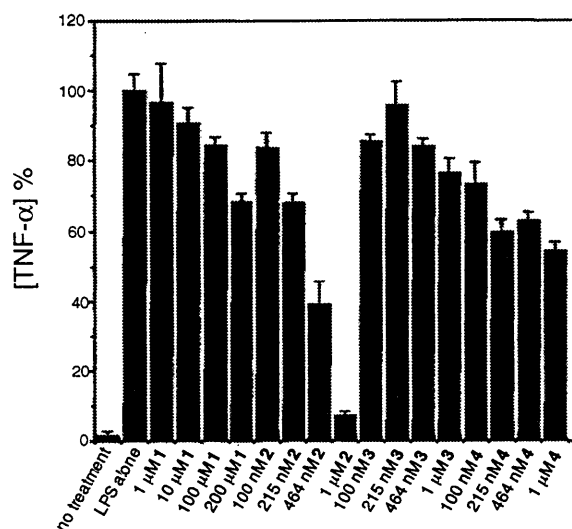


Figure 7.2. Inhibition of TNF- α production from LPS-stimulated THP-1 cells by thalidomide and analogs. Cells were rendered LPS responsive as described in text and treated with varying concentrations of compounds as indicated plus 1 $\mu\text{g}/\text{mL}$ LPS. After 16 hr TNF- α was analyzed in culture supernatants by ELISA.

fluorine, tetrachlorothalidomide (**3**) and tetrabromothalidomide (**4**) were prepared in an analogous manner. Both analogs are much less active than tetrafluorothalidomide at inhibiting TNF- α secretion (Figure 7.2). These observations suggest that the increase in potency is unique to fluorine substitution.

CC-1104 (**5**) has been reported to inhibit TNF- α production at concentrations 30-fold lower than thalidomide (*15*). To test the effects of combining this improvement with tetrafluorine substitution, CC-1104 and its tetrafluorinated analog (**7**) were prepared (Figure 7.3). CC-1104 was indeed found to be more potent than thalidomide, though we did not observe as significant an increase in potency as previously reported, possibly due to different assay conditions used (Figure 7.4). The tetrafluoro-substituted analog **7**, however, was found to be over 100-fold more potent than CC-1104, with an IC₅₀ of approximately 100 nM.

The large increases in potency involved with tetrafluorine substitution raised suspicions that the novel compounds might be acting by a mechanism distinct from thalidomide. Thalidomide has been shown to be a specific inhibitor of TNF- α production, and does not affect levels of other cytokines, such as IL-1 β and IL-6 (*6*). Conversely, we found that tetrafluorophthalimides **2** and **7** are potent inhibitors of the secretion of these other cytokines as well. Inhibition of IL-1 β production occurs with IC₅₀ values of approximately 400 nM for either compound, and IL-6 production is half-maximally inhibited at 700 nM and 300 nM for compounds **2** and **7**, respectively. Like thalidomide, **2** and **7** caused decreased levels of TNF- α mRNA to accumulate (Figure 7.5A). However, the tetrafluorophthalimides did not alter the turnover rate of the TNF- α mRNA, in contrast with previous reports indicating that thalidomide destabilizes the TNF- α message (Figure 7.5B) (*7*). These experiments suggest that tetrafluorophthalimides decrease TNF- α production at the transcriptional level. Thus it would appear that the tetrafluorophthalimides inhibit TNF- α production by a mechanism distinct from thalidomide.

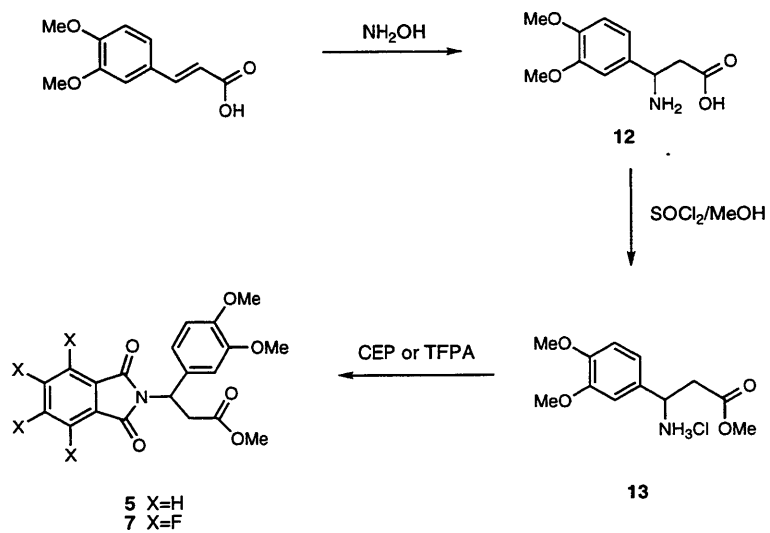


Figure 7.3. Synthesis of thalidomide analogs. Abbreviations: CEP, carboethoxyphthalimide; TFPA, tetrafluorophthalic anhydride.

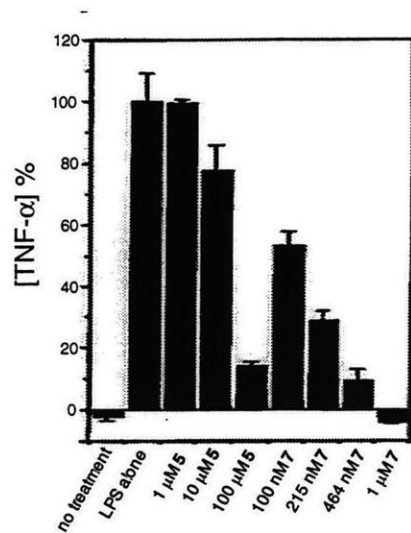


Figure 7.4. Inhibition of TNF- α production from LPS-stimulated THP-1 cells by compound **5** and its tetrafluorinated analog **7**. Cells were treated and culture supernatants were analyzed for TNF- α content as in Figure 7.2.

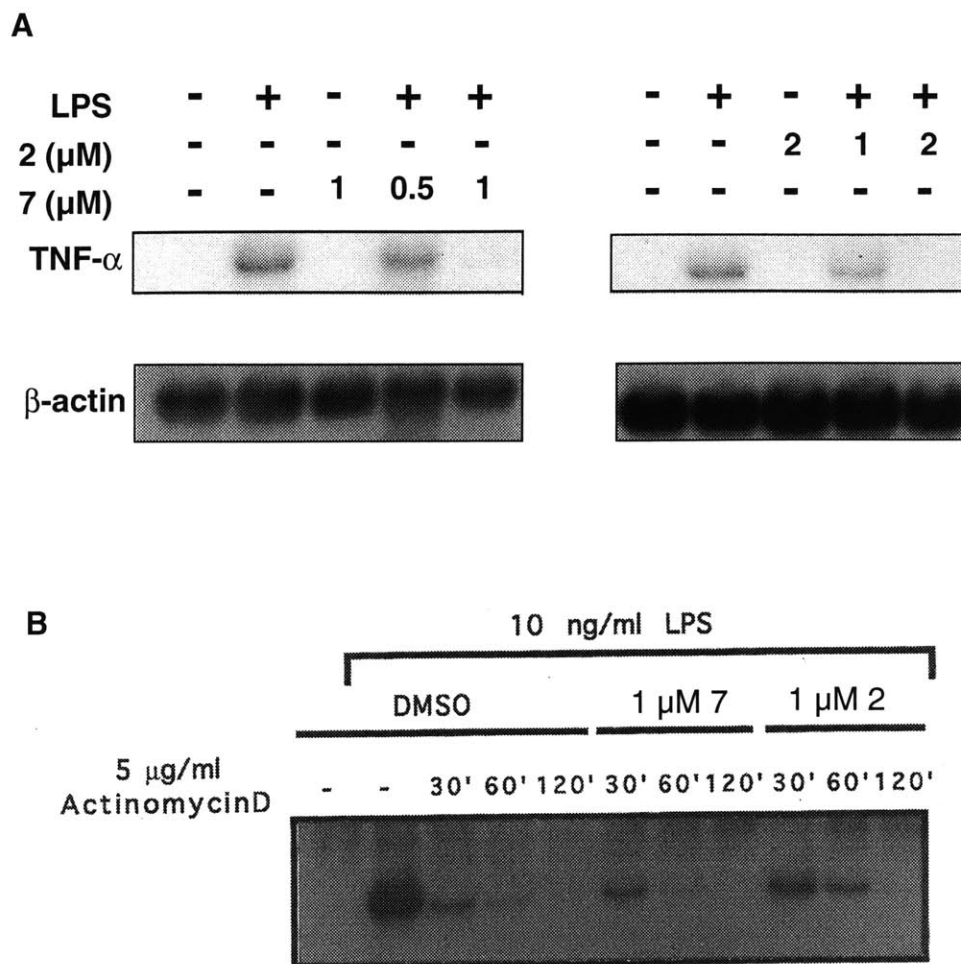


Figure 7.5. Tetrafluorophthalimides affect TNF- α production at the transcriptional level. A, Northern blot analysis of TNF- α mRNA in THP-1 cells stimulated with LPS in the presence or absence of tetrafluorophthalimides **2** and **7** as indicated. Cells were pretreated with drug for 1 hr and then stimulated with LPS for 1 hr prior to harvesting. B, Cells were first stimulated with LPS for 1 hr and then treated with actinomycin D in the presence or absence of tetrafluorophthalimides **2** and **7** as indicated. Cells were harvested at various times thereafter and analyzed for TNF- α mRNA by Northern blot analysis.

That tetrafluorophthalimides operate by a different mechanism than thalidomide suggests that they bind to a distinct target protein. Indeed, neither **2** nor **7** appears to bind α_1 -acid glycoprotein, the only reported thalidomide binding protein (Chapter 6), as determined by their inability to compete with a thalidomide photoaffinity label for binding to the protein (Figure 7.6). In order to detect tetrafluorophthalimide binding proteins, a photoaffinity label derived from **7**, the most active compound, was prepared (**9**, Figure 7.1). To ensure that modification of the drug did not result in loss of activity, the corresponding compound containing non-radioactive iodine was prepared and tested for its ability to inhibit TNF- α production from THP-1 cells. The tetrafluorophthalimide photoaffinity label maintained significant, though decreased, activity, with an IC₅₀ of approximately 2 μ M in this assay.

Incubation of HL-60 cell extracts with photoaffinity label **9** followed by irradiation resulted in the specific labeling of two protein bands, of 30 kD and 40 kD molecular weight (referred to from this point on as p30 and p40, respectively), as judged by the ability of excess cold **7** to compete for labeling (Figure 7.7). In contrast, neither tetrachlorothalidomide (**3**) nor CC-1104 itself (**5**) significantly inhibited labeling of either protein, suggesting that these proteins might specifically mediate the effects of the tetrafluorophthalimides.

To facilitate purification of p30 and p40, a derivative of **7** conjugated to biotin was prepared (**10**, Figure 7.1). HL-60 cytosolic extracts were incubated with **10** in the presence or absence of a 50-fold excess of competitor **7**. Proteins bound to the biotin conjugate were isolated on immobilized streptavidin beads. When the beads were subjected to SDS-PAGE, only the 40 kD protein could be detected (Figure 7.8). The presence of excess **7** during the binding reaction caused the 40 kD band to disappear. To isolate p40, the affinity chromatography procedure was done on a scale which produced approximately 1 μ g of protein. The protein band was excised from a Coomassie-stained polyacrylamide gel and digested with Lys-C endopeptidase. Peptides were extracted, separated by HPLC, and subjected to Edman degradation sequencing.

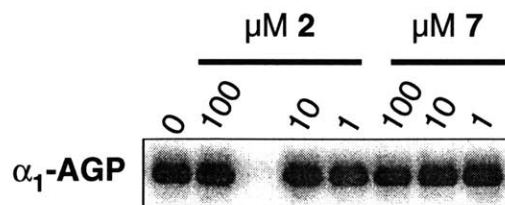


Figure 7.6. Tetrafluorophthalimides do not bind to α 1-AGP; α 1-AGP (2.5 μ g, 50 μ g/mL) was incubated with the indicated concentrations of drugs for 40 min prior to the addition of thalidomide photoaffinity label (1 μ Ci carrier free). After 40 min the reactions were irradiated and fractionated on SDS-PAGE followed by phosphorimager analysis.

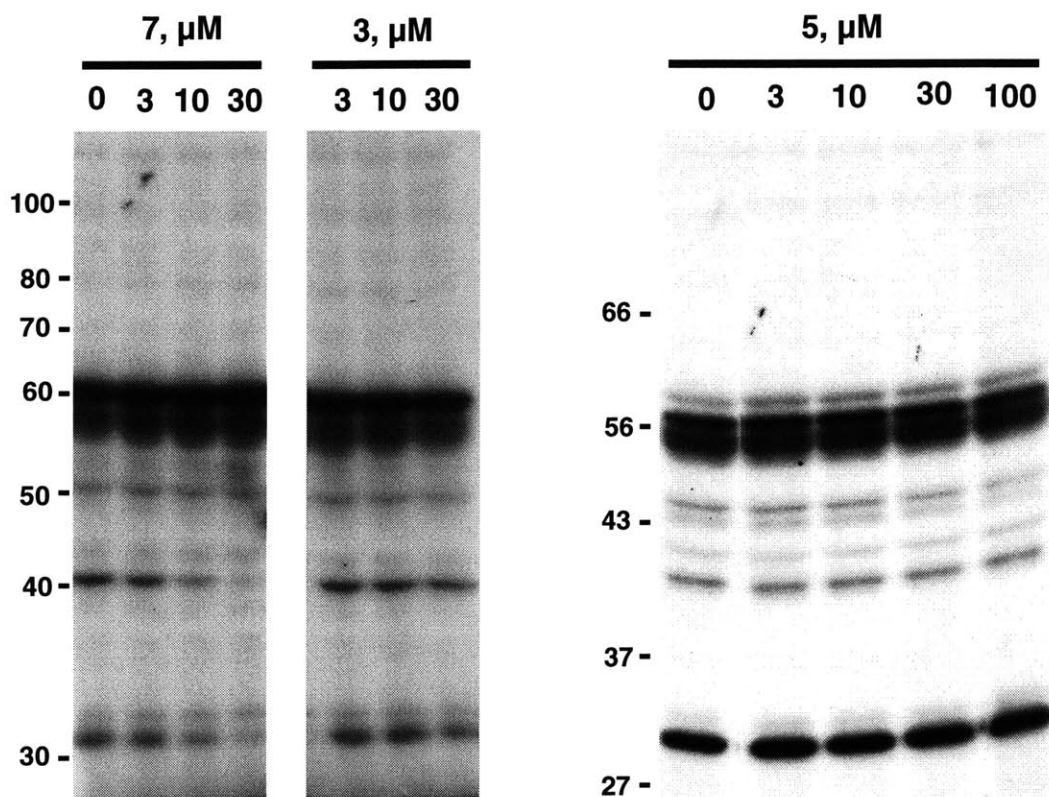


Figure 7.7. Detection of tetrafluorophthalimide binding proteins by photoaffinity labeling. HL-60 cell extracts were incubated with the indicated concentrations of tetrafluorophthalimide 7, tetrachlorothalidomide (3), or CC-1104 (5) for 30 min prior to the addition of photoaffinity label 9. After a further 30 min incubation in the dark, samples were irradiated and subjected to SDS-PAGE followed by autoradiography.

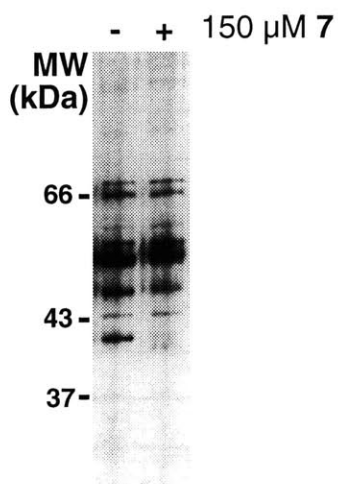


Figure 7.8. Affinity purification of p40. HL-60 cell extracts were incubated with biotin conjugate **10** in the presence or absence of a 50-fold excess of compound **7**, and tetrafluorophthalimide binding proteins isolated on immobilized streptavidin beads.

The peptide sequence data was used to search the protein sequence databank. All three peptides were found to be present within the sequence of a single 335 amino acid protein of unknown function, which had been cloned by virtue of its high homology to a putative yeast 27.5 kD protein identified from an open reading frame in the *S. cerevisiae* genome (NCBI Entrez accession number 3646128, Figure 7.9). The closest relatives to p40 of known function are the thioredoxins from plants, with the amino terminal portion of p40 being 32% identical to tobacco thioredoxin. Thioredoxin has been suggested to be important for activation of the transcription factor NF- κ B, which is known to be essential for TNF- α gene induction in LPS-stimulated monocytic cells (24,25,26). The binding of p40 by compounds which inhibit TNF- α induction raises the possibility that the novel protein may play a specialized role in the context of NF- κ B activation role similar to that previously prescribed to thioredoxin. To investigate this possibility, tetrafluorophthalimide **7** was tested for its ability to inhibit the LPS-induced activation of NF- κ B in THP-1 cells. As previously reported, LPS caused efficient activation of NF- κ B as judged by electrophoretic mobility shift assay (EMSA). Compound **7** caused only a partial decrease in NF- κ B activation in this assay at concentrations which completely abolish TNF- α gene induction (Figure 7.10A). Compound **7** was also tested for its effect in an NF- κ B-dependent reporter gene assay. THP-1 cells were transfected with a reporter plasmid containing the luciferase gene under the control of a multimerized NF- κ B binding site. Transfected cells were stimulated with LPS in the presence or absence of tetrafluorophthalimide **7**. Again, LPS-induced activation of the NF- κ B reporter gene was only partially reduced at concentrations which eliminate TNF- α production (Figure 7.10B). Furthermore, the same concentration of the compound also dramatically reduced the activation of a reporter gene under the control of the TNF- α promoter. These results indicate that tetrafluorophthalimides are likely to exert their effects on cytokine induction by affecting transcription factors other than NF- κ B.

Specific binding of p30 to biotin conjugate **10** could not be detected on one dimensional gels due to the low abundance of the protein and background binding of

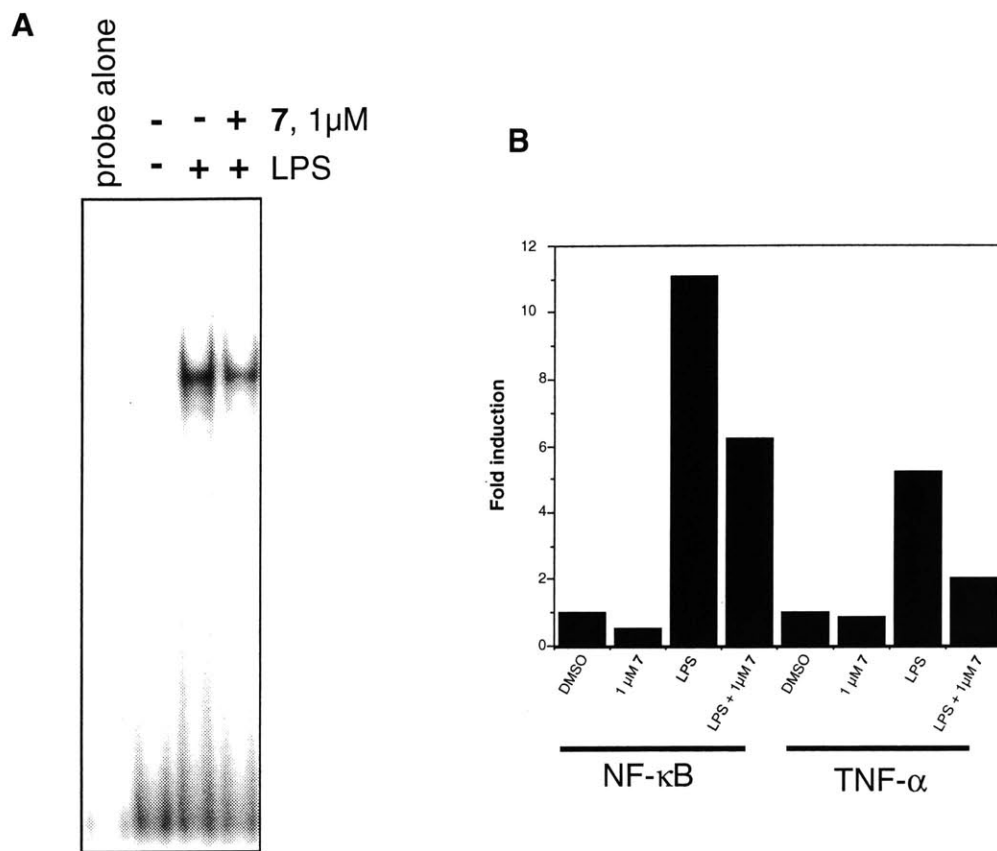


Figure 7.10. Effect of tetrafluorophthalimide 7 on NF- κ B activation. A, Electrophoretic mobility shift assay. THP-1 Cells were treated with or without 7 prior to LPS stimulation. Nuclear extracts were prepared and analyzed for the presence of NF- κ B with a consensus binding site oligonucleotide. B, Reporter gene assay. THP-1 cells were transfected with plasmids containing the luciferase gene under the control of either a multimerized consensus NF- κ B site or the human TNF- α promoter. Transfected cells were treated with 7 where indicated and stimulated with LPS for 6 hr prior to harvesting and analyzing for luciferase expression.

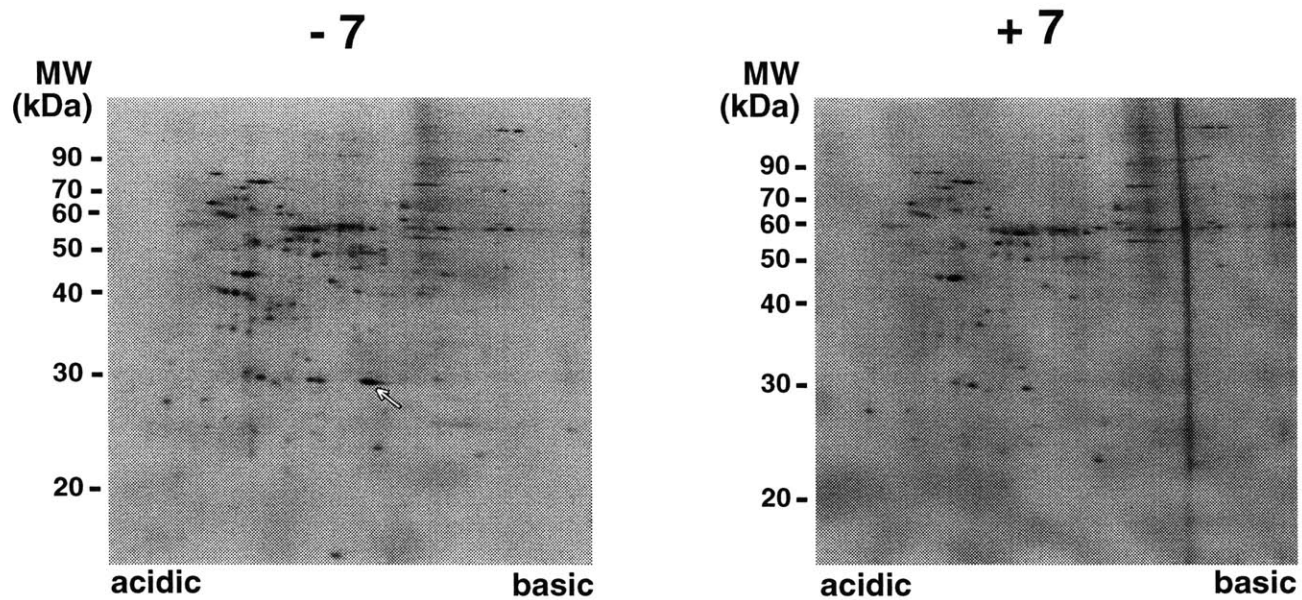


Figure 7.11. Affinity purification of p30. Tetrafluorophthalimide binding proteins from HL-60 cell extracts, isolated as in figure 7.8, were separated by two-dimensional gel electrophoresis (IEF/SDS-PAGE) and visualized by silver staining. The 30 kD protein, which does not appear if extracts are preincubated with excess tetrafluorophthalimide **7**, is indicated with an arrow.

proteins of similar molecular weight. However, when eluates from beads were subjected to two dimensional gel electrophoresis, binding of a 30 kD protein could be detected which was abrogated by the presence of excess competitor **7** during the binding reaction (Figure 7.11). Isolation of p30 in sufficient purity and yield to allow for its identification required several purification steps. As it was determined that some of the background in the 30 kD region was due to binding of glutathione S-transferases (GSTs, data not shown), extracts were first cleared with glutathione Sepharose. GST-cleared extracts were passed over a DEAE column, and the flowthrough fraction was concentrated and incubated with biotin conjugate **10**. Purified protein was isolated on immobilized streptavidin. Under these conditions, a 30 kD band could be detected by one dimensional electrophoresis which was not present if excess **7** was present during binding to **10** (Figure 7.12). The desired protein band was excised from silver-stained polyacrylamide gels and digested with trypsin, and the extracted peptides were subjected to MALDI-TOF mass spectrometry.

Seven of the nine peaks from the mass spectrum matched with high accuracy a recently identified protein of 28 kD predicted molecular weight (Table 7.1). This protein was cloned by virtue of its upregulation in cells which have lost the ability to undergo apoptosis in response to ionizing radiation (R. Kodym and M. Story, personal communication). The protein also bears high homology (80%) to a glutathione-dependent dehydroascorbate reductase recently cloned from the rat (Figure 7.13, 27). The assignment was confirmed in two ways. First, the remainder of the original tryptic digest was treated with methanolic thionyl chloride, which transforms carboxylic acids into methyl esters. The methylated peptides were again analyzed by mass spectrometry. The major peaks in the resulting spectrum corresponded to the predicted quantitative methylation products of peptides identified to be present in the mixture from the original spectrum. Since false positive assignments in database searches with peptide masses generally result from peptides of distinct amino acid composition which are close in molecular weight and not from 'scrambled' peptides, the methylation data strongly

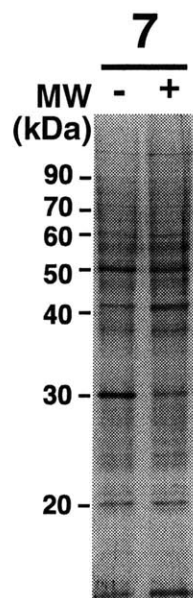


Figure 7.12. Purified p30. The 30 kD protein was purified from HL-60 cell extracts as described in the text. During the final affinity chromatography step, either tetrafluorophthalimide **7** (right lane) or carrier solvent alone (left lane) was included during binding to biotin-drug conjugate **10**. Material was subjected to SDS-PAGE and visualized by silver staining.

Table 7.1. The MALDI-TOF mass spectrum of a tryptic digest of p30 suggests identity with a recently cloned homolog of rat glutathione-dependent dehydroascorbate reductase (GDAR). The methylated mass refers to the major peak in the spectrum following treatment with methanolic thionyl chloride. The number in parentheses refers to the implied number of carboxyl groups in the peptide derived from the increase in mass upon methylation (14 Da per carboxylic acid), which in each case corresponds exactly to the predicted increase from the assigned peptide.

Measured Mass (Da)	Calculated Mass (Da)	Methylated Mass (Da)	GDAR Homolog Peptide Sequence	Peptide Location
926.38	926.419	954.415 (2)	FCPFAER	31-37
1074.561	1074.631	1088.62 (1)	VPSLVGSFIR	123-132
1095.481	1095.563	1123.56 (2)	NKPEWFFK	58-65
1320.621	1320.691	1348.71 (2)	GSAPPGPVPEGSIR	12-25
1356.601	1356.644	none	EDYAGLKEEFR	137-147
1813.811	1813.872	1883.92 (5)	SQNKEDYAGLKEEFR	133-147
1941.871	1941.967	2011.96 (5)	SQNKEDYAGLKEEFRK	133-148
1405.711	none	1433.8 (2)	none	-
2807.311	none	none	none	-

suggest that the isolated protein is indeed encoded by the recently cloned human gene.

Secondly, tetrafluorophthalimide binding proteins isolated by biotin-streptavidin affinity chromatography alone were subjected to SDS-PAGE followed by immunoblotting with antibodies raised against the novel protein (Figure 7.14). A protein of 30 kD which reacts with this antibody was found to bind to the beads. Binding was abrogated by the presence of excess competitor 7. Thus it would appear as if the tetrafluorophthalimide-binding p30 and the novel dehydroascorbate reductase homolog are identical proteins.

Discussion

Our results demonstrate that fluorine substitution dramatically increases the potency of a series of phthalimide inhibitors of TNF- α production. Fluorine is a close steric mimic of hydrogen, and incorporation of fluorine into drugs often improves their biological activity (28). Such improvements have been attributed to either the enhanced lipophilicity of fluorinated compounds or to stereoelectronic changes imparted to compounds by fluorine substitution resulting in more avid binding to their respective target molecules. Several lines of evidence support the contention that fluorinated thalidomide derivatives are an

```

1  M R F C P F A E R T R L V L K A K G I R H E V I N I N L K N K P E W F F K K N P human p30
1  M R F C P F A Q R T L M V L K A K G I R H E I I N I N L K N K P E W F F E K N P rat GDAR

41 F G L V P V L E N S Q G Q L I Y E S A I T C E Y L D E A Y P G K K L L P D D P Y human p30
41 F G L V P V L E N T Q G H L I T E S V I T C E Y L D E A Y P E K K L F P D D P Y rat GDAR

81 E K A C Q K M I L E L F S K V P S L V G S F I R S Q N K E D Y A G L K E E F R K human p30
81 E K A C Q K M T F E L F S K V P S L V T S F I R A K R K E D H P G I K E E L R K rat GDAR

121 E F T K L E E V L T N K K T T F F G G N S I S M I D Y L I W P W F E R L E A M K human p30
121 E F S K L E E A M A N K R T A F F G G N S L S M I D Y L I W P W F Q R L E A L E rat GDAR

161 L N E C V D H T P K L K L W M A A M K E D P T V S A L L T S E K D W Q G F L E L human p30
161 L N E C I D H T P K L K L W M A T M Q E D P V A S S H F I D A K T Y R D Y L S L rat GDAR

201 Y L Q N S P E A C D Y G L human p30
201 Y L Q D S P E A C D Y G L rat GDAR

```

Figure 7.13. Alignment of human p30 with a recently cloned glutathione-dependent dehydroascorbate reductase (GDAR) from rat. Residues in the rat GDAR which differ from human p30 are boxed. Alignment was done using the program MegAlign.

10	-	+	+
7	-	-	+

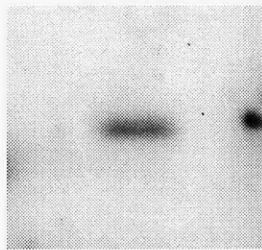


Figure 7.14. Confirmation that p30 is identical to a recently cloned homolog of GDAR. HL-60 cell extracts were preincubated with or without tetrafluorophthalimide 7 as indicated prior to the addition of either biotin-drug conjugate 10 or carrier solvent alone. Proteins bound to immobilized streptavidin beads were analyzed by immunoblotting against antibodies to the GST homolog.

exceptional case in which their mechanism of action bears apparently no relation to that of the parent compound. For example, thalidomide, but not tetrafluorophthalimides, destabilizes the TNF- α message. In addition, while thalidomide exclusively inhibits the production of TNF- α from stimulated monocytic cells, **2** and **7** inhibit production of IL-1 β and IL-6 as well. Furthermore, tetrafluorophthalimides have been shown recently to differ in their stereospecificity of action from thalidomide (29,30). These observations suggest that nonfluorinated and fluorinated phthalimides mediate inhibition of cytokine production by distinct mechanisms and through interaction with different target proteins.

Interestingly, recent reports also suggest that the non-fluorinated phthalimidocinnamic acid derivatives developed at Celgene may operate through a mechanism distinct from the parent compound, thalidomide. CC-3052, which differs from CC-1104 (**5**) only in that one of the phthalimide carbonyl groups has been reduced to methylene, has also been shown to affect TNF- α production at the level of transcription, and did not alter the stability of the TNF- α mRNA (31). Furthermore, this compound, and not thalidomide, was shown to inhibit the type IV phosphodiesterase (PDE IV) at concentrations close to those needed to inhibit TNF- α production. PDE IV inhibitors have attracted interest as anti-inflammatory compounds due to the ability of elevated cAMP levels to antagonize LPS-induced cytokine production, and a number of such compounds are in clinical development to treat inflammatory diseases such as rheumatoid arthritis (32). Tetrafluorophthalimides probably do not fall into this class of compounds, as PDE IV inhibitors do not inhibit production of the broad spectrum of cytokines affected by **2** and **7**. In addition, the nonfluorinated CC-1104 (**5**) does not appear to bind the two tetrafluorophthalimide binding proteins, p30 and p40.

Two proteins from monocytic cells were identified which bind to tetrafluorophthalimides. The 40 kD protein was identified as the product of a recently cloned gene encoding a protein predicted to be 38 kD in molecular weight (Figure 7.9). The protein is most homologous to the conceptual protein product of a yeast open reading frame which was identified from the *S. cerevisiae* genomic sequence (being 52% identical and 70%

similar at the amino acid level). The most closely related protein of known function is the small redox protein thioredoxin; the amino terminal region of p40 has highest homology to thioredoxins of plant origin (having 33% identity and 66% similarity to tobacco thioredoxin). In fact, p40 can be depicted as being comprised of three 'thioredoxin repeat' regions, each homologous to the entire thioredoxin sequence, with the two carboxy terminal repeats having higher homology to glutaredoxin and being most closely related to each other. The putative yeast homolog is smaller (27.5 kD), and bears only two thioredoxin repeats (Figure 7.9).

The biochemical activity of p40 is at this point unknown. Thioredoxin catalyzes the reduction of disulfide bonds in substrate proteins and thereby allows redox enzymes such as ribonucleotide reductase to participate in multiple rounds of catalysis *in vivo*. Reduction is mediated by an absolutely conserved pair of closely spaced cysteine residues which become oxidized to a disulfide during the reaction (33). Thioredoxin is in turn regenerated by an NADPH-dependent thioredoxin reductase. Thioredoxin has been implicated in several signal transduction pathways. It is believed to be important for maintaining members of the NF- κ B family of transcription factors, which are crucial for inflammatory cytokine induction, in a reduced state required for activity (24,25). Thus it is tempting to speculate that a thioredoxin homologous enzyme might have arisen to play a more specialized role in signaling. The tetrafluorophthalimides, however, only partially inhibit NF- κ B activation in activated monocytic cells as judged either by NF- κ B-dependent reporter gene activation or by EMSA (Figure 7.10), suggesting that p40 does not directly effect the redox state of NF- κ B.

The arrangement of repeated regions found in p40 is reminiscent of the protein disulfide isomerases which are important for proper disulfide bond formation for proteins in the secretory pathway (34). Each thioredoxin repeat of p40, however, bears only the carboxy terminal of the two cysteine residues (Figure 7.9). It therefore seems unlikely that p40 has either disulfide reducing or oxidizing activity. Two groups of enzymes are known which share structural homology with thioredoxin but lack one of the two

conserved cysteine residues. These are the glutathione peroxidases (which bear a selenocysteine residue at the analogous site) and the peroxiredoxins, which include thioredoxin peroxidases (35-37). Both of these groups of enzymes catalyze the reduction of peroxides, with the concomitant oxidation of the conserved cysteine or selenocysteine. The enzymes differ with regard to their source of electrons, with the glutathione peroxidases being regenerated by glutathione, thioredoxin peroxidases being regenerated by thioredoxin, and an unknown reductant acting on the other peroxiredoxins. Whether p40 has a similar biochemical activity to these enzymes and how such an activity might play a role in TNF- α gene induction is the subject of future studies.

The 30 kD protein was cloned by virtue of its upregulation in cells which fail to undergo apoptosis in response to ionizing radiation, though a role for the protein in resistance to apoptosis has not yet been established. The protein has significant homology to GST (29% identity and 49% similarity to soybean GST), binds to glutathione, but has not been demonstrated to have GST enzymatic activity (R. Kodym and M. Story, personal communication). Recently a glutathione-dependent dehydroascorbate reductase was cloned from the rat which has 76% identity (87% similarity) to p30 (27). This high degree of homology suggests that p30 is likely to have this enzymatic activity as well. Future work will be required to determine if this is the case and whether tetrafluorophthalimides are inhibitors of this activity. Though the role for such an enzyme in cytokine induction is unclear, it is anticipated that the effects of dehydroascorbate reductase inhibitors could be overcome by treating cells with excess reduced ascorbate. Experiments to test the effects of reduced ascorbate on sensitivity to tetrafluorophthalimides will constitute future work on these inhibitors.

Reactive oxygen species have been presumed to play a role in several signal transduction pathways, including the mitogenic Ras pathway, by virtue of the ability of antioxidants to diminish signaling (38,39). Antioxidants have been shown to prevent activation of NF- κ B as well in an indirect manner. In prokaryotes, two transcription factors, SoxR and OxyR, are known to be activated by direct oxidation by reactive oxygen

species (40,41). In the context of signal transduction and gene activation in mammalian cells, however, the protein molecules involved both in mediating production of oxygen species and in carrying such signals by acting as oxidative sensors in the context of signal transduction have not been identified. The finding that compounds which block LPS-mediated signal transduction in monocytic cells bind to two proteins which may play roles in redox regulation raises the possibility that reactive oxygen species are involved in unexplored aspects of this signaling pathway as well. Future work will be required to establish what role if any these proteins play in the regulation of cytokine induction in monocytes.

References for Chapter 7

1. Koch, H. P. (1985) Thalidomide and congeners as anti-inflammatory agents. *Prog. Med. Chem.* **22**, 165-242.
2. Sheskin, J. (1965) Thalidomide in the treatment of lepra reactions. *Clin. Pharmacol. Ther.* **6**, 303-306.
3. Vogelsang, G. B., et al. (1992) Thalidomide for the treatment of chronic graft-versus-host disease. *N. Engl. J. Med.* **326**, 1055-1058.
4. Jacobson, J. M., et al. (1997) Thalidomide for the treatment of oral aphthous ulcers in patients with human immunodeficiency virus infection. *N. Engl. J. Med.* **336**, 1487-1493.
5. Reyes-Terán, G., Sierra-Madero, J. G., Martínez del Cerro, V., Arroyo-Figueroa, H., Pasquetti, A., Calva, J. J., and Ruiz-Palacios, G. M. (1996) Effects of thalidomide on HIV-associated wasting syndrome: a randomized, double-blind, placebo-controlled clinical trial. *AIDS* **10**, 1501-1507.
6. Sampaio, E. P., Sarno, E. N., Galilly, R., Cohn, Z. A., and Kaplan, G. (1991) Thalidomide selectively inhibits tumor necrosis factor α production by stimulated human monocytes. *J. Exp. Med.* **173**, 699-703.
7. Moreira, A. L., Sampaio, E., Zmuidzinas, A., Frindt, P., Smith, K. A., and Kaplan, G. (1993) Thalidomide exerts its inhibitory action on tumor necrosis factor α by enhancing mRNA degradation. *J. Exp. Med.* **177**, 1675-1680.
8. McBride, W. G. (1961) Thalidomide and congenital abnormalities. *Lancet* **ii**, 1358.
9. Lenz, W. (1962) Thalidomide and congenital abnormalities. *Lancet* **i**, 45.
10. Clemmensen, O. J., Olsen, P. Z., and Andersen, K. E. (1984) Thalidomide neurotoxicity. *Arch. Dermatol.* **120**, 338-341.
11. Ockenfels, H., Köhler, F., and Meise, W. (1976) Teratogene Wirkung und Stereospezifität eines Thalidomid-Metaboliten. *Pharmazie* **31**, 492-493.
12. Blaschke, V. G., Kraft, H. P., Fickentscher, K., and Köhler, F. (1979) Chromatographische Racemattrennung von Thalidomide und teratogene Wirkung der Enantiomere. *Arzneim.-Forsch.* **29**, 1640-1642.
13. Fabro, S., Smith, R. L., and Williams, R. T. (1967) Toxicity and teratogenicity of optical isomers of thalidomide. *Nature* **215**, 296.
14. Wnendt, S., Finkam, M., Winter, W., Ossig, J., Raabe, G., and Zwingenberger, K. (1996) Enantioselective inhibition of TNF- α release by thalidomide and thalidomide-analogues. *Chirality* **8**, 390-396.
15. Muller, G. W., Corral, L. G., Shire, M. G., Wang, H., Moreira, A., Kaplan, G., and Stirling, D. I. (1996) Structural modifications of thalidomide produce analogs with enhanced tumor necrosis factor inhibitory activity. *J. Med. Chem.* **39**, 3238-3240.
16. Corral, L. G., Muller, G. W., Moreira, A. L., Chen, Y., Wu, M., Stirling, D., and Kaplan, G. (1996) Selection of novel analogs of thalidomide with enhanced tumor necrosis factor a inhibitory activity. *Mol. Med.* **2**, 506-515.

17. Nishimura, K., Hashimoto, Y., and Iwasaki, S. (1994) Enhancement of phorbol ester-induced production of tumor necrosis factor α by thalidomide. *Biochem. Biophys. Res. Commun.* **199**, 455-460.
18. Shibata, Y., Sasaki, K., Hashimoto, Y., and Iwasaki, S. (1994) Tumor necrosis factor α production enhancers with a phenylphthalimide skeleton. *Biochem. Biophys. Res. Commun.* **205**, 1992-1997.
19. Steiger, R. E. *Org. Synth. Coll. Vol. 3*, 91-93.
20. Muller, G. W. (1995) Imides as inhibitors of TNF alpha. International patent # WO 95/01348.
21. Shevchenko, A., Wilm, M., Vorm, O., and Mann, M. (1996) Mass spectrometric sequencing of proteins from silver-stained polyacrylamide. *Anal. Chem.* **68**, 850-858.
22. Robins P., Pappin D. J., Wood R. D., and Lindahl T. (1994) Structural and functional homology between mammalian DNase IV and the 5'-nuclease domain of *Escherichia coli* DNA polymerase I. *J. Biol. Chem.* **269**, 28535-28538.
23. Dignam, J. D., Lebovitz, R. M., and Roeder R. G. (1983) Accurate transcription initiation by RNA polymerase II in a soluble extract from isolated mammalian nuclei. *Nucleic Acids Res.* **11**, 1475-1489.
24. Matthews, J. R., Wakasugi, N., Virelizier, J.-L., Yodoi, J., and Hay, R. T. (1992) Thioredoxin regulates the DNA binding activity of NF- κ B by reduction of a disulphide bond involving cysteine 62. *Nucl. Acids Res.* **20**, 3821-3830.
25. Hayashi, T., Ueno, Y., and Okamoto, T. (1993) Oxidoreductive regulation of nuclear factor κ B: involvement of a cellular reducing catalyst thioredoxin. *J. Biol. Chem.* **268**, 11380-11388.
26. Trede, N. S., Tsytsykova, A. V., Chatila, T., Goldfeld, A. E., and Geha, R. S. (1995) Transcriptional activation of the human TNF- α promoter by superantigen in human monocytic cells: role of NF- κ B. *J. Immunol.* **155**, 902-908.
27. Ishikawa, T., Casini, A. F., and Nishikimi, M. (1998) Molecular cloning and functional expression of rat liver glutathione-dependent dehydroascorbate reductase. *J. Biol. Chem.* **273**, 28708-28712.
28. Filler, R., Kobayashi, Y., and Yagupolskii, L. M., Eds. (1993) *Organofluorine Compounds in Medicinal Chemistry and Biomedical Applications*. (Elsevier, Amsterdam).
29. Miyachi, H., Azuma, A., Hioki, E., Iwasaki, S., Kobayashi, Y., and Hashimoto, Y. (1996) Cell type-/inducer-specific bidirectional regulation by thalidomide and phenylphthalimides of tumor necrosis factor-alpha production and its enantio-dependence. *Biochem. Biophys. Res. Commun.* **226**, 439-444.
30. Niwayama, S., Loh, C., Turk, B. E., Liu, J. O., Miyachi, H., and Hashimoto, Y. (1998) Enhanced potency of perfluorinated thalidomide derivatives for inhibition of LPS-induced tumor necrosis factor- α production is associated with a change of mechanism of action. *Bioorg. Med. Chem. Lett.* **8**, 1071-1076.
31. Marriot, J. B., Westby, M., Cookson, S., Guckian, M., Goodburn, S., Muller, G., Shire, G., Stirling, D., and Dalglish, A. G. (1998) CC-3052: a water soluble analog

- of thalidomide and potent inhibitor of activation-induced TNF- α production. *J. Immunol.* **161**, 4236-4243.
32. Davidsen, S. K., and Summers, J. B. (1995) Inhibitors of TNF- α synthesis. *Exp. Opin. Ther. Patents* **5**, 1087-1100.
 33. Holmgren, A. (1995) Thioredoxin structure and mechanism: conformational changes on oxidation of the active-site sulfhydryls to a disulfide. *Structure* **3**, 239-243.
 34. Bardwell, J. C. A. and Beckwith, J. (1993) The bonds that tie: catalyzed disulfide bond formation. *Cell* **74**, 769-771.
 35. Martin, J. L. (1995) Thioredoxin—a fold for all reasons. *Structure* **3**, 245-250.
 36. Kang, S. W., Baines, I. C., and Rhee, S. G. (1998) Characterization of a mammalian peroxiredoxin that contains one conserved cysteine. *J. Biol. Chem.* **273**, 6303-6311.
 37. Schröder, E., and Ponting, C. P. (1998) Evidence that peroxiredoxins are novel members of the thioredoxin fold superfamily. *Protein Sci.* **7**, 2465-2468.
 38. Sen, C. K. and Packer, L. (1996) Antioxidant and redox regulation of gene transcription. *FASEB J.* **10**, 709-720.
 39. Irani, K., Xia, Y., Zweier, J. L., Sollott, S. J., Der, C. J., Fearon, E. R., Sundaresan, M., Finkel, T., and Goldschmidt-Clermont, P. J. (1997) Mitogenic signaling mediated by oxidants in Ras-transformed fibroblasts. *Science* **275**, 1649-1652.
 40. Hidalgo, E., Ding, H., and Dimple, B. (1997) Redox signal transduction: mutations shifting [2Fe-2S] centers of the SoxR sensor-regulator to the oxidized form. *Cell* **88**, 121-129.
 41. Zheng, M., Åslund, F., and Storz, G. (1998) Activation of the OxyR transcription factor by reversible disulfide bond formation. *Science* **279**, 1718-1721.